

THE PROPERTIES OF SOME COMPLEXES AND
SALTS CONTAINING THE MALONATE OR THE
C-SUBSTITUTED MALONATE GROUP.

A thesis presented for the degree of
Doctor of Philosophy in the Faculty
of Science of the University of London

by

SOROUR AMIRHAERI

July 1981

Bedford College, London

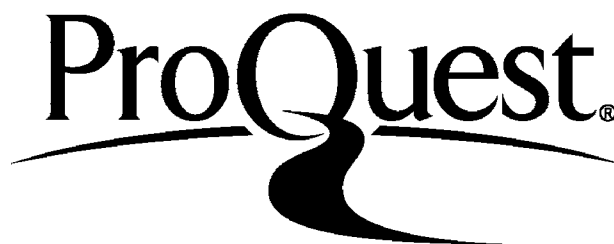
ProQuest Number: 10098399

All rights reserved

INFORMATION TO ALL USERS

The quality of this reproduction is dependent upon the quality of the copy submitted.

In the unlikely event that the author did not send a complete manuscript and there are missing pages, these will be noted. Also, if material had to be removed a note will indicate the deletion.



ProQuest 10098399

Published by ProQuest LLC(2016). Copyright of the Dissertation is held by the Author.

All rights reserved.

This work is protected against unauthorized copying under Title 17, United States Code
Microform Edition © ProQuest LLC.

ProQuest LLC
789 East Eisenhower Parkway
P.O. Box 1346
Ann Arbor, MI 48106-1346

ACKNOWLEDGEMENTS

I wish to thank my supervisor, Dr. M.E. Farago, for her constant help and encouragement, and also Professor G.H. Williams, the academic staff, particularly Dr. K.E. Howlett for his valuable assistance, and the technical staff of the Department of Chemistry, Bedford College.

My thanks are due to Dr. G. Marriner of the Geology Department, Bedford College, for all her help with the X-ray diffraction experiments, Professor T. Blundell of Birkbeck College for the use of single-crystal photograph facilities, Mr. I. Sayer, Birkbeck College for Mössbauer spectra and also Mr. A. Taha, Imperial College for his assistance with computer graphics.

The Educational Department of the Iranian Government is thanked for the award of a studentship, 1975-1978.

ABSTRACT

Methods have been devised for the preparation of some malonate and C-substituted malonate salts and complexes with various metal ions. The solid state ultraviolet, visible and infrared spectra have been measured and discussed with respect to the bonding of the compounds.

Infrared spectra studies confirmed that all complexes involve bonding through the carboxyl oxygen. Infrared analysis of these complexes confirmed the presence of two bands between $1600-1500\text{ cm}^{-1}$ and $1400-1350\text{ cm}^{-1}$. This differs from the position of such bands in the free acids, which upon coordination causes these bands to be shifted to lower or higher frequencies. The formation of these complexes through the carboxyl oxygen atoms has been confirmed from the X-ray analysis. The visible electronic spectra of the transition metal complexes indicated the most probable stereochemical shapes of the metal ion. The magnetic properties of Cu(II), Ni(II), Co(II), Fe(III), Mn(III) and Cr(III) complexes of malonate, ethyl and benzylmalonate were studied over a wide range of temperatures. The magnetic susceptibilities of all the compounds were found to be normal. Hence the Curie-Weiss Law was obeyed.

The Mössbauer spectra of iron(III)malonate, ethyl and benzylmalonate complexes exhibited a similar pattern characteristic of a high-spin octahedral structure. X-ray crystallographic data of Zn(II), Cd(II), Ca(II), Ba(II), Co(III) and Al(III)malonate and Zn(II) ethylmalonate complexes are reported. However, X-ray powder photographs of Zn(II) malonate confirmed it as isomorphous with Co(II) and Ni(II)malonate. The crystal structure of Al(III) malonato complexes were studied by the single-crystal method and the cell parameters were obtained.

Finally, ^1H n.m.r. and ^{13}C n.m.r. of some malonic acids and the chelated malonate group and the exchange of α -protons with deuterium from the solvent D_2O are reported.

CONTENTS

	<u>Page No.</u>
CHAPTER I: INTRODUCTION	6
1 Investigations of the structure of malonate compounds	6
2 X-ray powder studies of bivalent metal malonates	17
3 Malonates of trivalent metals	20
References	31
CHAPTER II: PREPARATIVE METHODS	33
1 Metal malonate compounds	33
2 Metal ethylmalonate compounds	38
3 Metal benzylmalonate compounds	44
References	52
CHAPTER III: VISIBLE AND ULTRAVIOLET SPECTROSCOPY	53
1 Introduction	53
2 Experimental methods	54
3 Results and discussion	54
References	66
CHAPTER IV: INFRARED ABSORPTION SPECTROSCOPY	69
1 Introduction	69
2 Results and discussion	73
3 Malonato metal compounds	73
4 Ethylmalonato metal compounds	83
5 Benzylmalonato metal compounds	92
References	104

	<u>Page No.</u>
CHAPTER V: MAGNETOCHEMISTRY	106
1 Introduction	106
2 Experimental	112
3 Diamagnetic susceptibility and diamagnetic correcting constants	115
4 Results and discussion	117
References	165
CHAPTER VI: X-RAY DIFFRACTION THEORY	168
1 The general nature of crystals	168
2 X-rays and crystal structure	170
3 Determination of the crystal structure	174
4 Principles of X-ray powder photographs	175
5 Experimental and results	182
References	210
CHAPTER VII: MÖSSBAUER SPECTROSCOPY	211
1 Introduction. Theory and application	211
2 Results and discussion	214
References	218
CHAPTER VIII: ^1H AND ^{13}C NMR STUDIES OF DICARBOXYLIC ACIDS AND THEIR METAL (III) COMPLEXES	219
1 Introduction	219
2 Results and discussion	220
References	229
CHAPTER IX: GENERAL CONCLUSIONS	230
PUBLICATIONS	237

CHAPTER I INTRODUCTION

1.1 Investigations of the structure of malonate compounds*

There has been recent interest in the malonate group. Malonate ion, $\bar{\text{O}}\text{OC}-\text{CH}_2-\text{CO}\bar{\text{O}}$, exhibits flexible stereochemistry and variable modes of binding with metal ions. It is known from the literature^{1,2} that malonic acid may chelate with the coordinated atoms to form four-membered as well as six-membered rings. However, there is a decided preference for six-membered chelate ring formation by malonate except in Ca(II) ³ and Nd(III) complexes,⁴ where only four-membered chelate rings are formed. X-ray structural analysis has shown that the conformation of the six-membered malonate chelate ring is greatly dependent on its environment in the solid state.^{1,4-7} The boat conformation appears to be the most common in malonate structures,^{4,7-11} but the chair conformation has been observed.¹⁰ However, the variety of observed bridging interactions underlines their importance in carboxylate metal crystalline structures. These bridged bonds are probably responsible for the extensive polymeric units commonly found in such derivatives and are obviously important in determining the crystalline structures.

Lanthanoid compounds

The conformations of the malonate ion in lanthanoid malonate complexes have been studied in a series of X-ray investigations involving $\text{Nd}_2 \text{ mal}_3 \cdot 8\text{H}_2\text{O}$ ⁹, $\text{Nd}_2 \text{ mal}_3 \cdot 6\text{H}_2\text{O}$ ⁴ and $\text{Eu}_2 \text{ mal}_3 \cdot 8\text{H}_2\text{O}$.¹⁰

In $\text{Eu}_2(\text{mal})_3 \cdot 8\text{H}_2\text{O}$ ¹⁰ there are three different europium(III) malonate stereochemistries: both four and six-membered chelate

* The references for this section are on pages 31 and 32.

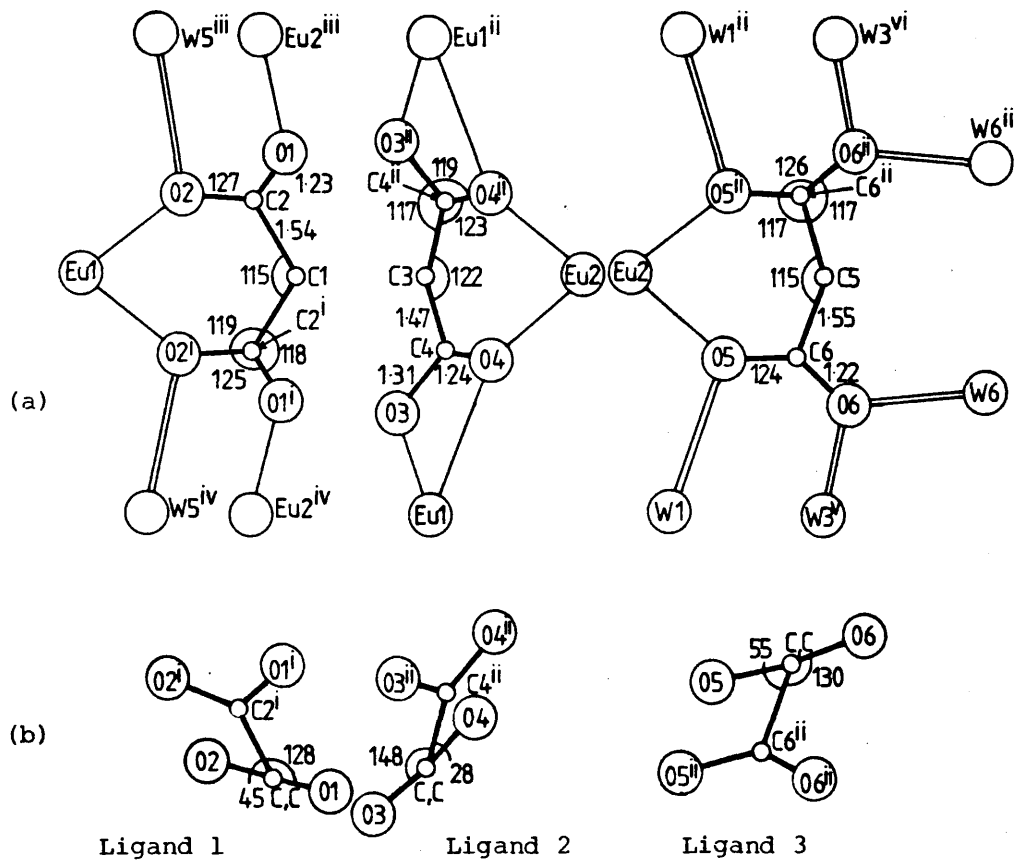


Fig.1.1.1. (a) The coordination around Eu ions.

(b) The three malonate ions in $\text{Eu}_2(\text{mal})_3 \cdot 8\text{H}_2\text{O}^{10}$.

rings and extensive bridging. The two europium ions have different coordination numbers. One europium is surrounded by nine oxygen atoms contributed by three malonate groups and three water molecules, with Eu-O in the range 2.37-2.84Å. The other europium is surrounded by eight oxygens contributed by four malonate groups and two water molecules with Eu-O bond distances in the range 2.37-2.48Å. The malonate ions form six-membered chelate rings with europium. The rings formed by ligand No. 1 and 2 have a boat conformation with the europium ion and the methylene carbon atom at the same side of the OCCO-plane, while the ring formed by ligand 3 adopts a chair conformation with the europium ion and methylene carbon atom at opposite sides of the OCCO-plane. The three malonate ions, together with the coordination around the Eu are indicated in Figure 1.1.

Basic Scandium malonate

In basic scandium malonate¹¹ $\text{Sc}(\text{OH})\text{mal} \cdot 2\text{H}_2\text{O}$ the malonate ion forms a six-membered chelate ring with the Sc ion. Each Sc ion is octahedrally surrounded by three carboxylate oxygens contributed by two malonate ions, two hydroxy oxygens and one water oxygen. The structure is composed of infinite Sc-hydroxo malonate chains which are linked by hydrogen bonds. Within each chain the Sc ions are bonded in pairs by double oxygen bridges formed by the hydroxy ions, and the Sc pairs are in turn linked by carboxylate bridges Sc-O(1) C(1) O(2)-Sc*. The bond distances and angles within the malonate are similar to other malonate structures.⁹ These are shown in Figure 1.2b.

Calcium malonate

The conformation of the malonate ligand in calcium malonate³ differs considerably from that found in other metal malonate compounds where only four-membered rings are formed. The structure of calcium

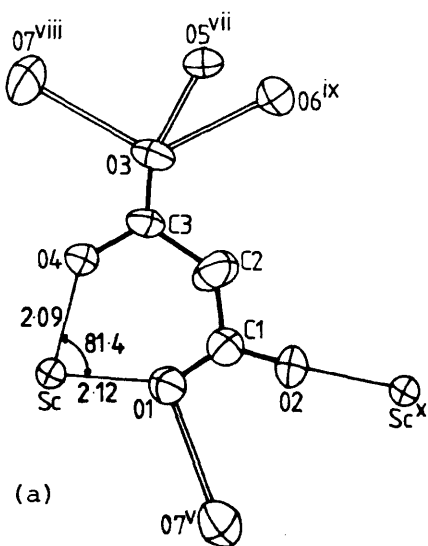
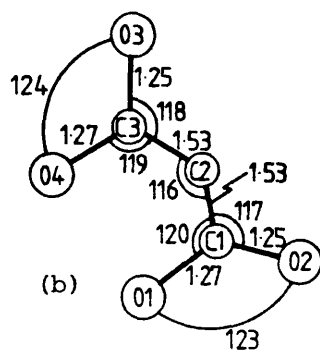


Fig.1.2. (a) The coordination in Sc malonate. $2\text{H}_2\text{O}^{11}$.



(b) The bond distances (Å) and angles ($^{\circ}$) within the malonate ion in Sc malonate. $2\text{H}_2\text{O}^{11}$.

malonate dihydrate is reported (Briggman and Oskarsson, 1977¹; Karipides et al; 1977³). Although the coordination of the malonate was the same in both investigations, the crystal data are slightly different. The crystal data reported by Karipides et al³ were confirmed in this investigation (see chapter VI for the basic salt). It seems very probable therefore that the calcium malonate dihydrate reported by both sets of workers is really the basic salt since their X-ray structural data on this compound have not been accompanied by chemical analysis proving the identity of the compound.

The calcium ion in this compound is eight coordinated^{1,3} and is bound to six oxygen atoms from four different malonate ions and two water molecules. All four oxygen atoms of a malonate ligand participate in binding Ca(II) ions. The two malonate carboxylate groups coordinate in different manners. One carboxylate group C(1)-O(1)-O(2) binds three different Ca(II) ions forming a four-membered ring with one Ca(II) and unidentate bridge linkages to two other Ca(II) ions. The unidentate carboxylate bridge bonds Ca-O(1^a) and Ca-O(2^b) are found in metal carboxylate complexes in particular in Ca(II) carboxylates (Fig.1.3.). These bridge bonds are responsible for the extensive polymeric units found in these complexes. In Ca(II)malonate the Ca-O(1^a), 2.397Å and Ca-O(2^b), 2.424Å, bridge bonds are shorter than all the nonbonding Ca(II) carboxylate oxygen distances.

More recently Marsh and Schomaker¹³ refined the structure reported by Karipides et al in space group C2/m in agreement with Briggman et al and this work rather than in C2, and the bond distances and angles were corrected accordingly. It was found that in calcium malonate dihydrate both O(5) and O(6) form hydrogen bonds rather than only O(5) reported by Karipides et al³.

Studies have also been carried out more recently on the structure of calcium malonate dihydrate by the neutron diffraction method¹².

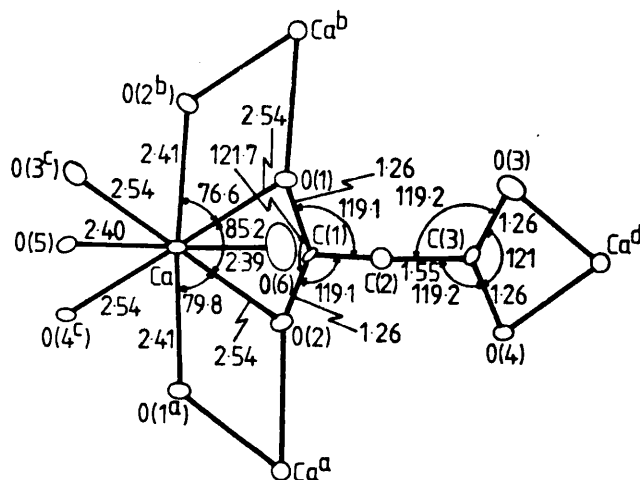


Fig.1.3. The coordination polyhedron in
Ca malonate. $2\text{H}_2\text{O}^3$.

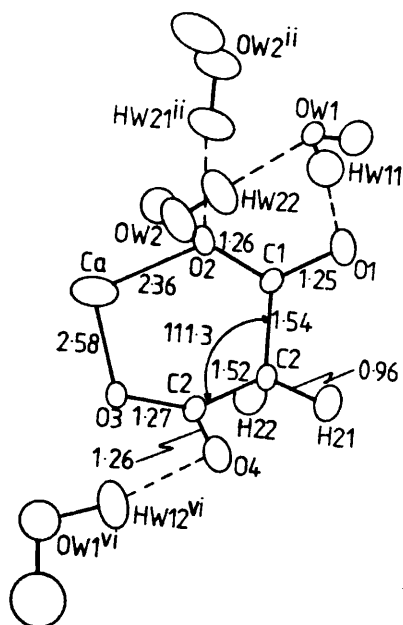


Fig.1.4. The coordination in
Ca malonate. $2\text{H}_2\text{O}^{12}$.

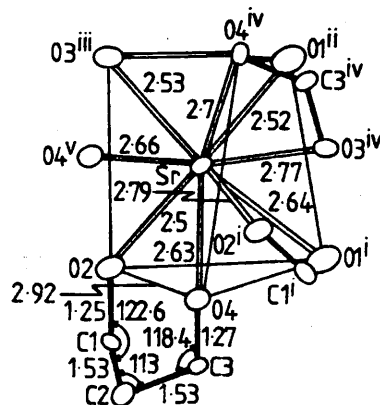


Fig.1.5. The coordination polyhedron
in Sr malonate anhydrous¹.

This compound differs appreciably from the structure of the compound discussed above and is probably the true dihydrate. In this compound each malonate ion is coordinated to four different Ca^{2+} ions. The malonate ion forms a six-membered ring with the Ca^{2+} ion. The coordination around the $\text{Ca}(\text{II})$ ion is shown in Fig.1.4. The two halves of the malonate ion are in quite different environments; the bond lengths and angles around C(1) are different from those around C(3). The malonate chelate ring has a boat conformation with Ca^{2+} which is similar to that observed in Sr malonate¹. The C-C-C angle is 111.3° (112.5° in Sr malonate). The C-C-C angle is 109.5° ; close to tetrahedral value in Ca malonate reported by both Briggman¹ and Karipides et al³, suggesting considerable relaxation of bond angle strain. The crystal data of calcium malonate dihydrate reported by different workers are listed in Table 1.0.

Strontium malonate

In anhydrous Sr malonate the compound is composed of a three dimensional network linked nine-coordinate Sr^{2+} complex¹. The malonate ion forms one six and two four-membered rings. The Sr ion is coordinated by nine carboxylate O atoms forming a distorted tricapped trigonal prism (Fig.1.5). It is found that the relative interatomic distances and angles within the four ligand halves $\text{C} - \text{C} \begin{array}{l} \diagup \text{O} \\ \diagdown \text{O} \end{array}$ are not significantly different and agree well with those found in other malonate compounds. However, if the C-C-C angle (in six-membered ring) is disregarded there are no differences between bond distances and angles in the Ca malonate³ and Sr malonate (112.5° in Sr malonate and 109.5° in Ca malonate).

Table 1.0 Crystal data for "calcium malonate"

Compound	a	b (Å)	c	β (deg)	space group	Ref.
"Ca mal.2H ₂ O"	13.8707	6.8120	6.8040	106.289	C2/m	1
"Ca mal.2H ₂ O"	13.955	6.855	6.835	106.28	C2/m	3,13
Ca mal,Ca(OH) ₂ .1½H ₂ O	13.9278	6.8559	6.8639	106.137	C2/m	This work
Ca mal.2H ₂ O	8.7767	7.7540	9.8836	106.406	P2 ₁ /C	12

Sodium malonate

In sodium malonate monohydrate, $\text{Na}_2\text{C}_3\text{H}_2\text{O}_4 \cdot \text{H}_2\text{O}$, each Na^+ ion is coordinated by five carboxylate oxygen atoms and one water molecule forming distorted octahedra¹⁴. The malonate ion (Fig.1.6.) forms a six-membered chelate ring with one of the Na^+ ions and a four-membered ring with the other. The conformation of the malonate ion is similar to those found in rare-earth malonates with six-membered chelate rings, and Sr malonate.¹ The C-C distances agree well with those found in Ca mal and Sr mal. The C(3)-O(3) bond distances involving O(3) hydrogen bonding are lengthened and C(3)-O(4) are shortened as compared to those observed in the other carboxylate group. The Na-O bond lengths are between 2.41 and 2.49Å.

Beryllium malonate

The crystal structure of potassium bis (malonato) beryllate hemihydrate, $\text{K}_2[\text{Be}(\text{C}_3\text{H}_2\text{O}_4)_2] \cdot \frac{1}{2}\text{H}_2\text{O}$ has recently been reported.¹⁵ The Be^{2+} ion is coordinated tetrahedrally by four carboxylate oxygen atoms contributed from two malonate groups. The Be-O bond distances are in the range 1.609-1.623Å. The conformation about the beryllium atom is shown in Figure 1.7.

Magnesium bis (hydrogen malonate) dihydrate

In $\text{Mg}(\text{C}_3\text{H}_3\text{O}_4)_2 \cdot 2\text{H}_2\text{O}$, the Mg ion is surrounded by four carboxylate O atoms (Mg-O=2.045Å) and two water O atoms (Mg-O=2.06Å) forming a slightly distorted octahedron.¹⁶ Fig.1.8. The hydrogen malonate ion forms a six-membered chelate ring which is almost planar with Mg^{2+} ion, with a C-C-C angle of 119.8°. A similar conformation of the hydrogen malonate ion is found in potassium hydrogen malonate, with a C-C-C angle of 119.4°.³⁷

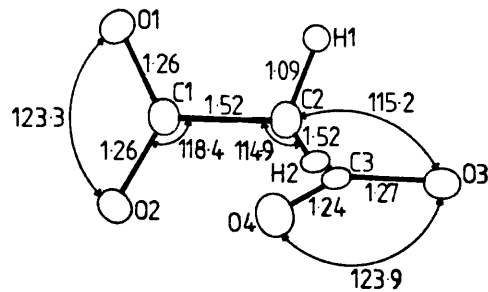


Fig.1.6. The bond lengths (\AA) and angles ($^\circ$)
in Na malonate. H_2O^{14} .

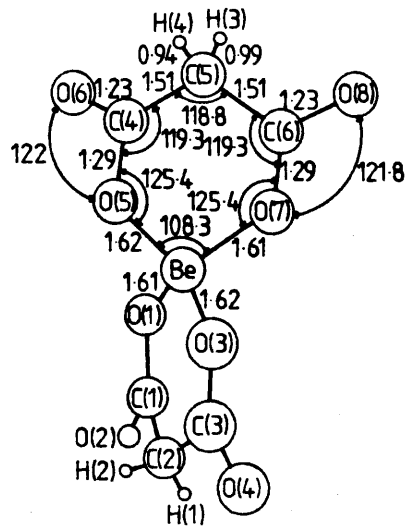


Fig.1.7. The coordination in Be malonate. $\frac{1}{2} \text{H}_2\text{O}^{15}$.

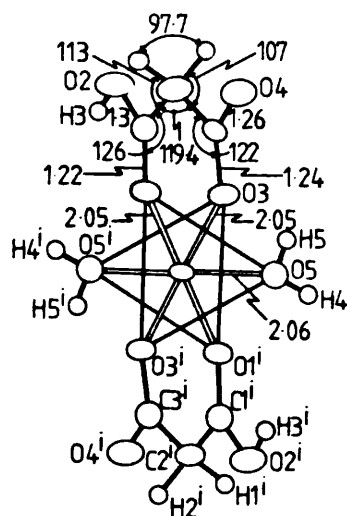


Fig.1.8. The coordination polyhedron around Mg(II) ion in $\text{Mg}(\text{H mal})_2 \cdot 2\text{H}_2\text{O}^{16}$.

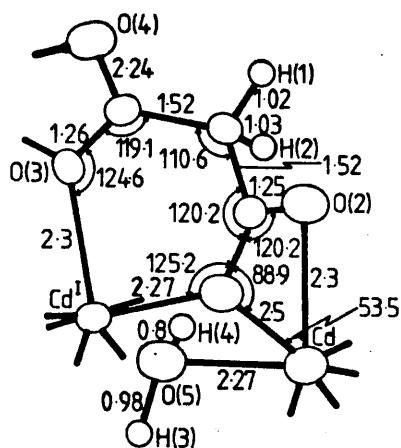


Fig.1.9. The coordination around Cd(II) ion in $\text{Cd malonate} \cdot \text{H}_2\text{O}^7$.

Cadmium malonate

In cadmium malonate monohydrate,⁷ the structure consists of one six-membered and two four-membered chelate rings. Each malonate ligand chelates three symmetry-related cadmium atoms with two of the oxygen atoms also in bridging positions and makes each of the malonate carboxyl groups tetradentate. The coordination about Cd is completed with one water molecule to give a coordination number of seven. The lattice formed is polymeric and further strengthened by hydrogen bonding of water hydrogen atoms. The Cd-O distances vary from 2.27-2.5Å, also the bridging oxygen atoms are not equally shared between cadmium atoms, the bonds in this case are shorter on the six-membered chelate ring side. The structural details are shown in Figure 1.9.

1.2 X-ray powder studies of bivalent metal malonates

A series of malonate derivatives of bivalent cations of the type $MC_3H_2O_4 \cdot 2H_2O$ where $M = Mg(II),^{17} Zn(II),^{17} Mn(II),^{17} Co(II),^{18} Ni(II)^{19}$ have been studied by the powder method and the space groups have been determined. Although the empirical formula units are similar, the indicated malonates are reported to crystallise in different space groups, suggesting a variation in metal ion-malonate coordination. These powder studies are far enough to specify their formula and to determine their crystalline system and to establish their isomorphism. However, bivalent $Co^{2+}, Ni^{2+}, Zn^{2+}$ malonate compounds are found to be monoclinic with $\beta \neq 90^\circ$ and they are isomorphous, whereas $Mg^{2+},^{17,20,21} Mn^{2+}, Fe^{2+}^{22}$ are orthorhombic and isomorphous. These results are similar to those of the other metal-carboxylate compounds^{23,24} having an octahedral arrangement around the metal ions. The complete X-ray analyses of these compounds with the exception of Mn(II) malonate have not yet been reported.

Manganese malonate dihydrate

Preliminary studies of manganese malonate have been made by Walter-Levy et al.¹⁷ and later by Gupta and Chand.²⁰ A complete crystal structure of the compound has been carried out more recently²¹ which confirmed the previous lattice parameters. In the crystal, each Mn^{2+} ion is octahedrally coordinated by four carboxylate O atoms from three different malonate ions and two trans water O atoms with Mn-O distances ranging from 2.13 to 2.23Å. The water molecules and the surrounding oxygen atoms form a distorted octahedron (Fig. 1.10.). Within the malonate ion the bond lengths and angles are normal. The malonate ligands adopt the envelope conformation, as in most complexes of the malonate ligand.⁵ In the crystal, all four H atoms from the two water molecules are involved in hydrogen bonding which holds the polymeric layers together.

Copper malonate

The structure of copper malonate has been investigated by various workers²⁵⁻²⁷ both by powder and single crystal x-ray methods. The salt which was prepared by neutralization of malonic acid with copper carbonate has three waters of crystallization and is reported to be monoclinic with cell parameters $a = 10.62$, $b = 21.00$, $c = 13.5\text{Å}$, $\beta = 111^\circ$, space group $P2_1/n$, $Z = 16$.

Copper malonate tetrahydrate which was prepared by reaction of malonic acid and copper hydroxide at 25°C has been studied by the powder method²⁶. The compound belongs to the triclinic symmetry group with unit cell parameters $a = 7.630$, $b = 10.33$, $c = 5.28\text{Å}$, $\alpha = 103.14^\circ$, $\beta = 99.06^\circ$, $\gamma = 108.54^\circ$. The distances between the planes and relative intensities of diffraction lines are also reported.

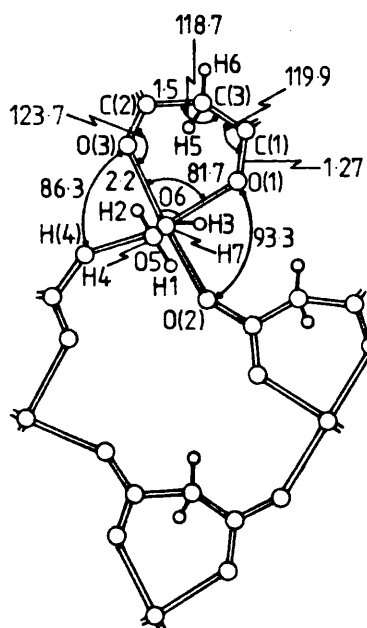


Fig.1.10. The crystal structure of Mn malonate. $2\text{H}_2\text{O}$ ²¹.

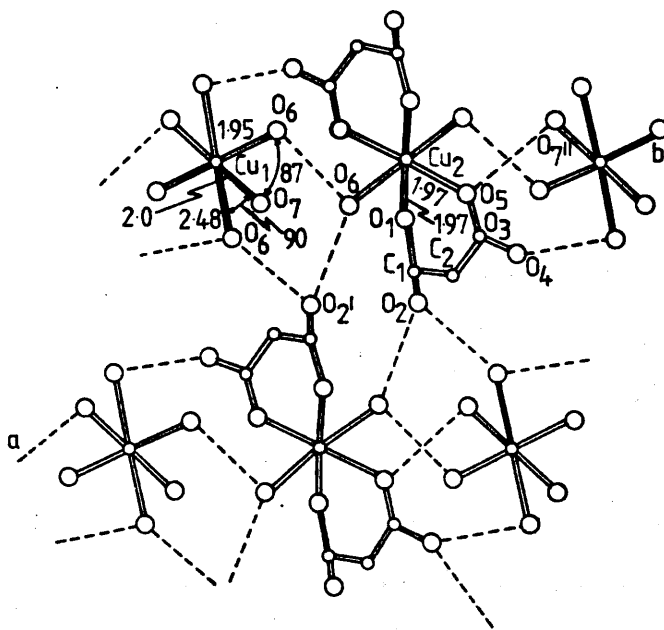


Fig.1.11. The crystal structure of Cu malonate. $4\text{H}_2\text{O}$ ²⁷.

The complete X-ray analysis of copper malonate tetra hydrate²⁷ later confirmed this result. Although the salt was prepared by using a different method of synthesis (i.e. equal volumes of 1M solutions of potassium hydrogen malonate and Cu(II) chloride) similar unit cell parameters were obtained.²⁷

The crystal structure with formula $[\text{Cu mal}, 4\text{H}_2\text{O}]_2$ is constructed from two different types, i.e. anions $[\text{Cu}(\text{mal})_2 \cdot 2\text{H}_2\text{O}]^{2-}$ and cations $[\text{Cu}(\text{H}_2\text{O})_6]^{2+}$. In the complex of the first type - dimalonato cuprate, the Cu atom is surrounded by two malonate ions which form two six-membered rings. The fifth and sixth positions are occupied by two water molecules.²⁷ (Fig.1.11).

The interatomic distances and angles in malonate are similar with that of malonic acid.²⁸ Similar structures have been reported for the corresponding oxalato complexes.²⁹

In a complex of second type the copper atom coordinates six water molecules with $\text{Cu}-\text{O}_6 = 1.95$, $\text{Cu}-\text{O}_7 = 2.0$, $\text{Cu}-\text{O}_8 = 2.47$, Å; $\text{O}_6\text{CuO}_7 = 87.1^\circ$; $\text{O}_8\text{CuO}_6 = 92.9^\circ$; $\text{O}_8\text{CuO}_7 = 90.0^\circ$. The hydrogen bonds form between the O2 atom of the carboxylate group of the malonate ion and the anionic complexes from the neighbouring layer.

1.3 Malonates of trivalent metals

Some comparisons can be made between tris (oxalato) complexes and tris (malonato) complexes of M(III) ions. It is known that the complex ions of the type $\text{M}(\text{ox})_3^{3-}$ possess similar configurations and the same coordination number six. Preliminary X-ray examination³⁰ indicates the exact correspondence of the molecular formulae of the potassium tris oxalato complexes of Al^{3+} , V^{3+} , Cr^{3+} , Mn^{3+} and Fe^{3+} , and the isomorphism of their crystals, all of which occur in the monoclinic system with three water molecules per

mole of salt, but corresponding Co^{3+} , Rh^{3+} and Ir^{3+} complexes are triclinic and they contain, $3\frac{1}{2}$, $4\frac{1}{2}$ and $4\frac{1}{2}$ molecules of water.³¹

In the case of tris malonato complexes of M(III) ions it has been found that the tris malonato complexes of Al(III), Cr(III) and Fe(III) are isomorphous having similar octahedral environments around the metal ions. The complete X-ray analyses of Al(III) and Fe(III) malonato complexes have not been reported.

X-ray structural analyses of coordinated malonate ion in tris malonato metal complexes of the type $\text{K}_3 [\text{M}(\text{mal})_3]$, XH_2O (M = Cr, Mn, Co) have been reported^{2,5} where three six-membered malonate chelate rings are involved. In these complexes the metal is surrounded nearly octahedrally by the oxygen atoms of the malonate groups. The molecular geometry in $\text{Cr}(\text{mal})_3$ complexes is shown in Figure 1.12.

The Cr-O bond distances and angles indicate a regular octahedron. These values are well within the range observed in the chromium malonato complexes.^{8,38} The malonate conformation is highly dependent on its environment as predicted by Butler and Snow.³² In $\text{Cr}(\text{mal})_3$ complexes the five atoms CrO(1), O(1'), C(3), C(3') are almost coplanar. The conformation of the six-membered malonate chelate ring assumes an envelope conformation⁵ (Fig.1.13.a).

It is different however from that reported for $(-)[\text{Co}(\text{NO}_2)_2(\text{en})_2]$ (+) $[\text{Co}(\text{mal})_2(\text{en})]$, where the six-membered chelate rings adopt a flattened skew boat conformation³³ (Fig. 1.13.b), and for Na (+) $[\text{Co}(\text{en})(\text{mal})_2] \cdot 2\text{H}_2\text{O}$ ³² where both rings adopt a boat conformation (fig.1.13.c). The boat conformation is the most common in malonate structures. The chair conformations (fig.1.13.d) are said to be energetically unfavoured for malonato complexes.³²

The structures of some dimeric chromium (III) malonato complexes have been reported recently.^{8,38} In $[\text{Cr}(\text{mal})_2(\text{OH})]_2^{4-}$,

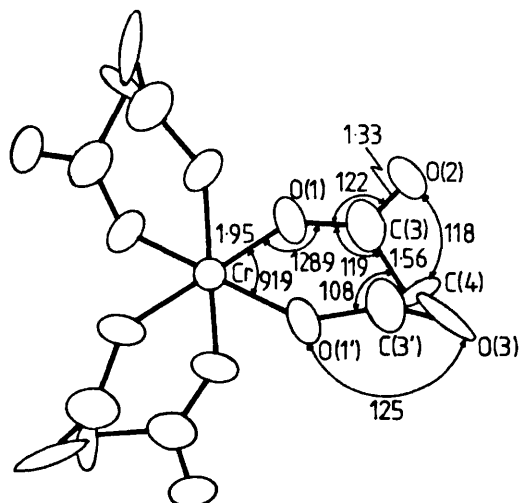


Fig.1.12. The geometry for $[\text{Cr}(\text{mal})_3]^{3-}$ anion⁵.

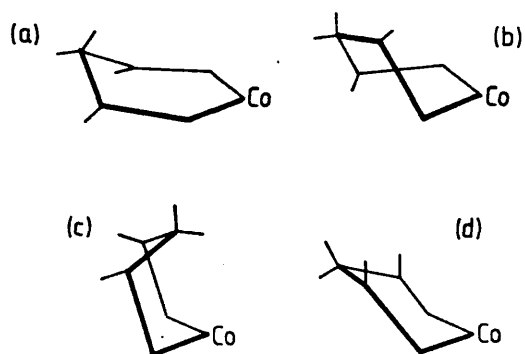


Fig.1.13. Malonate ring conformations: (a) envelope, (b) skewboat, (c) boat, (d) chair³².

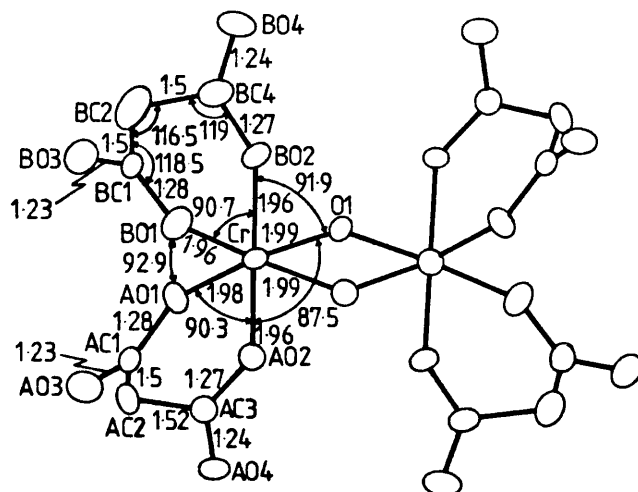


Fig.1.14. The geometry for $[\text{Cr}(\text{mal})_2(\text{OH})]_2^{4-}$ anion⁸.

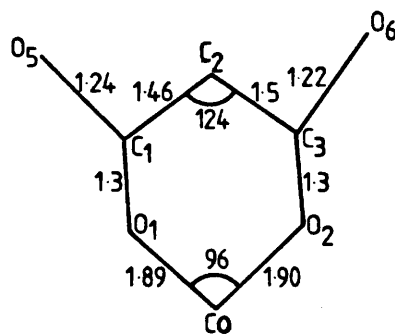


Fig.1.15. The projection of the Co-malonate in $[\text{Coen}(\text{mal})_2]^{-}$ ³³.

each chromium atom is six coordinated, approximately octahedral, the ligating atoms being two cis hydroxo groups and two cis malonate groups. The malonate ligands are bidentate, each coordinating through two oxygen atoms; the uncoordinated oxygen atoms are involved in extensive hydrogen bonding in the crystal. The four independent chromium - malonate oxygen distances with an average of 1.963Å, are shorter than the two Cr-O distances (1.987Å) in the bridging unit, Figure 1.14. Both malonate groups are in the boat conformation.

The X-ray crystal structure of $K_3[Co(mal)_3] \cdot 4H_2O$ has been reported⁵ and the cell parameters confirmed by this investigation (see Chapter VI). The molecular geometry of the Co malonate chelate ring is very similar to that observed for the $Cr(mal)_3$ complexes. The Co atom is surrounded octahedrally by the oxygen atoms of the malonate groups.^{32,33} Figure 1.15. shows the projection of the Co-malonate six-membered chelate ring in bis (malonate) ethylenediamine cobaltate (III). The bond distances and angles within the complex ion are normal and are in good agreement with those observed in other related complexes.⁶

The water molecules are not coordinated directly with the metal atoms, but link different parts of the structure by means of hydrogen bonding. The crystal structure of Mn(III) malonate complexes has been studied more recently by the single crystal diffraction method.² The results of X-ray analysis confirmed a distorted octahedral environment around the Mn^{3+} ion in both bis and tris Mn(III) malonate complexes.

Potassium trans-diaquo bis (malonate) manganese (III) dihydrate, $K[Mn(H_2O)_2(mal)_2] \cdot 2H_2O$ has the space group Pbcn, orthorhombic unit cell containing four molecular units with $a = 6.842$, $b = 13.49$, $c = 14.115\text{Å}$.

Each manganese atom is coordinated by four oxygens from the two malonate groups with equal bond distances ($M-O = 1.90\text{\AA}$) and two oxygens from the water molecules with longer bond distances ($M-O = 2.30\text{\AA}$). The arrangement of the molecule and bond distances and angles are given in Figure 1.16.

The bond distances and angles within the malonate ion are in agreement with the values for malonic acid²⁸ and substituted malonic acid.^{34,35} On comparison of the bond distances in Mn(II) malonate and bis malonate diaquo manganese (III) complexes, the Mn^{III}-H₂O distances of 2.30 Å in $[\text{Mn}(\text{mal})_2(\text{H}_2\text{O})_2]^-$ ions are slightly longer than those of Mn^{II}-H₂O (2.20 Å) in Mn mal, 2H₂O which confirms the suggestion² that bonds between Mn^{III} ions and water molecules are very weak and may be easily disrupted in solution.

Studies have also been carried out more recently on the structure of the complex known as $\text{K}[\text{Mn}(\text{mal})_2(\text{CH}_3\text{OH})]$ by X-ray analysis.³⁶ The crystals are triclinic, space group $P\bar{1}$, with $a = 8.55$, $b = 8.56$, $c = 8.95\text{\AA}$, $\alpha = 113.60$, $\beta = 94.78$, and $\gamma = 99.97^\circ$ and $Z = 2$.

The polymeric structure consists of carboxylate-bridged trans-bis (malonate) dimethanol manganese (III) and bis (malonate) manganese (III) anions and potassium cations. There are two different manganese atoms in the structure which have different octahedral environments (Fig. 1.17). Each of the two different manganese atoms is bound to four oxygen atoms of the malonate ligands with M-O distances of 1.91 Å similar to that of bis malonate diaquo manganese (III) complexes. The two remaining sites of the coordination octahedron around both manganese atoms are different. The Mn(1) atoms are linked to one of the oxygen atoms of the carboxylate groups of the malonate ligands with $\text{Mn}(1)-O = 2.26\text{\AA}$ chelating the Mn(2) atoms, while in Mn(2), the two remaining positions are occupied by methanol molecules with $\text{Mn}-O(\text{methanol}) = 2.203\text{\AA}$. The manganese-oxygen distances

Fig.1.16. The geometry for
 $[\text{Mn}(\text{mal})_2(\text{H}_2\text{O})_2]^{2-}$ anion².

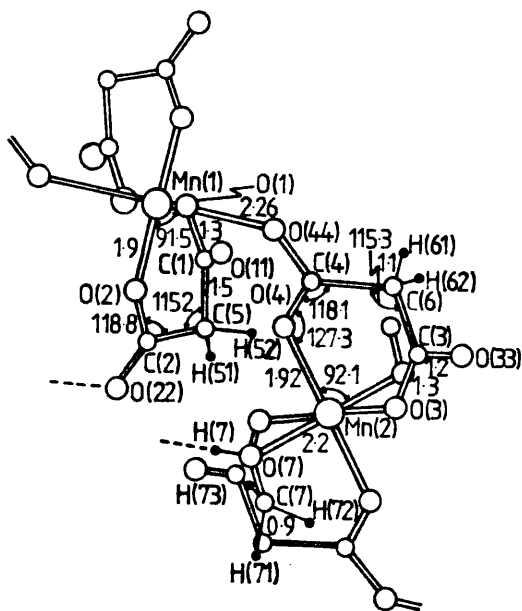
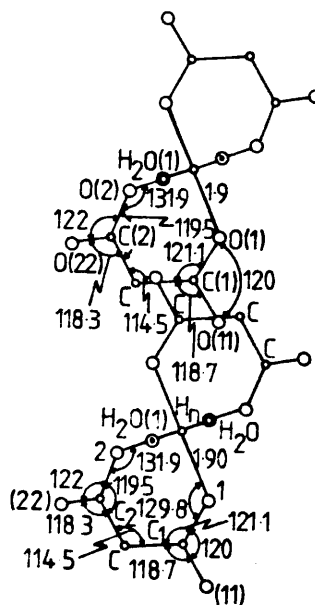
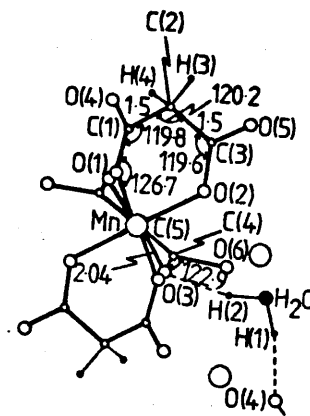


Fig.1.17. The geometry for
 $[\text{Mn}(\text{mal})_2(\text{CH}_3\text{OH})]^{36-}$ anion³⁶.

Fig.1.18. The geometry for
 $[\text{Mn}(\text{mal})_3]^{3-}$ anion³.



indicate the tetragonal elongation of the coordination octahedron around two different manganese atoms, similar to that found in $K[Mn(mal)_2(H_2O)_2] \cdot 2H_2O$ complexes. In $K[Mn(mal)_2(CH_3OH)]$, the two different malonate chelate rings adopt the envelope conformation, which is rather common in such compounds.³²

Hydrogen bonds are formed between the hydrogen atoms of the hydroxy groups of the methanol molecules and the oxygen atoms of the malonate ligands chelating the Mn(I) atom in a neighbouring cell.

In $K_3[Mn(mal)_3] \cdot 2H_2O^2$, a monoclinic unit cell, space group C2/c, has four molecules per unit cell with $a = 14.799$, $b = 7.850$, $c = 16.210 \text{ \AA}$, $\beta = 108.51^\circ$. In the crystal each manganese atom is coordinated octahedrally by six carboxylate oxygen atoms from three different malonate ions. The geometry of the molecule is shown in Figure 1.18.

The Mn-O bond distances of 1.92, 2.00 and 2.04 Å in the complex indicate the distortion from octahedral symmetry around the central manganese atom. The Mn-O bond distances in tris(malonato) complexes (Mn-O = 1.92-2.04 Å) are longer than the Mn-O distances (Mn-O = 1.90 Å) in the diaquo bis (malonato) manganese (III) complexes.² Hydrogen bonds are formed between the water and the oxygen atoms O(3) of the malonate ligands which may contribute to the stability of the crystal structure and it is shown that the H₂O-O(3) hydrogen bond influences the lengthening of the Mn-O(3) bond and therefore the geometry of the complex anion is more distorted.

Table 1.1. The bond lengths (Å), C-C-C bond angles (deg) and geometry in metal-malonate compounds

Compound	M-O	O-C	C-O	C-C	C-Ĉ-C	CO-NO*	Geometry	Ref.
Eu ₂ (mal) ₃ ·8H ₂ O	2.42, 2.51	1.24, 1.27	1.22-1.31	1.47-1.55	115, 122	8, 9	dist square antiprism	10
Sc(OH)mal·2H ₂ O	2.09, 2.12	1.27	1.25	1.53	115.7	6	octahedral	11
Na ₂ mal·H ₂ O	2.4, 2.45, 2.49	1.26, 1.26	1.22	1.52, 1.516	114.9	6	dist octahedral	14
KH mal	2.86, 2.88	1.29	1.22	1.52	119.4			37
K ₂ [Be(mal) ₂].½H ₂ O	1.609, 1.623	1.286, 1.282	1.23	1.50-1.51	118.8, 120.7	4	tetrahedral	15
Mg(Hmal) ₂ ·2H ₂ O	2.045, 2.06	1.22-1.24	1.257, 1.303	1.50-1.52	119.8	6	dist octahedral	16
"Ca mal·2H ₂ O"	2.54	1.255, 1.26	1.25, 1.26	1.533	109.3	8	bicapped trigonal prism	3
Ca mal·2H ₂ O	2.32-2.58	1.26-1.27	1.25, 1.26	1.52, 1.54	111.3		pentagonal bipyramid	12
Sr mal	2.6-2.7	1.25, 1.27	1.25, 1.26	1.525, 1.529	112.5	9	dist tricapped trigonal prism	1
Cd mal·H ₂ O	2.27-2.50	1.266, 1.26	1.25, 2.24	1.52	110.6	7	pentagonal bipyramid	7
Cu(mal) ₂ (H ₂ O) ₂ ·4H ₂ O	1.95, 1.96, 1.97	1.29, 1.31	1.22, 1.24	1.52, 1.54	110.0	6	tetragonal	27
Mn mal·2H ₂ O	2.13, 2.23	1.257	1.26, 1.24	1.51, 1.52	118.7	6	octahedral	21
K[Mn(mal) ₂ (H ₂ O) ₂].2H ₂ O	1.9, 2.30	1.28, 1.28	1.22, 1.24	1.53, 1.55	114.5	6	tetragonal	2
K[Mn(mal) ₂ (CH ₃ OH)]	1.90, 1.92, 2.20	1.298, 1.30, 1.28	1.22	1.50, 1.52	115.2, 115.3	6	tetragonal	36
K ₃ [Mn(mal) ₃].2H ₂ O	1.90, 2.0, 2.04	1.27, 1.28, 1.3	1.22, 1.24, 1.23	1.51, 1.52	120.9	6	dist octahedral	3
[Cr(mal) ₃] ³⁻	1.95	1.26	1.20, 1.33	1.56, 1.61	108.0	6	octahedral	5
[Cr(mal) ₂ OH] ⁴⁻	1.96	1.276	1.233	1.526	116.5	6	octahedral	8
[{Cr(en)(mal)(OH)} ₂] ₂ ·6H ₂ O	1.94, 1.95	1.24, 1.26	1.26, 1.28	1.49, 1.53	116.5	6	octahedral	38
(+)[Co mal ₂ en] ⁻	1.90 (mean)	1.29 (mean)	1.237 (mean)	1.475 (mean)	124.0, 125.0	6	octahedral	33
(+)[Co(CN) ₂ (mal)(NH ₃) ₂] ⁻	1.92, 1.93	1.277, 1.267	1.23, 1.247	1.519, 1.535	116.7	6	octahedral	6
Na(+)[Co(mal) ₂ (en)].2H ₂ O	1.897 (mean)	1.281	1.24	1.50	116.2, 118.2	6	octahedral	32

*coordination number

Table 1.2. Crystal data for malonate salts and malonate complexes

Compound	a	b (Å)	c	angles (deg)	system	space group	Z	Ref.
Eu ₂ (mal) ₃ ·8H ₂ O	12.220	8.100	20.545	α=β=γ=90	orthorhombic	Pnma	4	10
Sc(OH)mal·2H ₂ O	6.276	15.353	7.776	β=99.90	monoclinic	P2 ₁ /n	4	11
Na ₂ mal	7.7486	12.6419	5.7866	α=β=γ=90	orthorhombic	Pbc2 ₁	4	14
KH mal	9.473	11.559	4.726	β=91.6	monoclinic	C2/m	4	37
K[Be(mal) ₂] ₂ ·½H ₂ O	22.082	9.486	15.183	β=140.41	monoclinic	C2/c	8	15
Mg(H mal) ₂ ·2H ₂ O	4.9391	11.3100	9.6497	β=90.312	monoclinic	P2 ₁ /c	2	16
Mg mal·2H ₂ O	8.153	9.407	7.253	α=β=γ=90	orthorhombic	Pnab	4	17
"Ca mal·2H ₂ O"	13.955	6.855	6.835	β=106.28	monoclinic	C2/m	4	3
"Ca mal·2H ₂ O"	13.8707	6.8120	6.840	β=106.298	monoclinic	C2/m	4	1
Ca mal·2H ₂ O	8.7767	7.7540	9.8836	β=106.406	monoclinic	P2 ₁ /c	4	12
Ca mal,Ca(OH) ₂ ·1½H ₂ O	13.9278	6.8559	6.8639	β=106.137	monoclinic	C2/m	4	This work
Sr mal	6.7538	10.6270	12.6744	α=β=γ=90	orthorhombic	Pnan	8	1
Cd mal·H ₂ O	17.216	17.216	10.894	γ=β=90, γ=120	trigonal	R $\bar{3}$	18	7
Zn mal·2H ₂ O	11.059	7.411	7.294	β=95.32	monoclinic	I2/m	4	17
Zn mal·2H ₂ O	11.0625	7.4221	7.2901	β=95.275	monoclinic	I2/m	4	This work
Zn(H mal) ₂ ·2H ₂ O	9.732	11.254	4.928	γ=β=γ=90	orthorhombic	Pbam	2	17
Cu(mal) ₂ (H ₂ O)·4H ₂ O	7.68	10.16	5.32	α=100.0, β=93.7, γ=105.6	tetragonal	P $\bar{1}$	2	27
Ni mal·2H ₂ O	10.884	7.377	7.223	β=94.58	monoclinic	I2/m	4	17
Ni(H mal) ₂ ·2H ₂ O	9.762	11.047	4.921	α=β=γ=90	orthorhombic	Pb2 ₁ 2	2	17
Co mal·2H ₂ O	10.990	7.416	7.314	β=95.03	monoclinic	I2/m	4	17
Co(H mal) ₂ ·2H ₂ O	9.672	11.259	4.928	α=β=γ=90	orthorhombic	P2 ₁ /a	2	17

Table 1.2 continued

Compound	a	b Å	c	angles (deg)	system	space group	Z	Ref.
Fe mal. 2H ₂ O	8.229	9.452	7.285	α=β=γ=90	orthorhombic	P2 ₁ 2 ₁ 2 ₁	4	22
Mn mal. 2H ₂ O	9.62	7.36	8.33	α=β=γ=90	orthorhombic	Pca2 ₁	4	21
Mn mal. 2H ₂ O	8.334	9.611	7.367	α=β=γ=90	orthorhombic	Pmab	4	17
K[Mn(mal) ₂ (H ₂ O) ₂].2H ₂ O	6.842	13.491	14.115	α=β=γ=90	orthorhombic	Pbcn	4	2
K[Mn(mal) ₂ (CH ₃ OH)]	8.55	8.56	8.95	α=113.60, β=94.78, γ=99.97	triclinic	P $\bar{1}$	2	36
K ₃ [Mn(mal) ₃].2H ₂ O	14.799	7.850	16.210	β=108.51	monoclinic	C2/c	4	3
[Cr(mal) ₃] ³⁻	16.12	16.12	10.07	α=β=90, γ=120.0	trigonal, with hexagonal lattice parameters	R ₃₂	3	5
[Cr(mal) ₂ OH] ⁴⁻	8.937	10.279	8.310	α=75.20, β=76.01, γ=76.01	triclinic	P $\bar{1}$	1	8
[{Cr(en)(mal)(OH)} ₂].6H ₂ O	6.19	9.61	19.47	β=90.57	monoclinic	P2 ₁ /c	2	38
(+)[Co mal ₂ en] ⁻	10.58	7.98	7.99	α=122.8, β=105.3, γ=76.2	triclinic	P1	1	33
(+)[Co(CN) ₂ (mal)(NH ₃) ₂] ⁻	16.709	18.139	7.569	α=β=γ=90	orthorhombic	P2 ₁ 2 ₁ 2 ₁	4	6
Na(+)[Co(mal) ₂ (en)].2H ₂ O	13.46	14.24	7.344	α=β=γ=90	orthorhombic	P2 ₁ 2 ₁ 2 ₁	4	32
K ₃ [Co(mal) ₃].4H ₂ O	21.32	12.07	14.05	α=β=γ=90	orthorhombic	Pna2 ₁	8	5
K ₃ [Co(mal) ₃].4H ₂ O	21.3166	12.0672	14.0501	α=β=γ=90	orthorhombic	Pna2 ₁	8	This work
K[Co en ₂ (etmal) ₂]	19.16	16.67	14.34	β=104.30	monoclinic	P2 ₁ /c	8	This work
K ₃ [Al(mal) ₃].6H ₂ O	8.2633	13.0176	14.2399	β=67.99	monoclinic	P2 ₁ /c	4	This work

REFERENCES

1. B. Briggman, A. Oskarsson, *Acta Cryst.*, 1977, B33, 1900.
2. T. Lis, J. Matuszewski, B. Jezowska-Trez, *Acta. Cryst.*, 1977, B33, 1943.
3. A. Karipides and A.T. Reed, *J. Inorg. Chem.*, 1977, 16, 3299.
4. E. Hansson, *Acta. Chem. Scand.*, 1973, 27, 2813.
5. K.R. Butler and M.R. Snow, *J. Chem. Soc. Dalton.*, 1976, 251.
6. K. Torium, S. Sato and Y. Saito, *Acta. Cryst.*, 1977, B33, 1378.
7. M.L. Post and J. Trotter, *J. Chem. Soc. Dalton.*, 1974, 1922.
8. R.P. Scaringe, W.E. Hatfield, and D.J. Hodgson, *J. Inorg. Chem.*, 1977, 16, 1600.
9. E. Hansson, *Acta. Chem. Scand.*, 1973, 27, 2441.
10. E. Hansson, *Acta. Chem. Scand.*, 1973, 27, 2827.
11. E. Hansson, *Acta. Chem. Scand.*, 1973, 27, 2841.
12. J. Albertson, A. Oskarsson and C. Svensson, *Acta. Cryst.*, 1978, B34, 2737.
13. R.E. Marsh, V. Schomaker, *J. Inorg. Chem.*, 1979, 18, 2331.
14. A. Oskarsson, *Acta. Cryst.*, 1978, B34, 1350.
15. G. Duc, R. Faure and H. Loiseleur, *Acta. Cryst.*, 1978, B34, 2115.
16. B. Briggman and A. Oskarsson, *Acta. Cryst.*, 1978, B34, 3357.
17. L. Walter-Levy, J. Perrotey, and J.W. Visser, *Bull. Soc. Chim., Fr.*, 1973, 2596.
18. R. Lafont, G. Perinet and L.V. My, *Compt. Rendus.*, 1968, 267, 474.
19. L. van My, G. Perinet, F. Boubli and R. Lafont, *Compt. Rendus.*, 1970, 271, 69.
20. M.P. Gupta and P. Chand, *Curr. Sci.*, 1977, 46, 557.
21. T. Lis and J. Matuszewski, *Acta. Cryst.*, 1979, B35, 2212.
22. A. Kwiatkowski, J. Przedmojski and B. Pura, *Mat. Res. Bull.*, 1969, 4, 765.

23. A. Karipides and A.T. Reed, *J. Inorg. Chem.*, 1976, 15, 44.
24. A.T. Reed and A. Karipides, *Acta cryst.*, 1976, B32, 2085.
25. R. Rajan, *J. Chem. Phys.*, 1962, 37, 460.
26. F. Charbonnier and Y. Arnaud, *Compt. Rendus.*, 1972, 203, 275.
27. G.I. Dimitrova, A.V. Ablov, G.A. Kiosse, G.A. Popvich, T.I. Malinovski and I.E. Burshtein, *Duki, Akad. Nauk, SSSR.*, 1974, 216, 1055.
28. J.A. Goedkoop and C.H. MacGillarry, *Acta. cryst.*, 1957, 10, 125.
29. J. Lohn, *Acta. cryst.*, 1969, A25, 121.
30. I.E. Knaggs, *J. Chem. Soc. Trans.*, 1922, 121, 2069.
31. C.H. Johnson, *Trans. Faraday Soc.*, 1932, 28, 845.
32. K. Butler and M.R. Snow, *J. Chem. Soc. Dalton.*, 1976, 259.
33. K. Matsumoto and H. Kuroya, *Bull. Chem. Soc. Japan*; 1972, 45, 1755.
34. J.A. Kanters, G. Roelofsen, J. Kroon and J.A. Vliegthart, *Acta cryst.*, 1971, B27, 702.
35. U. Lepore, G.C. Lepore and P. Ganis, *Acta. cryst.*, 1975, B31, 2874.
36. T. Lis and J. Matuszewski, *J. Chem. Soc. Dalton.*, 1980, 6, 996.
37. J.G. Sime, J.C. Speakman, and R. Parthasarathy, *J. Chem. Soc.*, 1979, 1919.
38. J.W. Lethbridge, *J. Chem. Soc. Dalton.*, 1980, 10, 2039.

CHAPTER II PREPARATIVE METHODS

General Methods of Preparation of the Compounds*

Starting Materials

All chemicals were of reagent grade and were used without further purification.

Acids were obtained from BDH.

2.1 Metal-malonate Compounds

All simple malonate compounds except nickel malonate were prepared by the method by adding an equimolar quantity (plus a slight excess) of the solid metal carbonate to an equimolar quantity of an aqueous solution of malonic acid with continuous stirring and gentle heating at about 35°C for a few hours. The excess of carbonate was filtered off and washed with water; the filtrate was evaporated using a rotary evaporator. When sufficient salt had separated the mother liquor was decanted, and the crystals of salts were filtered off, washed and dried in air. These compounds all contain water of crystallisation. Nickel malonate dihydrate was prepared by the method of Ives and Riley.¹ After crystallisation in hot water, the salt was dried in air, very finely powdered, washed with absolute alcohol and water, and air dried. In the case of the barium and calcium malonates, the analysis results indicated that these compounds are basic salts. Recrystallisation was not effective in producing a pure non-basic compound. In the case of magnesium malonate, a more concentrated solution, lower temperature conditions and a longer reaction period were used. Under these conditions a pure compound resulted. However, the precipitate was allowed to stand in contact with the mother liquor at room temperature overnight before filtration, which might have been effective for purification of the compound as pointed out elsewhere² for analogous Ca(II) oxalate compounds. The analyses of carbon and hydrogen were

* The references for this section are on page 52.

Table 2.1. Analysis of malonato metal compounds

Empirical formula		%C	H	M ²⁺
Cu(II)(malonate).2½H ₂ O	F	17.0	3.30	29.94
	T	17.1	3.34	30.16
Na ₂ [Cu(mal) ₂ (H ₂ O) ₂]	F	20.7	2.3	18.30
	T	20.6	2.3	18.17
Zn(II)(malonate).2H ₂ O	F	17.5	2.90	32.2
	T	17.7	2.90	32.1
Co(II)(malonate).2H ₂ O	F	18.8	3.00	29.6
	T	18.3	3.07	29.9
Ni(II)(malonate).2H ₂ O	F	18.2	3.0	30.33
	T	18.3	3.1	29.83
Cd(II)(malonate).H ₂ O	F	15.2	1.6	48.15
	T	15.4	1.7	48.35
Ca(II)(malonate)Ca(OH) ₂ .1½H ₂ O	F	14.80	2.4	
	T	14.81	2.9	
Mg(II)(malonate).5H ₂ O	F	16.6	5.4	
	T	16.6	5.5	
2Ba(II)(malonate)Ba(OH) ₂ .2H ₂ O	F	10.2	1.4	
	T	10.5	1.4	

carried out by Miss M.E. Easton at Bedford College. Metals were determined by atomic absorption spectrophotometry³. These are listed in Table 2.1.

Preparation of sodium bis(malonato) diaquocuprate(II)

$\text{Na}_2[\text{Cu}(\text{mal})_2(\text{H}_2\text{O})_2]$ was prepared by the method of Riley.⁴ A pale blue powder was obtained.

Coordination Compounds of Trivalent Metals with Bidentate Ligand

Malonate

Preparation of compounds

Potassium tris (malonato) aluminate(III) 6-hydrate

$\text{K}_3[\text{Al}(\text{C}_3\text{H}_2\text{O}_4)_3] \cdot 6\text{H}_2\text{O}$ was prepared as described by Bailar and Jones⁵ for the corresponding tris (oxalato) complex. Recrystallisation was from the minimum of hot water. White crystals were obtained upon standing at room temperature and contained six molecules of water.

67g (0.1 mole) of aluminium sulphate $\text{Al}_2(\text{SO}_4)_3 \cdot 18\text{H}_2\text{O}$ was treated with a solution of 24 g (0.6 mole) of sodium hydroxide. The precipitated aluminium hydroxide was separated washed and boiled with a solution of 0.6 mole of potassium hydrogen malonate or a mixture of 0.3 mole of potassium malonate and 31.2 g (0.3 mole) of malonic acid in about 800 ml of water. Potassium malonate was prepared by neutralisation of the appropriate quantity of malonic acid 31.2 g (0.3 mole) and potassium carbonate 41.4 g (0.3 mole). The aluminium hydroxide which did not dissolve was filtered out and the filtrate was evaporated to crystallisation.

Sodium tris (malonato) ferrate(III) tetrahydrate

$\text{Na}_3[\text{Fe}(\text{C}_3\text{H}_2\text{O}_4)_3] \cdot 4\text{H}_2\text{O}$ was prepared by the method of Scholz.⁶ Recrystallisation was from water and alcohol. The pale green crystals tend to be light sensitive and on account of their photochemical decomposition, the compound was kept in a desiccator in the dark.

Potassium tris (malonato) cobaltate(III) tetrahydrate

The Method of Al-Obadie and Sharpe

Thomas⁷ reported the preparation of this compound by the lead dioxide oxidation of cobalt(II) malonate. More recently Al-Obadie and Sharpe⁸ attempted to make it by the use of the literature method for the corresponding oxalate complex.⁵ The method was unsuccessful, it failed at that step in which addition of alcohol to an aqueous solution should have precipitated the green crystals of the malonate complex of Co(III). However, the product was pink in colour due to the decomposition of Co(III) to Co(II) malonate.

However, the method of Lohmiller⁹ was tried under conditions where the pH of the solution was carefully controlled, since the compound is unstable in aqueous solution at low pH. There was a modification of the crystallisation step where adding alcohol to the green oil should precipitate the malonate complex of Co(III). Absolute ethanol was added to the dark green oil that was formed while scratching the inner surface of the vessel with glass stirring rod, and the supernatant liquid was then decanted and the process repeated until crystallisation of the oil began. The crystals were filtered off and washed with absolute methanol and stored in a vacuum desiccator in the dark. The compound tends to absorb water and decompose on exposure to air. It is thermally unstable and light sensitive in aqueous solutions, particularly at low pH. The solid form stored in a vacuum desiccator appears stable. The crystals did not appear homogeneous under the microscope. They were contaminated with some pink crystals which probably indicates decomposition. The low result for the carbon content indicates that the $K_3[Co(mal)_3] \cdot 4H_2O$ product might be contaminated with bis malonato species, i.e. $[Co(mal)_2(H_2O)_2]^-$ and Co(II) malonate, analogous to the solid-state decomposition¹⁰ of $K_3[Co(ox)_3] \cdot 3H_2O$.

Table 2.2 Analysis of malonate trivalent metal complexes

Empirical formula		%C	H	K	M ³⁺
K ₃ [Al(mal) ₃].6H ₂ O	F	19.2	3.1	20.84	
	T	19.3	3.2	21.00	
K ₃ [Co(mal) ₃].4H ₂ O	F	16.98	2.52	21.59	
	T	19.49	2.54	21.80	
K[Mn(mal) ₂ (H ₂ O) ₂]	F	21.70	2.40	12.50	18.30
	T	21.57	2.41	11.70	16.44
K[Cr(mal) ₂ (H ₂ O) ₂].3H ₂ O	F	18.70	3.50	10.15	13.80
	T	18.70	3.60	10.15	13.50
				Na	
Na ₃ [Fe(mal) ₃].4H ₂ O	F	21.72	2.68	13.62	11.06
	T	21.50	2.80	13.71	11.10

$[\text{Co}(\text{en})_2\text{mal}]\text{Br}$ and $\text{K}[\text{Co}(\text{en})\text{mal}_2]\text{H}_2\text{O}$ were prepared by the method described elsewhere.^{10,11}

Preparation of cis-bis (malonato)diaquo chromate(III) trihydrate

$\text{K}[\text{Cr}(\text{C}_3\text{H}_2\text{O}_4)_2(\text{H}_2\text{O})_2]$ was prepared by the method of Chang.¹³

The product was recrystallised from hot water and 95 per cent ethanol. The purple crystals were filtered, washed with 95 per cent ethanol and absolute ether, and air dried.

Malonato Manganates

Preparation of anhydrous potassium bis(malonato)diaquo manganate(III)

$\text{K}[\text{Mn}(\text{C}_3\text{H}_2\text{O}_4)_2(\text{H}_2\text{O})_2]$ was prepared by the method of Cartledge.¹⁴

The fine olive green crystals were left in the desiccator in the dark. All manganese(III) complexes decompose rapidly in the atmosphere not free from moisture and the organic solvents. They are unstable with respect to thermal or photochemical decomposition.

Analysis of M(III) malonates is given in Table 2.2.

2.2 Metal-ethylmalonate Compounds

These compounds were prepared by the similar method to that of the malonate compounds as described before.

Recrystallisation was also impossible due to the low solubility of these compounds. In the case of the nickel compound, as analysis indicates, it is contaminated with nickel hydroxide or is the basic salt. Attempted recrystallisations from water were unsuccessful. However, the purification of the nickel ethylmalonate was carried out by the grinding and washing method.¹ This treatment was found to be quite effective particularly in purifying of the nickel compound. The rest of the compounds were pure and recrystallisation was not needed. They all contain water of crystallisation except calcium ethylmalonate where the anhydrous salt was obtained.

There was difficulty in filtration of these compounds and

Table 2.3 Analysis of ethylmalonate metal compounds

Empirical formula		% C	H	M ²⁺
Cu(II)(etmal).2H ₂ O	F	26.10	4.59	27.45
	T	26.14	4.40	27.66
Zn(II)(etmal).2H ₂ O	F	25.63	4.50	27.98
	T	25.94	4.35	28.24
Co(II)(etmal).2H ₂ O	F	26.78	4.70	25.99
	T	26.68	4.48	26.18
2Ni(II)(etmal).Ni(OH) ₂ .3H ₂ O	F	23.15	3.98	34.20
	T	22.90	3.84	33.58
Cd(II)(etmal).H ₂ O	F	23.07	3.03	43.09
	T	23.05	3.09	43.15
Ca(II)(etmal)	F	34.86	3.52	
	T	35.28	3.55	
Mg(II)(etmal).3H ₂ O	F	28.10	5.31	
	T	28.80	5.80	
Ba(II)(etmal).½H ₂ O	F	22.05	2.58	
	T	21.72	2.55	

Whatman paper Grade 5V was used in all cases. Analysis is given in Table 2.3.

Coordination compounds of trivalent metals with ethylmalonate

Potassium tris(ethylmalonato)cobaltate(III) tetrahydrate

The preparation of the tris(ethylmalonato)cobaltate(III) by the method analogous to that used for the malonato complex was unsuccessful,^{9,15} although the pH of the solution was carefully controlled. Repeated attempts failed at the step in which addition of alcohol to an aqueous solution should have precipitated the ethylmalonate complex of Co(III). However deep pinkish colour crystals were always as the final products. Analysis results indicated that it was an impure Co(II) ethylmalonate.

Procedure 1

The method of Lohmiller and Wendlandt⁹ for the corresponding malonate complex was followed. Cobalt carbonate 5 g (0.042 mole) was slowly added in small portions to a boiling mixture of 6.34 g (0.048 mole) of ethylmalonic acid and potassium ethylmalonate (0.028 mole). Potassium ethylmalonate was prepared by the neutralisation of 3.7 g (0.028 mole) of ethylmalonic acid with 3.87 g (0.028 mole) of solid potassium carbonate. The violet coloured solution was cooled to room temperature and 12.7 g (0.096 mole) of ethylmalonic acid was added. Small amounts of solid potassium carbonate were then added until a pH of 6 was obtained followed by addition of 15 ml of 30% H₂O₂. The pH was then adjusted to pH 7 by addition of more potassium carbonate (vigorous oxidation reaction began). After the reaction subsided the green coloured solution was heated to 35°C and stirred for 1 hour in the dark. The solution was filtered and cooled to about 0°C and placed in a separating funnel. The addition of 150 ml of cold 95% ethanol gave a grey product to which more alcohol was added. The process was repeated several times, decanting the liquid before each

addition, but the pink crystals of the cobalt(II) salt were always as the final product.

Procedure 2

The literature method for the corresponding malonate complex¹⁵ was followed; it is also analogous to the preparation of the oxalate complex⁵ with the exception of the crystallisation step.

10 g (0.0402 mole) of cobalt acetate was added to a solution of 12.5 g (0.223 mole) of potassium hydroxide and 19.8 g (0.15 mole) of ethylmalonic acid in 20 ml of water with stirring. To the resulting Co(II) ethylmalonate 4.8 g (0.020 mole) of lead dioxide was added slowly followed by 5 ml of glacial acetic acid added a drop at a time. The solution was stirred in the dark for 1 hour during which time the colour changed from violet to dark green. The resulting solution was filtered directly into a flask containing 2-propanol (150 ml) and the violet coloured liquid was decanted from the green oil that was formed. The extraction was repeated several times. To the resulting extract 95% ethanol (10 ml) was added while scratching the inner surface of the vessel with a glass stirring rod. The supernatant liquid was decanted each time and the process repeated three times. Here again the pink Co(II) ethylmalonate crystals were always the final product. Analysis results indicated again that it was an impure Co(II) ethylmalonate.

[Co en₂ etmal]Br.H₂O was prepared as follows: 10 g of [Co en₂CO₃]Cl prepared by Dwyer's method,¹⁶ was treated with Ag₂O freshly precipitated from 11 g silver nitrate. The silver chloride (and the excess of silver oxide) was filtered off and ethylmalonic acid (5 g) was added. The mixture was shaken until the evolution of CO₂ had ceased. The volume of the solution was reduced to 40 cm³ on a rotary evaporator and KBr (8 g) was added to the hot solution. The crystals were filtered off from the ice-cold solution, washed with ice-cold

methanol, cold ether and dried in vacuum. The crude product was recrystallised from warm water and dried as before.

Ethylmalonate manganates

Preparation of anhydrous potassium bis (ethylmalonato) diaquo manganate(III)

$K[Mn(etmal)_2(H_2O)_2]$ was prepared by the method of Cartledge¹⁴ for the corresponding malonate complex.

Method

1.58 g (0.01 mole) of $KMnO_4$ and 3.30 g (0.025 mole) of ethylmalonic acid were shaken with about 150 ml of absolute methyl alcohol for about $\frac{1}{2}$ hour. It was necessary to allow the reaction mixture to stand for one week at $5^\circ C$ to complete the reaction. The cream product was filtered off and washed with cold methyl alcohol. It was stored in a desiccator in the dark. Recrystallisation of the product from methyl alcohol was not successful.

Potassium tris (ethylmalonato) aluminate(III) trihydrate

$K_3[Al(etmal)_3] \cdot 3H_2O$ was prepared by the similar method for the corresponding oxalate and malonate complex. The light yellowish liquid was concentrated and crystallised upon standing for 1 hour to creamy coloured crystals. These were collected and dried in a vacuum desiccator.

Method

A solution of 16.75 g (0.025 mole) of aluminium sulphate, $Al_2(SO_4)_3 \cdot 18H_2O$ was treated with a solution of 6 g (0.15 mole) of sodium hydroxide. The precipitated aluminium hydroxide was filtered off, washed and boiled with a solution of 0.15 mole of potassium hydrogen ethylmalonate, or a mixture of 0.15 mole of potassium ethylmalonate and 9.91 g (0.15 mole) of ethylmalonic acid in about 250 ml of water. Potassium ethylmalonate was prepared by neutralisation of the appropriate

Table 2.4 Analysis of ethylmalonate trivalent metal complexes

Empirical formula		%C	H	K	M ³⁺
K ₃ [Al(etmal) ₃].6H ₂ O	F	30.64	4.25	19.30	
	T	30.60	4.11	19.93	
K[Mn(etmal) ₂ (H ₂ O) ₂]	F	29.9	3.5	8.29	19.8
	T	30.7	4.1	10.02	14.07
Na					
Na ₃ [Fe(etmal) ₃].2H ₂ O	F	32.78	4.00	12.50	9.86
	T	32.69	4.02	12.51	10.13
N					
[Coen ₂ etmal]Br.H ₂ O	F	26.6	5.7	14.0	14.4
	T	26.6	5.9	13.8	14.4

quantity of 9.90 g (0.15 mole) of ethylmalonic acid and 10.37 g (0.15 mole) of potassium carbonate. The excess of aluminium hydroxide was filtered off and the light yellowish liquid was concentrated using a rotary evaporator. On standing for 1 hour creamy crystals were deposited.

Sodium tris (ethylmalonato) ferrate(III) dihydrate

$\text{Na}_3[\text{Fe}(\text{etmal})_3] \cdot 2\text{H}_2\text{O}$ was prepared by the method of Scholz for the corresponding malonate complex.⁶ The compound is light green, photosensitive and it tends to absorb water and decompose on exposure to air. It is thermally unstable. The compound was stored in a desiccator in the dark.

Method

A solution of 16.22 g (0.1 mole) of FeCl_3 in water was treated with about 380 ml of conc. ammonia. The precipitated ferric hydroxide was filtered out, and washed with water until the washings produced no precipitate with silver nitrate. The resulting $\text{Fe}(\text{OH})_3$ was added to a concentrated solution of 19.81 g (0.15 mole) of ethylmalonic acid and 0.15 mole of sodium ethylmalonate or a mixture of 19.81 g (0.15 mole) of ethylmalonic acid and 15.9 g (0.15 mole) of Na_2CO_3 in about 600 ml of water. The mixture was then digested for one day during which time the $\text{Fe}(\text{OH})_3$ slowly dissolved (by adding water and evaporating it again and again.) After filtering with suction (excess of $\text{Fe}(\text{OH})_3$) and washing, the resulting green liquid filtrate was evaporated to about 100 ml and allowed to cool. Small amounts of acetone were added to the light green gummy product to bring about the deposition of the complex as a pale green powder.

2.3 Metal-benzylmalonate Compounds

Attempts to obtain analogous salts containing anions of higher dicarboxylic acids as ligands have been successful. We have

examined the possibility of making benzylmalonate compounds by the method analogous to that used for malonate and ethylmalonate complexes.

Again there was great difficulty in the filtration of these compounds and a considerable foaming occurs during the process. This was particularly so with Co(II) benzylmalonate where experience showed that the reaction should be carried out at room temperature, and a longer period allowed for reaction, as the product which was formed at even low temperature was always contaminated with the brown Co(II) oxide. The reaction was carried out while stirring for 10 days and finally the stirred slurry mixture was filtered off many times (Whatman paper No. 5) until the excess of carbonate was completely removed and a clear solution was obtained. It was concentrated on the freeze drier. The pale pinkish precipitate which had coagulated was separated from the only slightly pink supernatant liquid by filtration. It was washed and dried.

In the case of nickel benzylmalonate a similar situation was observed, and finally the light greenish precipitate which was in contact with the mother liquor for a few days at room temperature was easily separated by filtration; it was obtained as a light green powder. It was washed and air dried; it contained two molecules of water of crystallisation.

Copper benzylmalonate crystallises as deep sky blue and contains half a molecule of water of crystallisation.

Zinc benzylmalonate crystallises as a bright white compound which contains two and a half molecules of water of crystallisation.

Magnesium, calcium and barium salts were basic.

Analyses were carried out and the results are summarised in Table 2.5. Again, recrystallisation of these compounds was impossible due to the very low solubility of the compounds. The compounds do not wet easily, forming a dry surface scum when water is added and on

Table 2.5 Analysis of benzylmalonate metal compounds

Empirical formula		%C	H	M ²⁺
Cu(II) (benzylmal) . $\frac{1}{2}$ H ₂ O	F	44.92	3.19	23.95
	T	45.37	3.42	24.00
Zn(II) (benzylmal) . $2\frac{1}{2}$ H ₂ O	F	39.72	4.22	20.95
	T	39.69	4.33	21.00
Co(II) (benzylmal) . 2H ₂ O	F	42.1	3.5	20.39
	T	41.8	4.2	20.52
Ni(II) (benzylmal) . 2H ₂ O	F	41.4	4.5	20.28
	T	41.8	4.2	20.46
Cd(II) (benzylmal) . H ₂ O	F	37.0	3.1	34.42
	T	37.2	3.1	34.80
Ca(II) (benzylmal) . Ca(OH) ₂	F	38.7	3.0	
	T	39.2	3.3	
Mg(II) (benzylmal) . Mg(OH) ₂ . 2H ₂ O	F	48.8	4.3	
	T	48.4	4.1	
Ba(II) (benzylmal) . Ba(OH) ₂ . $\frac{1}{2}$ H ₂ O	F	32.1	2.7	
	T	32.1	2.4	

shaking solutions of the benzylmalonate salts emulsions are formed and considerable foaming occurs during the process.

Coordination compounds of trivalent metals with benzylmalonate

Potassium tris (benzylmalonato) aluminate(III) trihydrate $K_3[Al(\text{benzyl mal})_3] \cdot 3H_2O$ was prepared by the similar method for the corresponding oxalate with the exception of crystallisation.⁵

Method

33.5 g (0.05 mole) of aluminium sulphate $Al_2(SO_4)_3 \cdot 18H_2O$ was treated with a solution of 12 g (0.3 mole) of sodium hydroxide. The precipitated aluminium hydroxide was filtered off, washed and boiled with a solution of 0.3 mole of potassium hydrogen benzylmalonate or a mixture of 29.13 g (0.15 mole) of benzylmalonic acid and 0.15 mole of potassium benzylmalonate.

(Potassium benzylmalonate was prepared by neutralisation of 29.13 g (0.15 mole) of benzylmalonic acid with 20.73 g (0.15 mole) of solid potassium carbonate in about 400 cc of water.) After additional stirring (magnetic stirrer) for a few minutes the resulting solution was filtered. Excess of aluminium hydroxide was filtered off (Whatman paper No. 54). After cooling at 5°C overnight a very sticky liquid was obtained. There was difficulty in obtaining the compound as crystals from the light yellowish gummy liquid. The addition of a number of solvents was also unsuccessful, and resulted the deposition of the complex. Finally the gummy liquid was concentrated to dryness. The product was a white shiny solid which was ground and stored in the desiccator. Recrystallisation of the compound was impossible although the complex is highly soluble in water but the gummy nature of the complex was the cause of unsuccessful crystallisation. Even the method of grinding and washing with acetone and ethanol was not effective in the production of a powder or crystals. However, the analysis results were satisfactory.

Sodium tris (benzylmalonato) ferrate(III) dihydrate

$\text{Na}_3[\text{Fe}(\text{benzylmal})_3] \cdot 2\text{H}_2\text{O}$ was prepared by the reaction of freshly made ferric hydroxide with a solution of sodium hydrogen benzylmalonate as described by Scholz⁶ for the corresponding malonate complex.

Method

A solution of 8.11 g (0.05 mole) of FeCl_3 in water was treated with ammonia, the colloidal precipitated ferric hydroxide was filtered out, and washed with water until the washings produced no precipitate with AgNO_3 (0.1 M). The precipitated $\text{Fe}(\text{OH})_3$ was added to a concentrated solution of 14.56 g (0.075 mole) of benzylmalonic acid and 0.075 mole of sodium benzylmalonate or a mixture of 14.56 g (0.075 mole) of benzylmalonic acid and 7.95 g (0.075 mole) of anhydrous sodium carbonate in about 100 cc of water. After additional stirring (magnetic stirrer) for a few minutes the mixture was then digested on the steam bath for a week. The $\text{Fe}(\text{OH})_3$ slowly dissolved (by adding water and evaporating again and again.) There was again difficulty in filtration of this complex due to the gummy liquid which was formed. However, the excess of ferric hydroxide was removed using Whatman paper No. 5 and the dark green liquid was concentrated. Here again there was a great deal of difficulty in the crystallisation of the gummy semi-solid. However, the deep green gummy liquid was concentrated on the rotary evaporator to nearly dryness and then left in the desiccator. The shiny product was ground in a mortar and pestle and stored in a vacuum desiccator in the dark. Recrystallisation was also impossible. The product was very pure and therefore purification was not needed. The compound is light, heat and moisture sensitive. The complex was stored in a vacuum desiccator in the dark and appears quite stable.

Benzylmalonate manganatesPreparation of anhydrous potassium bis (benzylmalonato) diaquo manganate(III)

$K[Mn(Benzylmal)_2(H_2O)_2]$ was prepared by the reaction of stoichiometric quantities of potassium permanganate and benzylmalonic acid in absolute methyl alcohol as described by Cartledge¹⁴ for the corresponding malonato complexes.

One hundredth of a mole (1.58 g) of potassium permanganate and 0.025 mole (4.85 g) of benzylmalonic acid were shaken with about 150 ml of absolute methyl alcohol and the reddish brown liquid which was obtained allowed to stand for one week at 5°C. It was then filtered off and the light brownish product was washed with absolute methyl alcohol and dried and stored in a vacuum desiccator in the dark.

Potassium tris (benzylmalonato) cobaltate(III) tetrahydrate

Repeated attempts to prepare $K_3[Co(benzylmal)_3].4H_2O$ by the method used for the corresponding malonate^{8,9} compounds again was unsuccessful. Although the pH of the solution was carefully controlled the attempts always failed at the step in which addition of alcohol to the aqueous solution should have separated the dark green oil from the aqueous solution. The complex tends to be very unstable. Finally the attempt was carried out in a very carefully controlled condition where all the apparatus was already cooled in the dry ice and acetone-bath. A similar method to that described by Lohmiller and Wendlant⁹ for the corresponding malonate complex was followed. 1.25 g (0.0105 mole) of $CoCO_3$ was added to a boiling mixture of 2.33 g (0.012 mole) of benzylmalonic acid and 0.007 mole of potassium benzylmalonate. This was prepared by the neutralisation of 1.35 g (0.007 mole) of benzylmalonic acid with 0.99 g (0.007 mole) of potassium carbonate in 21 ml of water. When the solution was cooled to room temperature 4.66 g (0.024 mole) of benzylmalonic acid was added. Small amounts of solid K_2CO_3 were then

added until a pH of 6 was obtained followed by 3.75 ml of 30% H_2O_2 added slowly. The pH was then readjusted to pH 7 by addition of more K_2CO_3 (a vigorous oxidation reaction began). After the reaction had subsided, the colour changed to deep green. The solution was then heated to 35°C and stirred in the dark for 1 hour. The solution was filtered and cooled to 0°C and placed in a separating funnel. The extraction of water and potassium benzylmalonate from the mixture was unsuccessful. The extraction was repeated several times and various proportions of solvents were examined and finally a mixture of acetone and chloroform was found to be successful in removal of the water and potassium benzylmalonate from the dark green oil that was formed. The extraction was repeated until a large amount of green solid and white mixture formed; this was filtered off immediately and the green oil was separated from the white potassium benzylmalonate. The process was repeated again with the acetone and chloroform each time while scratching the inner surface of the vessel with a glass stirring rod and supernatant liquid was decanted each time. However, the green oil that was separated decomposed rapidly to pink crystals at the final step where the attempt was made in the conversion of the oil into the crystals. From observation it could be seen that the complex does exist but at very low temperature (-60°C) and it is very unstable, highly sensitive to the light and to the atmosphere if this is not free from organic vapours. However, it decomposed before it could be isolated for analysis. The results of analysis indicated that the pink crystals of the cobalt(II) salt were the final product, analogous to that found for the Co(III) ethylmalonate complex.

Table 2.6 Analysis of benzylmalonato trivalent metal complexes

Empirical formula		%C	H	K	M ³⁺
K ₃ [Al(benzylmal) ₃].3H ₂ O	F	46.06	3.75	15.0	
	T	46.50	3.90	15.1	
K[Mn(benzylmal) ₂ (H ₂ O) ₂]	F	46.00	3.70	6.27	13.8
	T	46.69	3.92	7.60	10.68
				Na	
Na ₃ [Fe(benzylmal) ₃].2H ₂ O	F	48.77	3.75	9.23	7.4
	T	48.86	3.82	9.35	7.6

REFERENCES

1. D.J.G. Ives and H.L. Riley, J. Chem. Soc., 1931, 2004.
2. I.M. Kolthoff and E.B. Sandel, J. Phys. Chem., 1933, 468.
3. Elwell and Gidley, "Atomic absorption spectrophotometry", Pergamon Press, 1967.
4. H.L. Riley, J. Chem. Soc., 1929, 1307.
5. J.C. Bailar and E.M. Jones, Inorg. Syn., 1939, 1, 36.
6. A. Scholz, Montash. Chem., 1908, 29, 439.
7. W. Thomas, J. Chem. Soc., 1921, 119, 1140.
8. M.S. Al-Obadie and A.G. Sharpe, J. Inorg. Nucl. Chem., 1969, 31, 2963.
9. G. Lohmiller, W.W. Wendlandt, J. Inorg. Nucl. Chem., 1970, 32, 2430.
10. S.T. Spees and P.Z. Petrak, J. Inorg. Nucl. Chem., 1970, 32, 1229.
11. M.E. Farago and M.A.R. Smith, Inorg. Chim. Acta., 1975, 14, 21.
12. M.E. Farago and I.M. Keefe, Inorg. Chim. Acta., 1975, 15, 5.
13. J.C. Chang, Inorg. Syn., 16, 80.
14. G.H. Cartledge and P.M. Nichols, J. Amer. Chem. Soc., 1940, 62, 3057.
15. N. Kenten and S. Spees, J. Inorg. Nucl. Chem., 1971, 33, 2437.
16. F.P. Dwyer, A.M. Sargeson and I.K. Reid, J. Amer. Chem. Soc., 1963, 85, 1215.

CHAPTER III: VISIBLE AND ULTRAVIOLET SPECTROSCOPY^{1-3*}3.1 Introduction

Visible and u.v. spectroscopy are powerful tools in the investigation of structural aspects of chelates. The application of visible spectroscopy is limited to chelates of the transition metal ions, the lanthanides and the actinides. Ultraviolet spectroscopy is more generally applicable and can be useful in structural determination of all chelates since they all absorb this region.

In a typical transition metal chelate the observed spectrum in general, consists of a series of crystal field bands which are in the visible region and depend largely on the donor atom of the ligand and on the metal ion.

The crystal field transitions are of two types: the more intense spin-allowed transitions and the lower intensity spin-forbidden transitions, which usually appear as Shoulders on the spin-allowed transitions. The ultra-violet spectrum is complicated and consists of electronic transitions between the ligand and the metal (charge transfer) and also transitions within the ligand itself which are $\pi \rightarrow \pi^*$ or $\sigma \rightarrow \sigma^*$ transitions. The spectra of non-transition metal ion chelates usually result only from charge transfers and the ligand transitions.

The ligand transitions in all cases are characteristic of the coordinated ligand and not of the free ligand. However, the spectrum of the free ligand aids in classifying the transitions of the coordinated ligand. Interpretation of the results of spectral determinations would require a complete molecular orbital treatment, such treatments are rare and the methods used for such computations are only approximate in nature. The present situation is that the spectral results are used to test the theories, and the correlation of the spectrum with the theory

* the references for this section are on pages 66, 67 and 68.

gives a greater understanding of the bonding and interactions in chelates.

The visible spectra of transition metal ion chelates, however, can be understood and described quantitatively by crystal field theory or its extension, ligand field theory. An aid in making band assignments comes from the fact that spin or multiplicity-allowed transitions are broad while spin-forbidden transitions are usually sharp. Multiplicity-allowed $t_{2g} \rightarrow e_g$ transitions lead to an excited state in which the equilibrium internuclear distance between the metal ion and ligand is larger than in the ground state. In the course of the electronic transitions no change in distance can occur (Frank-Condon principle), so the electronically excited molecules are in vibrationally excited states with bond distances corresponding to the configuration of the ground state involved in the transition.

3.2 Experimental Methods

Visible and Ultraviolet Spectra in the Solid State

Since the complexes are insufficiently soluble in the common solvents, the spectra were recorded in powder form by the diffuse reflectance method.

The u.v. visible spectra of freshly ground samples were run on the Unicam SP700 recording spectra photometer using the SP735 solid state attachment with freshly prepared magnesium oxide in the reference beam.

3.3 Results and Discussion

Cr(III) d^3

In an environment of octahedral symmetry the ground state of Cr^{3+} ion is ${}^4A_{2g}$ and three spin-allowed transitions are expected: ${}^4A_{2g} \rightarrow {}^4T_{2g}$, ${}^4T_{1g}(F)$, ${}^4T_{1g}(P)$. The solution spectra of Cr(III) oxalato complexes have been reported by several workers.⁴⁻⁶ The results are

all very similar, having two absorption bands in the visible and near ultra violet at $\sim 17,400 \text{ cm}^{-1}$ and $24,000 \text{ cm}^{-1}$ characteristic of octahedral Cr(III) complexes. The crystal structure of tris(oxalato)chromium(III) complexes has been reported,⁷ which confirmed the earlier structure predicted by Mead.⁵ It has been found that six oxygen atoms of three oxalato groups surrounded the central chromium atom in an octahedral environment.⁷ The crystal structure of bis(oxalato)diaquo chromium(III) complex is known to be octahedral⁸. It has two bands in the visible region.⁹ The visible absorption spectra of tris(malonato), cis and trans-bis(malonato)diaquo complexes⁹⁻¹² are analogous to those of the Cr(III) oxalato complexes, each having two bands in the visible absorption spectra, and also show similarities to the crystal spectrum reported by Piper and Carlin¹³ and Hatfield.¹⁴ It was found by Hatfield that both Cr(III) malonato and Cr(III) oxalato complexes have similar octahedral structures. Recent X-ray structural analysis of some Cr(III) malonato complexes¹⁵⁻¹⁷ confirmed that the coordination is indeed octahedral.

In the solid state spectra of $\text{K}[\text{Cr}(\text{mal})_2(\text{H}_2\text{O})_2] \cdot 3\text{H}_2\text{O}$ two bands were observed at $18,200 \text{ cm}^{-1}$ and at $24,450 \text{ cm}^{-1}$ correspond to the transitions ${}^4\text{A}_{2g} \rightarrow {}^4\text{T}_{2g}(\text{F})$ and ${}^4\text{A}_{2g} \rightarrow {}^4\text{T}_{1g}(\text{F})$ respectively. The observed bands are similar to the absorption spectra of cis-bis(malonato)diaquo chromium(III) complex and those of the corresponding oxalate complex, which are consistent with a regular octahedral environment about the chromium atom.

Mn(III) d^4

The electronic and structural properties of high-spin manganese(III) complexes have been of unusual interest since the ground electronic state in octahedral complexes (${}^5\text{E}_g$) is subject to strong Jahn-Teller forces.

There are several reports concerning the spectra of six-coordinated high-spin Mn(III) complexes.^{13,18-24}

In all cases two prominent bands generally are observed, one near $20,000\text{ cm}^{-1}$ and the other in the range $5,000 - 15,000\text{ cm}^{-1}$ for complexes having six similar ligand atoms surrounding the manganese ion. Piper and Carlin^{13,21} and Barnum²² have interpreted their results in terms of an octahedral model and assigned the higher energy absorption as the spin-allowed, d-d transition ${}^5E_g \rightarrow {}^5T_{2g}$. The high energy absorption around $20,000\text{ cm}^{-1}$ (Band I) is easily identified, as it is the only quintet-quintet crystal field transition. The band observed at $22,200\text{ cm}^{-1}$ in bis(malonato)diaquo Mn(III), at $21,500\text{ cm}^{-1}$ in bis(ethylmalonato)Mn(III) and at $21,200\text{ cm}^{-1}$ in bis(benzylmalonato)Mn(III) complexes is undoubtedly the ${}^5E_g \rightarrow {}^5T_{2g}$ transition.

The lower energy absorption (Band II) $5,000 - 15,000\text{ cm}^{-1}$ in Mn(III) complexes has been suggested to be due to the following effects:

1. A spin forbidden transition from the ground state to ${}^3T_{1g}$ state (in O_h).
2. A spin-allowed transition between components of the 5E_g ground state subject to Jahn-Teller splitting.
3. The transition from ligand to metal "charge transfer".
4. The transition arises owing to a static or dynamic splitting of the E_g ground state.²⁰

In the study^{19,23} of tris malonato complexes a movement of Band I to higher energies in the bis(malonato)diaquo complexes together with reduction in intensity on going from tris(malonato) to bis(malonato) Mn(III) complexes has been considered characteristic of a tetragonal perturbation if water molecules occupy trans positions. However, from X-ray structure determination, Mn(III) malonato complexes are known to be tetragonally distorted.^{25,26} Our study of bis(malonato)diaquo, bis(ethylmalonato)diaquo and bis(benzylmalonato)diaquo complexes (Table 3.1) did not

show any intense absorption band in the near infrared as was found in the tris-bidentate malonate complexes by Dingle.¹⁹ It is because in bis-bidentate diaquo complexes one bidentate ligand is replaced by water molecules, as it was considered to be trans with D_{4h} symmetry. A corresponding band is replaced by a much less intense band at $15,100\text{ cm}^{-1}$ in bis(malonato)Mn(III), at $11,500\text{ cm}^{-1}$ in bis(ethylmalonato)Mn(III) and at $12,000\text{ cm}^{-1}$ in bis(benzylmalonato)Mn(III) complexes. Our results are in agreement with those of Dingle¹⁹ and Patel et al.,²³ though the nature of the low energy absorption is not certain. The spectra of six-coordinated Mn(III) complexes are not simple to interpret because of both static and dynamic Jahn-Teller effects.

Table 3.1 Solid state spectra of complexes of manganese(III)
(band positions in cm^{-1})

Complex	band I	band II
$\text{K}[\text{Mn}(\text{mal})_2(\text{H}_2\text{O})_2]$	22,200	15,100
$\text{K}[\text{Mn}(\text{etmal})_2(\text{H}_2\text{O})_2]$	21,500	11,500
$\text{K}[\text{Mn}(\text{benzylmal})_2(\text{H}_2\text{O})_2]$	21,200	12,000

Fe(III) d^5

Little is known of the details of Fe(III) spectra. This is because of the greater tendency of the trivalent ion to have charge transfer bands in the near ultraviolet region which have sufficiently strong low energy wings in the visible to obscure almost, completely in many cases, the very weak, spin-forbidden $d-d$ bands. However, the spectral features of iron(III) ions in octahedral surroundings are in accord with the theoretical expectations. The weakness of the bands and large numbers of the bands and variation in width of the bands

(with one being narrow) these are characteristic of a Fe(III) d^5 system explained in terms of ligand field theory²⁷. Although the solution spectra of an Fe(III) oxalate complex has been reported,^{4,28} the description of the absorption bands of Fe^{3+} in the visible and ultraviolet regions has not been made. The tris(oxalato)ferrate(III) complex is known to have an octahedral structure²⁹ and four bands have been observed in both solution²⁸ and the single-crystal spectra. The crystal spectrum of tris(malonato)ferrate(III) complex has been found¹⁴ to be similar to that of corresponding oxalate complex.¹³ The observed bands and assigned transitions reported by Hatfield¹⁴ are based on the known structure of the tris(oxalato)ferrate(III) complex. The results of solid state spectra of Fe(III) malonate, Fe(III) ethylmalonate and Fe(III) benzylmalonate complexes are very similar to those of single-crystal spectra, and on this basis, the observed bands in the reflectance spectra can therefore be assigned with a great deal of certainty by reference to the single crystal spectra.^{13,14} The solid state spectra of our Fe(III) complexes were poorly resolved. All the transitions are spin-forbidden and hence the intensities will be low. However in high-spin octahedral d^5 systems the transitions occur between the ${}^6A_{1g}$ ground state and the quartet excited states, which gives four absorption bands in the infrared and visible regions. The two observed bands at $10,400\text{ cm}^{-1}$ and $15,400\text{ cm}^{-1}$ in Fe(III) malonate, at $10,500\text{ cm}^{-1}$ and $15,400\text{ cm}^{-1}$ in Fe(III) ethylmalonate, at $11,600\text{ cm}^{-1}$ and $16,500\text{ cm}^{-1}$ in Fe(III) benzylmalonate complexes can be assigned to the transitions ${}^6A_{1g} \rightarrow {}^4T_{1g}(G)$ and ${}^6A_{1g} \rightarrow {}^4T_{2g}(G)$, respectively. Very similar absorption bands have been observed in some other iron(III) complexes.²² The sharp band of small intensity observed in the visible region at $22,600\text{ cm}^{-1}$ in Fe(III) malonate, at $22,500\text{ cm}^{-1}$ in Fe(III) ethylmalonate and at $22,700\text{ cm}^{-1}$ in Fe(III) benzylmalonate complexes accompanies transition to

the ${}^4A_{1g}(G)$, ${}^4E_g(G)$ levels. This band is much narrower than that for transition from ${}^6A_{1g}$ to the two first quartet levels ${}^4T_{1g}$, ${}^4T_{2g}$. The ${}^6A_{1g} \rightarrow {}^4A_{1g}(G)$, ${}^4E_g(G)$ transition occurs as a double band (with separation of $\sim 300 \text{ cm}^{-1}$) in Fe(III) malonate and Fe(III) ethylmalonate complexes. In the case of Fe(III) benzylmalonate complex the fourth band occurs as a slight shoulder on the sharp band towards the higher frequency side of the spectrum at $25,700 \text{ cm}^{-1}$. The weak shoulder has been observed in most octahedral Fe(III) complexes, and has been explained in terms of the splitting of the ${}^4A_{1g}$, 4E_g levels.^{13,14}

The results of our solid state spectra which are in close agreement with those of the crystal-spectrum, are strongly suggestive of the iron(III) ion in a regular octahedral environment in these complexes.

Table 3.2 Observed absorption bands and assigned transitions for octahedral Fe(III) complexes (band positions in cm^{-1})

Compound	${}^6A_{1g} \rightarrow {}^4T_{1g}(G)$	${}^6A_{1g} \rightarrow {}^4T_{2g}(G)$	${}^6A_{1g} \rightarrow {}^4A_{1g}, {}^4E_g$
$\text{Na}_3[\text{Fe}(\text{mal})_3] \cdot 4\text{H}_2\text{O}$	10,400	15,400	22,600 25,700 (w)
$\text{Na}_3[\text{Fe}(\text{etmal})_3] \cdot 2\text{H}_2\text{O}$	10,500	15,400	22,500 25,600 (w)
$\text{Na}_3[\text{Fe}(\text{benzylmal})_3] \cdot 2\text{H}_2\text{O}$	11,600	16,500	22,700 25,700 (sh)
$(\text{NH}_4)_3[\text{Fe}(\text{mal})_3] \cdot 3\text{H}_2\text{O}$ ¹³	11,090	15,720	22,660 22,880

Co(III) d^6

The visible absorption spectra of Co(III) spin paired complexes is expected to consist of transitions from the ${}^1A_{1g}$ ground state to the other singlet states.³² However, the two absorption bands found in

the visible spectra of regular octahedral Co(III) complexes represents transitions to the upper states ${}^1T_{1g}$ and ${}^1T_{2g}$. The absorption spectrum of octahedral Co(III) oxalato complexes are found to have two bands in the visible and near ultraviolet region.^{5,31} The u.v./visible spectra of the tris(malonato)cobaltate(III) ion consist of two bands situated at $16,500\text{ cm}^{-1}$ and $23,800\text{ cm}^{-1}$. These correspond to the transitions ${}^1A_{1g} \rightarrow {}^1T_{1g}$ and ${}^1A_{1g} \rightarrow {}^1T_{2g}$ respectively. In addition a third band is found as a shoulder on the low frequency side at $12,800\text{ cm}^{-1}$. A similar band at $13,000\text{ cm}^{-1}$ has been reported for the corresponding oxalate complex, which has been assigned to a $A_{1g} \rightarrow {}^3T_{1g}$ transition.³³ The solid state spectra of the Co(III) malonato complex is almost identical to that of the oxalato complex, indicative of a similar octahedral structure.

Co(II) d^7

The free ion spectrum is not defined completely. Apart from the 4P term, only the 2G and 2H terms have been assigned with certainty, which makes the assignment of the spectrum difficult. However, the Co^{2+} complexes can be obtained in regular tetrahedral and octahedral environments, which explains the large range of compounds for which the spectra have been studied.

An octahedrally coordinate Co(II) ion should have three spin-allowed d-d transitions, those from the ground state, ${}^4T_{1g}(F)$, to the states ${}^4T_{2g}$, ${}^4A_{2g}$ and ${}^4T_{1g}(P)$. Regular octahedral complexes such as the hexaquo cobalt(II) ion exhibit three bands.^{30,31} The visible absorption has been found³⁰ to be rather weak and placed in the blue part of the spectrum, accounting for the pale pink colour of the compound. The solid state spectra of Co(II) malonate, Co(II) ethylmalonate and Co(II) benzylmalonate compounds are similar to that of the $\text{Co}(\text{H}_2\text{O})_6^{2+}$ ion. They all have their strong band at $\sim 20,000\text{ cm}^{-1}$,

and the usual structure of the band with a less intense band (shoulder towards blue) which is an indication of octahedral Co(II) compounds.³¹

The band of $\text{Co}(\text{H}_2\text{O})_6^{2+}$ at $8,000 \text{ cm}^{-1}$ has been identified as the first octahedral field transition ${}^4\text{T}_{1g}(\text{F}) \rightarrow {}^4\text{T}_{2g}(\text{F})$. Similar bands were found for Co(II) malonate at $8,200 \text{ cm}^{-1}$, and for Co(II) ethylmalonate at $11,500 \text{ cm}^{-1}$, and at $8,100 \text{ cm}^{-1}$ for Co(II) benzylmalonate. The low intensity visible band at $\sim 16,000 \text{ cm}^{-1}$ in $\text{Co}(\text{H}_2\text{O})_6^{2+}$ has been identified as ${}^4\text{T}_{1g}(\text{F}) \rightarrow {}^4\text{A}_{2g}(\text{F})$. Corresponding bands^{are} observed at $16,600 \text{ cm}^{-1}$ in Co(II) malonate, at $16,700 \text{ cm}^{-1}$ in Co(II) ethylmalonate and at $15,400 \text{ cm}^{-1}$ in Co(II) benzylmalonate. The strongest band found in the spectrum at $20,200 \text{ cm}^{-1}$ in $\text{Co}(\text{H}_2\text{O})_6^{2+}$ is undoubtedly due to the transition ${}^4\text{T}_{1g}(\text{F}) \rightarrow {}^4\text{T}_{1g}(\text{P})$. Similar bands were observed at $20,000 \text{ cm}^{-1}$ for Co(II) malonate, at $19,500 \text{ cm}^{-1}$ for Co(II) ethylmalonate and at $19,100 \text{ cm}^{-1}$ for Co(II) benzylmalonate compounds. From the results of solid state spectra of Co(II) malonate, Co(II) ethylmalonate and Co(II) benzylmalonate, we could assume an octahedral configuration for these compounds. The results are shown in Table 3.3.

Table 3.3 Visible absorption spectra of octahedral Co(II) complexes
(band positions in cm^{-1})

Assignment	$[\text{Co}(\text{H}_2\text{O})_6]^{2+}$	Co(II)mal	Co(II)etmal	Co(II)benzylmal
${}^4\text{T}_{1g}(\text{F}) \rightarrow {}^4\text{T}_{2g}$	8,000	8,200	11,500	8,100
${}^4\text{T}_{1g}(\text{F}) \rightarrow {}^4\text{A}_{2g}$	16,000	16,600	16,700	15,400
${}^4\text{T}_{1g}(\text{F}) \rightarrow {}^4\text{T}_{1g}(\text{P})$	20,200	20,000	19,500	19,100

Ni(II) d⁸

Octahedral, tetrahedral, and square planar configurations occur in nickel complexes.³² In nickel(II) complexes of octahedral symmetry three transitions are allowed; from the ground state ${}^3A_{2g}$ to ${}^3T_{2g}(F)$, ${}^3T_{1g}(F)$, ${}^3T_{1g}(P)$. The spectrum of $\text{Ni}(\text{H}_2\text{O})_6^{2+}$ ion has indeed three absorption bands as is to be expected for six coordinate octahedral Ni(II) complexes.³²

In the solid state for Ni(II) malonate, Ni(II) ethylmalonate and Ni(II) benzylmalonate complexes three bands in the visible absorption characteristic of octahedral Ni(II) complexes were observed. The spectra of these complexes were similar to that of the aquo ion, and similarly the three observed bands in each spectrum can be assigned as a characteristic feature of the spectra of octahedral Ni(II) complexes. The results are shown in Table 3.4.

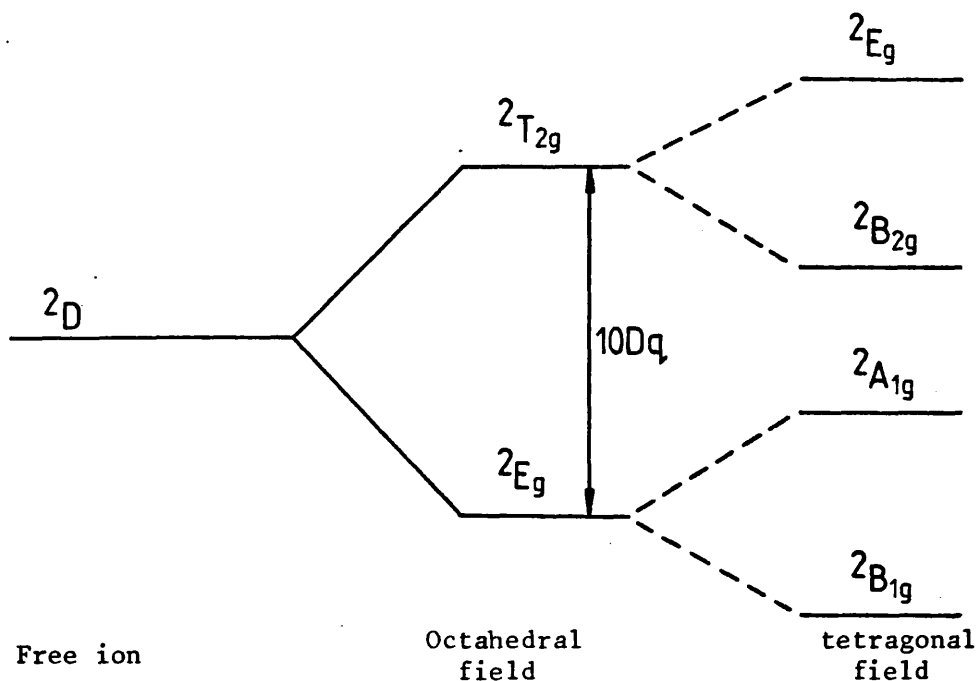
Table 3.4 Visible absorption spectra of octahedral Ni(II) complexes
(band positions in cm^{-1})

Assignment	$[\text{Ni}(\text{H}_2\text{O})_6]^{2+}$	Ni(II)mal	Ni(II)etmal	Ni(II)benzylmal
${}^3A_{2g} \rightarrow {}^3T_{2g}(F)$	8,500	8,300	8,300	8,200
${}^3A_{2g} \rightarrow {}^3T_{1g}(F)$	13,500	14,600	14,400	14,500
${}^3A_{2g} \rightarrow {}^3T_{1g}(P)$	25,300	25,300	24,800	24,900

Cu(II) d⁹

Copper Cu^{2+} with d^9 electronic configuration produces an E_g ground state in octahedral symmetry. Such a state is susceptible to Jahn-Teller forces which remove the degeneracy of the e_g orbitals.^{35,36} The result is either a tetragonal elongation or compression. An

elongated structure is usually assumed to be the most common example of Cu^{2+} coordination. For tetragonal Cu^{2+} complexes the octahedral doublet states ${}^2\text{E}_g$ and ${}^2\text{T}_{2g}$ will split as ${}^2\text{E}_g \rightarrow {}^2\text{A}_{1g} + {}^2\text{B}_{1g}$, ${}^2\text{T}_{2g} \rightarrow {}^2\text{E}_g + {}^2\text{B}_{2g}$. In elongated form the energy levels are as shown below, with ${}^2\text{B}_{1g}$ as the ground state:



Instead of the single ${}^2\text{T}_{2g} \leftarrow {}^2\text{E}_g$ transition of regular octahedra in a tetragonally distorted molecule the transition occurs between components of the E_g (in O_h) ground state and from the ground state to components of the T_{2g} state: ${}^2\text{B}_{1g} \rightarrow {}^2\text{B}_{2g}$, ${}^2\text{B}_{1g} \rightarrow {}^2\text{E}_g$. A further band at much lower energy is expected from ${}^2\text{B}_{1g} \rightarrow {}^2\text{A}_{1g}$ transitions. Electronic spectra theory predicts that tetragonal splitting of the e_g and t_{2g} level would produce a single broad band near $600 - 900 \text{ m}\mu$ which consists of several nearly superposed bands. This is in agreement with the results of Graddon³⁷ who studied the solution spectra of a number of $\text{Cu}(\text{II})$ carboxylate complexes. According to Graddon the single band observed at $14,280 \text{ cm}^{-1}$ in $\text{Cu}(\text{II})$ oxalate and $\text{Cu}(\text{II})$ malonate can be regarded as the only single transition required by crystal field theory for the

tetragonally coordinated cupric ion. The visible absorption spectra of a number of copper(II) α , ω -dicarboxylates of formula $[\text{Cu}(\text{OOC}(\text{CH}_2)_n\text{COO})]$ have been studied.^{38,40,41} The results confirmed that the electronic spectra of some of these Cu(II) carboxylate complexes contain an additional near-ultraviolet band. The appearance of a new band at $\sim 28,000 \text{ cm}^{-1}$ (band II) has been considered as "an indication of the linkage between the two copper atoms", as a result of dimeric structure. It has been suggested⁴⁰ that the absence of band (II) from the spectra of copper(II) oxalate and copper(II) malonate derivatives indicates that pairing of copper atoms does not occur. The solid state spectra of copper(II) oxalate has one band at $13,698 \text{ cm}^{-1}$. Its structure was proposed to consist of an infinite chain-like monomer,³⁸ which may involve interchange interaction to complete a distorted octahedron of oxygen atoms about each central copper atom. In fact the monomeric structure of Cu(II) oxalate has been confirmed by the recent single crystal X-ray analysis.³⁹ The copper atom is octahedrally coordinated by four oxygens from the two oxalate groups ($\text{Cu} - \text{O} = 1.96 \text{ \AA}$) and two oxygens from the water molecules ($\text{Cu} - \text{O} = 2.48 \text{ \AA}$). In the case of Cu(II) malonate compounds, the structural determinations by different workers are not in agreement with each other. It has been suggested as simple monomer,^{32,34} chain complexes,³⁶ and as distorted octahedral.³⁷ A recent ESR spectrum³⁸ of copper(II) malonate trihydrate indicates that the Cu^{2+} ion is octahedrally surrounded by oxygen atoms (visible band at $14,280 \text{ cm}^{-1}$ ⁴⁴). The complete X-ray crystal structure of copper(II) malonate confirmed that the coordination is indeed a distorted octahedron.⁴³ It was found that copper(II) malonate tetrahydrate with empirical formula $[\text{Cu}(\text{C}_3\text{H}_2\text{O}_4)_2 \cdot 4\text{H}_2\text{O}]_2$ is formed from two complexes of two different types. In the complex of the first type which is dimalonato cuprate, the copper atom is octahedrally surrounded by four oxygens of two malonate groups. The oxygen atoms of two water molecules are

(Cu - O = 2.48 Å) away from a copper atom to complete a distorted octahedron with four closer oxygen atoms (Cu - O distance, 1.96 - 1.97 Å) belonging to two malonate groups. The dimalonato cuprate is very similar to that of the dioxalato cuprate reported by Lohn.³⁹ In the complex of the second type $[\text{Cu}(\text{H}_2\text{O})_6]^{2+}$, the Cu atom coordinates six water molecules which are hydrogen bonded with the other oxygen atoms of two neighbouring malonates in the crystal lattice.

The bands observed in the diffuse reflectance spectra of the solid at $13,800 \text{ cm}^{-1}$ for Cu(II) malonate. 2.5 H₂O, at $14,000 \text{ cm}^{-1}$ for bis(malonato)diaquo Cu(II) complex, at $9,400 \text{ cm}^{-1}$ for Cu(II) ethylmalonate. H₂O and at $14,400 \text{ cm}^{-1}$ for Cu(II) benzylmalonate. H₂O tend to be broad as expected theoretically for the tetragonally coordinated Cu²⁺ ion with the usual Jahn-Teller distortion.⁴⁵

The interpretation of the visible spectra is not straight forward. However, if the environment is considered to have a static tetragonal distortion, then the splitting of the ²D term in crystal fields of octahedral-tetragonal symmetry should give two transitions, ${}^2B_{1g} \rightarrow {}^2A_{1g}$ and ${}^2E_g, {}^2B_{1g} \rightarrow {}^2B_{2g}$, however, it is unusual to observe such a clear separation of these two bands in the spectra of Cu(II) complexes and they usually tend to overlap and produce a single broad asymmetric band.

REFERENCES

1. F.A. Cotton and G. Wilkinson, "Advanced Inorganic Chemistry"., 2nd Ed., 1966.
2. D. Sutton, "Electronic Spectra of Transition Metal Complexes", 1968.
3. J.Lewis and R.G. Wilkins, "Modern Coordination Chemistry", 1960.
4. W. Lapraik, Chem. News., 1893, 25, 444.
5. A. Mead, Trans. Faraday Soc., 1934, 30, 1052.
6. C.K. Jørgensen, Acta Chem. Scand., 1955, 9, 1362.
7. J.N. Van Niekerk and F.R.L. Schoening, Acta Cryst., 1952, 5, 196.
8. J.N. Van Niekerk and F.R.L. Schoening, Acta Cryst., 1951, 4, 35.
9. J.C. Chang, J. Inorg. Nucl. Chem., 1968, 30, 945.
10. K.R. Ashley and K. Lane, J. Inorg. Chem., 1970, 9, 1795.
11. M.J. Frank and D.H. Hirehital, J. Inorg. Chem., 1972, 11, 776.
12. R.E. Hamm and R.H. Perkins, J. Amer. Chem. Soc., 1955, 77, 2083.
13. T.S. Piper and R.L. Carlin, J. Chem. Phys., 1961, 35, 1809.
14. W.E. Hatfield, J. Inorg. Chem., 1964, 3, 605.
15. K.R. Butler and M.R. Snow, J. Chem. Soc. Dalton., 1976, 251.
16. R.P. Scaringe, W.E. Hatfield and D.J. Hodgson, J. Inorg. Chem., 1977, 16, 1600.
17. J.W. Lethbridge, J. Chem. Soc., Dalton., 1980, 10, 2039.
18. J.P. Fackler and I.D. Chawla, J. Inorg. Chem., 1964, 3, 1130.
19. R. Dingle, Acta Chem. Scand., 1966, 20, 33.
20. T.S. Davis, J.P. Fackler and M.J. Weeks, J. Inorg. Chem., 1968, 7, 1994.
21. T.S. Piper and L.R. Carlin, J. Inorg. Chem., 1963, 2, 260.
22. D.W. Barnum, J. Inorg. Nucl. Chem., 1961, 21, 221.
23. J.I. Bullock, M.M. Patel and J.E. Salmon, J. Inorg. Nucl. Chem., 1969, 31, 415.

24. J.P. Fackler, T.S. Davis and I.D. Chawla, *J. Inorg. Chem.*, 1965, 4, 130.
25. T. Lis, J. Matuszewski and B. Jezowska-Trzebiatowska, *Acta Cryst.*, 1977, B33, 1943.
26. T. Lis and J. Matuszewski, *J. Chem. Soc., Dalton*, 1980, 6, 996.
27. F.A. Cotton and G. Wilkinson, "Advanced Inorganic Chemistry", 2nd Ed., 1966.
28. D.P. Graddon, *J. Inorg. Nucl. Chem.*, 1956, 3, 308.
29. N.S. Hush and R.J.M. Hobbs, "Progress in Inorganic Chemistry", 1968, 10, 345.
30. F.A. Cotton and G. Wilkinson, "Advanced Inorganic Chemistry", 1966, 2nd Ed., page 871.
31. C.J. Ballhausen and C.K. Jørgensen, *Acta Chem. Scand.*, 1955, 9, 397.
32. F.A. Cotton and G. Wilkinson, "Advanced Inorganic Chemistry", 1966, 2nd Ed., page 875.
33. L.H. James, *J. Chem. Phys.*, 1956, 25, 379.
34. F.A. Cotton and G. Wilkinson, "Advanced Inorganic Chemistry", 1966, 2nd Ed., page 882.
35. F.A. Cotton and G. Wilkinson, "Advanced Inorganic Chemistry", 1966, 2nd Ed., pages 873-901.
36. D. Sutton, "Electronic Spectra of Transition Metal Complexes", 1968.
37. D.P. Graddon, *J. Inorg. Nucl. Chem.*, 1958, 7, 73.
38. L. Dubiki, C.M. Harris, E. Kokot and R.L. Martin, *J. Inorg. Chem.*, 1966, 5, 93.
39. J. Lohn, *Acta Cryst.*, 1969, 25.
40. B.N. Figgis and D.J. Martin, *J. Inorg. Chem.*, 1966, 5, 100.
41. M. Kato, H.B. Janassen and J.C. Fanning, *Chem. Rev.*, 1964, 64, 99.
42. B.H. O'Connor and E.N. Maslen, *Acta Cryst.*, 1966, 20, 824.
43. G.I. Dimitrova, A.V. Ablov, G.A. Kiosse, G.A. Popovich, T.I. Malinovskii and I.F. Burshtein, *Ducki. Akad. Nauk. SSSR*, 1974, 216, 1055.

44. R. Rajan, *J. Chem. Phys.*, 1962, 37, 460.
45. J. Bjerrum, E.J. Ballhausen and C.K. Jørgensen, *Acta Chem. Scand.*, 1954, 8, 1275.

CHAPTER IV: INFRARED ABSORPTION SPECTROSCOPY*4.1 Introduction

Much work has been done in identifying the i.r. absorption bands with compounds analogous to those in this research, and it is intended to use previous work to help in band assignments.

The analysis is divided into several sections in order to observe the effects of different bonding species upon the i.r. bands. Our investigation is based on the i.r. absorption spectra of the compounds which have been prepared and would fall into the following categories:

1. Malonato metal complexes
2. Ethylmalonato metal complexes
3. Benzylmalonato metal complexes

Attempts have been made in the study of:

1. The shifts due to metal coordination or changes in the spectrum on coordination.
2. Carboxylic acid vibrations - C = O stretching vibrations.

Changes in the Spectrum on Coordination

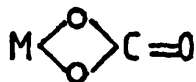
On coordination to a metal, the ligand bands in general are shifted to lower or higher frequencies. So the modes of vibration and the nature of the metal bond to the molecule will affect the intensity and position of the bands^{1,2,3}.

In a series of metal complexes having the same structure the magnitude of these band shifts becomes larger as the coordination bond becomes stronger. So it is possible to determine the order of strength of coordinate bonds by comparing the magnitudes of the band shifts.

Extensive infrared studies have been made on metal complexes of carboxylic acids⁴⁻⁷. In the study of the i.r. spectra of the carbonato metal complexes the nature of the metal-ligand bond was

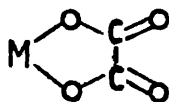
* The references for this section are on pages 104 and 105.

assumed to have covalent character.⁴



The results from i.r. spectra of some Co(III) carbonato complexes based on the normal coordinate analysis later confirmed the covalent nature of the coordination bond.⁵ Similar results have been reported for the M(III) oxalato complexes.⁷

Schemle et al.⁶ carried out a number of absorption studies of simple and complex metal oxalates. The results based on the normal coordinate analysis of the free oxalate ion indicate that in most metal oxalato complexes the ligands are coordinated to the central metal ion through the two oxygen atoms, the M-O bonds having some 50% covalent character.

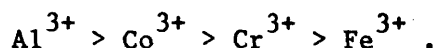


The literature investigations are mostly concerned only with the ligand vibrations and no direct information is available on the metal-oxygen vibrations in these complexes. Nevertheless the relationships between the metal-oxygen and the carbon-oxygen stretching frequencies of a series of oxalato metal complexes have been investigated.⁸ Their results suggest that the frequencies of the uncoordinated C=O stretching (ν_1 and ν_7 , around $1700 \sim 1600 \text{ cm}^{-1}$) increase and those of the coordinated C-O stretching bands (ν_8 , around $1450 \sim 1350 \text{ cm}^{-1}$ and ν_2 , around $1300 \sim 1200 \text{ cm}^{-1}$) decrease as the frequency of the metal oxygen (M-O) stretching band (ν_4 , around $600 \sim 500 \text{ cm}^{-1}$) increases in the order of

the metals $\text{Zn(II)} < \text{Cu(II)} < \text{Pd(II)} < \text{Pt(II)}$.

From these results it clearly indicates that the metal-sensitive bands both in the high and low frequency regions can be used as a measure of the strength of the coordinate bond.

The C=O and C-O stretching frequencies are not sensitive to the nature of the metal ion in the 1:3 metal-oxalate complexes. It was suggested by Nakamoto⁸ that this may be due to the broadening of the C=O stretching vibrations in octahedral complexes compared with those of the square or tetrahedral 1:2 oxalato complexes. Therefore the M-O stretching frequencies are found to be more useful as a measure of the strength of the coordinate bond than the C-O stretching bonds in the 1:3 complexes. The M-O stretching modes which appear in the low frequency region are more sensitive to the nature of the metal than are the ligand vibrations in the high frequency region. In the case of M(III) oxalato complexes the M-O frequency increases as the metal is changed in the order



However the metal-sensitive bands are not always easy to identify and the investigations mostly are concerned only with the ligand vibrations in these complexes.

Carboxylic Acid Vibrations

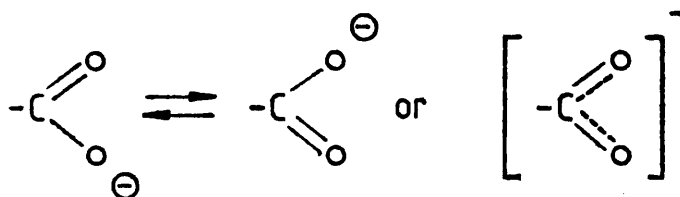
The infrared absorption spectra of the COO group in different environments are well established.³ The carboxyl group in a saturated acid, which can be regarded as ionised, exhibits a characteristic absorption band at $\sim 1725 - 1700 \text{ cm}^{-1}$. This band is often strong and is due to the C=O stretching vibration. Dicarboxylic acids often have two bands in this region, e.g. malonic acid shows two peaks at 1740 and 1710 cm^{-1} , oxalic acid has only one absorption band between 1710 and 1690 cm^{-1} , ethylmalonic acid absorbs strongly between 1740 - 1700 cm^{-1} , but in benzylmalonic acid two frequencies are shown at 1760

and 1735 cm^{-1} . The infrared spectra of a very considerable number of carboxylic acids have been reported.⁹

There are five bands to be considered in detecting a carboxyl group. The bands at $\sim 2500 - 2700\text{ cm}^{-1}$, near 1700 cm^{-1} , near 1420 cm^{-1} , near 1250 cm^{-1} and near 900 cm^{-1} . The first two are the most highly characteristic. The nature of these bands will be discussed later.

However, in the examination of an unknown compound in which a carboxyl group is postulated, the carboxyl intensity could reasonably be expected to be closely similar to that of the nearest known carboxylic acid with a similar structure around the COOH group.

The carboxyl group present in a salt is ionised and resonance is possible:



The characteristic carbonyl absorption is replaced by two bands between 1610 and 1550 cm^{-1} and between 1400 and 1300 cm^{-1} which correspond to the antisymmetric and symmetric vibrations of the COO^- group. Of these bands the former is more characteristic, and it is more constant in frequency whilst many other skeletal vibrations occur in the wide range $1400 - 1300\text{ cm}^{-1}$. When the ionised carboxyl group is coordinated to a metal it is seen to be somewhere between being an ionised and an unionised group and the vibration due to the antisymmetric stretching mode of the COO^- group occurs around $1650 - 1590\text{ cm}^{-1}$ depending on the nature of the metal. Therefore it is possible to distinguish between free and coordinated COO^- groups in these complexes and determine the degree of the coordination. In examining the effect of coordination on the COO stretching frequency, it is important to interpret the results

based on the structures obtained by X-ray analysis.

The results of X-ray analysis on sodium malonate monohydrate²¹ indicate that the two C-O bonds in the carboxyl group are equal, the bond distance being 1.26 Å. In Cr(III) malonato complex, however, the C-O bonds coordinated to the metal are lengthened (1.276 Å), while the uncoordinated C-O bonds are shortened (1.233 Å). This effect is common in coordinated carboxylate structures, but in malonato complexes most of such structures are polymeric utilizing the nonchelating oxygen atoms to continue the sequence,²²⁻²⁴ and the C-O distances are therefore more dependent on the environment, which would account for the differences in the C-O bond distances observed in other carboxylate groups.

Experimental

Infrared Spectroscopy Measurements

The spectra were measured on a Perkin Elmer infrared spectrophotometer Model 457 as Nujol or hexachlorobutadiene mulls, between KBr plates. The spectra of the solid complexes were also measured using the KBr method.

The spectrophotometer was calibrated using a polystyrene film.

4.2 Results and Discussion

The infrared absorption spectra of a number of metal compounds containing malonate, ethylmalonate, and benzylmalonate ligands are reported and some results of malonato, ethylmalonato, benzylmalonato complexes are included for comparison (see Tables 4.1 - 4.6).

The spectra have been compared with those of corresponding acids, and oxalato and malonato complexes.^{6,8,10}

4.3 Malonato Metal Compounds

Assignments of the observed frequencies of the infrared spectra of malonate metal compounds have been discussed^{6,11}. The

Table 4.1 The infrared spectra of some metal malonates and malonic acid (band position in cm^{-1})

Mg(II)mal. $5\text{H}_2\text{O}$	Ca(II)mal, $\text{Ca}(\text{OH})_2 \cdot 1\frac{1}{2}\text{H}_2\text{O}$	2Ba(II)mal, $\text{Ba}(\text{OH})_2 \cdot 2\text{H}_2\text{O}$	Cu(II)mal. $2\frac{1}{2}\text{H}_2\text{O}$	Co(II)mal. $2\text{H}_2\text{O}$	Ni(II)mal. $2\text{H}_2\text{O}$	Assignments
3520 (sh)	3500 (s, sh)	3620 (w)	3440 (w)	3450 (w)	3460 (s, b)	ν (OH)
3360 (m, b)	3200 (w, b)	3200 (s, b)	3200 (s, b)	3345 (m)	3200 (s)	ν (H_2O)
3240 (m)	3060 (w)			3200 (m)		
3100 (m)						
2970 (sh)	2990 (sh)	2990 (sh)		3015 (sh)	3025 (sh)	ν (CH)
2920 (sh)	2970 (sh)	2970 (sh)		2950 (sh)		
2905 (sh)	2950 (sh)	2950 (sh)		2920 (sh)	2920 (w)	
	2930 (sh)	2930 (sh)	2910 (sh)			
1700 (m)	1650 (w)	1665 (sh)		1670 (w)	1660 (sh)	(H_2O)
1610 (s)	1580-1560 (s, b)	1555 (s, b)	1590 (s, b)	1570 (s, b)	1580 (s, b)	ν (OCO) asym
1560 (s)						
1445 (sh)	1470 (w)	1440 (s)	1430 (s)	1450 (s)	1455 (m)	CH_2 bend
1405 (s)	1425 (w)	1405 (m)		1415 (w)	1380 (s)	ν (OCO) sym
1372 (m)	1365 (s)	1360 (s)	1370 (s)	1375 (s)	1365 (w)	ν (OCO) sym

Table 4.1 continued

Mg(II)mal. 5H ₂ O	Ca(II)mal, Ca(OH) ₂ ·1½H ₂ O	2Ba(II)mal, Ba(OH) ₂ ·2H ₂ O	Cu(II)mal. 2½H ₂ O	Co(II)mal.2H ₂ O	Ni(II)mal.2H ₂ O	Assignments
1285 (s)	1260 (m)	1260 (m)	1275 (m)	1285 (m)	1288 (m)	CH ₂ wag
1165 (w)	1160 (vw)	1170 (m)	1190 (m)	1238 (s)		
990 (m)			1160 (w)	1175 (m)	1179 (m)	ν(CC) asym
960 (m)	975 (m)	975 (m)	985 (sh)	1005 (sh)	973 (w)	ν(CC) asym
935 (w)	952 (s)	930 (sh)	966 (m)	975 (w)	965 (w)	ν(CC) sym
	872 (sh)		940 (w)	952 (s)	950 (s)	CH ₂ rock
852 (sh)	835 (w)	830 (w)	815 (w)	865 (w)	860 (w)	
740 (s,b)	720 (m)	695 (m)	740 (s)	780 (w)	790 (m)	OCO bend
672 (w)	660 (s)	625 (m)	600 (w,b)	722 (m)	730 (m)	OCO bend
600 (w,b)	598 (w)	590 (s)	522 (w)	670 (m)		OCO wag
550 (w)	540 (m)	545 (m)	455 (w)	575 (s)	578 (s,b)	ν(M-O) + (C-C)
485 (w)	485 (sh)	445 (vw)		480 (s)	540 (w)	+ ring
					489 (w)	

Table 4.1 continued

Zn(II)mal. 2H ₂ O	Cd(II)mal. H ₂ O	Malonic acid	Assignments
3460(s)	3440(m)		
3160(s)	3370(m, b)		$\nu(\text{H}_2\text{O})$
	3070(m)		
3025(w)	3010(w)	2980(s, b)	$\nu(\text{CH})$
2915(w)	2950(w)	2720(m, b)	$\nu(\text{OH})$
	2925(w)	2685(m, b)	
		2590(s, b)	
1660(w)	1640(w)		$\delta(\text{H}_2\text{O})$
1565(s, b)	1560(s, b)	1730(vs)	$\nu(\text{C=O})$ asym
		1710(vs)	
		1439(s)	$\nu(\text{Co}) + \delta(\text{OH})$
1450(s)	1450(s)	1422(s)	CH ₂ bend
1410(w)	1420(w)		$\nu(\text{OCO})$ sym
1375(s)	1380(s)	1310(s)	$\nu(\text{OCO})$ sym
1285(m)	1270(w)	1275(sh) 1219(s)	CH ₂ wag
1175(s)	1170(w)	1173(s)	$\nu(\text{CC})$ asym
		1155(w)	$\nu(\text{CC})$ asym

Table 4.1 continued

Zn(II)mal. 2H ₂ O	Cd(II)mal. H ₂ O	Malonic acid	Assignments
975 (w)	970 (w)	962 (m, sh)	ν (CC) sym
945 (w)	955 (w)	933 (m, sh)	CH ₂ rock
860 (m)	862 (w)		
790 (m)		920 (s)	π (OH)
720 (s)	730 (s)	770 (m)	δ (COOH)
670 (vw)	660 (sh)	654 (s)	π (COOH)
575 (m)	560 (m)		ν (M-O) + (C-C) + ring

vibrations of the malonate ion and malonic acid are quite similar except the antisymmetric and symmetric COO stretching vibrations of malonate ion which become the C=O stretching and C-O stretching vibrations coupled with in-plane OH deformation vibration of malonic acid. The results are listed in Table 4.1. A very strong band around 1600 - 1550 cm^{-1} and another near 1400 - 1350 cm^{-1} observed in the spectrum of all the simple malonate compounds can be assigned, respectively, to the antisymmetric and symmetric OCO stretching vibrations. These frequencies appear as a doublet in the spectrum of malonate ion.⁶ These frequencies become the C=O stretching (1735 cm^{-1}) and C-O vibrations coupled with in-plane OH deformation vibration (1439 and 1314 cm^{-1}) of malonic acid.⁹ The C-C stretching frequencies in the malonate compounds (seen as a doublet at ~ 1170 and ~ 970 cm^{-1}) correspond to the bands at 1174 and 960 cm^{-1} of malonic acid, which can be assigned to the symmetric and antisymmetric C-C stretching frequencies.

The broad band observed in the spectrum of malonic acid at ~ 900 cm^{-1} is due to the out-of-plane OH deformation vibration; it vanishes in the spectrum of the malonate ion.

The bands observed below 800 cm^{-1} can be assigned to OCO bending and wagging vibrations of the malonate ion and correspond to the COOH in-plane and out-of-plane deformation vibrations of malonic acid. Fairly constant bands observed in malonic acid and the malonate compounds at ~ 1460, ~ 1300 cm^{-1} and 900 cm^{-1} may be assigned to the CH_2 bending, wagging and rocking respectively.

However the malonate compounds of various metals studied have similar i.r. spectra except in the region of those frequencies characteristic of ionised carboxyl groups. The antisymmetric COO stretching frequency is known to be sensitive to a change in the metal, the relationship between this frequency and some physical property of the metal has been discussed by several investigators.^{12,13} For instance, Kagarise¹²

has shown for the salts of some carboxylic acids that a linear relationship exists between the antisymmetric COO stretching frequency and the electronegativity of the alkaline-earth metal constituent of the molecule increasing in the order Sr(II) < Ca(II) < Mg(II) < Be(II). It was also suggested¹³ that the COO stretching frequency is a function of the combined effect of mass, radius and electronegativity of the central metal atom. From the data listed in Table 4.1 it is observed that there is a good relationship between the COO⁻ stretching frequency and the electronegativity of the alkaline-earth metals, in the order Mg(II) > Ca(II) > Ba(II), in good agreement with the stability constants reported for these compounds.¹⁴ This order is in perfect agreement with recent X-ray structural analyses on alkaline-earth malonate compounds²⁵⁻²⁸ which indicated that the strength of M-O bonds decreases along the series of these compounds (see Table 1.1).

However, IR spectra results indicate that coordination occurs through the carboxyl oxygen atoms. A previous investigation⁸ showed that the nature of the metal to ligand bond (M-O) could be determined from the C-O stretching frequencies without determining the low frequencies characteristic of the M-O stretching vibrations. That is, the frequencies of the uncoordinated C=O stretching bands (1700 ~ 1600 cm⁻¹) increase and those of coordinated C-O stretching band decrease as the frequency of the metal oxygen (M-O) stretching increases. These results suggest that as the M-O bond becomes stronger, the O-C bond coordinated to the metal becomes weaker and the C-O bonds free from coordination and the C-C bonds become stronger. These results are in accordance with recent X-ray structural analyses. X-ray analysis of several alkaline earth malonate compounds²⁵⁻²⁸ indicates that the O-C bonds bonded to the metal are lengthened and the uncoordinated C-O bonds are shortened as the M-O bonds are shortened in the same order as mentioned above.

The discussion regarding to the position of the metal-sensitive bands in the lower frequency region requires the consideration of M-O stretching modes which appear at low frequencies. For the assignment of these low frequency bands a normal coordinate analysis of the whole chelate ring should be carried out. Results are available in the case of divalent metal chelates.⁸

It was observed that in the case of simple malonato compounds there is a shift of the antisymmetric and symmetric COO stretching to higher and lower frequencies respectively, as the metal is changed in the order: Cd(II) < Zn(II), Co(II) < Ni(II) < Cu(II).

The strength of the M-O bond increases along the series of these compounds. The magnitude of the M-O stretching frequencies and the stability constants of these compounds¹⁵ change in the same direction; this is expected, since an increase in the M-O bond order means higher stability of the complex.

Assignment of the Observed Frequencies of the Malonate Metal Complexes

The assignments of malonic acid and its simple metal compounds can be used to interpret the spectra of the metal coordination complexes. The bands for similar complexes are reported¹⁰.

The broad band $\sim 3500 \text{ cm}^{-1}$ is due to the water of crystallization indicated by empirical formulae of these complexes. A similar band is observed in the hydrated malonate salts. In basic Ca(II) and Ba(II) malonate compounds the corresponding band occurs, together with a sharp singlet band at higher frequencies at $\sim 3500 \text{ cm}^{-1}$ and 3620 cm^{-1} respectively. The latter band is of the type usually found¹⁷ in the hydroxy species and is characteristic of the free OH stretching frequency.

The strong absorption bands observed near 1630 cm^{-1} in the spectra of the complexes correspond to the broad band at 1563 cm^{-1} in the spectrum of simple malonato compounds which has been assigned to

Table 4.2 The infrared spectra of some metal-malonate complexes (band position in cm^{-1})

$\text{K}_3[\text{Al}(\text{mal})_3] \cdot 6\text{H}_2\text{O}$	$\text{K}_3[\text{Co}(\text{mal})_3] \cdot 4\text{H}_2\text{O}$	$\text{Na}_3[\text{Fe}(\text{mal})_3] \cdot 4\text{H}_2\text{O}$	$\text{K}[\text{Mn}(\text{mal})_2(\text{H}_2\text{O})_2]$	$\text{Na}_2[\text{Cu}(\text{mal})_2(\text{H}_2\text{O})_2]$	$\text{K}[\text{Cr}(\text{mal})_2(\text{H}_2\text{O})_2] \cdot 3\text{H}_2\text{O}$	Assignments
3400(w)	3490(sh)	3430(w)	3400(m,b)	3350(s)	3550(w)	$\nu(\text{H}_2\text{O})$
3240(m)	3340(w)	3230(w)	3200(m,b)	3220(s)	3410(m)	
	3200(w)					
2900(m)	2960(sh)	2930(s)	2930(w)	2940(s)	2920(s,b)	$\nu(\text{CH})$
			2910(sh)			
1640(s,b)	1570(s,b)	1625(s,b)	1625(s,b)	1610(s)	1595(s,b)	$\nu(\text{OCO})$ asym
				1580(s)		
1440(m)	1430(w)	1450(w)	masked	1430(m)	1420(m)	CH_2 bend
1400(w)	1410(sh)	1390(s)	1405(sh)	1405(m)	1385(m)	$\nu(\text{OCO})$ sym
1370(s)	1360(s,b)		1350(s,b)	1365(m)	1338(m)	
1290(m)	1310(sh)	1305(m)	1280(m)	1290(m)	1288(m)	CH_2 wag
	1268(m)	1280(m, sh)				
1185(m)	1190(m)	1208(w)	1170(sh)	1185(m)	1180(w)	$\nu(\text{C-C})$ asym
990(m)	985(m)	1150(m)	1150(w)	990(w)	990(m)	
			1015(w)			
965(s)	958(s)	973(m)	965(m)	973(s)	960(m)	$\nu(\text{C-C})$ sym
		960(m)				
940(w)	940(w)	935(s)	940(sh)	940(s)	945(m)	CH_2 rock
795(w)	810(w)	815(w)	740(m)	830(m)	812(w)	OCO bend
	765(w)	780(m)				
730(s)	735(sh)	735(s)	725(sh)	740(s)	752(m)	OCO bend.
	700(w)	720(sh)				

Table 4.2 continued

$K_3[Al(mal)_3] \cdot 6H_2O$	$K_3[Co(mal)_3] \cdot 4H_2O$	$Na_3[Fe(mal)_3] \cdot 4H_2O$	$K[Mn(mal)_2(H_2O)_2]$	$Na_2[Cu(mal)_2(H_2O)_2]$	$K[Cr(mal)_2(H_2O)_2] \cdot 3H_2O$	Assignments
597 (w)	660 (w)	562 (s)	578 (m)	650 (w)	645 (w)	OCO wag
560 (w)	590 (m,b)	562 (s)	578 (m)	623 (s)	545 (m)	$\nu(M-O) + \nu(C-C)$
505 (sh)	550 (sh)	499 (w)	480 (m)	570 (m)	515 (w)	+ ring
475 (m)	480 (w)	453 (m)	480 (m)	472 (m)	465 (m)	
	450 (w)					

the antisymmetric stretching vibration. The absorption band near 1380 cm^{-1} of the complexes (corresponding to 1405 cm^{-1} of the simple malonate compounds), can be assigned to the OCO symmetric stretching vibration. However the antisymmetric OCO stretching frequency in malonate complexes is higher than the corresponding OCO frequency in simple malonate compounds, and the symmetrical OCO frequency of complexes is lower than those of the simple malonate compounds. These results are in excellent agreement with recent X-ray structural analyses,^{29,30} which indicate that the O-C bonds coordinated to the metal are longer, i.e. weaker ($1.28 - 1.3\text{ \AA}$), and the C-O bonds free from coordination are shorter ($1.22 - 1.24\text{ \AA}$), therefore stronger in malonate complexes as compared to the O-C and C-O distances of 1.26 and $1.25 - 1.26\text{ \AA}$, respectively observed in simple malonate compounds (see Table 1.1). Our results are in agreement with those of Schmelz,¹⁰ suggesting that the metal to ligand bond of malonate metal complexes is more ionic than in oxalate metal complexes. The OCO bending vibrations are also affected by coordination. It can be seen from the table that the OCO bending of the simple malonate compounds near 800 cm^{-1} splits into two peaks in the 1:3 complexes. A similar effect has been reported previously for the 1:3 oxalato complexes,¹⁶ which has been explained on the basis of the normal coordinate treatment to be due to the effect of the coupling between the ligands in octahedral 1:3 complexes.

4.4 Ethylmalonato Metal Compounds

The infrared absorption spectra of these compounds are similar to those of malonate compounds, except for the appearance of new bands in the region $1100 - 1350\text{ cm}^{-1}$, where a group of bands known as a band progression³ appears with more or less regular spacings. Bellamy pointed out that the number and position of the bands in this region depend on the chain length.

However, the number of these sets of absorption bands which

Table 4.3 The infrared spectra of some metal etmalonates and ethylmalonic acid (band position in cm^{-1})

Mg(II)etmal. $3\text{H}_2\text{O}$	Ca(II)etmal.	Ba(II)etmal. $1/2 \text{H}_2\text{O}$	Cu(II)etmal. $2\text{H}_2\text{O}$	Co(II)etmal. $2\text{H}_2\text{O}$	2Ni(II)etmal, Ni(OH) $_2 \cdot 3\text{H}_2\text{O}$	Assignments
3320(s,b)	3340(w)	3360(w)	3340-3100(s,b)	3340-3260(s,b)	3540(w)	$\nu(\text{OH})$
2990(m)	2982(w)	2970(w)	2985(sh)	2995(m)	3360(s,b)	$\nu(\text{H}_2\text{O})$
2970(m)	2962(s)	2962(w)	2962(w)	2970(m)	2970(m)	νCH
2950(w)	2940(s)	2940(w)	2940(sh)	2950(sh)	2910(sh)	
2880(w)	2880(s)	2900(w)				
		2880(w)	2870(w)	2880(sh)	2880(w)	
1585(s,b)	1570(s,b)	1550(s,b)	1610-1540(s,b)	1580-1540(s,b)	1600-1550(s,b)	$\nu(\text{OCO}) \text{ asym}$
1462(w)	1450(w)	1440(s)	1460(w)	1462(m)	1460(sh)	CH_2 bend
1445(w)			1440(w)	1440(w)	1440(sh)	CH_3 bend
1430(w)	1430(w)	1410(s,b)	1420(w)	1425(w)	1430(m)	CH_2 bend
1385(sh)	1375(w)		1385(w)	1385(w)	1385(w)	CH_3 def
1365(m)	1360(m)	1365(s)	1360(s)	1360(s)	1355(m)	$\nu(\text{OCO}) \text{ sym} + \text{CH}_3 \text{ def}$
1335(m)	1330(m)	1325(m)	1335(m)	1332(w)	1330(sh)	CH_2 twist and wag
1310(s)	1300(s)	1290(s)	1312(s)	1310(s)	1302(s)	
1265	1255(s)		1272(m)	1265(w)	1265(sh)	
1242(m)	1240(sh)	1240(m)	1242(s)	1240(m)	1240(sh)	CH_2 wag
		1220(m)				
1152(w)	1170(sh)	1170(m)	1155(w)	1155(sh)	1220(sh)	$\nu(\text{C-C})$
					1130(sh)	
1093(s)	1090(sh)	1090(m)	1092(w)	1092(m)	1090(s)	C-C str or CH_3 def
1038(m)	1035(s)	1050(w)	1035(s)	1035(m)	1035(w)	

Table 4.3 continued

Mg(II) etmal. 3H ₂ O	Ca(II) etmal.	Ba(II) etmal. 1/2 H ₂ O	Cu(II) etmal. 2H ₂ O	Co(II) etmal. 2H ₂ O	2Ni(II) etmal, Ni(OH) ₂ ·3H ₂ O	Assignments
980 (m)	980 (s)	960 (sh)	982 (w)	980 (m)	980 (sh)	v (C-C)
960 (m)	945 (s)	940 (s)	960 (w) 940 (sh)	955 (m)	950 (w)	
900 (m)	893 (s)	897 (m)	900 (w)	895 (w)	890 (sh)	CH ₂ rock
850 (w)	845 (s)	840 (s)	880 (w)	860 (sh)	860 (sh)	
825 (w)						
800 (m)	805 (s)	790 (s)	800 (m)	800 (w)	800 (m)	δ (OCO)
770 (sh)	770 (s)		762 (w)	760 (sh)	762 (w)	δ (OCO)
		735 (m)				
730 (m)	720 (s)	710 (s, b)	720 (m)	730 (w)	730 (m)	
685 (s)	660 (s)	660 (s)	695 (m)	680 (m)	660 (m)	OCO wag
560 (m, b)	580 (m)	580 (s)	590 (m, b)	560 (s)	565 (w)	v (M-O) + ring
	555 (m)	550 (m)				
500 (w)	495 (s)	505 (s)	485 (m)			
445 (m)	440 (m)	430 (w)	450 (w)	450 (m)		

Table 4.3 continued

Zn(II)etmal. 2H ₂ O	Cd(II)etmal. H ₂ O	ethylmalonic acid	Assignments
3300(s,b)	3330(s,b)		$\nu(\text{H}_2\text{O})$
2995(w)	2962(m)	2980(w)	νCH
2950(sh)	2910(sh)	2920(w)	
2880(sh)	2870(w)	2880(w)	
1620		2840(w)	
		2700-2500	νOH
		2720(w)	
		2670(w)	bonded OH + aliphatic combination
		2600(w)	
1620-1560(s,b)	1555(s,b)	1740-1700(vs,b)	$\nu(\text{C=O})$
1462(w)	1460(w)	1465(sh)	$\nu\text{OCO asym}$
1445(w)	1435(s)		CH_2 bend
1420(w)	1420(sh)	1455(m)	CH_3 bend
		1420(s)	$\text{COOH, OH bend} + \text{CH}_2$ bend
1385(sh)	1380(s)	1375(sh)	CH_3 def
1360(s)	1350(m)		$\nu\text{OCO sym} + \text{CH}_3$ def
1335(w)	1335(sh)	1328(vw)	CH_2 twist and wag
1310(m)	1305(s)	1300(s)	
1268(m)	1255(w)	1270(m)	$\text{COOH, C-O str} + \text{CH}$ wag

Table 4.3 continued

Zn(II)etmal). 2H ₂ O		Cd(II)etmal. H ₂ O		ethylmalonic acid	Assignments
1240(m)	1240(w)	1230(m)	1230(m)		CH ₂ wag
	1225(sh)	1200(m)	1200(m)		
1145(m)	1140(v,w)	1118(sh)	1118(sh)		v(C-C)
1093(m)	1095(m)	1090(s)	1090(s)		
1035(m)	1040(w)	1045(m)	1045(m)		C-C str or CH ₃ def
980(m)	970(m)	940(s,b)	940(s,b)	π(OH)	v(C-C)
960(m)	948(w)				
895(m)	890(w)	880(sh)	880(sh)		CH ₂ rock
860(sh)	855(sh)				
800(w)	805(s)	780(s)	780(s)	δ(COOH)	δ(OCO)
760(w)					
715(w)	725(sh)				δ(OCO)
690(m)	700(w)	678(s)	678(s)	π(COOH)	OCO wag
	672(s)				
560(m)	550(m)				
450(w)	530(w)				v(M-O)+ring

Table 4.4 The infrared spectra of some ethylmalonate complexes (band position in cm^{-1})

$\text{K}_3[\text{Al}(\text{etmal})_3] \cdot 6\text{H}_2\text{O}$	$\text{Na}_3[\text{Fe}(\text{etmal})_3] \cdot 2\text{H}_2\text{O}$	$\text{K}[\text{Mn}(\text{etmal})_2(\text{H}_2\text{O})_2]$	Assignments
3515 (w)	3520 (m)	3360 (s,b)	$\nu\text{H}_2\text{O}$
3300-3100 (s,b)	3400 (s)		
2980 (sh)	2970 (m)	2970 (s)	νCH
2960	2940 (m)	2940 (m)	
2930 (w)	2880 (s)	2880 (m)	
2870	2850 (sh)	2850 (sh)	
1640-1610 (s,b)	1615 (s,b)	1580 (s,b)	$\nu\text{OCO asym}$
1465 (sh)	1465 (sh)	1460 (sh)	CH_2 bend
1420 (s)	1425 (sh)	1430 (m)	CH_2 bend and CH_3 def
	1390 (m)	1382 (sh)	
1340 (m)	1345 (s)	1360 (s)	$\nu\text{OCO sym, CH}_3$ def
1315 (sh)	1330 (sh)	1330 (w)	CH_2 twisting and wag
1305 (sh)	1310 (s)	1305 (sh)	
1270 (sh)	1275 (m)	1290 (sh)	
1240 (m)	1240 (s)	1245 (w)	CH_2 wag
1210 (w)	1210 (sh)	1185 (w)	$\nu(\text{C-C})$
1140 (w)	1140 (m)	1155 (w)	$\nu(\text{C-C})$
1090 (m)	1090 (m)	1125 (m)	C-C str or CH_3 def
		1095	
1055 (w)	1055 (w)	1050 (w)	
1035 (w)	1035 (w)	1025 (m)	

Table 4.4 continued

$K_3[Al(etmal)_3] \cdot 6H_2O$	$Na_3[Fe(etmal)_3] \cdot 2H_2O$	$K[Mn(etmal)_2(H_2O)_2]$	Assignments
980 (sh)	955 (s)	955 (sh)	$\nu(C-C)$
960 (m)	955 (s)	955 (sh)	$\nu(C-C)$
900 (w)	892 (m)	915 (w)	CH_2 rock
820 (s)	805 (sh)	805 (m)	$\delta(OCO)$
810 (s)	800 (sh)		
735 (m)	735 (s)	765 (w)	$\delta(OCO)$
720 (m)	730		
680 (m)	690 (w)	695 (m)	OCO wag
570 (s)	555 (s)	565 (w)	$\nu(M-O) + ring$
		525 (vw)	
480 (m)	470 (m)	470 (w)	
440 (m)	450 (w)		

are associated with wagging and twisting motions of methylene groups is known to have some relationship to the number of carbon atoms in a methylene chain; it is approximately equal to or greater by half than half the number of carbon atoms depending on whether the latter is even or odd. From the table it can be seen that there is an increase of number of these bands in the case of ethylmalonato metal compounds. These bands which remain fairly constant in the acid and the series of compounds studied appear at ~ 1330 , ~ 1300 , ~ 1260 , ~ 1240 , $\sim 1150 \text{ cm}^{-1}$ compared to the bands at $\sim 1280 \text{ cm}^{-1}$ and 1180 cm^{-1} in the malonato metal compounds. More of these progression bands were apparent for the salts than for the corresponding acid, and this is due to the removal of an interfering peak (at $\sim 1350 \text{ cm}^{-1}$) attributable to the C-O-H grouping.

The assignment of the COO symmetric band, which falls in the region of the symmetric deformation of the CH_3 group, is difficult. Also any bands due to the group $\text{CH}_3\text{-CH}_2$ which appear in a similar region and the presence of many bands in this region makes any assignment ambiguous. However, there are two bands one, at $\sim 1385 \text{ cm}^{-1}$ and another strong broad band at $\sim 1350 \text{ cm}^{-1}$, which may be assigned to the methyl group deformation and the symmetric COO stretching frequencies respectively. The former remains almost unchanged in value in the acid and the corresponding salts.

The COO antisymmetric stretching frequencies lie at $1600 - 1550 \text{ cm}^{-1}$ somewhat lower than those of the malonate compounds and are shifted to higher frequency as the metal is changed in the order $\text{Cd(II)} < \text{Zn(II)}$, $\text{Co(II)} < \text{Ni(II)} < \text{Cu(II)}$. The relative stabilities of these compounds follow a similar order¹⁴. A linear relationship was also observed between the antisymmetric COO stretching frequency and the electronegativity of the alkaline-earth metals in the order $\text{Ba(II)} < \text{Ca(II)} < \text{Mg(II)}$ as in the case in malonate compounds. The strength of M-O bonding also increases along the series, in agreement

with those of malonate compounds.

All the hydrated compounds show a broad band at $\sim 3420 - 3300 \text{ cm}^{-1}$ ($\nu \text{ H}_2\text{O}$). In basic Ni(II) and Ba(II) ethylmalonate salts the corresponding bands occur together with a sharp single band at ~ 3540 and 3400 cm^{-1} respectively, which is characteristic of the free OH stretching frequency, although it occurs at somewhat lower frequencies than is normally observed for these bands.

The region $1500 - 1300 \text{ cm}^{-1}$, where the frequencies of CH_3 and CH_2 deformation appear is interesting; malonate compounds show a single band only, at $\sim 1450 \text{ cm}^{-1}$ with higher intensity. On passing from malonate to ethylmalonate compounds, the band at 1450 cm^{-1} connected with the CH_2 deformation vibration splits into a pair at ~ 1460 and 1425 cm^{-1} due to the introduction of $\text{CH}_3\text{-CH}_2$ groups. The other CH_2 group deformation vibration at $\sim 1280 \text{ cm}^{-1}$ in malonate compounds is more intense and splits in ethylmalonate compounds to 1265 and 1240 cm^{-1} bands owing to the presence of CH_3 and CH_2 .

The other constant frequencies of ethylmalonate and ethylmalonic acid are found at ~ 1090 and $\sim 1035 \text{ cm}^{-1}$ which could be the results of either the stretching vibrations of the C-C bond or the CH_3 deformation vibration. In ethylmalonate metal complexes the band at 1035 cm^{-1} appears as a doublet at 1035 and 1055 cm^{-1} .

Several bands have been observed below 800 cm^{-1} ; by analogy with malonate compounds these bands can be assigned to the OCO deformation vibrations of the ethylmalonate ion and the COOH in-plane and out-of-plane deformation vibrations of ethylmalonic acid. The OCO deformation vibration of the simple ethylmalonate around 800 cm^{-1} splits in the ethylmalonate M(III) complexes.

The region below 600 cm^{-1} contains several bands. On examining the spectra of the acid and its salts below 600 cm^{-1} , the new bands appearing in the region $560 - 450 \text{ cm}^{-1}$ are tentatively assigned to M-O

stretching modes. The corresponding band is shifted to higher frequency in the ethylmalonate metal complexes.

4.5 Benzylmalonato Metal Compounds

The infrared absorption spectra of benzylmalonic acid, bivalent metals and tris-benzylmalonate metal complexes have been studied. Most of the observed frequencies in the region $4000 - 400 \text{ cm}^{-1}$ have been reported in terms of being characteristic of either the aliphatic, aromatic or carboxylic portions of the molecule. The assignments made in the following discussion are based on a comparative study of these and data from the literature.³ These are listed in Tables 4.5 and 4.6.

Results and Discussions

The observed frequencies are divided into three groups; vibrations of aliphatic portions (methylene groups), vibrations of the aromatic portions (phenyl groups) and vibrations of the carboxyl groups. The interpretation of the observed spectrum in terms of vibrations involving the aliphatic and aromatic portions of the molecule is straightforward.³ The only doubtful assignment is that of the bending mode of the methylene group adjacent to the COOH group. However the strong band observed at 1410 cm^{-1} has been considered for this frequency.

The infrared absorption spectra of benzylmalonic acid and its compounds are very similar. As expected those frequencies which are characteristic of the aliphatic and aromatic portions of the molecule will remain nearly unchanged in going from the acid to the salts and complexes (Table 4.5, 4.6), whereas those frequencies related to the carboxyl group are markedly changed.

However, the C=O stretching vibrations of the acid can be assigned to the strong double band at 1760 and 1730 cm^{-1} , somewhat higher than those of the ethylmalonic acid and malonic acid itself. The C-O stretching coupled with OH deformation vibration gives the strong bands at

Table 4.5 The infrared spectra of some metal benzylmalonates and benzylmalonate complexes (band position in cm^{-1})

	Mg(II)benzylmal, $\text{Mg}(\text{OH})_2 \cdot 2\text{H}_2\text{O}$	Ca(II)benzylmal, $\text{Ca}(\text{OH})_2$	Ba(II)benzylmal, $\text{Ba}(\text{OH})_2 \cdot 1/2\text{H}_2\text{O}$	Cu(II)benzylmal, $1/2\text{H}_2\text{O}$	Ni(II)benzylmal, $2\text{H}_2\text{O}$	Assignments
3600 (sh)		3610 (w)				$\nu(\text{OH})$
3360 (sh)	3420 (w,b)	3380 (w,b)		3630 (m)	3350 (s,b)	$\nu(\text{H}_2\text{O})$
3090 (sh)	3080 (w)	3090 (s)		3550 (m)	3200 (m)	
3060 (sh)	3060 (w)	3060 (vw)		3080 (w)	3085 (sh)	aromatic; CH str
3030 (sh)	3030 (m)	3030 (w)		3060 (w)	3060 (w)	
2960 (sh)	2960 (sh)	2960 (sh)		3025 (m)	3030 (w)	
2930 (sh)	2925 (w)	2930 (vw)		2990 (sh)	2970 (sh)	aliphatic; CH str
2860 (sh)	2860 (w)	2860 (sh)		2930 (w)	2950 (sh)	
2830 (sh)	2830 (w)	2830 (sh)		2890 (sh)	2930 (w)	
				2850 (vw)	2870 (sh)	
1950 (vw)	1880 (w)				2830 (w)	
1885 (vw)				1970 (vw)		aromatic; combinations
				1950 (vw)		
				1665 (s)		
1590 (vs,b)	1570 (s,b)	1568 (s,b)		1610 (s)	1570 (vs,b)	ν as (C=O)+ring
1555 (sh)	1540 (sh)	1540 (sh)		1590 (s)	1540 (sh)	vibration
				1550 (s)		
1495 (m)	1495 (w)	1495 (m)		1495 (m)	1495 (m)	aromatic C-C str
1452 (sh)	1455 (s)	1455 (sh)		1452 (s)	1452 (vw)	aliphatic; CH bend
				1432 (m)		in CH_2
1440 (s)	1440 (sh)	1440 (s)				
1420 (sh)	1420 (sh)	1420 (sh)		1420 (sh)	1420 (s,b)	

Table 4.5 continued

Mg(II)benzylmal, Mg(OH) ₂ ·2H ₂ O	Ca(II)benzylmal, Ca(OH) ₂	Ba(II)benzylmal, Ba(OH) ₂ ·1/2H ₂ O	Cu(II)benzylmal, 1/2H ₂ O	Ni(II)benzylmal, 2H ₂ O	Assignments
1405 (sh)	1385 (sh)	1385 (sh)	1385 (sh)	1395 (sh)	aliphatic, C-H
1350 (s)	1355 (s) 1340 (sh)	1330 (s,b)	1350 (vs)	1355 (m)	bend + ν(OCO)sym
1320 (sh)	1325 (w)		1325 (sh)	1315 (w)	aromatic ring breath
1290 (vw)	1290 (w)	1290 (w)	1295 (w)	1295 (w)	in plane C-H
1240 (vw)	1240 (w)	1230 (w)	1240 (vw)		aliphatic C-H wag
1212 (sh)	1210 (w)		1215 (sh)	1215 (sh)	aromatic
1205 (sh)		1205 (sh)	1205 (w)	1205 (sh)	
1175 (sh)	1173 (sh)	1170 (sh)	1178 (m)	1175 (m)	
1155 (sh)	1155 (sh)	1155 (sh)	1160 (vw)	1155 (sh)	
1110 (vw)	1105 (sh)	1110 (sh)	1110 (vw)	1110 (vw)	aromatic
			1100 (vw)		
1079 (w)	1079 (w)	1079 (vw)	1070 (m)	1080 (m)	aromatic + aliphatic C-C str
1030 (w)	1030 (vw)	1030 (vw)	1030 (w)	1030 (m)	aromatic CH bend in plane def of ring
1005 (vw)	993 (vw)				
965 (m)	970 (m)	965 (vw)	968 (m)	960 (m)	aliphatic CH ₂ rock
910 (w)	909 (w)	910 (vw)	912 (m)	912 (w)	aromatic
850 (sh)	863 (s)	862 (w)	880 (m)		
			855 (s)	850 (m)	aromatic
825 (sh)	838 (w)	825 (sh)	822 (w)	820 (w)	aromatic

Table 4.5 continued

Mg(OH) ₂ ·2H ₂ O	Ca(II)benzylmal, Ca(OH) ₂	Ba(II)benzylmal, Ba(OH) ₂ ·1/2 H ₂ O	Cu(II)benzylmal, 1/2 H ₂ O	Ni(II)benzylmal, 2H ₂ O	Assignments
755 (vw)	760 (sh)	753 (m)	755 (s)	750 (w)	aromatic C-H bend
735 (sh)	745 (m)	735 (sh)			
725 (sh)	715 (s)	725 (sh)		720 (w)	
700 (m)	695 (s)	700 (s)	700 (s)	700	
665 (vw)	650 (s)	655 (sh)	650 (m)	670 (vw)	OCO deformation
			610 (m)	600 (vw)	
570 (vw)	570 (m)	570 (vw)	578 (m)	570 (w)	ν(M-O) + ν ring
555 (sh)		555 (sh)		560 (sh)	
530 (sh)	535 (s)	535 (sh)			
465 (sh)	455 (sh)	460 (sh)	480 (w)	470 (sh)	

Table 4.5 continued

	Zn(II)benzylmal. 2½H ₂ O	Cd(II)benzylmal .H ₂ O	K ₃ [Al(benzylmal) ₃] .3H ₂ O	Na ₃ [Fe(benzylmal) ₃] .2H ₂ O	K[Mn(benzylmal) ₂ (H ₂ O) ₂]	Assignments
3560(w)	3360(sh)	3430(s,b)	3420(s,b)	3360(s,b)	ν(H ₂ O)	
3280(s,b)						
3085(sh)	3080(sh)	3082(w)	3083(w)	3080(sh)	aromatic; CH str	
3060(sh)	3060(sh)	3060(w)	3060(m)	3060(w)		
3030(w)	3025(w)	3030(m)	3030(m)	3030(w)		
2980(vw)	2960(sh)	2960(sh)	2960(sh)	2960(sh)	aliphatic; CH str	
2940(sh)	2930(w)	2930(w)	2930(w)	2930(sh)		
2930(sh)	2920(w)					
2890(vw)	2870(sh)	2870(sh)	2860(w)	2870(sh)		
2850(sh)	2850(sh)	2855(w)				
1960(vw)		1950(w)	1950(w)	1950(w)	aromatic; combinations	
1890(vw)		1880(w)	1880(vw)	1880(w)		
				1815(m)		
1600(vs,b)	1560(s,b)	1635(vs,b)	1610(vs,b)	1590(s,b)	ν as (C=O)+ring vibrations	
1580(sh)						
1540(sh)	1535(sh)					
1495(sh)	1495(w)	1495(w)	1495(m)	1495(m)	aromatic C-C str	
1452(sh)	1452(sh)	1452(sh)	1452(s)	1452(vw)	aliphatic, C-H bend in CH ₂	
1435(s)	1445(s)					
1415(s)	1420(sh)	1420(sh)	1420(sh)			
1385(sh)	1395(sh)			1420(vw)		

Table 4.5 continued

$Zn(II)benzylmal \cdot H_2O$	$K_3[Al(benzylmal)_3 \cdot 3H_2O]$	$Na_3[Fe(benzylmal)_3 \cdot 2H_2O]$	$K[Mn(benzylmal)_2(H_2O)_2]$	Assignments
1350(m,b)	1370(s)	1400(s)	1400(s)	aliphatic, C-H bend + $\nu(OCO)$ sym
1320(m)	1330(vw)	1315(w)	1315(sh)	aromatic ring breadth
	1320(sh)	1290(sh)		in plane C-H
1278(m)	1285(w)	1260(m)	1280(sh)	aliphatic CH wag
1235(w)	1240(vw)	1230(m)	1230(vw)	
1212(vw)	1215(sh)	1205(vw)	1205(sh)	aromatic
1205(vw)	1205(sh)			
1175(vw)	1175(sh)	1180(w)	1155(w)	
1165(w)	1165(vw)	1155(sh)		
	1125(w)			
1100(m)	1105(sh)	1110(m)	1110(vw)	aromatic
1079(w)	1075(m)	1078(w)	1080(m)	aromatic + aliphatic
1025(w)	1025(w)	1030(w)	1030(m)	C-C str
		1000(vw)		aromatic CH bend in plane def of ring
965(s)	960(m)	962(s)	960(vw)	aliphatic CH_2 rock
915(sh)	915(sh)	915(m)	915(w)	aromatic
872(w)	885(w)	885(m)	870(w)	aromatic
855(w)	840(w)	862(m)	855	

Table 4.5 continued

$Zn(II)$ benzylmal. $2\frac{1}{2}H_2O$	$Cd(II)$ benzylmal $.H_2O$	$K_3[Al(benzylmal)_3]$ $.3H_2O$	$Na_3[Fe(benzylmal)_3]$ $.2H_2O$	$K[Mn(benzylmal)_2(H_2O)_2]$	Assignments
820 (m)	825 (sh)	810 (w)	820 (sh)	820 (sh)	aromatic
765 (m)					
745 (w)	750 (m)	745 (s)	750 (m)	750 (m)	aromatic C-H bend
725 (m)	715 (sh)	700 (s)	700 (s)	700 (s)	
660 (vw)	650 (sh)	660 (vw)	670 (sh)	610 (w)	OCO deformation
595 (m)	590 (w)	610 (m)	590 (m)		
575 (w)	575 (m)	570 (w)	570 (sh)	570 (w,b)	$\nu(M-O) + \nu$ ring
555 (w)		550 (w)	555 (w)		
530 (w)	530 (w)	535 (vw)		530 (w)	
470 (sh)	465 (sh)	490 (s)	460 (w)	460 (sh)	

Table 4.6 The infrared spectra of benzylmalonic acid (band position in cm^{-1})

Assignments	
3120(m)	aromatic; CH str and OH str COOH
3070(w)	
3030(w)	
3000(w)	
2940(w)	aliphatic, CH str
2925(sh)	
2855(sh)	
2800(sh)	
2720(sh)	COOH; bonded OH + aliphatic combinations
2660(w)	
2580(w)	
2530(w)	
1955(w)	aromatic; combinations
1890(w)	
1860(w)	
1760(vs)	COOH, free C = O str + CH_2 bend
1735(s)	
1685(s)	
1602(w)	aromatic, combination
1585(w)	aromatic C-C str
1495(m)	
1452(s)	aliphatic, C-H bend in CH_2
1443(w)	$\nu(\text{CO}) + \delta(\text{OH})$
1425(sh)	

Table 4.6 continued

	<u>Assignments</u>
1410(vs)	CH ₂ bend
1348(w)	aromatic ring breath in plane CH
1320(m)	
1270(vs)	COOH, C-O str + aliphatic CH wag
1240(s)	COOH; CO str
1205(s)	aromatic
1185(sh)	
1162(s)	
1155(sh)	
1082(w)	aromatic + aliphatic C-C str
1052(m)	
1030(w)	aromatic, C-H bend in plane
1000(w)	def of ring
950(s)	aliphatic, CH ₂ rock
915(w)	aromatic
865(s)	aromatic; COOH, OH bend
845(w)	aromatic
830(w)	aromatic
750(s)	aromatic, CH out of plane def
700(s)	
665(sh)	π COOH
655(s)	

1410 cm^{-1} and 1270 and 1240 cm^{-1} respectively. In benzylmalonate compounds the corresponding band disappears and is replaced by the strong broad bands between $\sim 1550 - 1510 \text{ cm}^{-1}$ and $\sim 1400 - 1300 \text{ cm}^{-1}$, which can be assigned to antisymmetric and symmetric COO stretching vibrations, respectively. Malonic acid, ethylmalonic acid and corresponding compounds have shown similar effects. The assignments of the bands in the region 1600 - 1500 cm^{-1} is difficult. The COO antisymmetric stretching is expected in this region as well as the aromatic C=C stretching frequencies, and the presence of many bands in this region makes any assignment ambiguous. However the bands due to the phenyl group at ~ 1610 and 1585 cm^{-1} can be easily identified in the spectra of the benzylmalonic acid. On passing from the acid to the salts these bands are obscured or appear as shoulders on the main strong broad band of COO antisymmetric stretching frequencies. The fairly constant band observed in the acid and all the compounds at 1495 cm^{-1} is also due to the aromatic C=C stretching frequencies. The strong double bands observed at 1452 and 1440 cm^{-1} may, by analogy with those of the malonate and ethylmalonate compounds, be assigned to the CH_2 deformation vibration.

In the spectra of benzylmalonate compounds the symmetrical COO stretching falls in the region of the CH deformation modes, so that only an approximate value can be given for this frequency.

Absorptions below 1300 cm^{-1} are very similar to those of the ethylmalonate compounds. The absorption bands at 1290 and 1240 cm^{-1} correspond to those at ~ 1270 and $\sim 1240 \text{ cm}^{-1}$ of ethylmalonate compounds and may therefore be assigned to the CH_2 deformation vibrations. In benzylmalonate compounds both bands are much reduced in intensity. The bands observed at ~ 1320 and $\sim 1290 \text{ cm}^{-1}$, and the double band at 1200 and 1215 cm^{-1} are the aromatic and aliphatic CH deformation vibrations, respectively. The other constant frequencies of the acid and the compounds are found in the region $1200 - 650 \text{ cm}^{-1}$. A series of strong

bands appear between $1000 - 650 \text{ cm}^{-1}$ which are related to the aromatic CH-out-of-plane deformation vibrations. The strongest bands in this region are found at 700 and 750 cm^{-1} . They remain almost unchanged in the acid and the corresponding compounds. These bands and a series of relatively weak bands at 1200 , $1175 - 1110$, $\sim 1080 \text{ cm}^{-1}$ are characteristic frequencies of the mono substituted aromatic compounds. The aromatic CH stretching vibrations produce bands close to 3030 cm^{-1} on the side of the main, much stronger CH_2 absorption bands below 3000 cm^{-1} .

All the hydrated complexes show a strong broad band around 3350 cm^{-1} , due to the stretching vibrations of the water molecules. In the spectra of Mg(II) , Ca(II) and Ba(II) benzylmalonates a sharp singlet band occurs at a higher frequency around 3610 cm^{-1} as a shoulder on the broad water band. The latter band is of the type usually found in hydroxy complexes¹⁷ and is characteristic of the free OH stretching frequency.

Here again the relationship exists between the antisymmetric COO frequency and the electronegativity of the alkaline-earth metal constituent of the molecules, as in the case of malonate and ethylmalonate alkaline-earth metal compounds. It was also found that the COO antisymmetric stretching frequency is shifted as the bivalent metal is changed, in the same direction observed for the malonate and ethylmalonate M(II) compounds having similar structure. The results are in good agreement with the stability order of divalent metal compounds of other ligands.^{14,18}

The C=O and C-O stretching frequencies can be used as a measure of the strength of the coordination bonds in a series of metal carboxylate complexes. In a series of metal oxalato complexes, the frequencies of uncoordinated C=O stretching bands increase, and those of coordinated C-O stretching decrease, as the frequency of the M-O stretching band increases. The magnitude of these band shifts becomes larger as

the coordination bond becomes stronger. On comparison of the I.R. absorption spectra of the malonate, ethylmalonate and benzylmalonate compounds (see Tables) it is seen that the magnitude of these band shifts is in the order ethylmalonate < malonate < benzylmalonate. These results suggest that the strength of the coordination bond to the metal increases along the series, which also suggest that the benzylmalonato compounds are more stable than the corresponding malonate and ethylmalonate compounds. This is expected since benzylmalonic acid has greater strength of bonding to the metal ion.¹⁹

The effect of substitution on the stability of some malonate ions has been studied.²⁰ It has been pointed out, that the substitution of the ethyl group causes a slight decrease in the stability of the malonate ion, while the substitution of the benzyl group increases the coordination power of the carboxylate ion, and therefore increases the strength of bonding to the metal¹⁹.

The infrared spectra of the benzylmalonate salts and benzylmalonato metal complexes are very similar, except that in the complexes, the antisymmetric and symmetric COO frequency are shifted to higher and lower frequencies respectively than the corresponding simple salts, in agreement with the results of malonate and ethylmalonate metal complexes. The magnitude of this shift in Al(III) benzylmalonato complexes is higher than that of the Fe(III) complexes which may indicate stronger M-O bonding. This is consistent with the results of those of other M(III) carboxylate complexes.^{7,8}

REFERENCES

1. K. Nakamoto and P.J. MacCarthy, "Spectroscopy and structure of metal chelates compounds", John Wiley and Sons Inc., 1968.
2. K. Nakamoto, "Infrared spectra of inorganic and coordination compounds", Inc. N.Y., 1963.
3. L.J. Bellamy, "Infrared spectra of complex molecules", Methuen, 1964, London.
4. K. Nakamoto, J. Fujita, S. Tanaka and M. Kobayashi, J. Amer. Chem. Soc., 1957, 79, 4904.
5. J. Fujita, A.E. Martell and K. Nakamoto, J. Chem. Phys., 1962, 36, 339.
6. M.J. Schmelz, T. Miyazawa, S.I. Mizushima, T.J. Lane and J.V. Quagliano, Spectrochim. Acta., 1957, 9, 51.
7. D.P. Graddon, J. Inorg. Nucl. Chem., 1956, 3, 308.
8. J. Fujita, A.E. Martell and K. Nakomoto, J. Chem. Phys., 1962, 36, 324.
9. M.C. Flett, J. Chem. Soc., 1951, 962.
10. M.J. Schmelz, I. Nakagawa, S.I. Mizushima and J.V. Quagliano, J. Amer. Chem. Soc., 1959, 81, 287.
11. K. Kuroda and M. Kubo, J. Phys. Chem., 1960, 64, 759.
12. R.E. Kagarise, J. Phys. Chem., 1955, 59, 271.
13. B. Ellis and H. Pyszora, Nature., 1958, 181, 181.
14. A.E. Martell and M. Calvin, "Chemistry of the metal chelate compounds", p. 193.
15. A.E. Martell and M. Calvin, "Chemistry of the Metal Chelate Compounds", p. 514.
16. J. Fujita, A.E. Martell and K. Nakomoto, J. Chem. Phys., 1962, 36, 331.

17. K. Nakomoto, "Infrared spectra of inorganic and coordination compounds", Inc. N.Y., 1963, p. 82.
18. V.S.K. Nair and S. Parthasarathy, *J. Inorg. Nucl. Chem.*, 1970, 32, 3289.
19. A.E. Martell and M. Calvin, "Chemistry of the metal chelate compounds", p. 409.
20. D.J.G. Ives and H.L. Riley, *J. Chem. Soc.*, 1932, 1766.
21. A. Oskarsson, *Acta Cryst.*, 1978, B34, 1350.
22. E. Hansson, *Acta Chem. Scand.*, 1973, 27, 2827.
22. E. Hansson, *Acta Chem. Scand.*, 1973, 27, 2441.
23. E. Hansson, *Acta Chem. Scand.*, 1973, 27, 2841.
24. M.L. Post and J. Trotter, *J. Chem. Soc. Dalton.*, 1974, 1922.
25. G. Duc, R. Faure and H. Loiseleur, *Acta Cryst.*, 1978, B34, 2115.
26. B. Briggman and A. Oskarsson, *Acta Cryst.*, 1978, B34, 3357.
27. B. Briggman, A. Oskarsson, *Acta Cryst.*, 1977, B33, 1900.
28. A. Karipides and A.T. Reed, *J. Inorg. Chem.*, 1977, 16, 3299.
29. T. Lis, J. Matuszewski, B. Jezowska-Trez, *Acta Cryst.*, 1977, B33, 1943.
30. T. Lis and J. Matuzewski, *Acta Cryst.*, 1979, B35, 2212.

CHAPTER V: MAGNETOCHEMISTRY^{1-7*}

5.1 Introduction

(1) Normal Paramagnetism

The theory of paramagnetic and electric susceptibilities has been fully described by Van Vleck.⁷ If a substance with a permanent magnetic moment μ is placed in a magnetic field with the molecular magnets free to orient themselves, they will be subjected to two opposing effects. These are (i) the magnetic field of strength H which tends to align all molecular magnets in the same direction as that of the field, and (ii) the thermal agitation (the kT effect), which tends to randomise the direction of the molecular magnets. Clearly, as T decreases, the effect of the applied field becomes relatively stronger. In an ideal system, in which the dipoles are so far apart that no interaction takes place between them, the molar paramagnetic susceptibility is inversely proportional to the absolute temperature:

$$\chi_M = \frac{N\mu^2}{3kT} \quad (1)$$

where N is Avogadro's number, μ is the permanent magnetic moment, k the Boltzmann constant, and T the absolute temperature. From this expression it follows that

$$\mu = \sqrt{\frac{3kT \chi_M}{N}} \quad (2)$$

When a value of χ_M is determined for a paramagnetic substance, it is necessary for precise work to correct for the diamagnetic contribution and for the temperature - independent paramagnetism, TIP, sometimes called Van Vleck high frequency paramagnetism. A susceptibility which has been corrected for the presence of diamagnetic components is denoted

* The references for this section are on pages 165, 166 and 167.

by "corrected molar susceptibility" χ_M^{corr} or χ_M' which equals $\chi_M - \chi_D$ where χ_D is the sum of the diamagnetic contributions to the susceptibility. The value of the magnetic moment obtained using χ_M' is called the "effective magnetic moment", μ_{eff} . Substituting for the fundamental constants in the above expression we obtain the relationship:

$$\mu_{\text{eff}} = 2.84 \sqrt{\chi_M' \times T} \text{ B.M.} \quad (3)$$

Magnetic moments are now expressed in Bohr magnetons (B.M.); this is the natural unit of magnetism and equals the magnetic moment of an electron assumed to be "spinning" on its own axis. It is given by the expression $eh/4\pi mc$ and has the numerical value of 9.273×10^{-21} erg gauss⁻¹. The value of μ obtained from the above formula is a constant only when χ_M is proportional to $1/T$. The temperature dependence of the magnetic susceptibility of a paramagnetic substance is given in the ideal case by Curie's law:

$$\chi_M = \frac{C}{T} \quad (4)$$

where T represents the absolute temperature, and C is the Curie constant. Curie's law is generally applicable to a magnetically dilute system, that is, one in which magnetic interaction between neighbouring molecules is negligible. The susceptibilities of many paramagnetic substances change with temperature according to the modified Curie law (Curie-Weiss law):

$$\chi_M = \frac{C}{T + \theta} \quad (5)$$

where θ is a constant known as the "Weiss constant" at least over a considerable range of temperature. P. Weiss obtained this expression by consideration of the mutual interaction of the elementary magnets or molecular magnetic fields. The value of θ is constant over a smaller or greater temperature range, the significance of this is discussed by

Selwood.⁶ The magnetic susceptibility of many compounds is much better expressed by the Curie-Weiss law than by the Curie law alone, but no particular significance can, in general, be attached to θ . θ is an empirical factor and is simply a measure of how the origin of the paramagnetism, in the system, departs from the ideal basis on which the Curie law is derived.

(2) Temperature-independent Paramagnetism (TIP) or "Van Vleck high frequency paramagnetism"

Van Vleck's treatment of paramagnetism refers only to atoms in which the spin angular momenta, s , of all the electrons can combine to form a resultant S , and independently the orbital angular momenta l combine to form a resultant L . Application of Van Vleck's theory⁷ to various paramagnetic systems is rather complex, but it accounts for departures from the Curie-Weiss law. It depends entirely on the magnitude of the spin multiplet intervals as compared to Boltzmann distribution factor, kT . This gives rise to three specific situations in which the spin multiplet intervals may be (1) small, (2) large, or (3) nearly equal, as compared with kT . The import of this terminology is quoted from Van Vleck.⁷ The final results of Van Vleck's calculations are as follows.

(1) Multiplet intervals small compared to kT :

$$\chi_M = \frac{N\beta^2}{3kT} [4S(S+1) + L(L+1)] \quad (6)$$

where S and L are the resultant spin and orbital moments, respectively. This expression is used for calculating susceptibilities of ions of most transition-group elements when no orbital quenching takes place.

(2) Multiplet intervals large compared to kT :

$$\chi_M = \frac{N\beta^2 J(J+1)}{3kT} + \frac{N\beta^2}{6(2J+1)} \left[\frac{F(J+1)}{h\nu(J+1;J)} - \frac{F(J)}{h\nu(J+1;J)} \right] \quad (7)$$

where β is the Bohr magneton and

$$F(J) = \frac{1}{J} [(S + L + 1)^2 - J^2][J^2 - (S - L)^2]$$

(3) Multiplet intervals comparable to kT :

In this case, the effect of the quantum number J is comparable with kT . This case involves summation of the contributions of atoms with different values of J . The number N_J , that is the number of atoms in a mole with a given value of J , is determined by the Boltzmann temperature factor

$$\chi_M = N \sum_{J=|L-S|}^{L+S} \frac{\{[g_j^2 \beta^2 J(J+1)/3kT] + \alpha_j\} (2J+1) e^{-W_j^0/kT}}{\sum_j (2J+1) e^{-W_j^0/kT}} \quad (8)$$

According to Van Vleck when the multiplet intervals are small or large compared to kT , the Curie law should be obeyed, neglecting the temperature-independent paramagnetic contribution to susceptibility arising from high-frequency elements. But where the multiplet intervals are comparable to kT , Boltzmann distribution between various energy levels occurs, which results in large departures from the Curie law.

The Magnetic Properties of the First Transition Group Elements and their Ions

Various efforts have been made to calculate the effective moments of the ions of the elements of the first row transition series. It has been found that, in general, none of the theoretical formulae fits the experimental data perfectly but the best agreement with experiment is obtained by completely neglecting the orbital contribution, the $L(L+1)$ term, from $\mu_{\text{eff}} = \sqrt{4S(S+1)+L(L+1)}$ B.M., leaving what is often referred to as the so-called 'spin only' expression

$$\mu_{\text{eff}} = \sqrt{4S(S+1)} = \sqrt{n(n+2)} \quad \text{B.M.}$$

This effect is commonly known as "quenching" of the orbital contribution and in transition metal complexes it can be interpreted in terms of the

crystal-field theory by a change in symmetry.

During complex formation the presence of a ligand field removes the degeneracy of the d-orbitals and thereby, the rotation mechanism to transform the orbital into an equivalent and degenerate orbital which does not already contain an electron with the same spin becomes impossible. For complexes with octahedral symmetry the equivalence of the $d_{x^2-y^2}$ and d_{xy} orbitals has been destroyed, the consequence of this is that the important source of orbital contribution in the free ion is no longer possible and hence their orbital contribution of 2 units vanishes. The t_{2g} set of orbitals remain degenerate and consequently are capable of giving an orbital contribution to the magnetic moment unless occupied by paired electrons. Hence the t_{2g}^3 electronic configuration does not contribute to the orbital angular momentum because any attempt at rotation will put two electrons of the same spin in a single orbital, contrary to the exclusion principle. Further, since $d_{x^2-y^2}$ and d_{z^2} orbitals, being of different shapes, cannot be transformed into each other by rotation about any axis, there can be no orbital contribution associated with this pair of orbitals.

In Table 5.1 are listed experimental and theoretical (spin-only) values of the magnetic moments of a number of metals of the first row transition series. It may be observed that the experimental values, in general, agree fairly well with theory, there is little departure from the spin-only moment in those configurations where complete quenching of the orbital contribution is required (d^8 , d^9), but no particular agreement with the theory is obvious when the quenching is incomplete (d^7). Thus it is possible in principle to use the spin only formula to calculate the magnetic moments of these ions in octahedral environments.

*Table 5.1 Magnetic moments of first row transition metal spin-free configurations 111.

No. of d electrons	L	S	Free ion ground term	$\mu = [4S(S+1) + L(L+1)]^{1/2}$ B.M.	$\mu_{s.o.} = [4S(S+1)]^{1/2}$ B.M.	μ observed at 300 K
1	2	$\frac{1}{2}$	$2D$	3.00	1.73	1.7-1.8
2	3	1	$3F$	4.47	2.83	2.8-2.9
3	3	$\frac{3}{2}$	$4F$	5.20	3.87	3.7-3.9
4	2	2	$5D$	5.48	4.90	4.8-5.0
5	0	$\frac{5}{2}$	$6S$	5.92	5.92	5.8-6.0
6	2	2	$5D$	5.48	4.90	5.1-5.7
7	3	$\frac{3}{2}$	$4F$	5.20	3.87	4.3-5.2
8	3	1	$3F$	4.47	2.83	2.9-3.9
9	2	$\frac{1}{2}$	$2D$	3.00	1.73	1.7-2.2
10	0	0	$1S$	0.00	0.00	0

*Table 5.2 Quenching of the orbital contribution, to the magnetic moment, due to the ligand field

No. of d-electrons	Free ion ground terms	Stereochemistry			Quenching of orbital contribution	Tetrahedral	
		Octahedral	ligand field ground term	Quenching of orbital contribution		$e^n t_2^m$ ground configuration	ligand field ground term
1	$2D$	t_{2g}^1	$2T_{2g}$	No	e^1	$2E$	Yes
2	$3F$	t_{2g}^2	$3T_{1g}$	No	e^2	$3A_2$	Yes
3	$4F$	t_{2g}^3	$4A_{2g}$	Yes	$e^2 t_2^1$	$4T_1$	No
4	$5D$	$t_{2g}^3 e_g^1$	$5E_g$	Yes	$e^2 t_2^2$	$5T_2$	No
		t_{2g}^4	$3T_{1g}$	No	-	-	-
5	$6S$	$t_{2g}^3 e_g^2$	$6A_{1g}$	Yes	$e^2 t_2^3$	$6A_1$	Yes
		t_{2g}^5	$2T_{2g}$	No	-	-	-
6	$5D$	$t_{2g}^4 e_g^2$	$5T_{2g}$	No	$e^3 t_2^3$	$5E$	Yes
		t_{2g}^6	$1A_{1g}$	Yes	-	-	-
7	$4F$	$t_{2g}^5 e_g^2$	$4T_{1g}$	No	$e^4 t_2^3$	$4A_2$	Yes
		$t_{2g}^6 e_g^1$	$2E_g$	Yes	-	-	-
8	$3F$	$t_{2g}^6 e_g^2$	$3A_{2g}$	Yes	$e^4 t_2^4$	$3T_1$	No
9	$2D$	$t_{2g}^6 e_g^3$	$2E_g$	Yes	$e^4 t_2^5$	$2T_2$	No

*taken from reference 56.

5.2 Experimental

Magnetic Susceptibility Measurement down to 'Liquid Nitrogen Temperature'

The low temperature measurements need a cryostat to maintain the low environmental temperature of the specimen. This cryostat necessitates a wide pole gap (approximately 6 cm) and so, in order to achieve reasonable fields for this type of measurement the Newport equipment is fitted with special pole tips to ensure that the positioning of the sample is not critical. To perform susceptibility measurements at low temperatures by the Gouy method a number of basic units are required. In the case of the Newport equipment they are:

1. Magnet and power supply capable of producing sufficient field intensity.
2. Semi-microbalance.
3. Cryostat for maintaining specimen and transducers in a nitrogen atmosphere at the low temperature.
4. Specimen temperature measurement and control units.

The general arrangement of the balance and cryostat is shown diagrammatically in Figure 5.1.

Magnetic susceptibilities were determined by the Gouy method using a Newport variable-temperature balance. The Gouy tube was calibrated using $\text{Hg}[\text{Co}(\text{CNS})_4]$ of known susceptibility¹ = 16.44×10^{-6} c.g.s. units decreasing by 0.05×10^{-6} per degree temperature rise, near room temperature.

All measurements were made over the temperature range 113 - 293 K, and with different field strengths (i.e., different magnetic currents) to confirm the absence of any ferromagnetic impurities.

A tube calibration constant (factor β) must be obtained before measurements can be made with a substance of known susceptibility. A number of readings were taken with different packing of the tube using

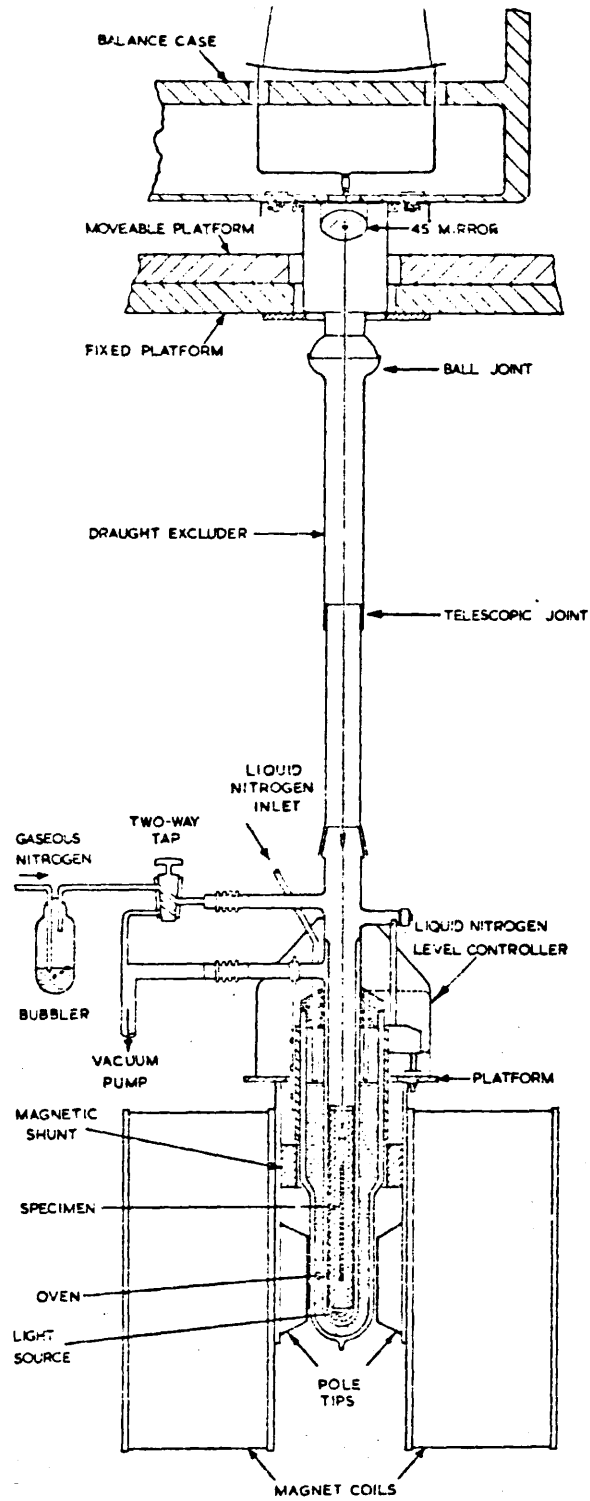


Fig.5.1. A diagram of the general arrangement of the balance and cryostat of the Newport equipment.

Hg[Co(CNS)₄] as calibrant. The determination and calculation of magnetic susceptibilities were performed according to the direction of Figgis and Lewis,² using the expression

$$10^6 \chi = \frac{\alpha + \beta F'}{W}$$

where α is a constant allowing for the displaced air, and equal to 0.029 x specimen volume, β is the 'tube calibration constant', W is the weight of the specimen, and F' is the force on the specimen, i.e. $(F - \delta)$, F being the observed force, δ is tube correction factor. In order to find δ i.e. the diamagnetism of the tube, the empty tube is weighed with the field on and off, the difference being δ . Since the glass tube is diamagnetic δ is a negative quantity. δ should be subtracted from the observed force (F) in order to obtain the force on the specimen alone (F').

<u>Calculation of β for the first tube</u>	mass/g
Weight of empty Gouy tube without field applied	7.71340
Weight of empty Gouy tube with field applied (10A)	7.71240
Weight of empty Gouy tube with field applied (15A)	7.71200
Weight of Gouy tube, filled with water	8.73942
Weight of Gouy tube, filled with Hg[Co(CNS) ₄] without field applied	9.63465
Weight of Gouy tube and Hg[Co(CNS) ₄] with field applied (10A)	9.68142
Weight of Gouy tube and Hg[Co(CNS) ₄] with field applied (15A)	9.69875
Temperature	20°C

At 10 amps
$$\beta = \frac{\chi \times W - \alpha}{F'}$$

$$= \frac{16.44 \times 1.92125 - 0.029821}{47.77}$$

$$= 0.660572 \times 10^{-6} \text{ c.g.s. units}$$

At 15 amps
$$\beta = \frac{16.44 \times 1.92125 - 0.029821}{65.5}$$

$$= 0.4817639 \times 10^{-6} \text{ c.g.s. units}$$

β for the second tube

$$W = 1.6887 \quad \delta = -1.33 \text{ mg}$$

$$\alpha = 0.0253582 \quad F' = 42.68 \text{ mg}$$

$$\begin{aligned} \text{At 10 amps} \quad \beta &= \frac{16.44 \times 1.6887 - 0.0253582}{42.68} \\ &= \frac{0.6498798 \times 10^{-6}}{\text{c.g.s. units}} \end{aligned}$$

$$\begin{aligned} \text{At 15 amps} \quad \beta &= \frac{16.44 \times 1.6887 - 0.0253582}{59} \\ &= \frac{0.4701164 \times 10^{-6}}{\text{c.g.s. units}} \end{aligned}$$

The diamagnetic contributions of the ligands were calculated from the observed susceptibility measurements of the corresponding acids.

In the case of hydrated compounds the susceptibility of each hydrate was determined and the contribution from water molecules² ($\chi_{\text{H}_2\text{O}} = -13 \times 10^{-6}$) was subtracted from it to obtain χ_{para} .

A correction was also included for the diamagnetism of the metal itself. Allowing for the diamagnetism, the effective magnetic moment, μ was calculated from the molar susceptibilities χ_M as

$$\mu = 2.84 [(\chi_M - \chi_{\text{dia}})T]^{\frac{1}{2}}$$

5.3 Diamagnetic Susceptibility and Diamagnetic Correcting Constants

The literature reports data of the susceptibilities of a large number of organic anions including some for malonate ion. These values deduced either theoretically or experimentally for the malonate ion by various workers are often widely different, and the selection of such values which should be undoubtedly correct could not be done from values available in the literature. Parasad and co-workers⁸ used graphical methods to determine the susceptibility of the malonate ion, by measuring the molar susceptibilities of a large number of malonate salts of different elements of the periodical table. The susceptibilities reported by them are not a fixed quantity, and these values not only differ from

one another according to their combination with different groups of elements, but are also not in agreement with the calculated values from Pascal's constants. The diamagnetic susceptibilities of the malonate ion have been determined experimentally on samples of the free acid.^{9,10} Asai et al.⁹ reported the value of (-46×10^{-6}) for the observed and calculated susceptibilities of the malonate ion, while later Dubicki et al.¹⁰ reported another value (-56×10^{-6}) . Such differences, in some cases, also arise from the fact that the calculated values of the molar susceptibilities reported in the literature for the malonate anion by various workers are also often widely different. The difference in the calculated and observed values can be attributed to bond effects which have not been considered in calculating the molar susceptibilities of the organic acids. Where the bond effects for atoms constituting the organic anions have, however, been taken into account, the susceptibility of the malonate ion has been calculated to be (-39.8×10^{-6}) ¹¹ in exact agreement with our calculated values.

In order to check the observed literature values of the molar susceptibility of the malonate anion, and to examine the accuracy of the theoretical calculations, the magnetic susceptibilities of the malonate, ethylmalonate, and benzylmalonate ligands were deduced directly from measurements on the acids. In order to average the errors of packing, if any, measurements were made with three separate fillings of the same acid and an average of the three closely agreeing values of the susceptibility thus obtained was taken as the final value of the specific susceptibility. The diamagnetic susceptibility of malonate, ethyl malonate and benzylmalonate were obtained by subtracting the susceptibility of the hydrogen ($\chi_H = -2.93 \times 10^{-6}$ from Pascal's data) from the molar susceptibility of the corresponding acid, assuming strict additivity. The observed values obtained were in excellent agreement with the theoretically calculated values. In the case of malonate anion the

susceptibility was found to be inconsistent with the values reported by previous workers. The susceptibilities of ethylmalonate and benzylmalonate anions do not appear to have measured by any previous workers. The results are given in Table 5.3 column 2 along with the values obtained by the graphical method by Parasad and co-workers in column 3. Columns 4 and 5 give, respectively, the experimental values of previous workers,^{9,10} and those calculated by Pascal's atomic constants. All the values of susceptibilities are expressed in -1×10^{-6} c.g.s. units.

Table 5.3

Anions ^a	This work (obs) 293 K	χ anions			Other workers (obs) ref.9,10	Pascal's cal. ref.2
		Li-Na-K	Mg-Zn-Cd ref. 8	Ca-Sr-Ba		
Malonate	39.8	45.5	52.0	53.0	46.0 56.0	39.8
Ethylmalonate	63.5					63.5
Benzylmalonate	100.5					100.8

a: from observed value for free acid - 5.86 for 2 protons

5.4 Results and Discussion

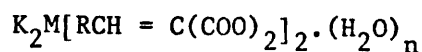
Ni(II)

The magnetic susceptibilities of Ni(II) malonate, Ni(II) ethylmalonate and Ni(II) benzylmalonate were measured between 113 - 313 K. The variation with temperature of the molar susceptibilities and the effective magnetic moments are given in Tables 5.5 - 5.7. All the compounds studied are of high-spin type, and the values of magnetic moments range between 3.17 - 3.2 B.M. for Ni(II) malonate, 3.1 B.M. for Ni(II) ethylmalonate and 3.1 - 3.2 B.M. for Ni(II) benzylmalonate complexes.

Moments were independent of the temperature, with $\theta = -2^\circ$ for Ni(II) malonate and $\theta = 0$ for the other two complexes.

Ni(II) shows magnetic moment values for two unpaired electrons in octahedral and tetrahedral complexes while its square planar complexes are diamagnetic.^{1,4} Six covalent octahedral paramagnetic complexes with an $^3A_{2g}$ ground term, associated with low orbital contribution to the magnetic moment, have the moment range (2.9 - 3.3 B.M.), and the moment should be independent of temperature, apart from small increases at higher temperature which arise from the T.I.P. contribution (temperature independent paramagnetism). The variation of paramagnetic susceptibility for a number of anhydrous Ni(II) complexes of the organic acids including those of Ni(II) oxalate have been studied¹³ over the temperature range 310 - 423 K. The magnetic moment of the anhydrous Ni(II) oxalate has been reported to be slightly below the spin-only value; $\mu = 2.75$ B.M.; it seems likely that those moments which are below spin-only value are in error. Bhatnagar's data for these Ni(II) complexes, give magnetic moments slightly lower than spin-only values, and the Weiss constants found for these compounds are not small, as the theory requires; however, his values of susceptibilities have been calculated from these large θ values, and the moments have been obtained accordingly. No explanation of the results has been put forward, and the details of his experimental method and the kind of calibration used are lacking. It has been proposed² that the magnetic dilution in Ni(II) oxalate may not be adequate. If the compound is indeed magnetically dilute, the departure of his results from those expected from theory can be partially explained in terms of the experimental error. The magnetic moment of 3.1 B.M. at room temperature was later reported¹⁵ for the Ni(II) oxalate dihydrate, whose structure is known¹⁴ to be octahedral. The nickel atom is in an octahedral environment of oxygen atoms (two

from two water molecules and four from two different oxalato groups). Normal room temperature magnetic behaviour has been observed¹⁵ for a number of high-spin complexes of Ni(II) with substituted malonic acids $R-CH = C(COOH)_2$ and a number of derivatives of the following type:



R =	M = Ni	μ_{eff} (B.M.)	M = Co	μ_{eff} (B.M.)
	n		n	
$C_6H_5 -$	3	3.52	3	5.45
$O-ClC_6H_4 -$	4	3.64	3	5.98
$p-ClC_6H_4 -$	6	3.71	2	6.13
$p-CH_3OC_6H_4 -$	5	3.68	3	5.78
$p-NO_2C_6H_4 -$	7	3.69	5	6.14

The high values of magnetic moments and their variations could be correlated by consideration of the strength of the parent acids and substitutions in the benzene ring which need not be discussed here.

Ploquin¹⁶ reported the results of magnetic susceptibilities of various organic salts of bivalent nickel, which have a normal magnetic behaviour at room temperature. The magnetic moment at room temperature of Ni(II) malonate dihydrate is given as 3.27 B.M. in agreement with our work. Rao et al.¹⁷ confirmed Ploquin¹⁶ results, and suggested a six covalent octahedral structure for this complex. The structure of Ni(II) malonate dihydrate has been investigated by X-ray powder methods,^{18,19} since no single crystals have been prepared. The results obtained from the X-ray powder method are sufficient to prove the structural formula to be Ni malonate, $2H_2O$. The compound is monoclinic with four molecules per unit cell, and is isomorphous with both Co(II) and Zn(II) malonate. No details of complete structural analysis have been obtained so far. (X-ray structural results are discussed in Chapter VI). Our results

Table 5.5 Variation of magnetic susceptibility and moment with
temperature (112-323 K). All χ values in c.g.s. units

Compound Ni (II)mal, 2H₂O Field 10 amps

Temp/K	χ_g	$\chi_M \times 10^6$	$\chi'_M \times 10^6$	$\frac{1}{\chi'_M} \times 10^6$	$\mu_{\text{eff}}(\text{B.M.})$
112.5	56.2090	11061.4	11140.0	0.8977×10^{-4}	3.179
132.5	48.1569	9476.9	9555.5	1.0465×10^{-4}	3.196
152	42.0051	8266.2	8344.8	1.1983×10^{-4}	3.199
172	37.3663	7353.4	7432.0	1.3455×10^{-4}	3.210
192.5	33.3558	6564.1	6642.7	1.5054×10^{-4}	3.211
212	29.7885	5862.1	5940.7	1.6833×10^{-4}	3.187
233	27.2837	5369.2	5447.8	1.8356×10^{-4}	3.200
253.5	25.2145	4962.0	5040.6	1.9839×10^{-4}	3.210
273	23.4481	4614.4	4693.0	2.13084×10^{-4}	3.215
293	21.9641	4322.3	4400.9	2.2722×10^{-4}	3.224
313	20.4986	4034.0	4112.6	2.4316×10^{-4}	3.222
323	19.8712	3910.5	3989.1	2.5069×10^{-4}	3.224

Diamagnetic correction = -78.6×10^{-6} c.g.s. units

Variation of molar susceptibility with temperature is shown in Figs.5.5-5.19

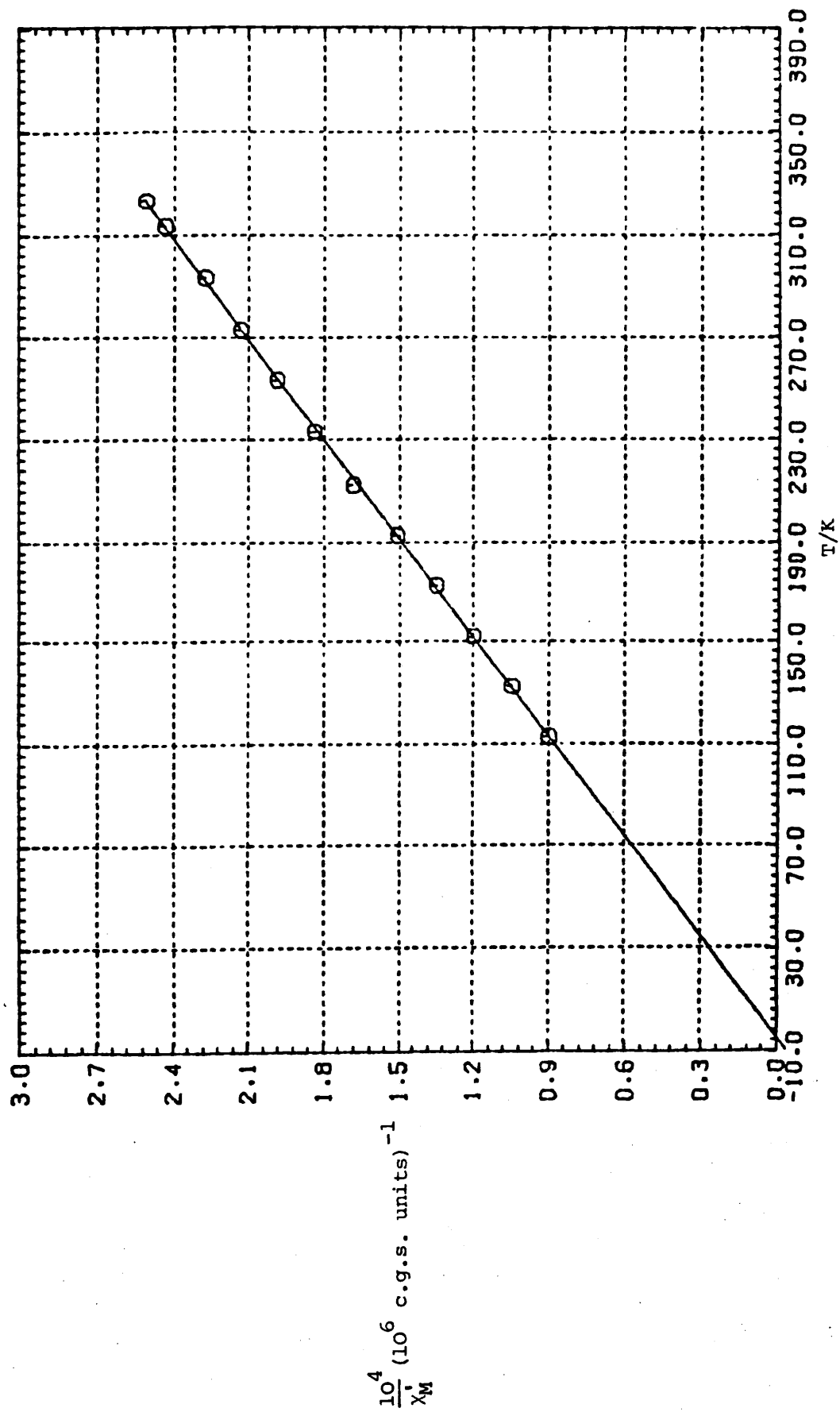


Fig.5.5. Ni(II)mal.2H₂O

Table 5.6. Variation of magnetic susceptibility and moment with temperature (112-323 K). All χ values in c.g.s. units

Compound $2\text{Ni(II)etmal.Ni(OH)}_2 \cdot 3\text{H}_2\text{O}$ Field 10 amps

Temp/K	χ_g	$\chi_M \times 10^6$	$\chi'_M \times 10^6$	$\frac{1}{\chi'_M} \times 10^6$	$\mu_{\text{eff}}(\text{B.M.})$
112	63,4791	10651.4	10803.5	0.92563×10^{-4}	3.124
132.5	53,5553	8986.2	9138.4	1.0943×10^{-4}	3.125
152	46,2365	7758.2	7910.3	1.2642×10^{-4}	3.114
171	40,5883	6810.4	6962.6	1.4363×10^{-4}	3.099
191.5	36,1403	6064.1	6216.2	1.6087×10^{-4}	3.098
212.5	32,9199	5523.7	5675.9	1.7618×10^{-4}	3.119
233	29,8973	5016.6	5168.7	1.9347×10^{-4}	3.117
253.5	27,3035	4581.4	4733.5	2.1126×10^{-4}	3.111
273	25,1513	4220.2	4372.3	2.2887×10^{-4}	3.103
293	23,467	3937.6	4089.7	2.44452×10^{-4}	3.109
313	21,8682	3669.4	3819.0	2.6185×10^{-4}	3.105
323	21,2103	3559.0	3708.6	2.6965×10^{-4}	3.108

Diamagnetic correction = -152.12×10^{-6} c.g.s. units

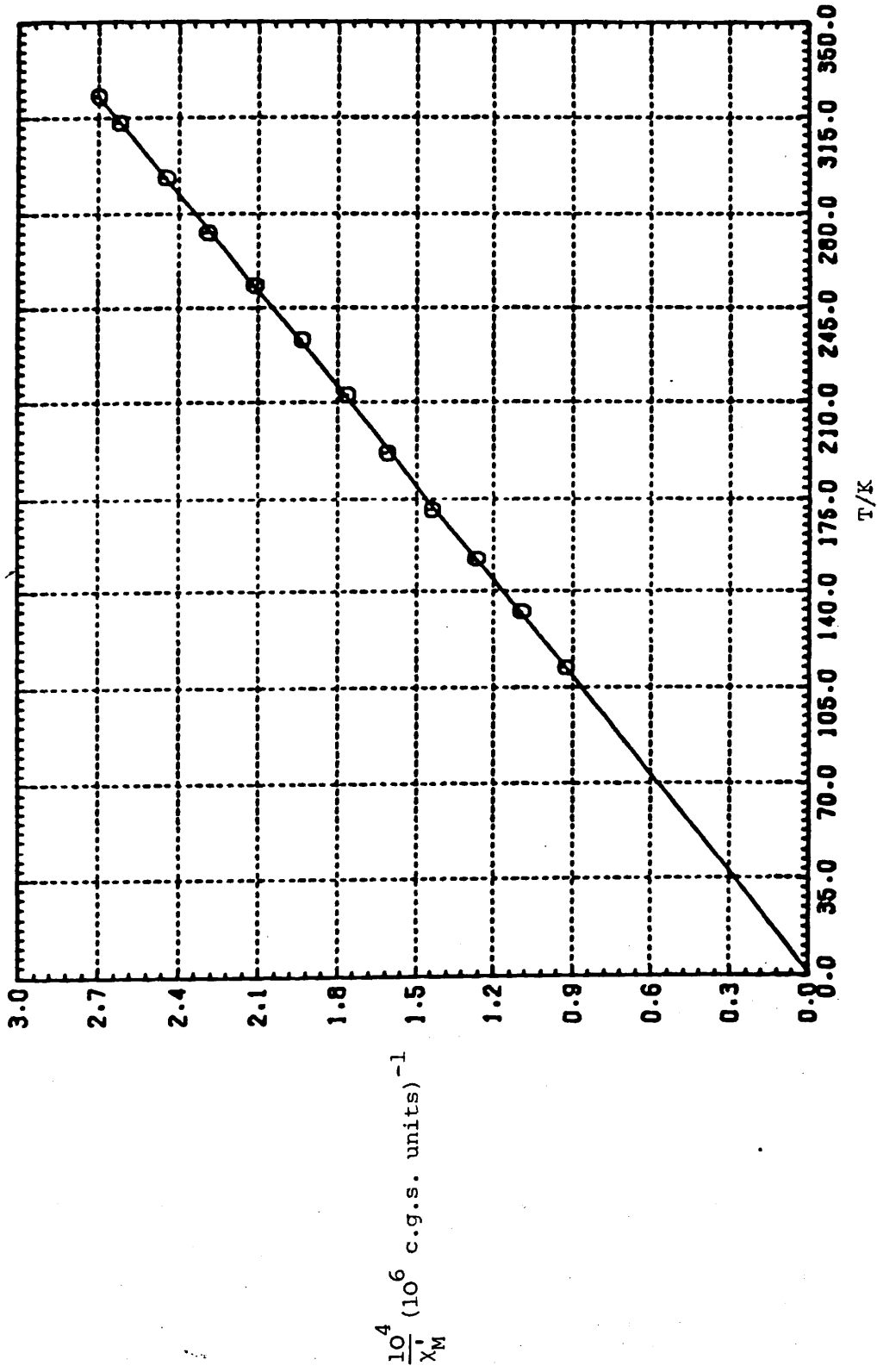
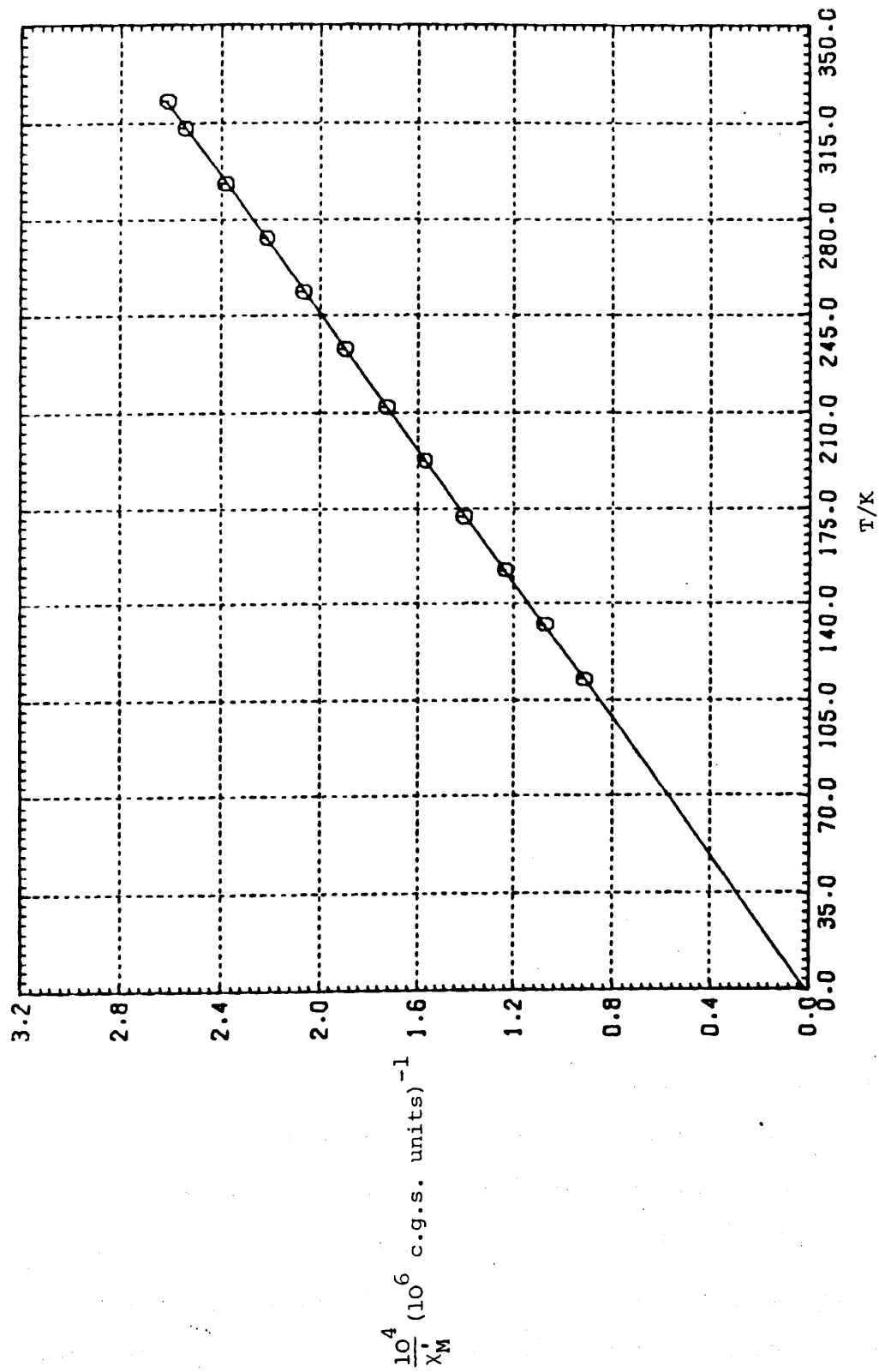
Fig.5.6. $2Ni(II) etnal, Ni(OH)_2 \cdot 3H_2O$

Table 5.7. Variation of magnetic susceptibility and moment with temperature (112-323 K). All X values in c.g.s. units

<u>Compound</u> Ni(II)benzylmal.2H ₂ O		Field 10 amps			
Temp/K	χ_g	$\chi_M \times 10^6$	$\chi'_M \times 10^6$	$\frac{1}{\chi'_M} \times 10^6$	eff (B.M.)
112.5	37.4995	10759.2	10898.8	0.91753×10^{-4}	3.145
132.5	31.9135	9156.5	9296.1	1.0757×10^{-4}	3.152
152	27.727	7955.2	8094.9	1.2353×10^{-4}	3.150
127	24.3769	6994.1	7133.8	1.4018×10^{-4}	3.146
192.5	21.7897	6251.8	6391.4	1.5646×10^{-4}	3.150
212	19.7103	5655.2	5794.8	1.7257×10^{-4}	3.148
233	17.9033	5136.8	5276.4	1.8952×10^{-4}	3.149
253.5	16.3975	4704.7	4844.3	2.0643×10^{-4}	3.147
273	15.2587	4378.0	4517.6	2.2136×10^{-4}	3.154
293	14.1552	4061.4	4201.0	2.3804×10^{-4}	3.151
313	13.2189	3792.7	3932.3	2.5430×10^{-4}	3.151
323	12.8529	3687.7	3827.3	2.6128×10^{-4}	3.158

Diamagnetic correction = -139.62×10^{-6} c.g.s. units

Fig.5.7. Ni(II)benzylmal.2H₂O

are in agreement with those of Rao¹⁷ suggesting a six-coordinate octahedral environment about the Ni atom in Ni(II) malonate and its analogous Ni(II) ethylmalonate and Ni(II) benzylmalonate complexes, and these results are consistent with the diffuse reflectance spectrum, which lends further support for the proposed structure for these compounds (see Chapter III).

Co(II)

From the magnetic point of view two different stereochemical arrangements are expected for cobalt(II) (d^7 systems). These are octahedral, $t_{2g}^5 e_g^2$, and tetrahedral, $t_2^4 e^3$ complexes.

High spin octahedral complexes with ${}^4T_{1g}$ ground terms possess moments in the range 4.7 - 5.2 B.M. at room temperature, and the moment should vary with temperature, and the moments of high-spin octahedral complexes, which are higher than spin-only values, arise from the unquenched orbital contribution of both the ground state $t_{2g}^5 e_g^2$ and the first excited state, $t_{2g}^4 e_g^3$, and as a result a relatively large orbital contribution to the moment occurs in these types of complexes, whereas in tetrahedral high-spin complexes, the contribution to the moment is quite small and the experimental moments are smaller than those for the corresponding octahedral complexes, and the moments do not vary as much with temperature. Nyholm²⁰ has suggested that this distinction may be used as a diagnostic tool to differentiate between six and four coordination complexes.

The magnetic susceptibilities of Co(II) malonate, Co(II) ethylmalonate and Co(II) benzylmalonate compounds were carried out over a range of temperature. The observed magnetic moment values range between 4.74 - 4.76 B.M. for Co(II) malonate, 4.72 - 4.75 B.M. and 4.8 - 5.0 B.M. for Co(II) ethylmalonate and Co(II) benzylmalonate respectively. The moments vary with temperature, as expected for the Co(II) ion in an octahedral environment. It was found that the Curie-Weiss

law was obeyed over the temperature range studied. The Weiss constants are $\theta = -24^\circ$ for Co(II) malonate, $\theta = -12^\circ$ for Co(II) ethylmalonate and $\theta = -20^\circ$ for Co(II) benzylmalonate complexes. Such values of θ are of the same order as those in the literature expected for the high-spin Co(II) octahedral complexes. The normal paramagnetic behaviour at room temperature of a number of anionic Co(II) complexes of substituted malonic acid, $R-CH = C(COOH)_2$ with $R = C_6H_5$ and its chloro, methoxy and nitro derivatives of the formula $K_2Co[RCH = C(COO)_2]_2 \cdot (H_2O)_n$ have been reported¹⁵ (see page 119). The room temperature magnetic moments of these compounds have been found to vary from 5.5 - 6.1 B.M. depending on the nature of the substituent in this series of complexes. The magnetic moment of octahedral Co(II) malonate is reported to vary with temperature, ($\theta = -58^\circ$), having a value of 4.97 B.M. at room temperature.¹³ The magnetic susceptibilities of Co(II) malonate have been measured at room temperature¹⁷. The structure has been found by the powder method to be isomorphous with malonates of nickel and zinc.^{19,21} The details of complete X-ray structural analysis have not yet been reported.

High spin octahedral cobalt(II) malonate has a moment of 5.2 B.M. at room temperature.¹⁷ The values of the magnetic moments found in this work for salts of Co(II) with malonate, ethylmalonate and benzylmalonate at room temperature are slightly lower than those reported by Ranade and Rao.¹⁷ The reason for this is not quite clear. However similar low magnetic moments for Co(II) oxalate have been reported.¹³ According to Figgis and Lewis,⁴ the moments below about 4.7 B.M. are in error, the compounds may not be octahedral in stereochemistry or are not magnetically dilute. From the available data of X-ray powder diffraction of Co(II) malonate,^{19,21} it is clear that there is no evidence of any metal-metal interaction. Although the magnetic moments of tetrahedral Co(II) ions are expected to be lower than those of octahedral systems (see page 111) the diffuse reflectance spectra i.e., the

Table 5.8. Variation of magnetic susceptibility and moment with temperature (113-293 K). All χ values in c.g.s. units

Compound Co(II)mal.2H₂O

Field 10 amps

Temp K	χ_g	$\chi_M \times 10^6$	$\chi'_M \times 10^6$	$\frac{1}{\chi'_M} \times 10^6$	$\mu_{\text{eff}}(\text{B.M.})$
113	102.812	20256.1	20334.7	4.9177×10^{-5}	4.740
133	90.1663	17764.7	17843.3	5.6044×10^{-5}	4.742
153	79.5485	15672.7	15751.3	6.3488×10^{-5}	4.742
173	71.6072	14108.1	14186.7	7.0488×10^{-5}	4.748
193	65.2160	12848.9	12927.5	7.7354×10^{-5}	4.757
213	59.3100	11685.3	11763.9	8.5006×10^{-5}	4.742
233	54.7999	10796.7	10875.3	9.1951×10^{-5}	4.748
253	50.9151	10031.4	10110.0	9.8912×10^{-5}	4.753
273	47.2861	9316.4	9395.0	10.644×10^{-5}	4.743
293	44.3435	8736.6	8815.2	11.344×10^{-5}	4.747

Diamagnetic correction = -78.6×10^{-6} c.g.s. units

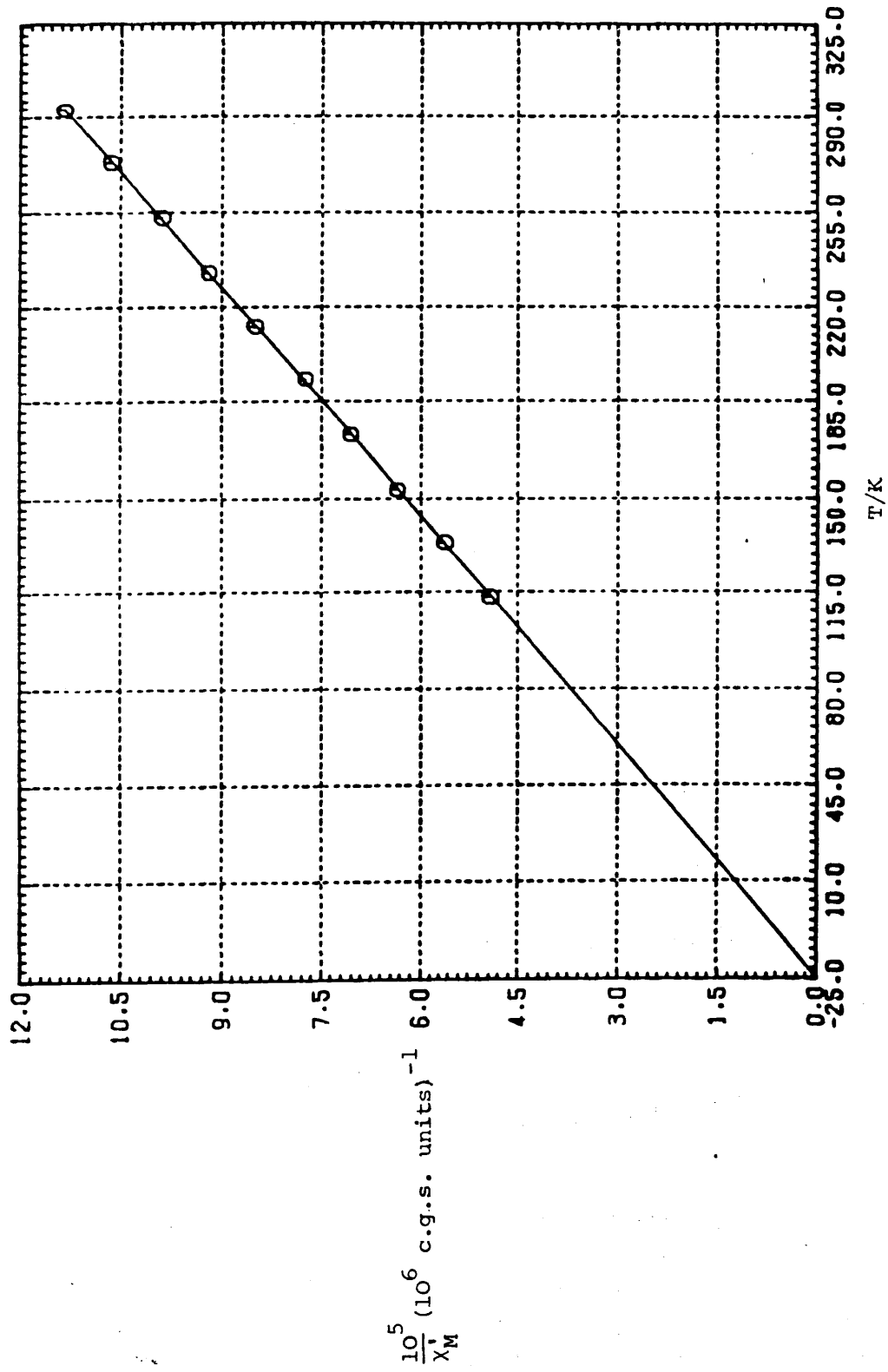
Fig.5.8. Co(II)mal.2H₂O

Table 5.9. Variation of magnetic susceptibility and moment with temperature (112-323 K). All χ values in c.g.s. units

Compound Co(II)etmal.2H₂O

Field 10 amps

Temp/K	χ_g	$\chi_M \times 10^6$	$\chi'_M \times 10^6$	$\frac{1}{\chi'_M} \times 10^6$	μ_{eff} (B.M.)
112.5	94.1445	22089.9	22192.2	4.5061×10^{-5}	4.720
132.5	84.9200	19113.4	19215.7	5.2041×10^{-5}	4.732
152	74.3747	16739.9	16842.2	5.9375×10^{-5}	4.720
171.5	66.4022	14945.5	15047.8	6.6455×10^{-5}	4.719
191.5	59.4720	13385.7	13488.0	7.414×10^{-5}	4.705
212.5	54.2503	12210.4	12312.7	8.1217×10^{-5}	4.716
233	49.7256	11192.0	11294.3	8.8540×10^{-5}	4.724
253.5	45.7486	10296.9	10399.2	9.6161×10^{-5}	4.719
273	42.5526	9577.5	9679.8	10.331×10^{-5}	4.717
293	39.7149	8938.8	9041.2	11.061×10^{-5}	4.716
313	37.4883	8437.7	8540.0	11.709×10^{-5}	4.731
323	36.4385	8201.4	8303.7	12.043×10^{-5}	4.737

Diamagnetic correction = -102.32×10^{-6} c.g.s. units

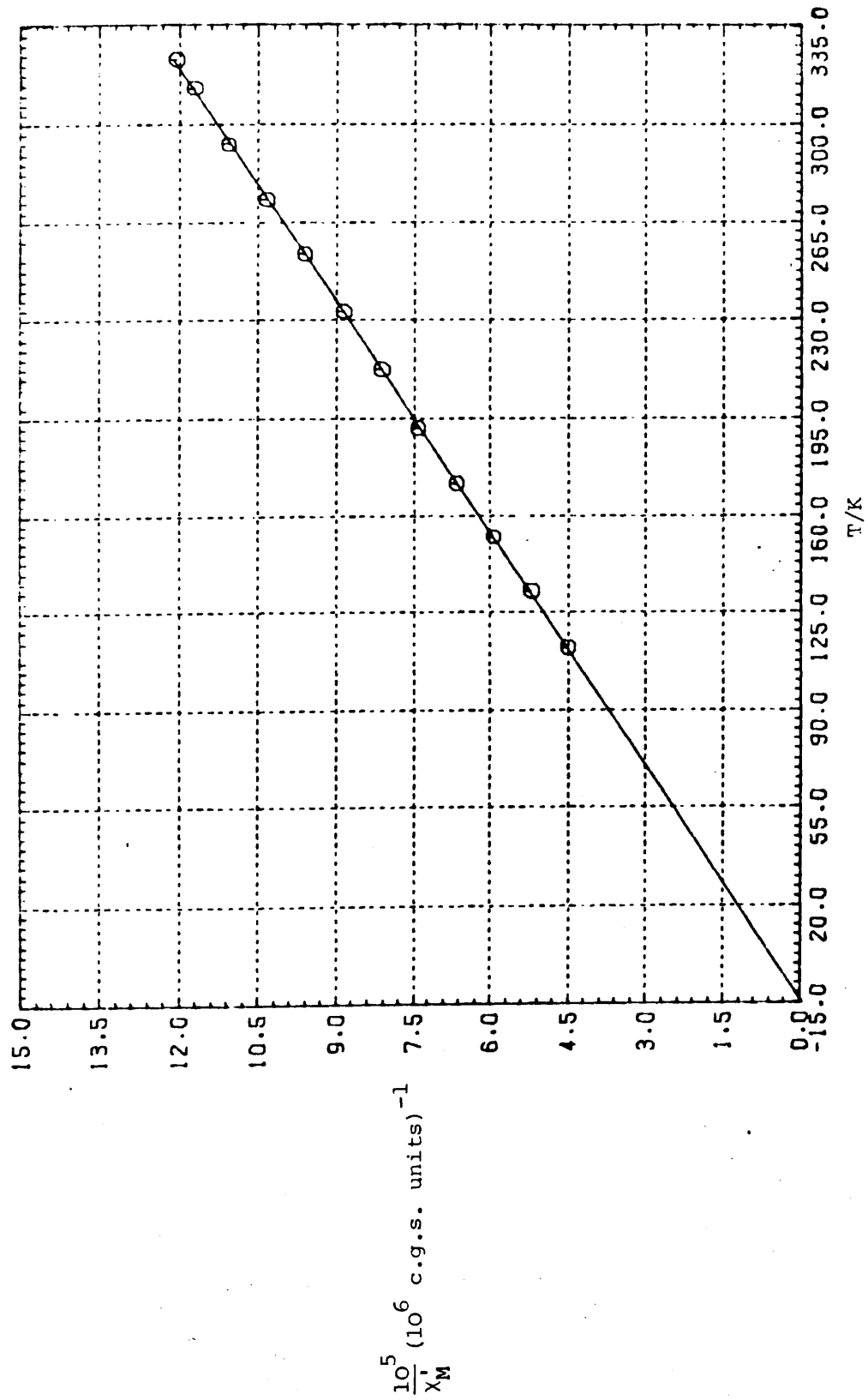
Fig.5.9. Co(II)etmal.2H₂O

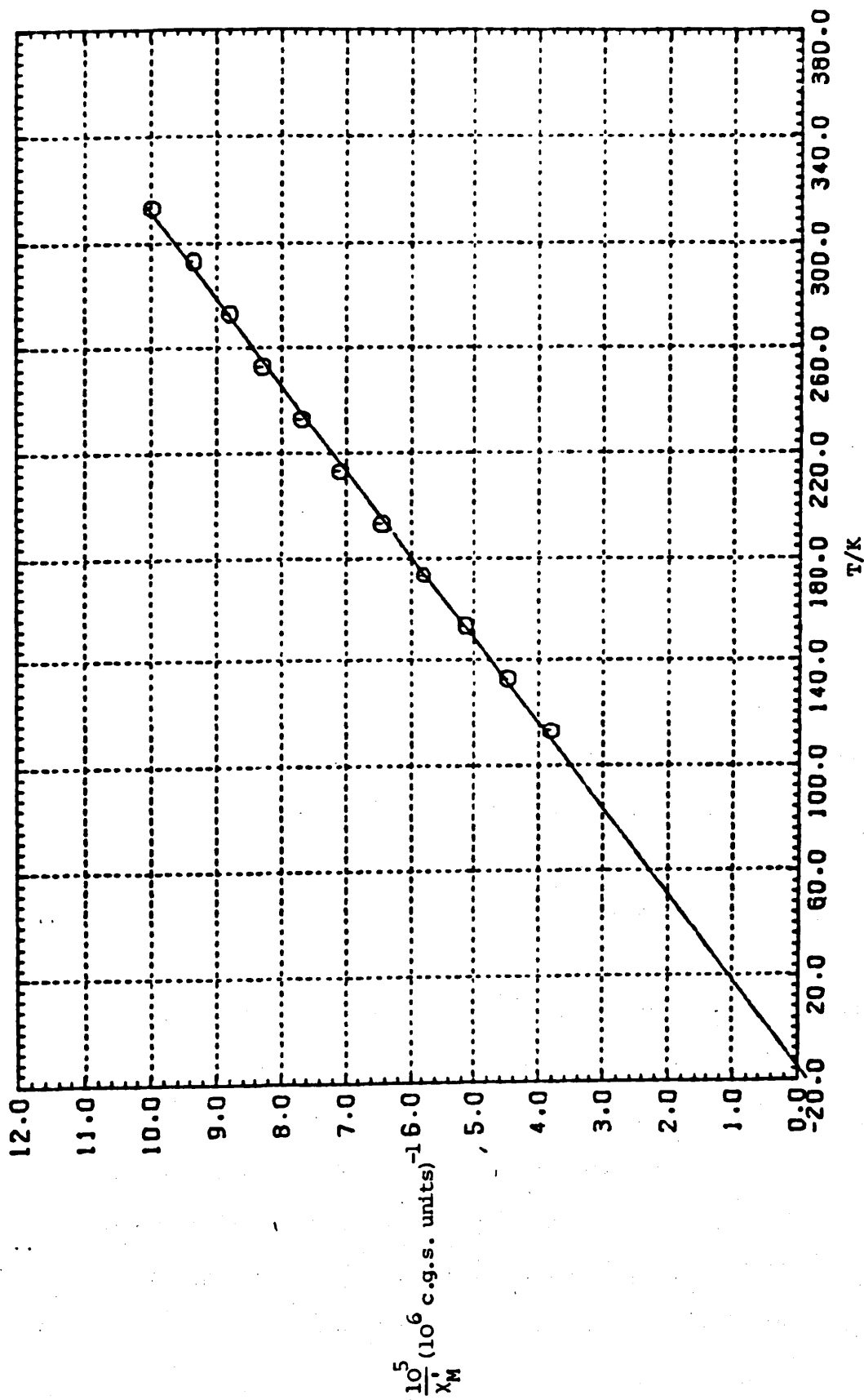
Table 5.10. Variation of magnetic susceptibility and moment with temperature (113-293 K). All χ values in c.g.s. units

Compound Co (II)benzylmal. $2H_2O$

Field 10 amps

Temp /K	χ_g	$\chi_M \times 10^6$	$\chi'_M \times 10^6$	$\frac{1}{\chi'_M} \times 10^6$	$\mu_{\text{eff}}(\text{B.M.})$
113	90.6364	26025.9	26165.5	3.8218×10^{-5}	4.883
133	77.1470	22152.5	22292.1	4.4859×10^{-5}	4.890
153	67.3145	19329.1	19468.7	5.1365×10^{-5}	4.902
173	59.6153	17118.3	17257.9	5.7944×10^{-5}	4.907
193	53.5800	15385.3	15524.9	6.4413×10^{-5}	4.916
213	48.6844	13979.5	14119.2	7.0826×10^{-5}	4.925
233	44.8696	12884.1	13023.7	7.6783×10^{-5}	4.947
253	41.5275	11924.5	12064.1	8.2891×10^{-5}	4.962
273	39.12720	11235.2	11374.8	8.7913×10^{-5}	5.005
293	36.7275	10546.2	10685.8	9.3582×10^{-5}	5.025

Diamagnetic correction = -139.62×10^{-6} c.g.s. units

Fig.5.10. Co(II)benzylmal.2H₂O

intensity and the positions of the bands in the visible region of Co(II) malonates (see page 61) show that only high-spin octahedral complexes are present.

Fe(III)

The magnetic moments and susceptibilities of Fe(III) malonate, Fe(III) ethylmalonate, and Fe(III) benzylmalonate complexes were measured between 113 - 293 K and are shown in the Tables. All three sets of compounds are of high-spin type, and the following magnetic moments (Bohr magnetons) have been found for the sodium salts: Ferrimalonate (+4H₂O) 5.9, Ferriethylmalonate (+2H₂O) 5.9 and Ferribenzylmalonate (+2H₂O) 5.85; corresponding to 5 unpaired electrons. The plots of $1/\chi_M'$ versus T give straight lines through the origin, i.e. $\theta = 0^\circ$.

In an octahedral environment the high-spin Fe³⁺ complexes are expected to possess moments very close to the spin-only value of 5.92 B.M., which are independent of temperature (see page 111). Magnetic measurements have been carried out on Fe(III) oxalato complexes, and used to determine the nature of the bonding of the iron in the system.^{22,23} The magnetic moment of this compound is reported by Johnson²² to be 5.75 B.M. at 291 and 90 K with $\theta = 4^\circ$. The moment of this compound was later reported^{24,25} to be 5.92 B.M. over the range 80 - 300 K with $\theta = 0^\circ$. Similar magnetic moment values have been given recently²⁶ for this complex at room temperature, which are in better agreement with theory than those early data of Johnson.²²

According to Curtis et al.²⁷ "ionic" (highly paramagnetic) ferrioxalato complexes have moments of 5.88 and ferrimalonato complexes of 5.87 B.M. which are independent of temperature ($\theta = 0^\circ$). The crystal structure of potassium ferrioxalate has been reported.²⁸ The iron atom is octahedrally surrounded by six carboxyl oxygen atoms. The complex is isomorphous with the oxalato complexes of Al(III) and Cr(III).²⁹ Hatfield³⁰ found that the crystal spectrum of Fe(III) malonato complexes

Table 5.11. Variation of magnetic susceptibility and moment with temperature (112-293 K). All χ values in c.g.s. units

Compound $\text{Na}_3[\text{Fe}(\text{mal})_3] \cdot 4\text{H}_2\text{O}$ Field 10 amps

Temp/K	χ_g	$\chi_M \times 10^6$	$\chi'_M \times 10^6$	$\frac{1}{\chi'_M} \times 10^6$	$\mu_{\text{eff}}(\text{B.M.})$
112	79.2429	38434.2	38636.0	2.5883×10^{-5}	5.908
132.5	67.8829	32924.4	33126.2	3.0188×10^{-5}	5.950
152	58.9889	28610.7	28812.5	3.4707×10^{-5}	5.943
171.5	51.7193	25084.8	25286.6	3.9547×10^{-5}	5.914
191.5	46.1010	22359.8	22561.6	4.4323×10^{-5}	5.903
212	41.6404	20196.4	20398.2	4.9024×10^{-5}	5.906
233	37.9106	18387.3	18589.1	5.3795×10^{-5}	5.910
253	34.9414	16947.2	17149.0	5.8312×10^{-5}	5.916
273	32.382	15705.9	15907.7	6.2863×10^{-5}	5.918
293	30.182	14638.8	14840.6	6.7383×10^{-5}	5.922

Diamagnetic correction = -201.8×10^{-6} c.g.s. units

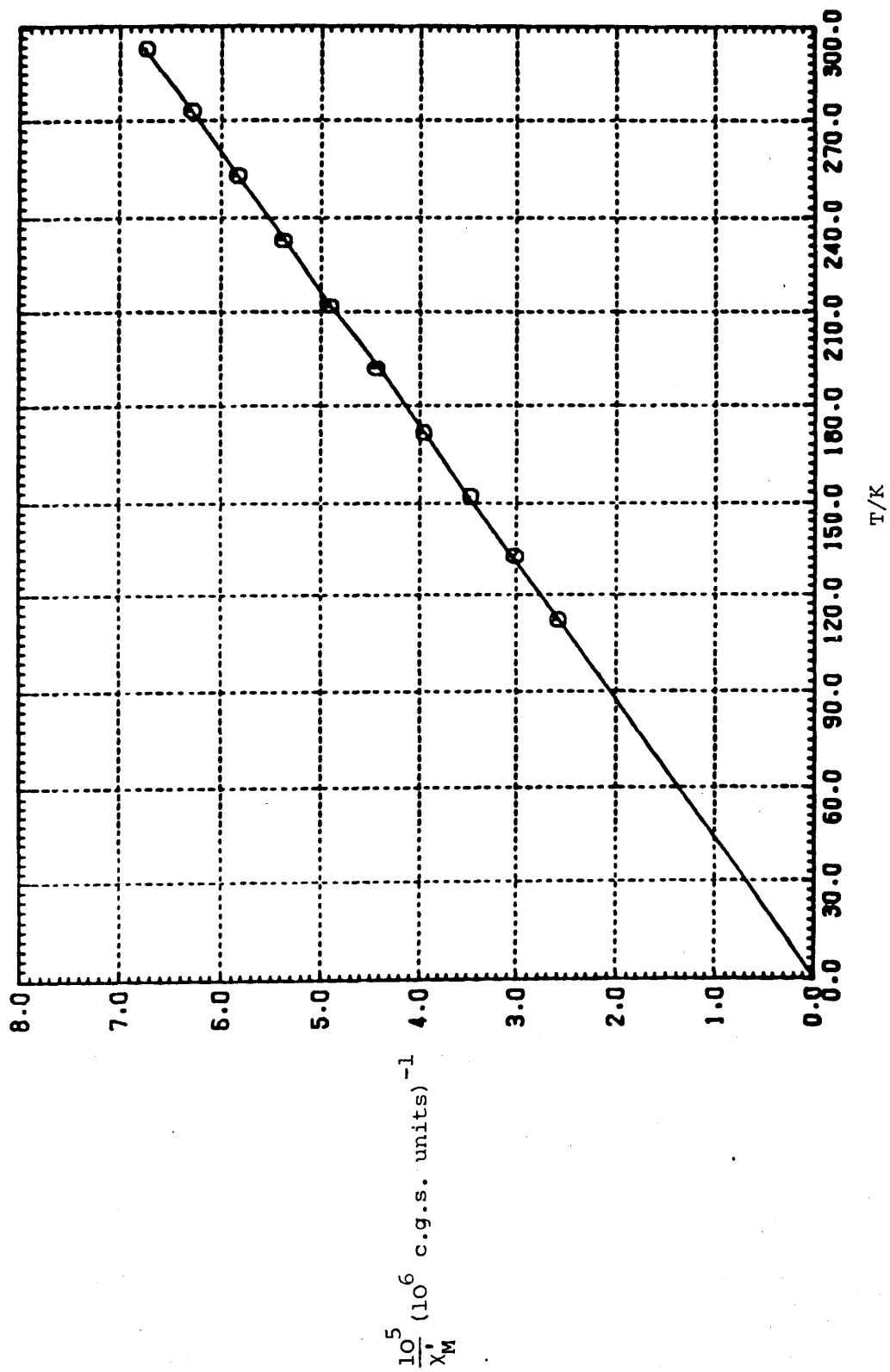
Fig.5.11. $\text{Na}_3[\text{Fe}(\text{mal})_3] \cdot 4\text{H}_2\text{O}$

Table 5.12. Variation of magnetic susceptibility and moment with temperature (112-293 K). All χ values in c.g.s. units

Compound $\text{Na}_3[\text{Fe}(\text{etmal})_3] \cdot 2\text{H}_2\text{O}$

Field 10 amps

Temp/K	χ_g	$\chi_M \times 10^6$	$\chi'_M \times 10^6$	$\frac{1}{\chi'_M} \times 10^6$	$\mu_{\text{eff}}(\text{B.M.})$
112.5	69.6358	38380.8	38653.7	2.5871×10^{-5}	5.922
132.5	59.0439	32542.8	32815.8	3.0473×10^{-5}	5.922
152	51.3682	28312.3	28585.3	3.4983×10^{-5}	5.920
172	45.4433	25046.7	25319.7	3.9495×10^{-5}	5.927
192.5	40.7298	22448.8	22721.8	4.4011×10^{-5}	5.940
212	36.9659	20374.3	20647.3	4.8433×10^{-5}	5.942
233	33.7729	18614.4	18887.4	5.2945×10^{-5}	5.958
253.5	30.9773	17073.6	17346.5	5.7648×10^{-5}	5.955
273	28.5044	15710.6	15983.5	6.2564×10^{-5}	5.932
293	26.5813	14650.7	14923.6	6.7008×10^{-5}	5.939

Diamagnetic correction = -272.96×10^{-6} c.g.s. units

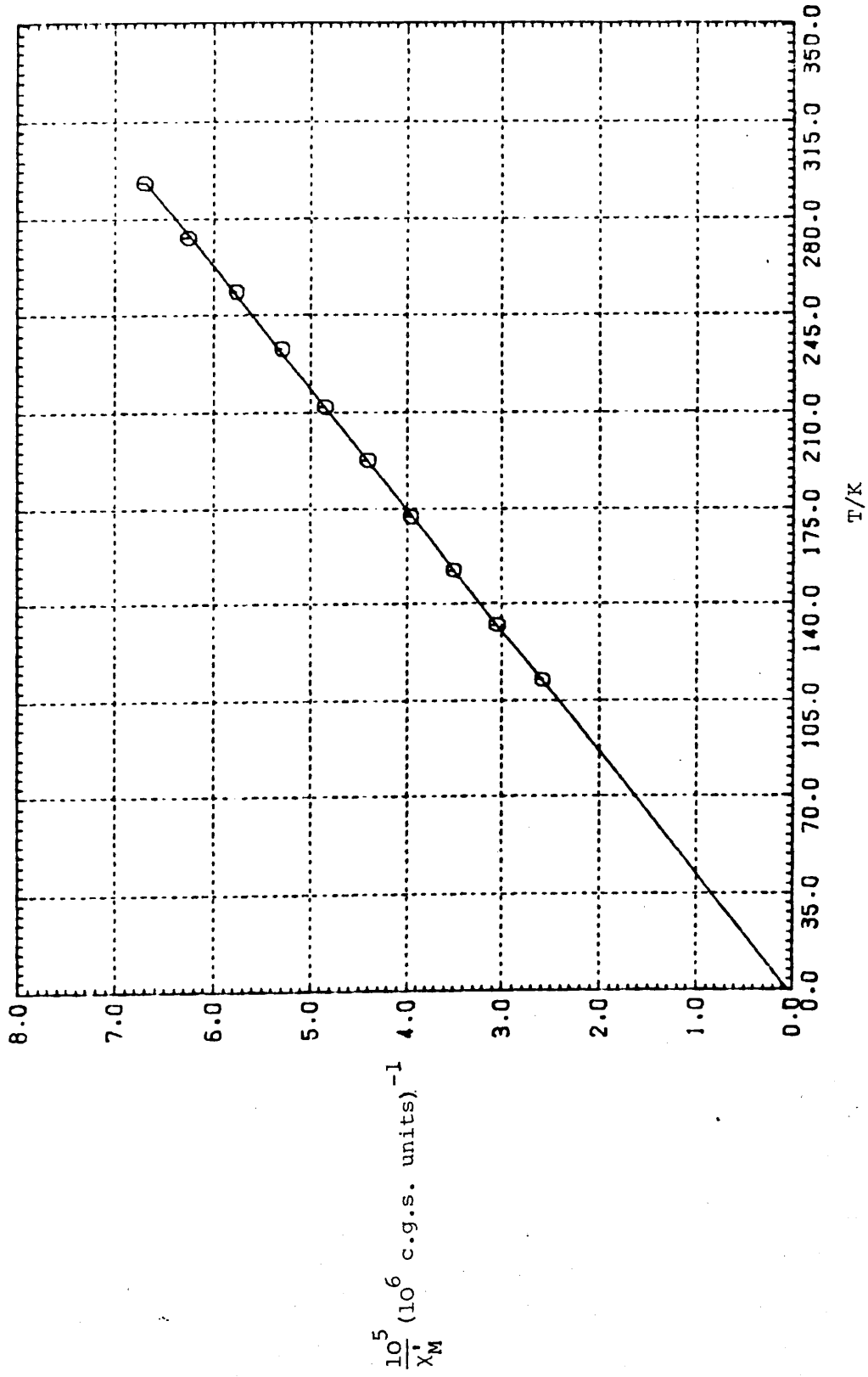
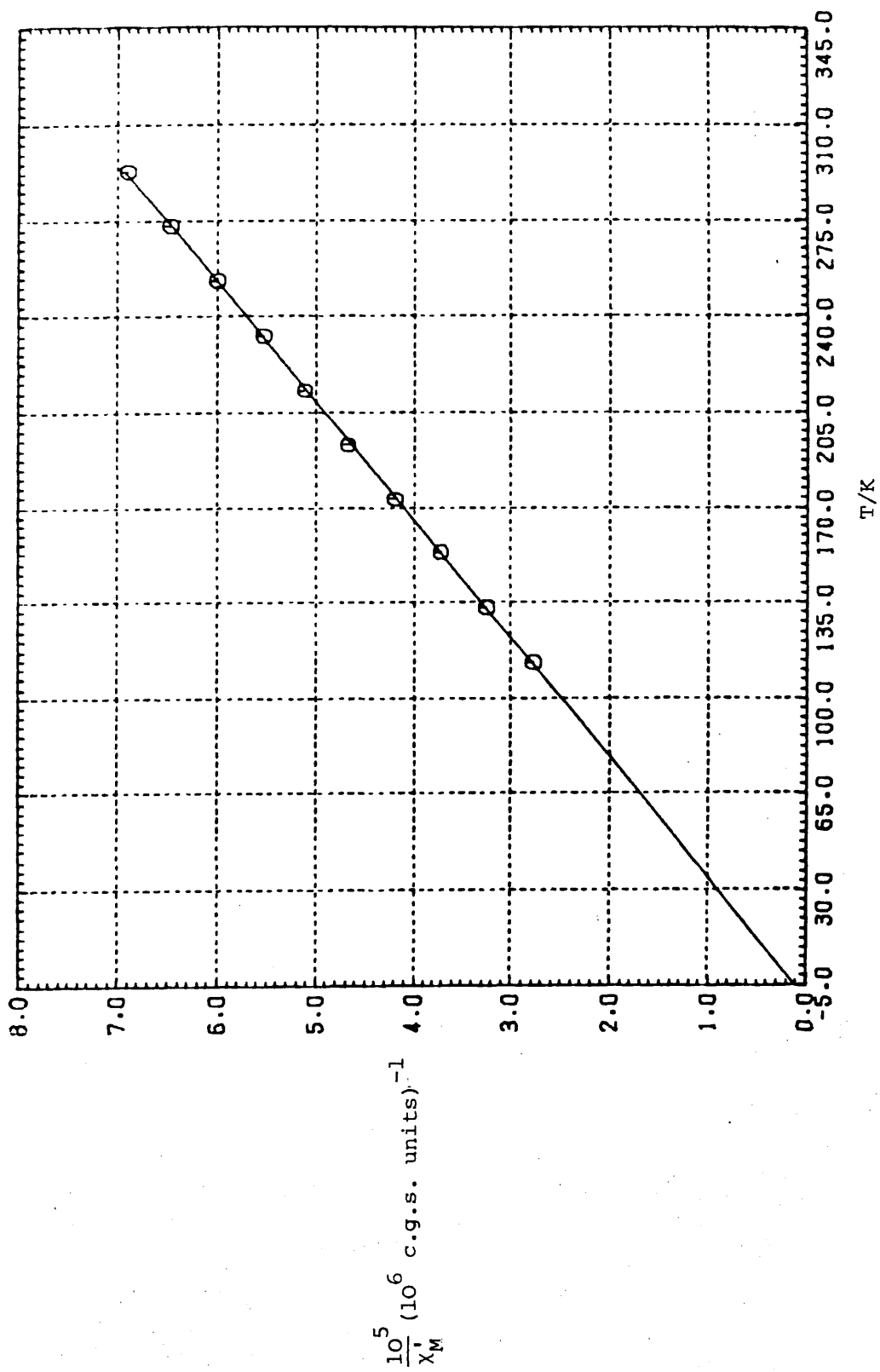
Fig.5.12. Na[Fe(etmal)₃].2H₂O

Table 5.13 . Variation of magnetic susceptibility and moment with temperature (113-293 K). All χ values in c.g.s. units

Compound $\text{Na}_3[\text{Fe}(\text{benzylmal})_3] \cdot 2\text{H}_2\text{O}$ Field 10 amps

Temp/K	χ_g	$\chi_M \times 10^6$	$\chi'_M \times 10^6$	$\frac{1}{\chi_M} \times 10^6$	$\mu_{\text{eff}}(\text{B.M.})$
113	48.3633	35662.0	36046.9	2.7742×10^{-5}	5.732
133	41.2714	30432.4	30817.3	3.2449×10^{-5}	5.75
153	36.02703	26565.5	26950.4	3.7105×10^{-5}	5.767
173	31.8372	23476.1	23860.9	4.191×10^{-5}	5.770
193	28.5241	21033.0	21417.9	4.669×10^{-5}	5.774
213	26.0013	19172.7	19557.6	5.1131×10^{-5}	5.796
233	23.9996	17696.8	18081.6	5.5305×10^{-5}	5.829
253	22.0895	16288.3	16673.1	5.9977×10^{-5}	5.833
273	20.4426	15073.9	15458.8	6.4688×10^{-5}	5.834
293	19.142	14114.8	14499.7	6.8967×10^{-5}	5.854

Diamagnetic correction = -384.86×10^{-6} c.g.s. units

Fig.5.13. $\text{Na}_3[\text{Fe}(\text{benzylmal})_3] \cdot 2\text{H}_2\text{O}$

is similar to that of oxalato system³¹ and confirmed their isomorphism. The Mössbauer spectra point to an octahedral high-spin Fe(III) system for Fe(III) oxalato complexes, which confirms the early data of Johnson²² and Curtis.²⁷ The magnetic moments of Fe(III) malonate complexes in the present study are similar to those reported by Curtis,²⁷ and also in good agreement with those of similar Fe(III) oxalato complexes,²⁴⁻²⁶ and these results are also consistent with the diffuse reflectance spectra; suggesting therefore a high-spin octahedral symmetry for Fe(III) malonato complexes, and by comparison a similar structure could be ascribed for the Fe(III) ethyl, and Fe(III) benzylmalonato complexes. Another piece of evidence reinforcing this suggestion is provided by the Mössbauer spectrum which strongly supports the proposed structure of these complexes (see Chapter VII).

Cr(III)

The complexes of Cr^{3+} are mostly of the octahedral type. In an environment of octahedral symmetry the ground term of the Cr^{3+} ion is ${}^3A_{2g}$. The moment is expected to be independent of temperature (θ zero or very small), and slightly below the spin-only value of 3.88 B.M. for three unpaired electrons (see Table 5.1,5.2).

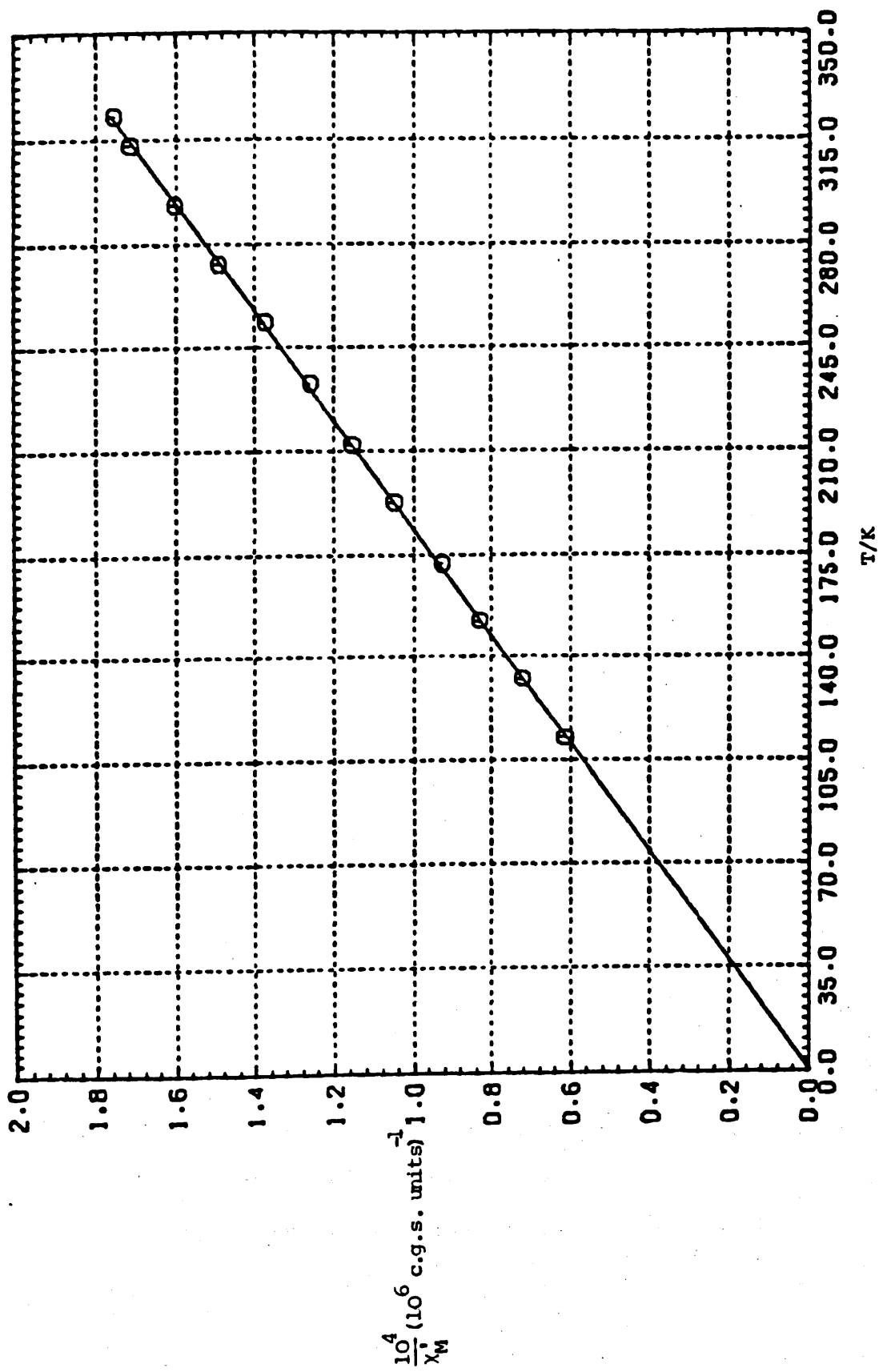
The magnetic susceptibility of a magnetic dilute system of octahedral Cr(III) oxalato complexes has been studied²² at room temperature and recently by other workers^{24,25} over an extended temperature range. The results are similar. Weiss constants are small and the moments are slightly below the spin-only value by the spin-orbit coupling effect. A magnetic moment of 3.84 B.M. was observed²⁴ for ionic $\text{K}_3[\text{Cr}(\text{ox})_3] \cdot 3\text{H}_2\text{O}$ complex whose structure has recently been found by X-ray analysis to be octahedral.²⁴ The complex is isomorphous with the complexes of Al(III) and Fe(III) oxalate.²⁹ It has been suggested³⁰ that $\text{Cr}(\text{mal})_3^{3-}$ ions occupy positions which are identical with those of $\text{Fe}(\text{mal})_3^{3-}$ ions, and they are isomorphous. The crystal structure of

Table 5.14. Variation of magnetic susceptibility and moment with temperature (112-323 K). All X values in c.g.s. units

Compound $K[Cr(mal)_2(H_2O)_2] \cdot 3H_2O$ Field 10 amps

Temp/K	χ_g	$\chi_M \times 10^6$	$\chi'_M \times 10^6$	$\frac{1}{\chi'_M} \times 10^6$	$\mu_{eff}(B.M.)$
112.5	41.8060	16107.4	16277.9	0.6143×10^{-4}	3.843
132.5	35.4652	13664.3	13834.8	0.7228×10^{-4}	3.845
152	30.8506	11886.4	12056.9	0.8294×10^{-4}	3.845
172	27.6511	10653.7	10824.2	0.9239×10^{-4}	3.875
192.5	24.3390	9377.5	9548.0	1.0473×10^{-4}	3.850
212	22.0445	8493.5	8664.0	1.1542×10^{-4}	3.849
233	20.1745	7773.0	7943.5	1.2589×10^{-4}	3.864
253.5	18.4594	7112.2	7282.7	1.3731×10^{-4}	3.859
273	16.9816	6542.8	6713.3	1.4896×10^{-4}	3.845
293	15.7709	6076.3	6246.8	1.6008×10^{-4}	3.842
313	14.7199	5671.4	5841.9	1.7118×10^{-4}	3.840
323	14.3667	5535.3	5705.8	1.7526×10^{-4}	3.855

Diamagnetic correction = -170.5×10^{-6} c.g.s. units

Fig.5.14. $K[\text{Cr}(\text{mal})_2(\text{H}_2\text{O})]_3\text{H}_2\text{O}$

$K[Cr(ox)_2(H_2O)_2] \cdot 3H_2O$ has been determined by Van Niekerk and Schoening.³² The four oxygen atoms and two water molecules surrounding the central chromium atom form an octahedral arrangement

The visible spectra of the malonato complexes of Cr(III) are similar to those of the Cr(III) oxalato complexes.^{33,34} The shift of the bands to the shorter wavelength from the tris-malonato to cis-diaquo complexes is also as for the corresponding oxalato complexes³³. It has been found by Hatfield³⁰ that the crystal spectra of the tris(malonato) chromium(III) complexes are similar to those of octahedral tris(oxalato) chromium(III) complexes. The complete X-ray analysis of Cr(III) malonato complexes³⁵⁻³⁷ later confirmed this result, which lends further support for the octahedral structure of these complexes.

The magnetic moment of 3.84 B.M. was found for $cis-K[Cr(mal)_2(H_2O)_2] \cdot 3H_2O$ over the temperature range 112 - 313 K. The moments were independent of temperature, with $\theta = 0^\circ$ after the manner expected for the Cr^{3+} ion in an octahedral environment.

Our results of the magnetic moment and the visible spectrum are in agreement with those obtained for the analogous oxalato complexes,^{24,25,33,34} and the diffuse reflectance spectra results are also consistent with those reported values,^{33,44,45} suggesting therefore a similar octahedral structure for this complex.

Mn(III)

In an environment of octahedral symmetry the d^4 configuration can give rise to compounds of either the high-spin or the low-spin type. For the high-spin type the ground term is the 5E_g from the 5D term of the free ion, and the magnetic moment is expected to lie slightly below the spin-only value for four unpaired electrons (4.90 B.M.) and to be independent of temperature (θ small).

A large number of complex compounds of trivalent manganese have been reviewed by Goldenberg.³⁸ Magnetic measurements have been

carried out on Mn(III) oxalato complexes and used to determine the nature of the bonding of the manganese in the system.²² The magnetic moment of octahedral high-spin $K_3[Mn(C_2O_4)_3] \cdot 3H_2O$ is reported by Johnson²² to be 4.88 B.M. with $\theta = 14^\circ$ and by Goldenberg³⁸ 4.81 B.M. at 291 K. The magnetic results however indicate that the complex ion is stabilized by ionic linkages.

The magnetic moment of potassium bis (malonato) diaquo manganese dihydrate has been reported³⁹ to have a value of 4.37 B.M. at 323 K which is much lower than the theoretical value of 4.90 B.M. obtained for the spin-only approximation of Mn^{3+} ion in an octahedral environment. The moment of this compound has been recently reported⁴⁰ to be 4.90 B.M. at 300 and 90 K with $\theta = 0^\circ$, which is in better agreement with theory than the early data³⁹. The low magnetic moment found³⁹ for potassium dioxalato-dihydroxo-manganate is likely to be due to the presence of a small amount of magnetic exchange. It has however been suggested⁴ that there are Mn-O-Mn linkages in place of some of the hydroxyl groups. Recent experimental studies⁴⁰ of the paramagnetic susceptibilities of several high-spin octahedral bis(malonato)diaquo manganese(III) salts; of general formula $M'[(C_3H_2O_4)_2(H_2O)_2Mn] \cdot nH_2O$, (where $M' = K^+$ or Na^+ , $n = 2$; $M' = Li$, $n = 3$; $M' = NH_4^+$, $n = 0$) and of potassium tris(malonato) manganese(III), $K_3[(C_3H_2O_4)_3Mn] \cdot 3H_2O$, have shown that they usually obey the Curie-Weiss law with a temperature independent magnetic moment of 4.80 - 5.1 B.M. with θ values close to 0° , which is expected in octahedral spin-free manganese(III) complexes. Since high-spin d^4 systems contain a degenerate ground state in octahedral symmetry, Jahn-Teller distortions are expected with two opposite trans Mn-O bonds longer than the other four and this is borne out in the crystallographic structure. A structural study⁴¹ with X-rays has now confirmed a distorted octahedron around the Mn^{3+} ion for both the bis and tris(malonato)manganese(III) complexes. Moreover, the Mn-Mn

distances of 2.99 and 3.35 Å are considered to be long enough to eliminate any interaction between Mn atoms.

The magnetic moments and susceptibilities of Mn(III) malonato, Mn(III)ethylmalonato and Mn(III) benzylmalonato complexes were studied over a temperature range of 113 - 293 K. On account of the high photosensitivity and general instability of manganic complexes, utmost precaution was taken during the measurements to avoid possible decomposition of the samples. However, for each complex, either two or three samples were prepared in the dark and their magnetic moments were measured accordingly. The results revealed that all three sets of compounds are of high-spin type and they obey the Curie-Weiss law over the temperature range studied. The room temperature moment of 5.0 B.M. was found for Mn(III) malonato complex, with $\theta = 2^\circ$ which is in excellent agreement with the reported value.⁴⁰ In the case of Mn(III) ethyl and benzylmalonato complexes, when the magnetic moments were calculated from experimental values of the mass susceptibilities, it was found that the values did not check that theoretically for Mn^{3+} with four unpaired electrons, assuming only the spin moments to be effective. The observed susceptibility value of Mn(III) ethylmalonato complex at 293 K is 46.46×10^{-6} c.g.s. and that of Mn(III) benzylmalonato complex is 32.60×10^{-6} c.g.s., similar to that of the Mn(III) malonato complex with $\chi = 31.94 \times 10^{-6}$ c.g.s. at 293 K. The room temperature moments in Mn(III) ethyl and benzylmalonato complexes were higher than the value expected for the high-spin manganese(III) ion. The moments also decrease continuously with decreasing temperature, i.e., their reciprocal molar susceptibilities vary linearly with temperature, the lines intercepting the temperature axis to give small values for the Weiss constants, with $\theta = 2^\circ$ for Mn(III) malonate, $\theta = 16^\circ$ for both Mn(III) ethyl and benzylmalonato complexes. Similar θ values were found for some Mn(III) oxalato²² and malonato complexes.⁴⁰ The moments of both anhydrous

sodium and potassium bis(malonato)manganese(III) complexes have been found to decrease with lowering of the temperature⁴⁰ (90 to 300 K). At 300 K μ_{eff} is 5.5 B.M. and 5.01 B.M. and θ is 16° and 8° respectively. It is suggested that this decrease is due to some slight magnetic interaction presumably because of bridging.

The discrepancies of the measured magnetic moments for Mn(III) ethyl and benzylmalonato complexes from the theoretical predictions seem to be outside the experimental error of most of the measurements concerned. A survey of the literature revealed that this defect in moment was not peculiar to these Mn(III) compounds, but that it existed in the certain other compounds of manganese,³⁸ and in most cases no clearly defined explanation had been advanced. The experimental data on Mn compounds generally show large effective moments and this is said to be due to partial oxidation, perhaps combined with some temperature independent paramagnetism. It is known that the simple manganic ion has a large oxidation potential and it is difficult to manipulate because of the readiness with which it disproportionates into the manganous ion and manganese dioxide. The magnetic moments of the simple and complex salts of manganese reported by Goldenberg³⁸ are mostly higher than the theoretical values. The compounds prepared were always contaminated. It has however, been found that in fact such deviations are due to the presence of certain amount of impurities. When the necessary corrections for the paramagnetic contribution of the respective amounts of the impurities were made, the values of μ agreed well with theory. The anomalously high magnetic moments of Mn(III) ethyl and benzylmalonato complexes are very likely to be due to the contamination of the samples with finely divided manganese dioxide suspended on the complexes. It is very difficult to exclude the formation of manganese dioxide along with the compounds. An impurity with the high magnetic susceptibility of MnO_2 could seriously interfere with the measurement

of the susceptibilities of the compounds. However, traces of the impurities were shown to have no noticeable effect on the spectroscopic analysis in the visible region, as was pointed out elsewhere.⁴² Mn(III) ethyl and benzylmalonato complexes were prepared by the method of Cartledge and Nichols⁴³ for the corresponding malonate complexes, by the reaction of stoichiometric quantities of potassium permanganate and either ethyl or benzylmalonic acid in non-aqueous medium (absolute methanol). These conditions appear to be favourable for the formation of highly magnetic oxides of manganese which would account for high value for μ_{eff} . Analysis of both complexes showed that they contained more manganese than the formula indicates.

Mn found 19.8%; calc. for $\text{K}[\text{Mn}(\text{etmal})_2(\text{H}_2\text{O})_2]$: 14.07%

Mn found 13.8%; calc. for $\text{K}[\text{Mn}(\text{benzylmal})_2(\text{H}_2\text{O})_2]$: 10.67%.

A detailed study was made. It was assumed that the magnetic moment values would be altered linearly if the complexes were contaminated with MnO_2 , probably formed along with the compounds. From the analyses Mn(III) ethylmalonate was composed of 11.45% MnO_2 and 88.5% of the complex, and similarly, Mn(III) benzylmalonate was composed of 6.24% of MnO_2 and 93.76% of the complex, and the magnetic moments were therefore calculated on the actual manganese contents. χ for MnO_2 was taken to be 46.58. When corrected for this, the room temperature moments of 4.93 B.M. and 5.01 B.M. were obtained for Mn(III) ethyl and benzylmalonato complexes respectively, in excellent agreement with theory. Clearly it is impossible to establish the origin of these anomalous magnetic moments in the absence of structural analysis. However, complete crystallographic information is available for potassium bis(malonato)diaquo manganate(III) by x-ray analysis.⁴¹ This compound was also known to give rise to two bands in the visible region of the spectrum.⁴⁰

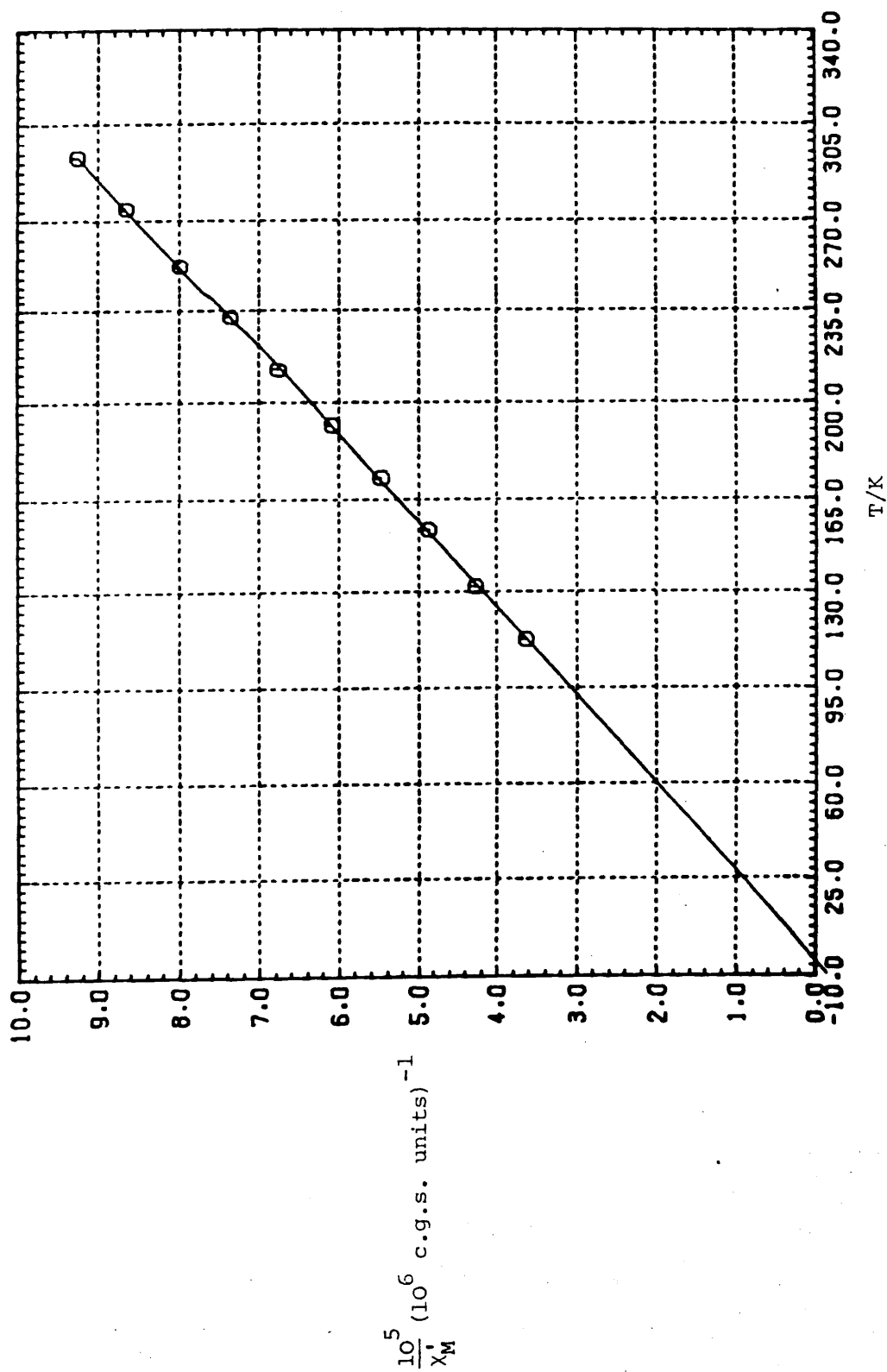
Our results of the magnetic moments of Mn(III) malonato

Table 5.15. Variation of magnetic susceptibility and moment with temperature (112-293 K). All χ values in c.g.s. units

Compound $K[Mn(mal)_2(H_2O)_2]$ Field 10 amps

Temp/K	χ_g	$\chi_M \times 10^6$	$\chi'_M \times 10^6$	$\frac{1}{\chi_M} \times 10^6$	$\mu_{eff}(B.M.)$
112.3	81.8969	27367.5	27498.0	3.6366×10^{-5}	4.991
132	66.8687	23348.0	23478.5	4.2592×10^{-5}	5.000
153	61.1624	20438.6	20569.1	4.8617×10^{-5}	5.038
172.5	54.3859	18174.2	18304.7	5.4631×10^{-5}	5.047
191.5	48.7859	16302.8	16433.3	6.0852×10^{-5}	5.038
212	43.8662	14658.8	14789.3	6.7617×10^{-5}	5.028
232.5	40.3056	13468.9	13599.4	7.3532×10^{-5}	5.05
253	37.0704	12387.8	12518.3	7.9883×10^{-5}	5.054
274	34.2061	11430.7	11561.2	8.6496×10^{-5}	5.055
293	31.9429	10674.4	10804.9	9.2551×10^{-5}	5.053

Diamagnetic correction = -130.5×10^{-6} c.g.s. units

Fig.5.15. $K[Mn(mal)_2(H_2O)_2]$

complex in the present study are similar to those reported values,⁴⁰ and also in agreement with the corresponding Mn(III) oxalato complexes,²² and these results are also consistent with IR and diffuse reflectance spectra⁴⁰ suggesting, therefore a high-spin octahedral symmetry for Mn(III) malonato complexes. The IR and solid state spectra of Mn(III) ethyl and Mn(III) benzylmalonato complexes are very similar to those of malonato and oxalato Mn(III) complexes, therefore these complexes may also be considered to have a similar distorted octahedral structure. Verification of this conclusion must, of course, await a detailed crystallographic study of each of the complexes.

Cu(II)

The magnetic moments, and susceptibilities of Cu(II) malonate, sodium bis(malonato)diaquo Cu(II) complex, Cu(II) ethylmalonate, and Cu(II) benzylmalonate compounds were measured between 113 - 323 K. These are listed in Tables 5.16-5.19. All the compounds studied are, magnetically, perfectly normal bivalent copper complexes, and the observed room temperature magnetic moment values are 1.94 B.M. for Cu(II) malonate, 1.93 B.M. for bis(malonato) diaquo Cu(II), 1.90 B.M. for Cu(II) ethylmalonate and 1.93 B.M. for Cu(II) benzylmalonate complexes. It can be seen that the moments are all higher than the spin-only value, 1.73 B.M., for one unpaired electron, as expected for the Cu(II) ion in an octahedral environment in the absence of magnetic exchange. It was found that the Curie-Weiss law was obeyed over the liquid nitrogen temperature range with $\theta = -2^\circ$ for Cu(II) malonate, $\theta = +6^\circ$ for bis(malonato)diaquo Cu(II), $\theta = 0^\circ$ and 14° for Cu(II) ethyl and Cu(II) benzylmalonato complexes respectively.

The copper(II) carboxylates have been the subject of many investigations and a large amount of magnetic data on copper(II) complexes is available.⁴ These complexes are mostly found to have the distorted octahedral stereochemistry with ~ 1.9 B.M. as the moment for

the cupric ion, although a few are known which are square planar or approximate to a tetrahedral stereochemistry. On the basis of their magnetic moments at room temperature copper(II) compounds can be classified in two main groups. A great majority of these compounds show normal moments (1.8 - 2.0 B.M.), indicating the absence of any appreciable spin coupling between unpaired electrons belonging to copper atoms. On the other hand, a number of copper(II) compounds have been reported to show moments considerably smaller than the spin moment 1.73 B.M. for one unpaired electron (~ 1.4 B.M. or less). Thus some kind of spin interaction either of a direct nature⁴⁶ or of a super exchange process⁴⁷ (via intervening oxygen or other atoms) must be responsible for the subnormal moments. Ploquin¹⁶ measured the magnetic moments for a series of copper(II) salts of α, ω dicarboxylic acids ($\text{HOOC}(\text{CH}_2)_n \text{COOH}$), $n = 0-8$ at room temperature. Recently, Asai⁹ carefully re-examined the magnetic moments of the same series of compounds and tried to correlate the obtained moments with the probable structures of the copper(II) salts. It was found⁹ that all members of the series examined, with the single exception of the malonate ($n = 1$), gave subnormal magnetic moments, i.e. moments smaller than the spin-only value of 1.73 B.M., for a single unpaired electron. Copper(II) malonate has a slightly higher moment than the theoretical value, the difference being attributed to orbital contributions. The studies of the copper(II) compounds with subnormal magnetic moments have been extensive with copper(II) acetate (and its homologues) whose structure consists of a binuclear molecule,⁴⁸ in which the copper ions are bridged in pairs by four acetate groups to form a dimer molecule. The Cu-Cu distance is 2.64 Å. The subnormal magnetic moment of 1.20 B.M. has been reported⁹ for Cu(II) oxalate, whose structure has been suggested⁹ to comprise a dimeric structural network, or polymeric molecules involving coordination links rather than separate molecules having a single copper atom, or as dimeric molecules as in

copper(II) acetate monohydrate crystals.⁴⁸ In fact, the monomeric structure of Cu(II) oxalate has been confirmed by the recent single crystal analysis.⁴⁹ The copper atom is octahedrally coordinated by four oxygens from the two oxalate groups (Cu-O = 1.96 Å) and two oxygens from the water molecules (Cu-O = 2.48 Å).

In the case of malonate, the twisting of chains at the central carbon atoms renders the formation of such a network structure similar to that in Cu(II) oxalate altogether impossible. In fact the normal magnetic moment found⁹ for Cu(II) malonate suggests that the atom pairs of copper are not formed in the crystals.

A rough correlation is found^{10,50} between the appearance of a new band at $\sim 28,000 \text{ cm}^{-1}$ and the subnormal magnetic moments of the copper(II) carboxylates. The ultraviolet and visible spectra of the copper(II) α,ω -dicarboxylates with subnormal magnetic moments all show a new band at $\sim 28,000 \text{ cm}^{-1}$ (band II) both in solution and in the crystal which is suggested to be due to the copper-copper linkage as a result of dimeric structure. The reflectance spectra of copper(II) malonate and Cu(II) oxalate have a single broad band at⁵¹ $14,280 \text{ cm}^{-1}$ and¹⁰ $13,698 \text{ cm}^{-1}$ respectively. The near-ultraviolet band (band II) was not observed in copper(II) oxalate and copper(II) malonate derivatives in which no direct copper-to-copper link exists.⁵⁰ The results of magnetic moment data^{16,9} of the dimeric structures of Cu(II) salts of α,ω -dicarboxylic acids are also confirmed by infrared spectral data,⁵² especially by the variation of the C-O stretching and the CH₂ rotation bands. It is concluded that the formation of pairs of copper atoms leads to the distortion of the methylene chains in crystalline copper(II) α,ω -dicarboxylate complexes. It was found⁵² that the dependence of the shift of the antisymmetric COO stretching frequency of the copper(II) salts of these series from the normal position is similar to that of the variation of the magnetic moment of the copper(II) salts from the theoretical spin-

only moment for one odd electron, suggesting that these two quantities are related to each other. It was proposed that⁵² the electronic structure around the copper(II) ion or a pair of copper(II) ions causes the lowering of the magnetic moments and the band shift. The infrared spectral studies also indicate the monomeric nature of the Cu(II) malonate and oxalate compounds.⁵² A recent electron spin resonance study⁵³ also confirmed the formation of pairs of copper atoms in the copper(II) salts of higher carboxylic acids with subnormal magnetic moments in all cases except copper(II) malonate, supporting the conclusion made by Asai.⁹ The room temperature magnetic moments of both anhydrous^{9,10} and the various hydrates of Cu(II) malonate, $\text{CuC}_3\text{H}_2\text{O}_4 \cdot m\text{H}_2\text{O}$, $m = 1$,^{16,50} $m = 2$,¹⁶ $m = 2.5$ ¹⁰ $m = 3$,^{9,16,17} have been reported by different workers. These are shown in Table 5.4 together with the values found in the present study. It can be seen that the magnetic moment values vary somewhat from sample to sample, but in general the agreement is fairly good. The observed differences could arise from the fact that some workers have calculated the effective magnetic moment with or without taking into account the diamagnetic correction for the Cu(II) ion. Some have used the Pascal constants for the diamagnetic correction of the non metal part of the molecule, and some have used the experimental values. Moreover, the numerical values of Pascal's constants are different in detail from table to table. An observation worth making is that most of the magnetic measurements on Cu(II) malonate compounds have not been accompanied by accurate analysis proving the identity of the compound. Failure to establish purity may readily explain deviations in susceptibilities reported by various workers. In the case of copper(II) malonate compounds, the structural determinations by different workers are not in agreement with each other.^{10,50,54} It seems that the magnetic moment and structure of each compound depend strongly on the past history of the sample and its mode of preparation. The

Table 5.4 The magnetic moments of Cu(II) malonate

Compound	Temp/K	$\chi_M \times 10^6$ c.g.s. units	$\chi_{dia} \times 10^6$	μ_{eff} (B.M.)	Refs.
Cu(C ₃ H ₂ O ₄)	286	1358	-46	1.76	9
	RT	1370	-56	1.75	10
Cu(C ₃ H ₂ O ₄)·H ₂ O	300	1530		1.92	16
	300	1444	-34	1.86	46
Cu(C ₃ H ₂ O ₄)·2H ₂ O	300	1680		2.02	16
Cu(C ₃ H ₂ O ₄)·2½H ₂ O	RT	1395	-90	1.77	10
Cu(C ₃ H ₂ O ₄)·3H ₂ O	300	1598		1.95	16
	296	1513	-85	1.95	9
	296	1411		1.84	17
Cu(C ₃ H ₂ O ₄)·2½H ₂ O	293	1513	-85	1.94	This work
Na ₂ [Cu(C ₃ H ₂ O ₄) ₂ (H ₂ O) ₂]	293	1415	-132	1.93	This work

RT = room temperature

observed moment of 1.94 B.M. of copper(II) malonate in the present study is similar to that reported for the Cu(II) malonate trihydrate.⁹ A recent electron spin resonance spectrum⁵³ of copper(II) malonate trihydrate indicates an octahedral environment around the Cu²⁺ ion in this compound. The latter has a single broad band in the visible region of the spectrum.⁵¹ Dimitrova, et al.,⁵⁵ have carried out a complete X-ray analysis of copper(II) malonate tetrahydrate. It was found that the oxygen atoms of two water molecules are 2.48 Å distant from a copper atom to complete a distorted octahedron with four close oxygen atoms (Cu-O distance, 1.96 - 1.97 Å) belonging to two malonate groups.

The Cu(II) ethyl and benzylmalonate complexes have the same reflectance spectra and magnetic moment as the Cu(II) malonate (see Tables 5.16 - 5.19, Chapter III). Therefore these complexes may also be considered to have similar distorted octahedral structures.

Table 5.16. Variation of magnetic susceptibility and moment with temperature (112-323 K). All χ values in c.g.s. units

Compound $\text{Cu(II)mal} \cdot 2\frac{1}{2}\text{H}_2\text{O}$		Field 10 amps			
Temp/K	χ_g	$\chi_M \times 10^6$	$\chi'_M \times 10^6$	$\frac{1}{\chi'_M} \times 10^6$	$\mu_{\text{eff}}(\text{B.M.})$
112.5	18.9212	3985.4	4070.5	2.4567×10^{-4}	1.922
132.5	16.0669	3384.2	3469.3	2.8825×10^{-4}	1.926
152	14.0291	2954.9	3040.0	3.2894×10^{-4}	1.931
172	12.3229	2595.6	2680.7	3.7304×10^{-4}	1.928
192.5	11.0227	2321.7	2406.8	4.1549×10^{-4}	1.933
212	9.9422	2094.1	2179.2	4.5888×10^{-4}	1.930
233	9.0622	1908.8	1993.9	5.0154×10^{-4}	1.936
253.5	8.3343	1755.5	1840.6	5.4332×10^{-4}	1.940
273	7.7075	1623.4	1708.5	5.8530×10^{-4}	1.940
293	7.1840	1513.2	1598.3	6.2568×10^{-4}	1.943
313	6.639	1398.4	1483.5	6.741×10^{-4}	1.935
323	6.4497	1358.5	1443.6	6.9271×10^{-4}	1.940

Diamagnetic correction = -85.1×10^{-6} c.g.s. units

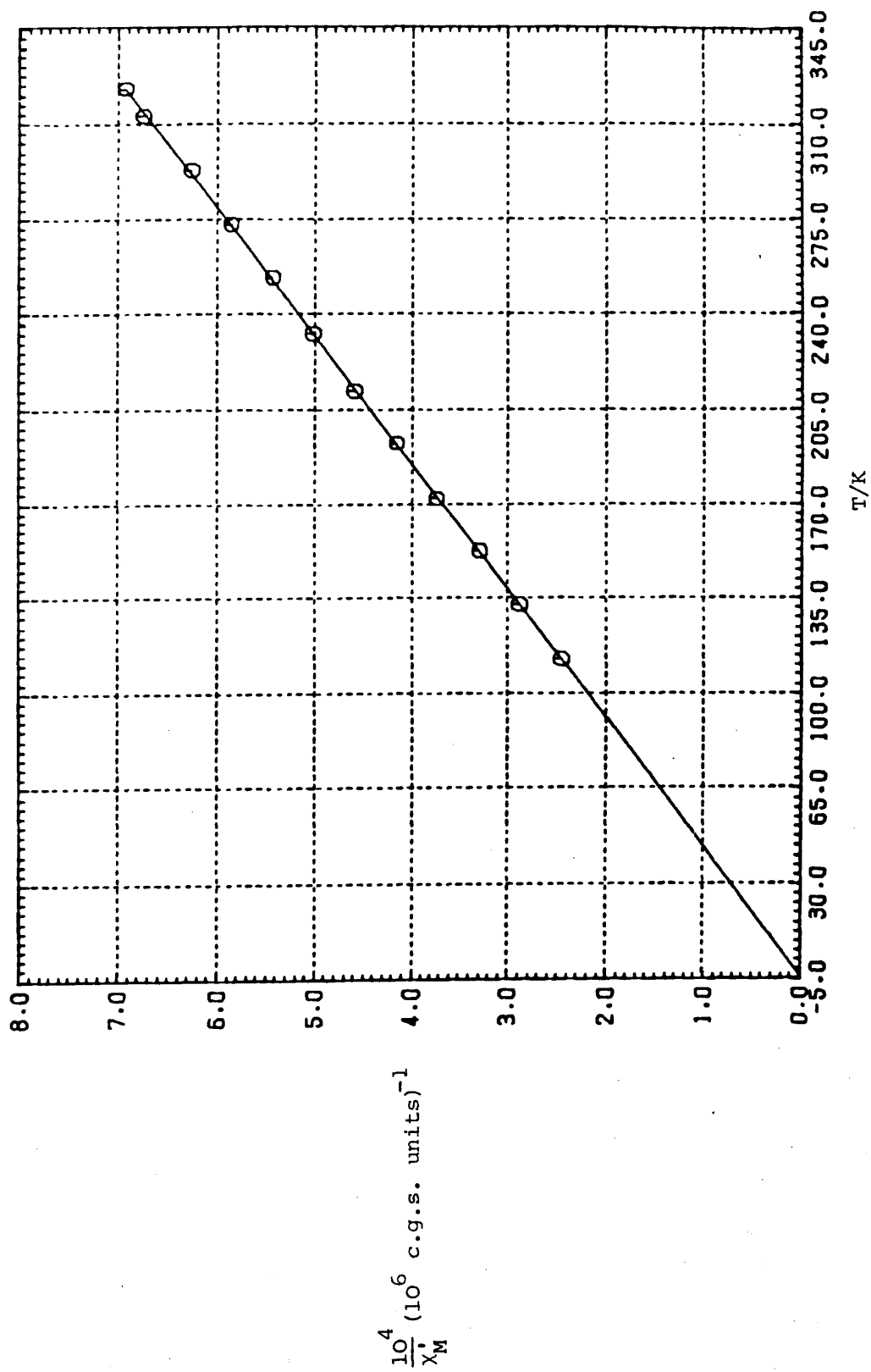
Fig.5.16. Cu(II)mal.2½H₂O

Table 5.17. Variation of magnetic susceptibility and moment with temperature (113-293 K). All χ values in c.g.s. units

<u>Compound</u> $\text{Na}_2[\text{Cu}(\text{mal})_2(\text{H}_2\text{O})_2]$		Field 10 amps			
Temp/K	χ_g	$\chi_M \times 10^6$	$\chi_M' \times 10^6$	$\frac{1}{\chi_M'} \times 10^6$	$\mu_{\text{eff}}(\text{B.M.})$
113	11.7071	4093.4	4225.4	2.3666×10^{-4}	1.962
133	9.8367	3439.4	3571.4	2.8×10^{-4}	1.957
153	8.5213	2979.5	3111.5	3.2139×10^{-4}	1.960
173	7.4275	2597.0	2729.0	3.6643×10^{-4}	1.951
193	6.6217	2315.3	2447.3	4.0861×10^{-4}	1.952
213	5.9313	2073.9	2205.9	4.5333×10^{-4}	1.947
233	5.3563	1872.8	2004.8	4.9879×10^{-4}	1.941
253	4.8392	1692.0	1824.0	5.4824×10^{-4}	1.929
273	4.4946	1571.6	1703.6	5.8701×10^{-4}	1.937
293	4.1501	1451.1	1583.1	6.3167×10^{-4}	1.934

Diamagnetic correction = -132×10^{-6} c.g.s. units

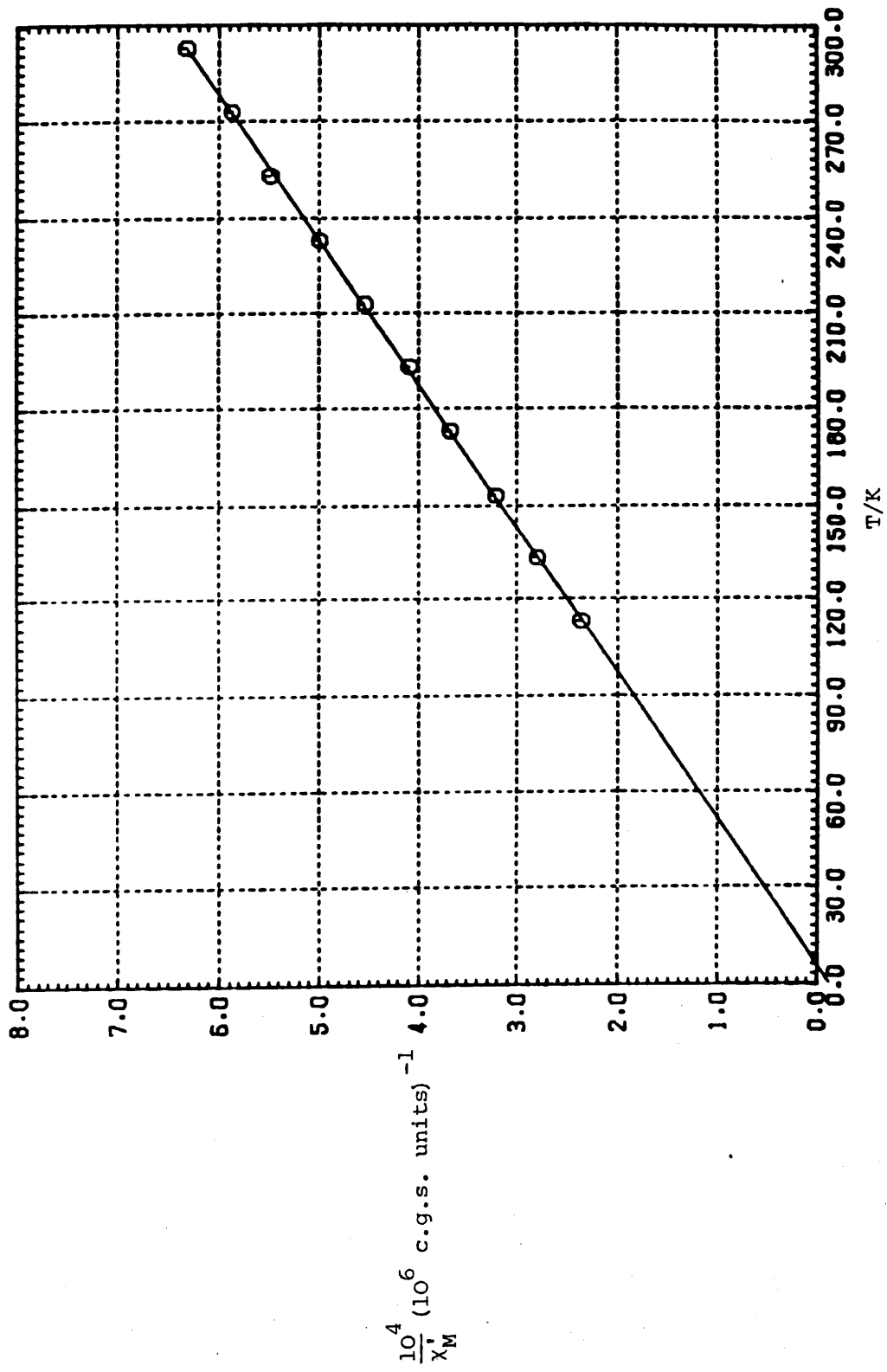
Fig.5.17. $\text{Na}_2[\text{Cu}(\text{mal})_2(\text{H}_2\text{O})_2]$

Table 5.18. Variation of magnetic susceptibility and moment with temperature (112-323 K). All χ values in c.g.s. units

Compound Cu(II) etmal.2H ₂ O		Field 10 amps			
Temp/K	χ_g	$\chi_M \times 10^6$	$\chi'_M \times 10^6$	$\frac{1}{\chi'_M} \times 10^6$	$\mu_{\text{eff}}(\text{B.M.})$
112.5	16.8749	3875.8	3978.1	2.5138×10^{-4}	1.900
132.5	14.3090	3286.4	3388.7	2.951×10^{-4}	1.903
152	12.4545	2860.5	2962.8	3.3752×10^{-4}	1.906
171.5	10.9073	2505.1	2607.5	3.8351×10^{-4}	1.900
191.5	9.7660	2243.0	2345.3	4.2638×10^{-4}	1.903
212.5	8.7694	2014.1	2116.4	4.7249×10^{-4}	1.905
233	7.9806	1833.0	1935.3	5.1672×10^{-4}	1.907
253.5	7.2777	1671.5	1773.8	5.6375×10^{-4}	1.904
273	6.6809	1534.5	1636.8	6.1096×10^{-4}	1.900
293	6.2411	1433.4	1535.7	6.5115×10^{-4}	1.905
313	5.8216	1337.1	1439.4	6.9474×10^{-4}	1.906
323	5.6296	1293.0	1395.3	7.1922×10^{-4}	1.906

Diamagnetic correction = -102.32×10^{-6} c.g.s. units

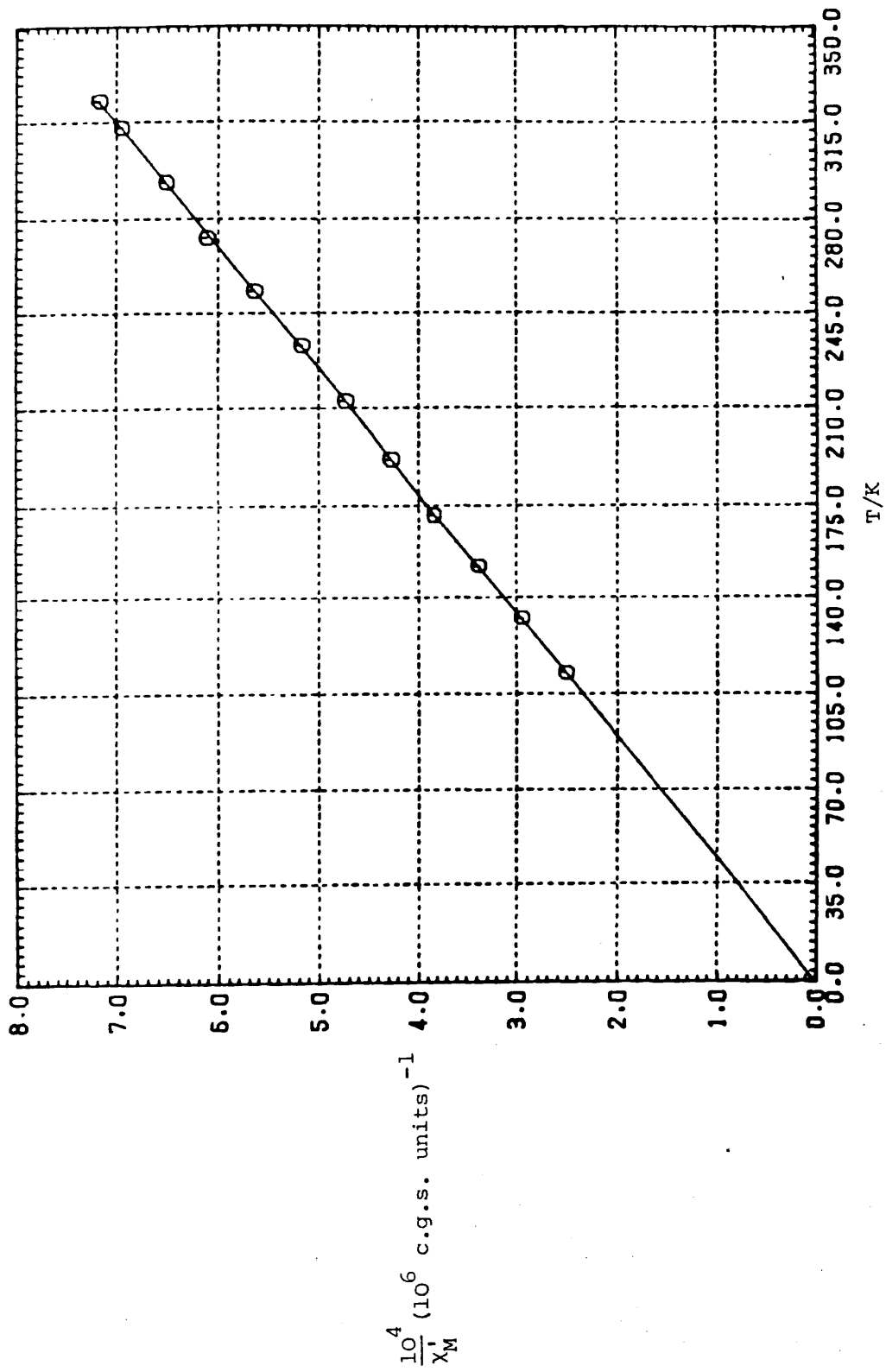
Fig. 5.18. Cu(II) etmal.2H₂O

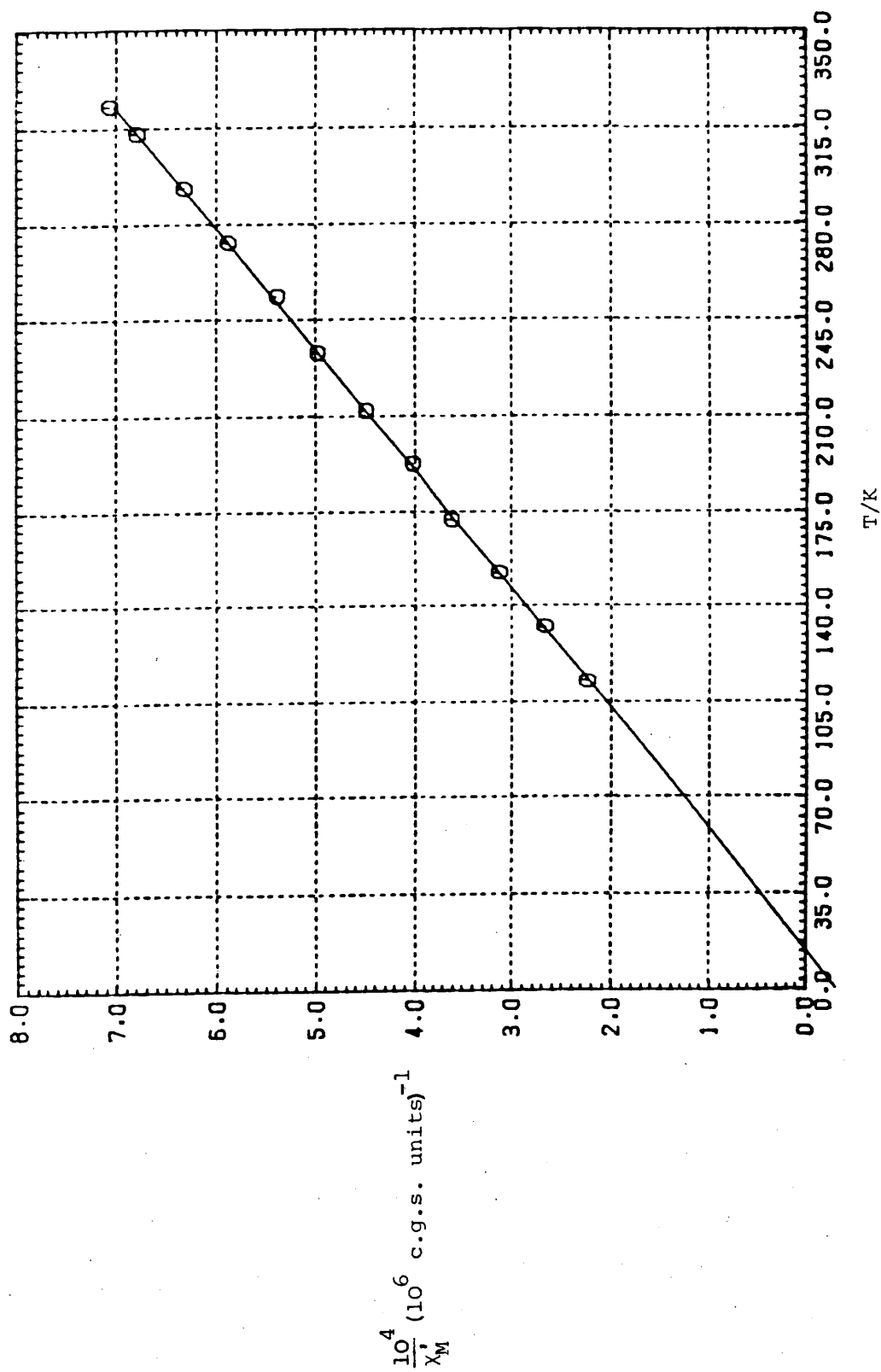
Table 5.19 . Variation of magnetic susceptibility and moment with temperature (112-323 K). All χ values in c.g.s. units

Compound Cu(II)benzylmal.1/2 H₂O

Field 10 amps

Temp/K	χ_g	$\chi_M \times 10^6$	$\chi'_M \times 10^6$	$\frac{1}{\chi'_M} \times 10^6$	$\mu_{\text{eff}}(\text{B.M.})$
112.5	16.3589	4330.6	4450.7	2.2468×10^{-4}	2.000
132.5	13.6927	3624.8	3744.9	2.6703×10^{-4}	2.000
152	11.6146	3074.7	3194.8	3.1301×10^{-4}	1.979
172	10.0329	2655.9	2776.1	3.6022×10^{-4}	1.962
192.5	8.9466	2368.4	2488.5	4.0185×10^{-4}	1.966
212	7.9581	2106.7	2226.8	4.4907×10^{-4}	1.951
233	7.1459	1891.7	2011.8	4.9707×10^{-4}	1.944
253.5	6.5591	1736.3	1856.5	5.3866×10^{-4}	1.948
273	5.9747	1581.6	1701.8	5.8763×10^{-4}	1.936
293	5.5232	1462.1	1582.2	6.3201×10^{-4}	1.934
313	5.1184	1355.0	1475.1	6.7793×10^{-4}	1.930
323	4.8938	1295.5	1415.6	7.0641×10^{-4}	1.920

Diamagnetic correction = -120.12×10^{-6} c.g.s. units

Fig.5.19. Cu(II)benzylmal.½H₂O

REFERENCES

1. F.A. Cotton and G. Wilkinson, "Advanced Inorganic Chemistry", 2nd Ed., 1966.
2. J. Lewis and R.G. Wilkins, "Modern Coordination Chemistry", Interscience, New York, 1960.
3. L.N. Mulay, "Magnetic Susceptibility", Part 1, 1963, 4.
4. B.N. Figgis and J. Lewis, "The magnetic properties of transition metal complexes", in: Cotton, F.A. (ed.), Progress in Inorganic Chemistry, vol. 6, Interscience, New York, 1964.
5. R.S. Nyholm, J. Inorg. Nucl. Chem., 1958, 8, 401.
6. P.W. Selwood, "Magneto Chemistry", Interscience, New York, 1943.
7. J.H. Van Vleck, "Electric and Magnetic Susceptibilities", Oxford University Press, 1932, London.
8. M. Prasad, S.S. Dharmatti, C.R. Kanekar and D.D. Khanolkar, J. Chem. Phys., 1950, 18, 941.
9. O. Asai, M. Kishita and M. Kubo, J. Phys. Chem., 1959, 63, 96.
10. L. Dubiki, C.M. Harris, E. Kokot and R.L. Martin, J. Inorg. Chem., 1966, 5, 93.
11. M. Prasad, S.S. Dharmati, C.R. Kanekar and M.G. Datar, Proc. Ind. Acad. Sci., 1950, 31A, 389.
12. B.N. Figgis and R.S. Nyholm, J. Chem. Soc., 1958, 4190.
13. S.S. Bhatnagar, M.L. Khannar and M.B. Nevgi, Phil. mag., 1938, 25, 234.
14. H. Pezeart, J. Duberant, J.P. Lagier and J. Wyart, Compt. Rend., 1968, 266, 1357.
15. A.M. Talati and B.V. Shah, Indian J. Chem., 1974, 12, 658.
16. J. Ploquin, Bull. Soc. Chim. France; 1951, 18, 757.
17. A.C. Ranade and V.V. Subbo Rao, Indian J. Chem., 1966, 4, 42.

18. L. Walter-Levy, J. Perrotery and J.W. Visser, *Bull. Chim. Soc.*, 1973, 2596.
19. L.G. Perinet, F. Doubli and R. Lafont, *Compt. Rend.*, 1970, 271, 69.
20. R.S. Nyholm, *J. Inorg. Nucl. Chem.*, 1958, 8, 420.
21. R. Lafont, G. Perinet and L.V. My, *Compt. Rend.*, 1968, 267, 474.
22. C.H. Johnson, *Trans. Faraday Soc.*, 1932, 28, 845.
23. F.A. Long, *J. Amer. Chem. Soc.*, 1941, 1353.
24. N. Perakis, J. Wucher and T. Karantassis, *Compt. Rend.*, 1954, 238, 475.
25. B.C. Guha, *Proc. Roy. Soc.*, 1951, A206, 353.
26. T.G. Dunne, *J. Chem. Educ.*, 1967, 44.
27. H.C. Clark, N.F. Curtis and A.L. Odell, *J. Chem. Soc.*, 1954, 63.
28. C. Oldeham, *Progr. Inorg. Chem.*, 1968, 10, 345.
29. I.E. Knaggs, *J. Chem. Soc.*, 1922, 121, 2071.
30. W.E. Hatfield, *J. Inorg. Chem.*, 1964, 3, 605.
31. T.S. Piper and R.L. Carlin, *J. Chem. Phys.*, 1961, 35, 1809.
32. J.N. VanNiekerc, F.R.L. Schoening, *Acta Cryst.*, 1952, 5, 196.
33. J.C. Chang, *J. Inorg. Nucl. Chem.*, 1968, 30, 945.
34. A. Mead, *Trans. Faraday Soc.*, 1934, 30, 1052.
35. K.R. Butler and M.R. Snow, *J. Chem. Soc. Dalton*, 1976, 251.
36. R.P. Scaringe, W.E. Hatfield and D.J. Hodgson, *J. Inorg. Chem.*, 1977, 16, 1600.
37. J.W. Lethbridge, *J. Chem. Soc. Dalton*, 1980, 10, 2039.
38. N. Goldenberg, *Trans. Faraday Soc.*, 1940, 36, 847.
39. J.T. Grey, *Amer. Chem. Soc.*, 1946, 605.
40. J.I. Bullock, M.M. Patel and J.E. Salmon, *J. Inorg. Nucl. Chem.*, 1969, 31, 415.
41. T. Lis, J. Matuszewski and B. Jezowska-Trzebiatowska, *Acta Cryst.*, 1977, B33, 1943.

42. T.S. Davis, J.P. Fackler and M.J. Weeks, *J. Inorg. Chem.*, 1968, 7, 1994.
43. G.H. Cartledge and P.M. Nichols, *J. Amer. Chem. Soc.*, 1940, 62, 3057.
44. K.R. Ashley and K. Lane, *J. Inorg. Chem.*, 1970, 9, 1795.
45. R.E. Hamm and R.H. Perkins, *J. Amer. Chem. Soc.*, 1955, 77, 2083.
46. B.N. Figgis and R.L. Martin, *J. Chem. Soc.*, 1956, 2837.
47. R.L. Martin and H. Waterman, *J. Chem. Soc.*, 1959, 1359.
48. J.N. VanNiekerk and F.R.L. Schoening, *Acta Cryst.*, 1953, 6, 227.
49. J. Lohn, *Acta Cryst.*, 1969, 22.
50. B.N. Figgis and D.J. Martin, *J. Inorg. Chem.*, 1966, 5, 100.
51. D.P. Graddon, *J. Inorg. Nucl. Chem.*, 1958, 7, 73.
52. K. Kuroda and M. Kubo, *J. Phys. Chem.*, 1960, 64, 759.
53. R. Rajan, *J. Chem. Phys.*, 1962, 37, 460.
54. B.H. O'Connor and E.N. Maslen, *Acta Cryst.*, 1966, 20, 824.
55. G.I. Dimitrova, A.V. Ablove, G.A. Kiosse, G.A. Popovich, T.I. Malinovskii and I.F. Burshtein, *Ducki. Akad. Nauk. SSSR.*, 1974, 216, 1055.
56. F.E. Mabbs and D.J. Machin, "Magnetism and Transition Metal Complexes", Chapman and Hall Ltd., 1973, London.

CHAPTER VI: X-RAY DIFFRACTION THEORY^{1-5*}

6.1 The General Nature of Crystals

The constancy of the external forms of well-developed crystals early led to the idea that they were built from blocks of a unit structure regularly repeated in space. Quantitative studies of the interfacial angles confirmed this idea and established a crystal as constituted of these units stacked side to side in three dimensions.

The geometrical properties of a crystal are conveniently described in terms of its crystallographic axes. These are three or sometimes four lines, meeting at a point. They are chosen so as to bear a definite relationship with characteristic features of the crystal, for example, the axes may coincide with or be parallel to the edges between principal faces. Where possible, the axes are chosen to be at right angles to each other. This is illustrated in Figure 6.1.

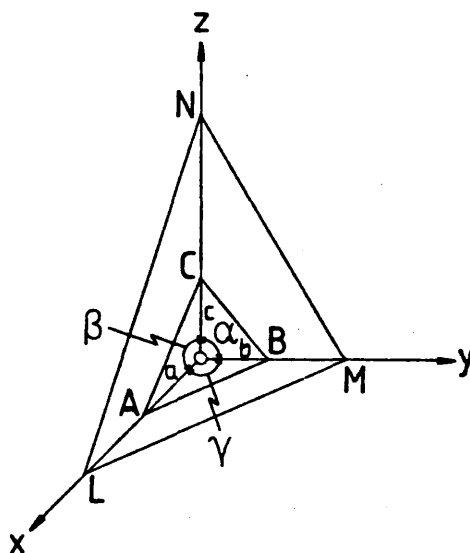


Figure 6.1. The crystallographic axes.

OX, OY and OZ are the crystallographic axes, the interaxial angles, α , β and γ are all as shown. A particular plane, (ABC), of the crystal

* The references for this section are on page 210.

is chosen as a standard or unit plane, in terms of which the crystal faces may be described. This plane must cut the three crystallographic axes, and is often a good face of the crystal. The intercepts where this plane cuts the axes, $OA = a$, $OB = b$, $OC = c$, are known as the crystal parameters. Their lengths are purely relative but their ratios are important and are used to describe the crystal. The law of rational indices states that the intercepts made on the crystallographic axes by the intersections of the plane parallel to possible crystal faces shall have values such as $\pm a/h$, $\pm b/k$, $\pm c/l$, in which h , k and l are integers, including zero. The three integers used to index the plane are called Miller indices. These indices are described as the reciprocal of the intercepts of the plane along each of the three crystallographic axes. Thus, if the original lattice planes had the indices (h, k, l) , resulting from intercepts $1/h$, $1/k$ and $1/l$, a single interleaving plane would cut the axes at half these distances from the origin, i.e. $\frac{1}{2}h$, $\frac{1}{2}k$, and $\frac{1}{2}l$, and have indices $(2h, 2k, 2l)$. For example, plane LMN has indices $(3, 3, 2)$ respectively in Figure 6.1.

A plane parallel to an axis is one of the types $(h, k, 0)$, $(h, 0, 1)$ or $(0, k, 1)$, and one parallel to two axes is one of the types $(h, 0, 0)$, $(0, h, 0)$ or $(0, 0, h)$. If the indices of a plane can be derived from another by multiplying throughout by -1 , then the two planes are parallel.

Every crystal possesses certain elements of symmetry. Externally, this appears as repetition of the crystal faces and their angles. A crystal is said to have an n -fold axis of symmetry when a rotation of $360^\circ/n$ about the axis produces an orientation which cannot be distinguished from the first. Another possible symmetry operation is inversion. This may be visualized in terms of the normals to the crystal faces. A 1-fold inversion axis, $\bar{1}$, means that in effect there is a centre of symmetry present and for each face on the crystal there will be

one parallel on the opposite side. Generally, crystals can be divided into seven different fundamental classes or systems on the basis of their external shapes. These are summarised in Table 6.1. A crystal is made up of an 'infinite' number of repeating groups. Each group constitutes a unit cell, this being the smallest portion of the crystal which possesses all the various kinds of symmetry which characterize the crystal as a whole. In general the unit cell is characterized by six parameters, three axial lengths and three interaxial angles (Fig.6.2). The lengths of the unit cell edges are designated a , b , c and the interaxial angles α , β , γ . The angle α is between b and c , β is between a and c and γ is between a and b .

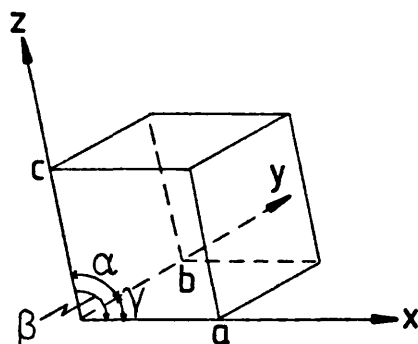


Figure 6.2. Unit cell.

6.2 X-rays and Crystal Structure

Important information concerning the arrangement of the atoms and molecules within crystals has been obtained from the measurements of the transmission and 'reflection' of X-rays. A crystal is a periodic three-dimensional array of atoms in which the interatomic distances are about 2×10^{-8} cm on the average. This fact reveals the

Table 6.1

System	Lattice constants	Essential symmetry
Cubic	$\alpha = \beta = \gamma = 90^\circ$ $a = b = c$	Four 3-fold axes
Tetragonal	$\alpha = \beta = \gamma = 90^\circ$ $a = b \neq c$	One 4-fold or 4-fold inversion axis
Hexagonal	$\alpha = \beta = 90^\circ; \gamma = 120^\circ$ $a = b \neq c$	One 6-fold or 6-fold inversion axis
Rhombohedral (Trigonal)	$\alpha = \beta = \gamma \neq 90^\circ$ $a = b = c$	One 3-fold or 3-fold inversion axis
Orthorhombic	$\alpha = \beta = \gamma = 90^\circ$ $a \neq b \neq c$	Three mutually perpendicular 2-fold axes (either rotation or rotation inversion)
Monoclinic	$\alpha = \gamma = 90^\circ; \beta \neq 90^\circ$ $a \neq b \neq c$	One 2-fold or 2-fold inversion axis
Triclinic	$\alpha \neq \beta \neq \gamma$ $a \neq b \neq c$	One 1-fold or 1-fold inversion axis

possibility of obtaining diffraction effects if radiation with a wavelength in this range ($1 - 2 \text{ \AA}$) is passed through a crystal. When a wave-front of X-rays passes over the atoms in a crystal, each atom scatters the X-rays. A crystal therefore acts as a three dimensional diffraction grating towards X-rays. According to Bragg, the crystal can be regarded simply as a series of identical parallel planes spaced at definite intervals, so-called lattice planes. When X-rays fall upon a lattice plane, its single lattice points become secondary radiation sources, which scatter the incident electromagnetic radiation in every direction of space. It can be shown that the scattered rays extinguish one another in every direction, with the exception of one direction, which can be obtained by considering the lattice planes as a mirror, from which the X-ray beam is reflected. However, an intense diffracted beam is obtained only if the rays reflected by the single lattice planes reinforce one another. The condition for this is that the path difference of the rays must be integral multiples of the wavelength. From Figure 6.3 it can be seen that the path difference of two neighbouring rays is $BC + CD$. d is the perpendicular distance between the two lattice planes. Since for $BC = CD$ the path difference is $2BC$, furthermore since $BC = d \sin \theta$, so the path difference is $2d \sin \theta$, this must be an integral number of wavelengths, that is $n\lambda$ where n is an integer. If this is so,

$$n\lambda = 2d \sin \theta \quad (1)$$

where θ is the angle which the X-ray beam makes with the lattice plane, and λ is the wavelength of the X-rays. This equation is known as Bragg's Law and is defined in terms of an interplanar spacing d and a glancing angle θ .

When a crystal diffracts X-rays in accordance with Bragg's Law, the scattered X-rays are said to constitute a reflection. Since the reflection is attributed to the plane (h, k, l) the reflection

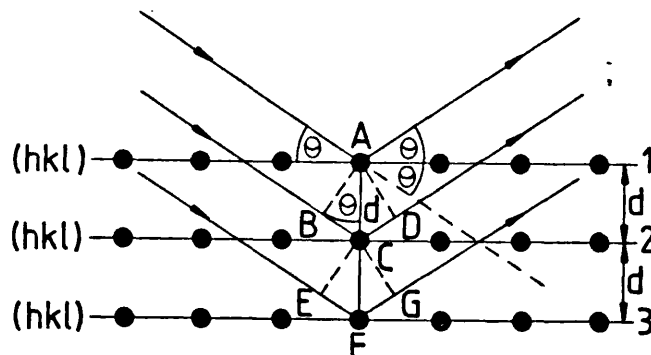


Figure 6.3. 'Reflection' of X-rays from the lattice planes of a crystal.

itself is designated h, k, l . It follows from the Bragg equation that, a particular reflection h, k, l can occur only at angle θ . In general reflection takes place from all possible planes (h, k, l) out to the limiting value of $d(h, k, l) = \lambda/2$, which occurs when θ is 90° . As the wavelength employed is usually much less than the maximum spacing, it is possible to observe reflections from a very large number of planes. In general, only a few planes are in position to reflect if the crystal is kept stationary, and it is therefore necessary to rotate the crystal if all the possible reflections are to be observed. When a crystal is rotated in a collimated beam of monochromatic X-rays, accordingly it reflects a large number of discrete beams in directions determined by the geometry of the crystal lattice. The diffracted beams may be recorded on a photographic plate as a series of spots (each spot corresponding with a particular set of planes in a crystal)

or by other types of counters.^{3,4} The mathematical analysis of the diffraction pattern gives the distribution of electron density in the crystal since the diffraction is caused primarily by the extranuclear electrons. Thus a picture of the structure can be built up consisting of sections or projections of the crystal lattice which show contours of equal electron density. The positions of the atoms are usually assumed to coincide with regions of maximum electron density.

6.3 Determination of the Crystal Structure

Space Group Symmetry^{1,3}

The application of the theory of space groups to crystal structure determination involves the assumption that equivalent sites of the crystal are occupied by identical atoms.

According to the theory of space groups there are 230 essentially different ways of arranging asymmetric but identical bodies in crystal lattice systems. These are so-called space groups. Any crystal can be classified into one of these space groups. The space group gives only the symmetry elements of a crystal lattice. Depending on the number of latticepoints in the unit cell, and their arrangement relative to the symmetry elements, an infinite number of arrangements is possible within each space group. The glide planes and screw axes are the symmetry elements of the crystal lattice which can be derived from the symmetry planes and rotational axes of symmetry by associating them with a translation. Information about the space group is sometimes obtainable from a simple study of X-ray reflections recorded, on the basis of the systematic absence of interference spots of certain type. The screw axis (rotation-translation) and glide plane (reflection-translation), which are of great importance from the point of view of the determination of the space group, can be found indirectly from such systematic absences. Such systematic absences are termed space group extinctions or simply

extinctions. A list of X-ray extinctions of a given crystal is thus characteristic of the repeating operation of the pattern of the crystal, i.e., of the space group of the crystal in hand. A complete list of space groups and the absences are set out in full detail in the international tables for X-ray crystallography and by Buerger.¹ When the space group is determined, the number of asymmetric units necessary to build up the symmetry of the space group and complete the identically repeating unit cell can be found easily. The translation appropriate to a space group is of atomic dimensions and is negligible when the crystal is considered as a macroscopic structure. In many cases it is possible to identify the crystal space group from the diffraction pattern, but unfortunately it is not usually possible to show the asymmetry of a structure in this way as nearly all crystals diffract as though they had a centre of symmetry. As a consequence, the interpretation of diffraction spectra may be ambiguous in some cases and the space groups must be confirmed by much more detailed study of the reflections and their intensities.

If the unit cell dimensions are determined, its volume, and, from the known density of the crystal, the number of molecules, Z , in the unit cell can be calculated.

$$Z = \frac{\rho v \times 0.6023 \times 10^{24}}{M}$$

where ρ is the density (g cm^3), v the volume (cm^3) of the unit cell, and M the molecular weight. If the space group has been determined, the number of atoms in equivalent positions contained by the unit cell can be deduced.

6.4 Principles of X-ray Powder Photographs^{2,5}

The value of X-ray diffraction as an investigator's tool in chemical analysis was greatly extended by the introduction of the powder

method by means of which X-ray diffraction photographs can be obtained not only of powdered crystals, but also of polycrystalline aggregates and of polycrystalline surfaces such as those of metals.

Most crystalline materials do not normally occur in sufficiently large single crystals, so that a powder of a large number of very tiny crystals must be utilized instead. There are many applications of the powder method, but two of these are of primary importance. Fundamentally, the powder method provides a way of investigating, within limits, the crystallography of the crystal in the powder. Secondly, since the powder diffraction diagram of a crystallite of a material is characteristic of the atomic arrangement in the material, it is like a fingerprint in that no two substances give rise to identical diagrams. Conversely, if two materials do give rise to identical diagrams, they must be the same material. It follows, therefore, that powder photographs of known materials can be used to identify the composition of an unknown material.

The indirect method of identification, in which the pattern of the unknown is compared with those of likely substances, has been much used. In such cases if a set of standard diagrams of known substances, or tabular representations of them are available, then it is usually possible to identify a pure substance with the aid of a set of rules for finding an unknown diagram among the standard diagrams. Such procedure can be used to great advantage when a group of structurally related compounds is being studied. In such a group, the common structural features often give rise to lines which are common to the whole group. The lines not common to the group, however, are the ones most helpful in distinguishing between the various members of the group. Thus, when studying isomorphous series such procedure can be most helpful in the identification of any member in the series assuming that the unknown has a structure similar to that of one of the known structure types.

The sample to be measured in the powder method is ground to a

fine powder, which is really an aggregate of a large number of tiny crystals (crystallites). The random orientation of these crystallites in the specimen ensures that every possible reflection plane is presented parallel to the specimen surface by at least some crystallites. If such a system is irradiated by monochromatic X-rays, the powder sample gives a diffraction pattern, consisting of a series of lines corresponding to Bragg reflection from each set of parallel planes and separated by distances determined by the characteristics of the crystal lattice from which they have been reflected.

Principles of the Calculation of Powder Patterns

Any diffraction pattern may be considered to consist of two aspects: (1) the positions of the diffraction lines, and (2) the intensities of the lines. The positions of the diffraction lines are related to the size and shape of the crystal lattice on which the crystal structure is built. This dependence is most commonly expressed by the Bragg relation:

$$\sin \theta_{hkl} = \frac{\lambda}{2d_{hkl}}$$

where θ_{hkl} is the Bragg angle, λ is the X-ray wavelength, and d_{hkl} is the interplanar spacing for the atomic planes represented by the Miller indices h , k and l (nh , nk , nl). The interpretation of a powder photograph requires the identification of all reflections. From the measured position of each line on the powder pattern, the Bragg angle θ , for that reflection line can be calculated. Each θ can be readily transformed into the interplanar spacing d_{hkl} for the planes responsible for the reflection of that line.⁶ Primarily, then a powder photograph yields a set of numerical values for the various d 's ($= \lambda/2 \sin \theta$) of the crystal sample, one d for each line of the powder photograph. A powder photograph is always interpretable up to this point (except for possible

complications due to d's so close together that they are unresolved, that is, so that one observed line is really two or more overlapping lines). The spacings can also be arrived at in another way, for they are functions of the cell edges a, b, and c, interaxial angles α , β and γ , and the indices of the reflecting planes(hkl). If the cell dimensions are known, a list of expected d_{hkl} values can be prepared and the list of calculated and indexed spacings can then be compared with the list of observed, but unindexed spacings, and the individual spacings in the latter may thus be identified. Normally, the cell dimensions are not known, therefore, the unit cell dimensions and indices must be determined in some way from the experimental d_{hkl} values. This is fairly easy in geometry when the cell angles are all 90° , and there are graphical procedures for assigning indices to powder photographs of crystals belonging to such systems.⁵ The relationship between d_{hkl} and the parameters which describe the direct lattice is very complicated for low-symmetry systems (orthorhombic, monoclinic or triclinic crystal) because too many variables are involved. It is more simply stated in terms of the reciprocal parameters, where

$$d_{hkl}^2 = h^2 a^{*2} + k^2 b^{*2} + l^2 c^{*2} + 2hka^*b^* \cos \gamma^* + 2hla^*c^* \cos \beta^* + 2klb^*c^* \cos \alpha^*$$

The quantities a^* , b^* , c^* , α^* , β^* and γ^* are the reciprocal lattice constants and are found from the real cell parameters through the equations:

$$\begin{aligned} a^* &= \frac{bc \sin \alpha}{V} & \cos \alpha^* &= \frac{\cos \beta \cos \gamma - \cos \alpha}{\sin \beta \sin \gamma} \\ b^* &= \frac{ac \sin \beta}{V} & \cos \beta^* &= \frac{\cos \alpha \cos \gamma - \cos \beta}{\sin \alpha \sin \gamma} \\ c^* &= \frac{ab \sin \gamma}{V} & \cos \gamma^* &= \frac{\cos \alpha \cos \beta - \cos \gamma}{\sin \alpha \sin \beta} \end{aligned}$$

$$V = abc(1 - \cos^2 \alpha - \cos^2 \beta - \cos^2 \gamma + 2 \cos \alpha \cos \beta \cos \gamma)^{\frac{1}{2}}$$

where a , b , c , α , β and γ are the real cell parameters and V is the volume of the unit cell. Using these relations or others which may be derived from them, it is possible to relate the positions of all the powder lines observed to the crystal lattice with no knowledge of the intensities of the lines. This means that, the set of positions of all the X-ray reflections from a crystal depend only on the dimensional characteristics of its atoms, while the intensities of the reflections hkl depend entirely on the arrangement of the atoms in the unit cell. Thus in the determination of the unit cell dimensions, only the positions of the reflections need be considered and the intensities may be ignored. If an unknown material is to be identified, it may be one pure substance or a mixture. In either case the observed intensities of the diffraction pattern need to be considered. In such cases a comparison of the interplanar spacings and the relative intensities of the observed set with those calculated, usually produces a correct identification, which, however, should only be accepted as final when the whole observed pattern is compared with that of the calculated structure and found to agree, both in spacings and relative intensities. The relative intensities based on 100 of the most intense lines observed, are usually sufficient for identification purposes.

The combination of the unit cell and the arrangement of atoms in it comprises the crystal structure itself. Therefore, the positions and relative intensities of the reflections of a crystal are characteristics of the crystal structure. Whether or not the powder diagram of an unknown crystal can be interpreted, at least this diagram is characteristic of the crystal and can be used as a "fingerprint" to distinguish it from other crystals, and hence to identify it. This is the philosophic basis for using the X-ray powder pattern in crystal identification.

Experimental

The powder pattern diffraction traces were recorded at room temperature using a Phillips PW1011 X-ray diffractometer with $\theta - 2\theta$ scan technique and with Ni-filtered $\text{CuK}\alpha$ radiation ($\lambda = 1.54178 \text{ \AA}$). The scan range and 2θ values for background measurements were determined by inspection of the graphical trace of each peak. The intensities and 2θ values of all independent reflections were recorded (2θ range $5 - 53^\circ$). Beyond this 2θ value very few reflections had significant intensities. The 2θ values measured from diffractometer chart and powder photographs were converted into the interplanar spacings (d) of the diffracting hkl planes, using the published X-ray diffraction tables of J.H. Fang and F. Donald Bloss (1966).⁶ The tables give d values corresponding to 2θ values in the range of $0.11^\circ - 180^\circ$, in increments of 0.01° for the most frequently used wavelengths.

Since direct X-ray diffraction study of these compounds has been proved to be difficult, an attempt was made to examine the structures of these complexes on the basis of the previously published data by: (i) the known crystal data of each corresponding compound were computed; (ii) the data set were then collected; these consisted of the diffraction angle 2θ and d spacings of the diffracting hkl planes. These were regarded as calculated values which are given in column 3 of each table; (iii) the reciprocal lattice levels (the values of hkl) for all the relevant spectra were estimated visually by comparing these with the data set computed of the previously published data in the first stage, assuming approximately the same cell dimensions. The results obtained by this method in most cases were found to be reasonably consistent.

All computations were performed on the University of London CDC computer by way of the crystallographic programmes developed by Dr Langford and Dr Marriner at Birmingham University Physics Department.^{7,8} Single crystal diffraction photographs were carried out with a single crystal

Pye Unicam oscillation/rotation camera, using $\text{CuK}\alpha$ radiation. The single-crystal photographs of Al^{3+} malonate complex were carried out at Birkbeck College using a precession camera.

The complete list of observed and calculated interplanar spacings, the relative reflection intensities, and the reflection indices when known are tabulated in Tables 6.3 - 6.10 for comparison.

Determination of the Unit Cell Dimensions with the Highest Accuracy. The minimization of errors by the use of an internal standard.

One simple and highly recommended method of correcting for all possible errors is to mix the substance under investigation with a standard substance whose spacings are known to the desired accuracy; the resulting powder photograph shows both patterns superimposed. For this purpose it is desirable to use a simple substance giving few lines, otherwise overlapping is frequent. Quartz was used in this investigation. Since the accurate 2θ values of quartz were known,² the peak shifts $\delta(2\theta)$ were then obtained, where $\delta(2\theta)$ is the difference between the known and the measured value of 2θ of the standard, which were then used to determine the precise spacings of the substance under investigation. For the best accuracy, the average errors were calculated by taking the average of all the individual errors, from which the position of the reflections on the chart paper, that is, the 2θ values of the substance, were corrected. The interplanar spacings were then obtained directly from the table for the corresponding diffraction angle 2θ . The d values thus determined together with the corresponding reflection indices when known were then computed. Applying the least-squares method, the unit cell dimensions were refined. The accuracy attainable by the internal standard procedure described is directly comparable with the accuracy to which the spacings

of the standard are known.

Calculation of the Tables

Relative intensity measurements

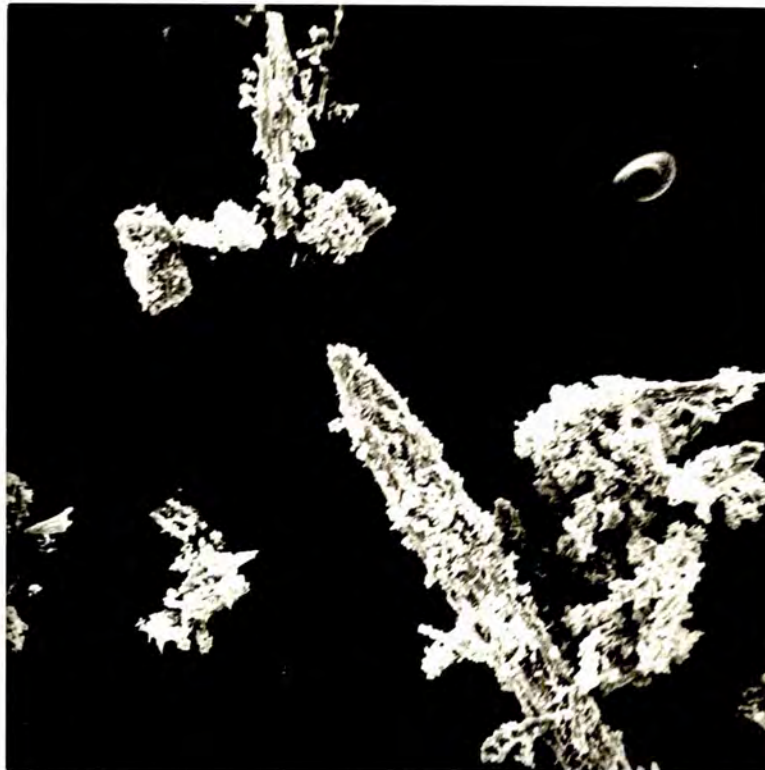
The column labelled I/I_1 in each table contains the relative intensities of these reflections based on 100 for the strongest intensity observed from the experimental diffractometer trace. If the profile was fully resolved its height was measured by counting squares on the chart paper. The relative intensities were readily found and listed by applying an "absolute scale factor" to the measured peak height. Such scale factor was chosen to scale the set to a maximum value, usually 100, for the strongest reflections observed, that is, the most intense reflection is arbitrarily assigned the value of 100 and the other intensities were scaled accordingly. These are listed in the first column of the tables for each corresponding d value.

X-ray Determinations

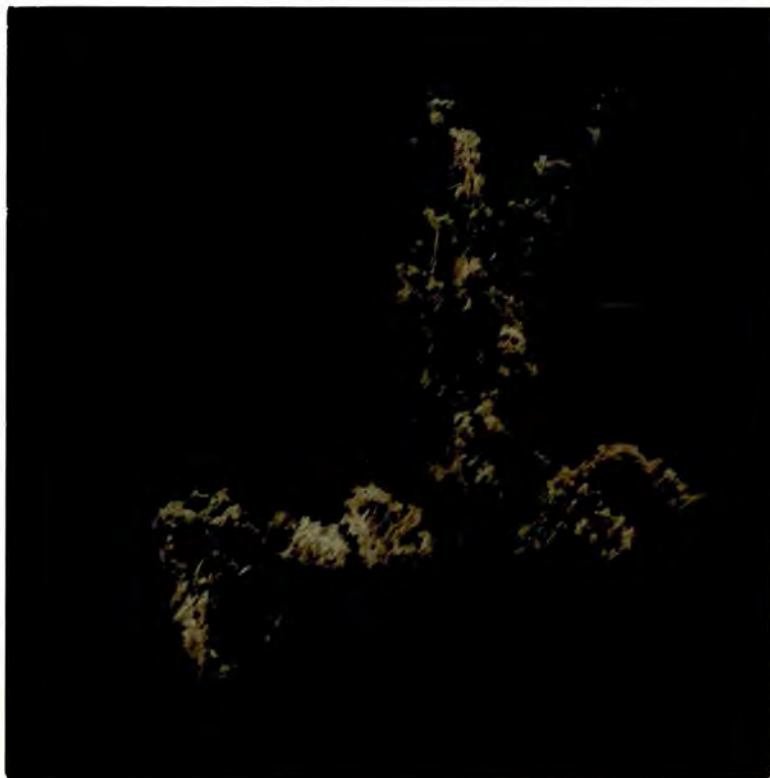
6.5 Experimental and Results

The structure of Ba (II) malonate dihydrate

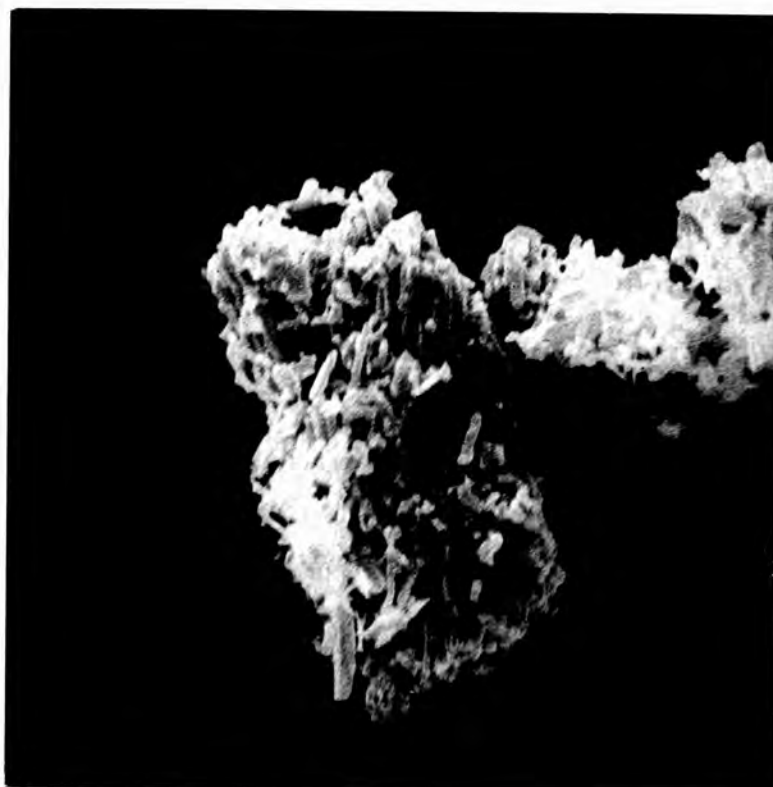
The crystal structure of this compound has been studied for the first time. The structures for the corresponding calcium and strontium compounds⁹ have been published, and they are different from each other. The data now obtained for barium malonate were examined to see if they fit either of the structures proposed for the calcium and strontium compounds. This analysis has been pursued only far enough to prove the structure to be of the strontium type. Weak and broad spectra, and doubling of peaks caused some difficulties in the recognition of any individually significant peaks in the spectra. The broadening may mean that some crystals have slightly different unit-cell dimensions from others; or that the unit-cell dimensions vary in different regions of the same crystals, owing to variations of composition



Slide 1. 2Bamal, Ba(OH)₂·2H₂O (×1,100)



Slide 2. Similar to the above (×2,200)



Slide 3. 2Bamal, $\text{Ba}(\text{OH})_2 \cdot 2\text{H}_2\text{O}$ ($\times 5,500$)

or to strains^{2,4}. In these circumstances certain crystals or parts of crystals give X-ray reflections at slightly different angles from others, and a broad line is the result. Alternatively, the broadening may mean that crystals are too small to yield a normal diffraction pattern⁵. In fact, when the crystallites are very small, the number of parallel planes available is too small for a sharp diffraction pattern to build up, and the lines in powder photographs become broadened. When differential broadening is encountered in powder photographs, it is often difficult to decide which is the most likely cause. In barium malonate, electron microscopic examination confirmed that the Ba malonate crystallites consist of very fine grains (see Slides) and it seems most reasonable to assume that the broadening is due to the very small size of the crystals. Further, when operating the X-ray diffractometer, the initial position of the chart is set manually and thus some correction might be anticipated. Attempts to solve this problem were made, using quartz as an internal standard substance, whose spacings are accurately known¹⁰. Measurement of the quartz reflections gives a calibration curve based on peak shifts measured under various conditions for quartz of known reflection angles, which can then be used for interpolating the precise spacings of the Ba malonate. For the best accuracy, the reading error due to the location of the centre of the line on the chart paper can be minimized by preparing and measuring several traces. Various mixtures of quartz and barium malonate were tried. For several such mixtures examined, the 2θ values and the intensities of quartz reflections in the mixture were obtained, and it revealed some significant variations from the initial measurements. Since the accurate 2θ values of quartz were known, $\delta(2\theta)$ were then obtained, where $\delta(2\theta)$ is the difference between the known and measured value of 2θ of the standard. By comparing the original diffractometer trace with three traces obtained using mixtures of barium malonate with quartz, the best

values of the reflection angles were determined. The 2θ values thus determined were then plotted against the $\delta(2\theta)$ of quartz, and the peak shifts corresponding to any 2θ values were read directly from this graph. Finally the improved values of 2θ were estimated in which at least some of the errors of the original diffractometer trace are removed. This gave a new set of 2θ values which were converted into the interplanar spacings (d). By computing the new sets of values of the proposed cell dimensions, the data were collected covering all the reciprocal lattice nets, hkl . At this stage of the refinement a new value for 2θ for each corresponding hkl value when known was computed and the probable error of the trial and refined cell dimensions were estimated by the method of least-squares, and were found to be negligible. Nevertheless the problem proved difficult, and the spectra finally obtained indicated 2 peaks, one at $2\theta = 24.0^\circ$ with quite weak intensity, as well as one with medium intensity at $2\theta = 24.52^\circ$, which could not be identified. Attempts to improve the data were made by a series of computations of the cell parameters using different values of β (106° , 95° , 92° , 91° , 91.5°). Of several such data obtained, the one having $\beta = 92^\circ$ gave the most satisfactory results, and the unit cell dimensions were then refined accordingly by a least-squares method as described before.

Table 6.2. Crystal data for $2\text{BaC}_3\text{H}_2\text{O}_4 \cdot \text{Ba}(\text{OH})_2 \cdot 2\text{H}_2\text{O}$

Trial cell dimensions:

$a = 7.0930$, $b = 9.5170$, $c = 12.7400 \text{ \AA}$,
 $\alpha = 90.00$, $\beta = 92.00$, $\gamma = 90.00 \text{ deg}$.

Refined cell dimensions:

$a = 7.0931$, $b = 9.5193$, $c = 12.7421 \text{ \AA}$,
 $\alpha = 90.00$, $\beta = 91.96$, $\gamma = 90.00 \text{ deg}$.

STD Errors in a , b and c are 0.0033, 0.0034 and 0.0050 \AA .

STD Errors in α , β and γ are 0.000, 0.037 and 0.000 deg.

No further attempt was therefore made to refine the structure, as it seemed very unlikely at this stage that further refinement would lead to a more reliable set of structural data. The observed and calculated d spacings are given together with the observed powder intensities in Table 6.3.

It may be seen that there is a general agreement between the observed and calculated values, remembering that this analysis is based on the known structure for the Sr compound. The reason for some discrepancies between the predicted and observed values is at present unknown. Some observations are worth making, e.g. the Sr malonate compound studied by Briggman and Oskarsson⁹ is in anhydrous form. Furthermore, X-ray structural data on both calcium and strontium malonate reported by them have not been accompanied by accurate analyses proving the identity of the compounds. Failure to establish purity may explain such deviations in the values. In fact, the X-ray analysis of Ca malonate studied by us also did not confirm their results (see page 190). However, from our own evidence as well as from the reported work it is known that the structure of the compound depends strongly on the past history of the sample and its mode of preparation. The compound examined in the present investigation is a basic salt and has the following analysis:

Found: C 10.2 ; H 1.4%

calculated for $2\text{BaC}_3\text{H}_2\text{O}_4$, $\text{Ba}(\text{OH})_2 \cdot 2\text{H}_2\text{O}$: C 10.5; H 1.4%

Although we extrapolate the cell parameters of barium malonate from that of strontium malonate, we have not provided a general proof of the structure. Without complete X-ray structural analysis it is not possible to assign an unequivocal structure to these complexes. Moreover, although the strontium and barium malonates show close resemblances in the values of their crystal angles, and they crystallise probably with

Table 6.3 Powder pattern data for 2Bamal, $\text{Ba}(\text{OH})_2 \cdot 2\text{H}_2\text{O}$

I_{obs}	$d(\text{\AA})$		h	k	l
	obs.	calcd			
s	12.5738	12.7346	0	0	1
	12.5738	12.7346	0	0	$\bar{1}$
vs	9.4083	9.5193	0	1	0
w	7.0530	7.0890	1	0	0
m	6.3301	6.3673	0	0	2
	6.3301	6.3673	0	0	$\bar{2}$
m	6.1721	6.1058	1	0	1
w	5.7910	5.6856	1	1	0
	4.2203	4.2449	0	0	3
w	4.2203	4.2449	0	0	$\bar{3}$
w,b	3.8096	3.8123	0	2	$\bar{2}$
	3.8096	3.8123	0	2	2
m,b	3.5872	3.5882	1	0	3
m	3.5353	3.5445	2	0	0
vw	3.4013	3.3866	1	2	$\bar{2}$
vw	3.3634	3.3576	1	1	3
m	3.2000	3.1893	2	1	1
vw,b	3.1589	3.1680	0	2	$\bar{3}$
	3.1589	3.1680	0	2	3
w,b	2.9766	2.9845	2	1	$\bar{2}$
w	2.9030	2.9071	2	1	2
vw	2.7648	2.7677	2	0	$\bar{3}$
vw	2.6595	2.6576	2	1	$\bar{3}$
m/w	2.5082	2.5026	1	2	$\bar{4}$
m/w	2.3860	2.3798	0	4	0
vw,b	2.3619	2.3630	3	0	0
w	2.3066	2.3092	3	0	1
vw,b	2.2659	2.2625	2	1	4
vw	2.1222	2.1224	1	2	5
vw	2.1002	2.0983	3	2	$\bar{1}$
vw	2.0736	2.0759	0	4	$\bar{3}$
	2.0736	2.0759	0	4	3
vw	2.0535	2.0527	1	0	$\bar{6}$
vw	2.0468	2.0464	3	1	$\bar{3}$
vw	2.0294	2.0271	3	2	$\bar{2}$
vw	1.9701	1.9708	1	1	6

Table 6.3 continued

I _{obs}	d (Å)		h	k	l
	obs	calcd			
vw	1.9256	1.9260	1	3	$\bar{5}$
w,b	1.9066	1.9061	0	4	$\bar{4}$
	1.9066	1.9061	0	4	4
w,b	1.8654	1.8671	3	3	1
vw	1.8554	1.8551	1	2	6
vw	1.8224	1.8221	1	5	$\bar{1}$
vw	1.8139	1.8151	2	1	$\bar{6}$
vw,b	1.7039	1.7035	3	0	5

the same symmetry, orthorhombic or monoclinic, they are not truly isomorphous. Microscopic examination of the barium malonate showed that these consisted of microcrystals or powder which are not suitable for single-crystal X-ray diffraction studies (see Slides), and their crystallographic study has for this reason proved a difficult task. In our opinion a detailed structural investigation of this compound and the close similarity between the two structures will lead to more definite results.

The Structure of Ca(II) malonate

The structure of this compound has been determined from its X-ray powder pattern, and has been fully refined by partial three-dimensional single-crystal X-ray diffraction photographs.

The crystal data both of Briggman and Oskarson (1967)⁹ and of Karipides (1977)¹¹ were examined. Our results are in agreement with those of Karipides (see Table 6.4). Both the previous sets of workers make reference to a so-called calcium malonate dihydrate, $\text{CaC}_3\text{H}_2\text{O}_4 \cdot 2\text{H}_2\text{O}$, which is described as monoclinic. It seems very probable that what the above workers called calcium malonate dihydrate is really a basic salt, in view of their similar method of preparing the compound (from the basic carbonate). The compound examined in the present study has the following analysis:

Found: C 14.80 ; H 2.4%

Calculated for $\text{CaC}_3\text{H}_2\text{O}_4 \cdot \text{Ca}(\text{OH})_2 \cdot 1\frac{1}{2}\text{H}_2\text{O}$: C 14.81 ; H 2.9%

Using quartz as an internal standard the X-ray diffractometer trace was shown to have an error of 0.087 cm. The corrected and calculated values of d spacings, and hkl values are given together with the observed powder pattern intensities in Table 6.4.

Single crystal X-ray work

A well-formed crystal was chosen, it was mounted around the C axis and the photograph was taken at room temperature using Cu-K α

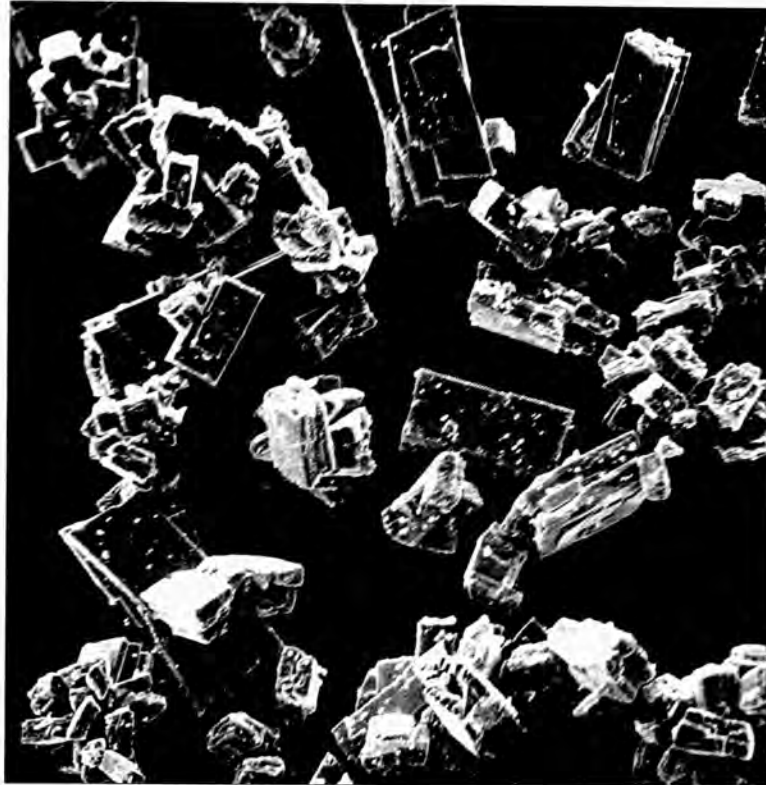
Table 6.4 Powder pattern data for Camal, $\text{Ca}(\text{OH})_2 \cdot 1\frac{1}{2}\text{H}_2\text{O}$

Sym. monoclinic

 $a = 13.9278$, $b = 6.8559$, $c = 6.8639 \text{ \AA}$ Volume = 629.59 \AA^3 $\alpha = 90.000$, $\beta = 106.137$, $\gamma = 90.000$ space group $C2/m$ $Z = 4$

I/I_1	$d(\text{\AA})$		h	k	l
	obs*	calcd			
100	6.6619	6.6895	2	0	0
< 1	6.0836	6.1014	1	1	0
1	4.7805	4.7912	1	1	$\bar{1}$
4	4.1216	4.1540	2	0	1
1	3.7216	3.7384	3	1	0
3	3.6245	3.6357	3	1	$\bar{1}$
7	3.4115	3.4279	0	2	0
39	3.3313	3.3492	2	0	$\bar{2}$
< 1	3.0369	3.0415	0	2	$\bar{1}$
< 1	3.0219	3.0415	0	2	1
1	2.9535	2.9688	3	1	1
< 1	2.8019	2.8199	3	1	$\bar{2}$
2	2.7557	2.7631	4	0	$\bar{2}$
4	2.6780	2.6768	2	0	2
< 1	2.6285	2.6440	2	2	1
2	2.2869	2.2848	2	0	$\bar{3}$
3	2.2373	2.2298	6	0	0
1	2.1371	2.1442	6	0	$\bar{2}$
< 1	2.1085	2.1098	2	2	2
2	2.0226	2.0168	3	3	$\bar{1}$
< 1	1.9349	1.9347	2	0	3
1	1.9024	1.9019	1	3	$\bar{2}$
3	1.8341	1.8382	3	3	$\bar{2}$
5	1.8102	1.8081	4	2	$\bar{3}$
< 1	1.7289	1.7270	3	1	3

* All the above data are based upon an average error of 0.0875



Slide 4. Camal, $\text{Ca}(\text{OH})_2 \cdot 1\frac{1}{2}\text{H}_2\text{O}$ ($\times 550$)



Slide 5. Similar to the above ($\times 2,200$)

radiation ($\lambda = 1.5418 \text{ \AA}$).

The unit cell dimensions obtained by single crystal photographs agree reasonably with the values reported for the similar compound recently.¹¹ The accurate values of the lattice parameters were obtained from powder data by least-squares refinement. Crystal data for $\text{CaC}_3\text{H}_2\text{O}_4 \cdot \text{Ca}(\text{OH})_2 \cdot 1\frac{1}{2}\text{H}_2\text{O}$:
 Monoclinic, space group C2/m , $Z=4$; $a = 13.9278$; $b = 6.8559$; $c = 6.8639 \text{ \AA}$;
 $\beta = 106.137^\circ$; $V = 629.59 \text{ \AA}^3$.

The crystals are shown in Slides 4 and 5.

The Structure of Zn(II) malonate dihydrate

The crystal structure of Zn(II) malonate dihydrate $\text{ZnC}_3\text{H}_2\text{O}_4 \cdot 2\text{H}_2\text{O}$ has been previously reported,¹² and the unit cell dimensions have been confirmed by the present investigation.

Attempts were made to re-examine the structural analysis of this compound from its X-ray powder diffraction pattern, using the data obtained by the above workers. An instrumental error of magnitude 0.1cm was obtained by applying the internal standard method, and the initial values were improved accordingly. The relative intensities of the possible reflections were measured by the method outlined above. A listing of final observed and calculated interplanar spacings and the relative intensities are compared in Table 6.5. Excellent agreement was achieved between the observed and calculated values obtained in the present work and those in the literature.¹² The crystals viewed in an electron microscope are shown in Slides 6, 7 and 8.

The Structure of Cd (II) malonate monohydrate

The crystal structure of this compound was investigated to compare it with the values of the polymeric Cd malonate monohydrate and dihydrate previously reported.¹³ Our results are not in agreement with the observations of Post and Trotter (1974) although their cell dimensions for both monohydrate and dihydrate were tried. The failure of

Table 6.5 Powder pattern data for $\text{Znmal}, 2\text{H}_2\text{O}$

Sym. monoclinic

a = 11.0625, b = 7.4221, c = 7.2901 Å Volume = 596.03 Å³ $\alpha = 90.000$, $\beta = 95.275$, $\gamma = 90.000$ Space group I2/m

Z = 4

I/I ₁	d(Å)		h	k	l
	obs*	calcd			
5	6.3256	6.3349	1	0	$\bar{1}$
3	6.1551	6.1553	1	1	0
10	5.8098	5.8205	1	0	1
100	5.5050	5.5078	2	0	0
45	5.1792	5.1897	0	1	1
68	3.9002	3.9075	2	1	$\bar{1}$
6	3.7033	3.7110	0	2	0
8	3.6494	3.6296	0	0	2
17	3.4013	3.4051	3	0	$\bar{1}$
5	3.2832	3.2911	3	1	0
4	3.1922	3.1993	1	1	$\bar{2}$
1	3.1655	3.1675	2	0	$\bar{2}$
9	3.1232	3.1291	1	2	1
7	3.0727	3.0776	2	2	0
9	2.9094	2.9103	2	0	2
3	2.5931	2.5948	0	2	2
2	2.5411	2.5447	3	1	$\bar{2}$
26	2.5014	2.5017	4	1	$\bar{1}$
7	2.4088	2.4092	2	2	$\bar{2}$
1	2.3679	2.3690	4	1	1
2	2.3394	2.3418	0	3	1
17	2.2981	2.2980	4	0	$\bar{2}$
	2.2908	2.2901	2	2	2
11	2.2100	2.2115	4	2	0
1	2.1774	2.1785	2	3	$\bar{1}$
6	2.1303	2.1324	2	3	1

Table 6.5. (continued)

I/I ₁	d(Å)		h	k	l
	obs*	calcd			
12	2.0588	2.0598	2	1	3
8	1.9529	1.9537	4	2	$\bar{2}$
5	1.8554	1.8555	0	4	0
3	1.8292	1.8295	4	2	2
8	1.7681	1.7677	6	1	$\bar{1}$
3	1.7586	1.7584	4	3	1
1	1.7307	1.7299	0	3	3

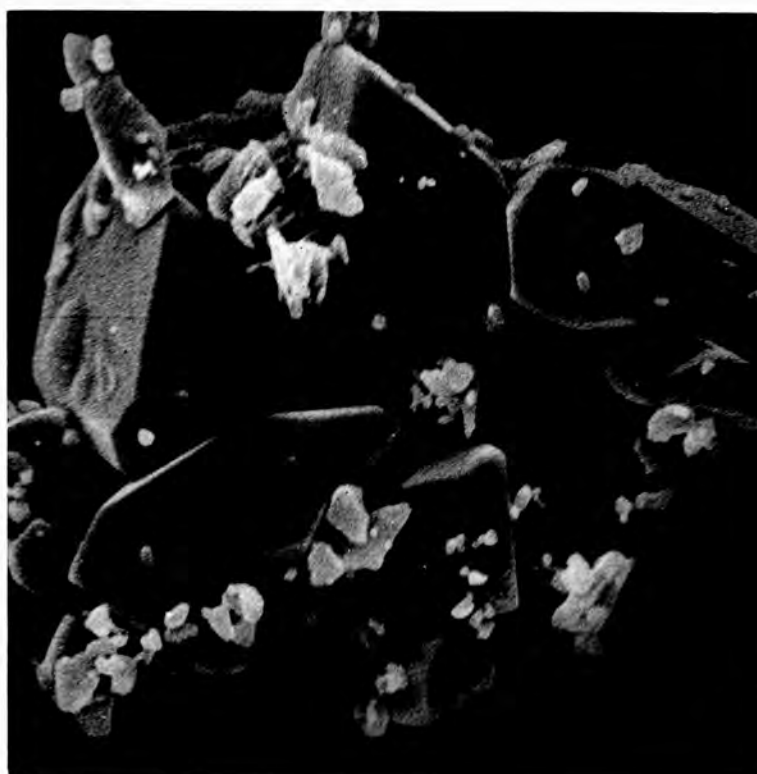
* All the above data are based upon an average error of 0.1cm



Slide 6. $\text{Znmal.}2\text{H}_2\text{O}$ ($\times 220$)



Slide 7. Similar to the above ($\times 1,100$)



Slide 8. Zn mal. 2H₂O (×5,500)

Table 6.6 Powder pattern data for $\text{Cdmal.H}_2\text{O}$

Observed d and 2θ values are given together with the observed intensities

2θ		$d(\text{\AA})$		I_{obs}
obs.	calcd.*	obs.	calcd.*	
8.40	8.1154	10.526	10.8944	vw
9.38	10.0554	9.4282	8.7965	s
10.40	10.2756	8.5057	8.6085	vs
12.19	11.8706	7.2604	7.4551	vw
12.99	13.1074	6.7543		vw
14.01	14.3960	6.3210	6.1525	w
14.74		6.1211		vw
15.53	15.7245	5.7056	5.6356	vw
16.70	16.2719	5.4472		vw,b
17.50	17.3316	5.0675	5.1165	m
17.85	17.8461	4.9689	4.9701	w,sh
18.09		4.9036		
18.75	19.2821	4.7324	4.6031	w
20.25	20.1893	4.3851	4.3982	w
20.72	20.6350	4.2867	4.3042	sh
20.92	21.4875	4.2462	4.1354	s
21.55		4.1159		
23.05	23.0031	3.8584	3.8662	m
24.02	23.8710	3.7047	3.7276	m
24.60	24.5124	3.6187	3.6315	w
25.25	25.2514	3.5270	3.5268	m
26.39	27.3164	3.2561	3.2647	w
28.23	28.6323	3.1611	3.1176	m
29.13	29.0257	3.0654	3.0763	w
30.20	30.4858	2.9592	2.9322	vw
30.60	30.8667	2.9214	2.8968	vw
32.33	32.2513	2.7690	2.7756	vw
34.62	34.5398	2.5909	2.5967	vw
35.35	35.3540	2.5390	2.5388	vw
36.33	36.1445	2.4727	2.4851	vw
26.75	36.6606	2.4454	2.4512	w/sh
36.90	37.0986	2.4358	2.4233	w
37.80	37.6747	2.3799	2.3876	m
39.92	39.8723	2.2583	2.2609	w
40.03	40.0466	2.2523	2.2514	w

Table 6.6 (continued)

2θ		$d(\text{\AA})$		I_{obs}
obs.	calcd.*	obs.	calcd.*	
42.01	41.9801	2.2007	2.1521	vw
42.49	42.4361	2.1274	2.1300	m
43.55	43.3229	2.0781	2.0885	vw
44.13	44.1594	2.0521	2.0508	w
45.10	45.0804	2.0102	2.0110	w
45.45	45.4504	1.9955	1.9955	w
46.50	46.7261	1.9529	1.9440	w,b
47.65	47.6332	1.9084	1.9091	w,b
48.08	48.3865	1.8923	1.8811	w
49.05	49.0650	1.8572	1.8567	w
50.45	50.4040	1.8089	1.8104	v,w
51.78	51.8224	1.7655	1.7634	w
52.90	52.9823	1.7307	1.7282	w,b
53.80	53.7458	1.7039	1.7055	w,b
54.20	54.2742	1.6922	1.6901	w,b

* J.C.S. Dalton, 1974, 1922.

repeated attempts suggested that either the two investigators were examining different compounds, or different crystalline forms are not in the same, but rather in different habits and different structures.

The compound used in the present work has the following analysis:

Found: C 15.2; H 1.6%

Calculated for $\text{CdC}_3\text{H}_2\text{O}_4 \cdot \text{H}_2\text{O}$: C 15.4 ; H 1.7%

Under the microscope the substance is seen to be powdered which is not suitable for single-crystal X-ray diffraction studies. The powder pattern diffraction traces were therefore obtained. The observed and calculated values of d spacings are presented in Table 6.6 together with the corresponding reflection angles.

The Structure of potassium tris (malonato) cobaltate (III) tetrahydrate

The unit cell dimensions of this complex have already been determined and published¹⁴, but the details of the X-ray powder diffraction pattern have not been recorded. Due to the high sensitivity of this complex, care was taken during the X-ray examination, wherein the compound was ground and packed in the dark, in order to minimize thermal and photodecomposition. Referring the crystals to a set of axes approximately similar to those in the compound previously reported¹⁴, the data were obtained. The degree of fit between the two patterns was very good, and the general appearance of reflections resembles very closely the corresponding calculated data based on the product obtained by Butler and Snow¹⁴.

The average error of magnitude 0.13 was obtained from which the corrections were made by the internal-standard procedure already described. The complete data of this complex are listed in Table 6.7

A comparison of the interplanar spacings of the observed set with the d's calculated indicates that the observed values are slightly high. This may be due to errors in the data selected for structural

Table 6.7 Powder pattern data for potassium tris (malonato) cobalt(III) tetrahydrate

Sym. orthorhombic

$a = 21.3166$, $b = 12.0672$, $c = 14.0501$ Å Volume = 3914.137 Å³

$\alpha = 90.000$, $\beta = 90.000$, $\gamma = 90.000$ Space group $Pna2_1$

Z = 8

I/I ₁	d(Å)		h	k	l
	obs*	calcd			
8	21.8705	21.3166	1	0	0
13	10.4761	10.5013	1	1	0
11	7.9924	7.9885	2	1	0
6	6.7224	6.6721	1	0	2
87	5.9336	5.8656	2	0	2
28	4.9388	4.9184	2	2	1
59	4.6107	4.6056	4	1	1
26	4.1540	4.2057	2	2	2
64	3.5381	3.5528	6	0	0
13	3.4309	3.444	6	0	1
15	3.3485	3.3360	2	0	4
100	3.2318	3.2154	2	1	4
11	3.0562	3.0514	0	3	3
69	2.9708	2.9761	7	0	1
4	2.9318	2.9328	4	0	4
13	2.8062	2.8065	6	2	2
8	2.7328	2.7368	0	1	5
28	2.6772	2.6828	2	4	2
10	2.6557	2.6508	2	1	5
17	2.5873	2.5825	3	4	2
17	2.5467	2.5473	0	2	5
33	2.5143	2.5184	1	4	3
60	2.4767	2.4775	2	2	5
20	2.4314	2.4345	4	1	5
10	2.3818	2.3786	0	5	1
6	2.3518	2.3512	7	2	3
11	2.3243	2.3242	9	1	0
13	2.3083	2.3079	6	2	4
8	2.2583	2.2602	7	1	4
14	2.2305	2.2319	2	5	2
9	2.0840	2.0819	9	1	3
13	2.0403	2.0398	10	0	2
5	1.9701	1.9715	1	1	7

Table 6.7 (continued)

I/I_1	$d(\text{\AA})$		h	k	l
	obs*	calcd			
9	1.9384	1.9379	11	0	0
4	1.9153	1.9155	3	5	4

* All the above data are based upon an average error of 0.13 cm

determination. The direct effect of inaccurate lattice constants is to cause the positions of the calculated diffraction lines to be shifted from their true position.

Single-crystal photographs of the microcrystalline powder of this complex could not be obtained.

The Crystal Structure of potassium tris (malonato)
aluminate (III) 6-hydrate

The crystal structure of this compound has not been reported. The structure of the corresponding oxalato complexes have been previously reported. It is shown that the potassium tris(oxalato) complexes derived from the trivalent metals aluminium, chromium and iron are isomorphic, belonging to monoclinic system. A literature survey revealed that the X-ray analysis of tris(malonato) complexes of Co(III) has been published so far. However a preliminary investigation by X-ray powder photographs indicated that the tris(malonato) complexes of Al(III) and Co(III) are not isomorphous. In fact the Co(III) malonato complex is orthorhombic whereas the Al(III) malonato complex is monoclinic.

X-ray measurements of the tris(Malonato)Al(III) complex were performed by single crystal and powder methods. A choice of space groups and unit cell dimensions was determined from precession photographs. The accurate values of the lattice parameters were obtained from powder data by least-squares refinement as described before.

The powder photograph was taken using CuK α radiation ($\lambda = 1.54178 \text{ \AA}$) using the procedure already described. The interplanar spacings were calculated from the diffraction pattern and all the reflection lines were indexed accordingly. The observed values of interplanar spacings are compared with those calculated values, together with the observed intensities and hkl values in Table 6.8.

Table 6.8 Powder pattern data for potassium tris(malonato)aluminate (III)
-6 hydrate

I _{obs}	d(Å)		h	k	l
	obs.	calcd			
vw	13.1924	13.2027	0	0	1
	13.1924	13.2027	0	0	$\bar{1}$
m/s	8.9432	9.2696	0	1	$\bar{1}$
	8.9432	9.2696	0	1	1
w	7.8372	7.6614	1	0	0
vs	6.6075	6.6013	0	0	2
	6.6075	6.6013	0	0	$\bar{2}$
w	5.8288	5.8379	0	2	1
	5.8288	5.8379	0	2	$\bar{1}$
m/w	5.1052	5.0656	1	2	1
m	4.5246	4.5280	1	2	2
w	4.3959	4.4009	0	0	3
	4.3959	4.4009	0	0	$\bar{3}$
vw	4.2909	4.3119	1	2	$\bar{1}$
w	4.1463	4.1691	0	1	$\bar{3}$
	4.1463	4.1691	0	1	3
w/m	3.9308	3.9233	2	1	1
w	3.8176	3.8215	1	3	1
w	3.7109	3.6749	2	1	0
m	3.5367	3.5535	1	0	4
s	3.4809	3.4779	2	2	1
vw	3.1557	3.1598	0	4	$\bar{1}$
	3.1557	3.1598	0	4	1
m	3.0655	3.0632	2	1	4
m	2.9951	2.9954	1	4	0
w	2.9280	2.9190	0	4	2
	2.9280	2.9190	0	4	$\bar{2}$
m	2.8693	2.8718	2	3	0
w	2.7968	2.7903	2	3	3
w	2.7442	2.7492	1	3	4
w/m	2.6158	2.6167	0	4	$\bar{3}$
	2.6158	2.6167	0	4	3
m	2.5636	2.5538	3	0	0
m	2.4767	2.4802	2	4	0
w	2.3830	2.3801	1	3	5
w	2.3559	2.3582	3	2	4

Table 6.8 (continued)

I_{obs}	obs. $d(\text{\AA})$	calcd	h	k	l
m	2.2659	2.2705	1	5	3
m	2.2064	2.2092	3	2	$\bar{1}$
w	2.1424	2.1426	1	4	5
vw	2.0790	2.0795	3	4	1
vw	2.0624	2.0614	4	0	3
m/w	2.0407	2.0441	0	5	$\bar{4}$
	2.0407	2.0441	0	5	4
vw	1.9689	1.9663	2	4	$\bar{3}$
vw	1.9470	1.9460	0	6	$\bar{3}$
	1.9470	1.9460	0	6	3
vw	1.9141	1.9154	4	0	0
vw	1.8953	1.8937	3	0	7
m/w	1.7719	1.7697	1	7	$\bar{1}$
vw	1.7421	1.7439	3	5	$\bar{1}$
w	1.7068	1.7072	4	4	1
w	1.6837	1.6851	4	1	7

The precession photographs indicate monoclinic crystal symmetry and the reflections $h0l$ with l even, and $0k0$ with k even are present which indicate the possible space group $P2_1/C$ (International Tables for X-ray Crystallography). Table 6.9 gives information concerning the crystal data.

Table 6.9 Crystal data

Composition	$K_3[Al(mal)_3] \cdot 6H_2O$
MW	558.523
crystal system	monoclinic
space group	$P2_1/C$
a (Å)	8.2633
b	13.0176
c	14.2399
β (°)	67.99
V (Å ³)	1420.19
z	4
D (g cm ⁻³)	2.6
systematic absences:	
$h0l$	$l = 2n + 1$
$0k0$	$k = 2n + 1$

The Structure of Zn(II) ethylmalonate dihydrate

The crystal symmetry of $Zn\ etmal \cdot 2H_2O$ has not been determined previously. A structural study with X-rays has now been made and interpreted as though the compound has the same symmetry as Zn malonate, namely that the crystals are monoclinic. Significant differences between these two representative structures were observed. Overcrowding in the acid radical could be the reason. Examination of the spectra shows that they differ greatly. The results are

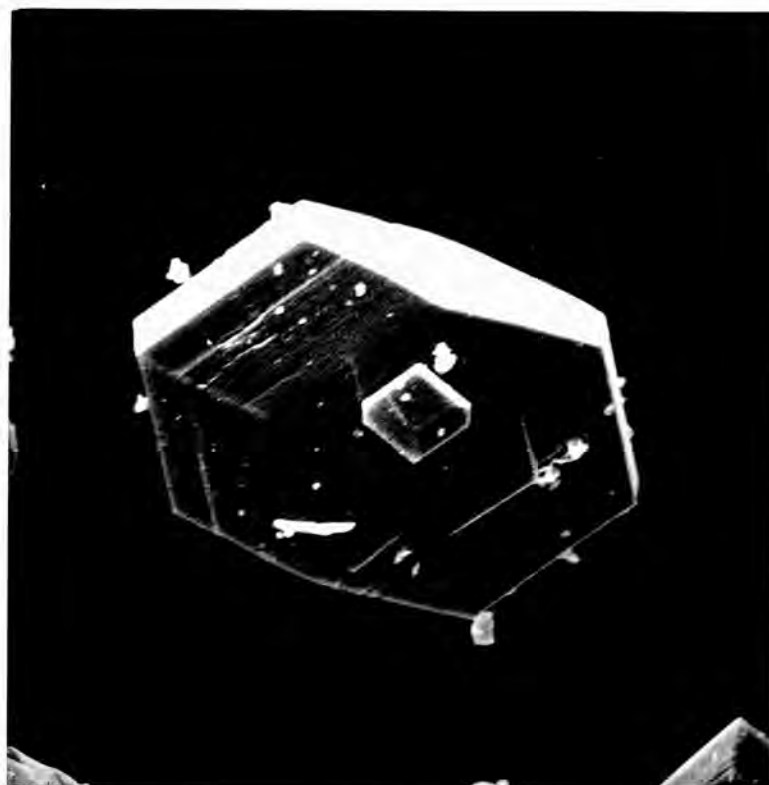
Table 6.10 Powder data for $Zn_{1-x}Mg_xO$

Observed d and 2θ values are given together with the
observed intensities

I_{obs}	d_{obs} (Å)	$2\theta_{obs}$	I_{obs}	d_{obs}	$2\theta_{obs}$
m	7.5957	11.65	m	2.5425	35.30
vs	6.7735	13.07	vw	2.4519	36.65
m	6.0137	14.73	w	2.4251	37.07
m	5.5083	16.09	w	2.3048	39.08
m	5.1552	17.20	w	2.2539	40.00
w	4.7881	18.53	w	2.2168	40.70
w/m	4.5314	19.59	w/m	2.1506	42.01
s	4.2806	20.75	w	2.1080	42.9
w	4.0971	21.69	w	2.0895	43.3
m	3.9567	22.47	w,b	2.0726	43.67
m	3.8850	22.89	w	1.9617	46.28
w	3.7967	23.43	w	1.9229	47.27
m/w	3.7308	23.85	w	1.8396	49.55
m	3.6000	24.73	vw	1.8129	50.33
w	3.5430	25.80	w/m	1.7208	53.23
w	3.3847	26.33	w	1.7083	53.65
w	3.2784	27.20			
w/m	2.1512	28.32			
m	3.0634	29.15			
w	2.9688	30.10			
w	2.9640	31.15			
vw	2.7883	32.10			
vw	2.6811	33.42			
vw	2.6610	23.68			
m	2.5996	34.50			



Slide 9. Znetmal.2H₂O (×550)



Slide 10. Similar to the above (×2,200)

given in Table 6.10.

Under the microscope the crystals appear colourless and very well formed, belonging to the orthorhombic system (Slides 9 and 10).

REFERENCES

1. M.J. Buerger, "X-ray crystallography", John Wiley, New York, 1953.
2. C.W. Bunn, "Chemical Crystallography", Oxford University Press, 1945.
3. G.H. Stout and L.H. Jensen, The Macmillan Company, London, 1968.
4. L.V. Azaroff, "Elements of x-ray crystallography", McGraw-Hill, 1968.
5. L.V. Azaroff and M.J. Buerger, "The Powder Method in x-ray crystallography", McGraw-Hill, New York, 1958.
6. J.H. Fang and F. Donald Bloss, "X-ray Diffraction Tables", Southern Illinois University Press, 1966.
7. J.I. Langford and G.F. Marriner, "Powder Pattern Programs", University of Birmingham Physics Publication, 1973.
8. J.I. Langford, "Powder Pattern Programs", J. App. Cryst., 1971, 4, 259-60.
9. B. Briggman and A. Oskarsson, Acta Cryst., 1977, B33, 1900.
10. T.Y. Borg and D.K. Smith, "Calculated X-ray Powder Pattern for Silicate Minerals", printed by the Geological Society of America in cooperation with the Mineralogist Society of America, 1969.
11. A. Karipides, J. Ault and A.T. Reed, J. Inorg. Chem., 1977, 16, 3299.
12. L. Walter-Levy, J. Perrotey and J.W. Visser, Bull. Chim. Soc. Fr., 1973, 2596.
13. M.L. Post and J. Trotter, J.Chem. Soc. Dalton; 1974, 1922.
14. K.R. Butler and M.R. Snow, J.Chem. Soc. Dalton; 1976, 251.

CHAPTER VII MÖSSBAUER SPECTROSCOPY^{1-3*}

7.1 Introduction. Theory and Application

Mössbauer spectroscopy is the study of γ -ray absorption or emission between the ground and excited state of a specific type of nucleus. It is a branch of spectroscopy which has been developed since 1958 and has proved to be a useful tool for investigation of electronic configurations and the structures of chemical compounds containing specific nuclei. Among the nuclei which have been found to show Mössbauer effects are ^{57}Fe , ^{61}Ni , ^{67}Zn , ^{117}Sn , ^{127}I , ^{129}I , ^{131}Xe , ^{195}Pt , and ^{197}Au .

The Mössbauer effect for iron depends on the fact that the nuclide ^{57}Fe which is formed in the decay of ^{57}Co has an excited state ($t_{1/2} \approx 10^{-7}$ sec) at 14.4 KeV above the ground state; this can lead to a very sharp resonance absorption peak. Thus if γ radiation from the ^{57}Co source falls on an absorber where the iron nuclei are in environment identical with that of the source, then resonance absorption of γ -rays will occur. However, if the Fe nuclei are in a different environment, no absorption occurs and the radiation is transmitted and can be measured. In order to obtain resonance absorption it is then necessary to impart a velocity to the absorber, relative to the source. This motion changes the energy of the incident quanta (Doppler effect) so that at a certain velocity there is correspondence with the excitation energy of the nuclei in the absorber. The usefulness of the Mössbauer effect is due to the fact that the resonant capture of the photon depends on several kinds of electron-nucleus interactions. In the absence of a magnetic field at the region of the nucleus the most important hyperfine interactions

* The references for this section are on page 218.

are the isomer shift and the nuclear quadrupole coupling.

The isomer shift (δ) is due to the interaction between the nuclear charge distribution and electrons with finite probability at the region of the nucleus (s electrons). It manifests itself as a shift from zero relative source-absorber velocity of the centroid of the resonance spectrum, it is a measure of the difference in electron charge density at the nucleus of the source and absorber atoms and thus is most clearly related to the nature of the chemical environments of the resonant nuclei. The isomer shift (δ) is a linear function of s electron density at the nucleus and is expressed as a velocity (mm/sec). The value of the Mössbauer isomer shift is a measure of the change in electron density at the nucleus. In the case of iron compounds, the isomer shift decreases with increasing electron density around the nucleus, thus it is to be expected that with iron complexes of various ligands the decreasing order of the isomer shift follows the increasing order of the covalence of the bond between the metal and donor atoms; that is to say, the nephelauxetic sequence.⁴

The nuclear quadrupole interaction is due to the coupling of the quadrupole moment of the Fe nucleus with an electric field gradient at the region of the nucleus arising from the asymmetry of external charges. It manifests itself as a splitting of the resonance curve into two peaks. The distance between peaks of the doublet, designated ΔE , is the quadrupole splitting. Thus the magnitude of the quadrupole splitting can serve as a measure of the inhomogeneity of the electric field of a Mössbauer nucleus. The electric field at the nucleus is determined primarily by the electronic configuration of the atom and consequently by the nature of the bonding, and secondly by the symmetry of the crystal lattice or of the molecular structure. The occurrence and the magnitude of

of quadrupole splitting are therefore of use for the study of chemical bonding or the symmetry of the compound. No quadrupole splitting occurs in the Mössbauer spectra of purely ionic compounds of iron (III), while the quadrupole splitting of some iron (III) compounds containing iron partly in ionic and partly in covalent bonds is small and depends slightly on the temperature.

The Mössbauer spectra of some iron (III) complexes with monocarboxylic acids have been investigated by some workers.^{5,6} These complexes were shown to be triangular - trinuclear in structure and contain bridging carboxylate ligands and a central bridging oxygen. The Mössbauer parameters have been published for a series of iron (III) salts of organic acids.⁷ There have been very few reports of Mössbauer studies of Fe (III) complexes with dicarboxylic acids. One recent paper reports on the magnetic properties and Mössbauer spectra of several polymeric iron (III) dicarboxylic acid complexes including those of malonic-acid.¹⁰ These complexes, however, are different from those studied in this work. The Mössbauer effect has been used to obtain a more direct indication of the valence state of the iron atom. Gallagher and Kurkjian⁷ utilized the Mössbauer effect to substantiate the changes in the oxidation state proposed from the thermal decomposition in Ferric oxalate and alkaline earth trioxalato ferrates. The successive products formed in the decomposition at 75° and 130°C of both hydrated and anhydrous potassium trioxalato-ferrate (III) were also established by the Mössbauer spectroscopy.⁹

Experimental

Mössbauer measurements was carried out at Birkbeck College. All values of isomer shifts are reported relative to a ⁵⁷Co-paladium source on powdered samples at 290.5 and 80 K. The Mössbauer spectra

results are shown in Figure 7.1.

7.2 Results and Discussion

The Mössbauer spectra of sodium salts of Fe (III) malonate, Fe(III) ethylmalonate and Fe(III) benzylmalonate complexes have a typical singlet absorption peak. The isomer shift values observed are 0.45 mm/sec for Fe(III) malonate, 0.42 mm/sec for Fe(III) benzylmalonate and 0.36 mm/sec for Fe(III) ethylmalonate complexes and are within the characteristic region associated with high-spin Fe(III) compounds.¹¹ These are similar to the values observed for oxalato Fe(III)^{7,8} and room temperature γ values of the polymeric malonato Fe(III) complexes reported recently.¹⁰ The prominent feature here is that all the complexes effectively have zero quadrupole splitting at both 290 and 70 K. This is expected since the quadrupole splitting of the common trivalent iron ($3d^5$) salts with the spherically symmetrical half filled d shell does not contribute to the electric-field gradient. The direct implication of zero quadrupole splitting is that these compounds possess O_h symmetry despite the presence of the chelate rings, which strongly suggests that the oxygen atoms are in very nearly perfect octahedral positions. The spectra consist of a broad peak with zero quadrupole splitting values at 290 and 70 K. The direct implication of this is that there is only one type of iron in the compounds. We are interested primarily in the isomer shift which is essentially the position of the center of the absorption band. In the case of iron compounds, there is a tendency for the more covalent compounds to show smaller isomer shifts, a smaller isomer shift corresponding to increased central electron density. The results of our Mössbauer spectra of Fe(III) malonate and substituted malonate complexes have shown that the substitution produces some changes in the bonding of the iron atom in these complexes. It can

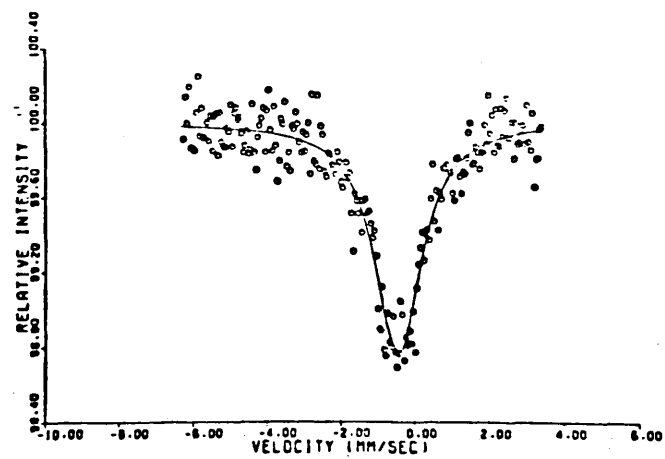
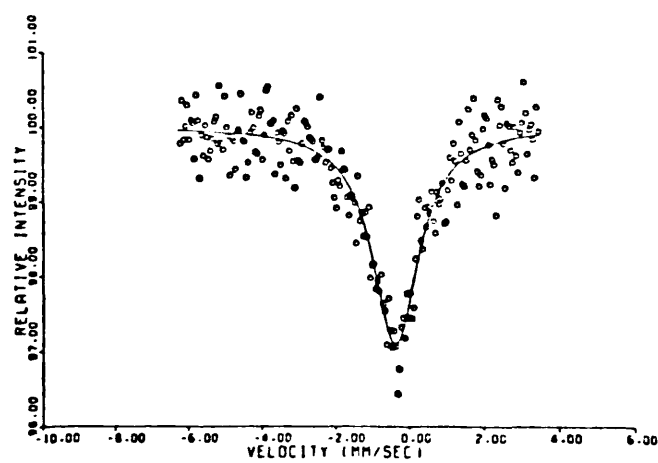
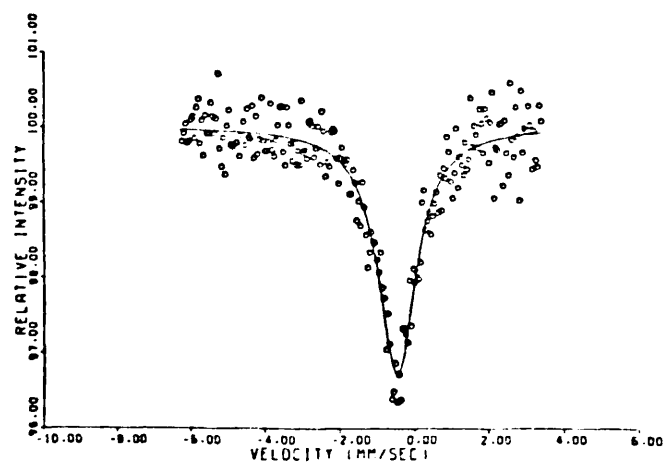


Fig.7.1. Mössbauer spectra of Fe(III) complexes:

(a) malonate; (b) etmalonate;

(c) benzylmalonate at 290 K

be seen that the isomer shift is smaller in ethylmalonate derivatives than in the corresponding benzylmalonate or the unsubstituted malonate itself. The values of the isomer shifts found for these complexes show the largest s-electron density at the iron nucleus observed with the substituted malonate iron (III) complexes. We attribute this decrease in the isomer shift essentially to the greater covalent character of the iron - ethyl and benzylmalonate bonds. The magnetic moment values of these compounds (see p.134) indicated a high-spin octahedral Fe(III). However, in short, the iron atom behaves somewhat as in a typical ionic ferric salt, little influenced by its organic ligands. There is a recent report¹⁰ on the Fe(III) malonato complex which has been formulated as $[\text{Fe}_3\text{O}(\text{O}_2\text{CCH}_2\text{CO}_2)_3(\text{H}_2\text{O})_3]\text{ClO}_4 \cdot 3\text{H}_2\text{O}$. The structure of the compound was postulated, using the magnetic properties, to be a trimeric iron with bridging carboxylate groups and a central common oxygen atom. The Mössbauer spectrum of this compound consists of two absorption bands. The isomer shift value, of 0.41 mm/sec reported is characteristic of high-spin Fe(III). The broad line observed has been attributed to be a consequence of iron being present in a variety of slightly different environments as a result of the polymeric structure of these complexes.

The Fe(III) malonato complex studied in the present investigation was prepared by a different method of synthesis (see page 35) and gave satisfactory analysis results (Table 2.2). Its infrared spectrum was similar to those reported for similar compounds (Table 4.2). Although X-ray data are not available for the Fe(III) malonato complex, the fact that chromium can replace iron isomorphously in these salts strongly supports an octahedral structure similar to that of Cr(III) malonate complexes, and not an oxo bridged structure as studied recently by Dziobkowski et al¹⁰. This result

is also in agreement with the magnetic moment obtained and with diffuse reflectance spectrum.

REFERENCES

1. T.C. Gibb, "Principles of Mössbauer Spectroscopy", Chapman and Hall, Publ., 1976.
2. A.E. Martell, "Coordination Chemistry", Litton Educational Publ., Inc., 1971, 1, 341.
3. N.N. Greenwood and T.C. Gibb, "Mössbauer-Spectroscopy", Chapman and Hall Ltd., London, 1971.
4. C.K. Jørgensen, "Absorption spectra and chemical bonding in complexes", Pergamon Press, Oxford, 1962.
5. A. Earnshaw, B.N. Figgis, and L. Lewis, J. Chem. Soc., 1966, 1056.
6. G.J. Long, W.T. Robinson, W.P. Tappmeyer, and D.L. Bridges, J. Chem. Soc. Dalton., 1973, 573.
7. Y. Takashima, T. Tateishi, Bull. Chem. Soc. Japan., 1965, 38, 1688.
8. P.K. Gallagher and C.R. Kurkjian, J. Inorg. Chem., 1966, 5, 214.
9. K.G. Dharmawardena and G.M. Bancroft, J. Chem. Soc., 1968, 2655.
10. C.T. Dziobkowski, J.T. Wroblewski, and D.B. Brown, J. Inorg. Chem., 1981, 20, 671.
11. L.R. Walker, G.K. Wertheim and V. Jaccarino, Phys. Rev. Lett., 1961, 6, 98.

CHAPTER VIII ^1H AND ^{13}C NMR STUDIES OF DICARBOXYLIC ACIDS
AND THEIR METAL (III) COMPLEXES

8.1 Introduction*

There have been several investigations of malonato complexes using ^1H n.m.r. particularly those of Co(III) complexes,^{1,2} in which certain conclusions regarding chelate ring conformations have been made.³ In the cases of malonato complexes studies have been made on complexes of the type $[\text{CoX}_2\text{mal}]$, where X is a chelate, concerning the lability of methylene protons of the malonate ring, and isotopic exchange rates. Values of ΔH^\ddagger , ΔS^\ddagger and the proposed mechanisms have been discussed⁴. Comparative conclusions have been made between the nature of the active methylene protons of the diethylmalonato ester and the malonato methylene protons of the above complexes.¹ Some work has been published recently on the application of ^{13}C n.m.r. spectroscopy to the study of cobalt (III) complexes, including those of aminopolycarboxylates,⁵⁻⁷ amino acids,⁸ and of diamines.^{9,10}

Experimental

^1H n.m.r. spectra were measured with a Perkin Elmer 60 MHz continuous wave spectrometer at 35°C, or with a Jeol Inc., JNMPS 100 Fourier transform 100 MHz spectrometer in the ^1H mode. Chemical shifts were relative to tertiary butanol as internal standard, or to external TMS. ^{13}C n.m.r. spectra were measured using the Jeol Fourier transform instrument in the ^{13}C mode. Most spectra were obtained using a D_2O lock, 8000 data points, repetition times between 3 and 10 seconds, and up to 6000 scans depending on the concentration of the sample. Concentrations were normally about

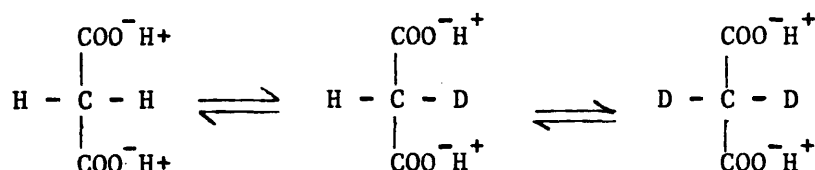
* The references for this section are on page 229.

0.2 g cm⁻³. Either tertiary butanol or p-dioxane were used as internal standards. Most ¹³C spectra were carried out at Rothamsted (some were measured by P.C.M.U., Harwell, where T.S.P. was used as internal standard, and some by U.L.I.R.S., King's College, London). ¹H n.m.r. spectra were measured at Bedford College.

8.2 Results and Discussion

1. N.M.R. spectra of malonic acid.

In D₂O the ¹H spectra of malonic acid in D₂SO₄ solution show that the single peak expected for the CH₂ signal splits into a triplet (2.1 ppm vs. t-butanol J ~ 7.3Hz) indicating the presence of the H-C-D group, with its signal superimposed on the singlet from the CH₂ group. The intensities of these signals were found to decrease with time as CD₂ is produced. Finally an equilibrium was reached with no further decrease in intensity of the signal, i.e.

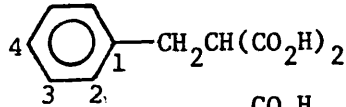


In NaOD/D₂O solutions a similar trend was observed, i.e. the appearance of the triplet, the intensity of which decreases with time.

In D₂O neutralised with Na₂CO₃ solution, malonic acid shows only a singlet from the CH₂ group (1.91 ppm vs. t-butanol) which remains unchanged for several hours.

The ¹³C n.m.r. spectrum of malonic acid in D₂O shows a signal of 171.57 ppm for the carbonyl shielding and a split signal at 42.4 ppm for the CH₂ resonance confirming the presence of CH₂, CHD and CD₂. The carbonyl resonance compares with a value of 170.4 ppm for a saturated solution in methanol.¹¹ In NaOH solution the

Table 8.1 ^{13}C n.m.r. signals of malonic acid, ethylmalonic acid, benzylmalonic acid and derivatives (δ in ppm vs.TMS)

Compound	Signal	D_2O soln	$\text{D}_2\text{O}/$ NaOD	$\text{Na}_2\text{CO}_3/$ D_2O	$\text{Al}(\text{mal})_3^{3-}$
$\text{CH}_2(\text{CO}_2\text{H})_2$	CO_2H	171.57	178.49	178.37	175.49
	CH_2	42.33	49.44	48.90	42.40
		41.43	48.73		
		40.64	47.92		
$\text{CH}_3\text{CH}_2\text{CH}(\text{CO}_2\text{H})_2$					$\text{Al}(\text{etmal})_3^{3-}$
	CO_2H	174.28	180.88	180.86	178.50
	CH	54.05	-	61.64	54.85
	CH_2	22.80	22.40	22.38	24.54
	CH_3	11.73	13.00	13.04	12.48
 $\text{C}_6\text{H}_5\text{CH}_2\text{CH}(\text{CO}_2\text{H})_2$					$\text{Al}(\text{benzylmal})_3^{3-}$
	CO_2H	173.21	179.86	180.00	177.38
	C_1	138.63	141.66	141.72	140.50
	C_2, C_3	129.53	129.38	129.46	129.62, 129.38
	C_4	127.71	126.95	127.04	127.25
	CH	54.42	61.7	61.21	55.41
	CH_2	35.17	37.11	37.24	36.19

carbonyl peak shifts to 178.37 ppm, and the methylene signal is split (Table 8.1). When malonic acid is neutralised in H_2O with Na_2CO_3 , then evaporated to dryness and redissolved in D_2O , the proton decoupled spectrum shows a singlet for the CH_2 resonance which persists for several hours. If neutralisation is carried out in D_2O , some exchange occurs during neutralisation, but the spectrum is then frozen for several hours and shows the peaks required for CH_2 , CHD and CD_2 species.

2. N.M.R. spectra of ethylmalonic acid.

Similar results were obtained here as for malonic acid. In D_2O solution ethylmalonic acid gives signals from the CH_3 group, - 0.28 ppm (triplet $J \sim 7.5$ Hz); CH_2 group, 0.65 ppm (quintet, $J \sim 7.6$ Hz); CH, 2.19 ppm (triplet $J \sim 7.24$ Hz). On standing, the triplet CH signal decreases and the CH_2 quintet broadens. Finally the CH triplet disappears and the CH_2 signal sharpens to a quartet. Similar effects are noticed when the acid is neutralised with Na_2CO_3 (Table 8.2). With an excess of NaOD the triplet CH signal has almost disappeared and the CH_2 signal is quartet when the first measurement is taken in the fresh solution.

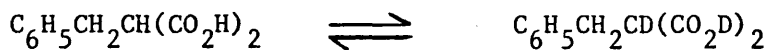
The ^{13}C n.m.r. spectrum of ethylmalonic acid in fresh D_2O solution exhibits a singlet for the CH resonance, which rapidly collapses to a complex triplet. When ethylmalonic acid is neutralised in H_2O with Na_2CO_3 , evaporated to dryness and dissolved in D_2O a singlet results for the CH resonance, which persists for several hours. No resonance is observed for the CH carbon in NaOH solution, indicating fast exchange. The ^{13}C n.m.r. spectrum of ethylmalonic acid is given in Table 8.1.

3. N.M.R. spectra of benzylmalonic acid.

The 1H n.m.r. spectrum of benzylmalonic acid in $CDCl_2$ is reported in Table 8.1. In this solvent there is no change in spectrum

for 24 hours.

In D₂O solution the spectrum is more complicated as a consequence of the slow exchange reaction:



After 30 minutes the singlet of the high field (CH₂) pattern has increased at the expense of the low field (CH) triplet. After 24 hours the low field triplet has disappeared and the high field pattern has become a singlet, indicating the presence of C₆H₅CH₂CD(CO₂D)₂. The ¹³C n.m.r. spectral data of benzylmalonic ethylmalonic and malonic acids are shown in Table 8.1.

Discussion

Free Acids and Anions

The ¹H n.m.r. spectra show that the methylene protons of all three malonic acids exchange with deuterium from the solvent in both acidic and basic solution. In neutral solution, however, this exchange is very slow. This is also supported by the results obtained in the ¹³C spectrum. The reactions are faster with ethylmalonic acid than for the unsubstituted compound. The results show that (Table 8.2) initially the CH₂ signal is a quintet, with splitting from neighbouring CH and CH₃ groups. When the exchange of D for H in the CH group is complete with excess of NaOH, the coupling of the CH₂ groups is now only with the methyl group, giving a quartet. As the exchange takes place the CH₂ signal becomes complicated as it arises from the quintet of the >CHCH₂CH₃ group superimposed on the quartet of the >CDCH₂CH₃ group. When half exchange has taken place, this gives rise to seven or eight bands.

The ¹³C n.m.r. spectra give expected values for the shielding in all acids. The results show that on formation of the anion¹² the carboxylate carbon signal shifts to lower field with a shift of +6.60 ppm for ethylmalonic acid, +6.92 ppm for malonic

Table 8.2 Splitting of CH₂ signal in ethylmalonic acid in
D₂O/Na₂CO₃ solution as α-H exchanges with D from solvent

Intensity	Splitting of CH ₂ signals	Time
CH:CH ₂ :CH ₃		
1:2:3	quintet	fresh solution
0.75:2:2	broad quintet	after two days
0.45:2:3	7 or 8 bands	after seven days
0:2:3	quartet	in excess of NaOD (fresh solution)

Table 8.3 ¹³C n.m.r. signals from malonate group (ppm vs.TMS).

Compound	Carboxyl	Methylene
Malonic acid/D ₂ O	171.57	42.23 41.43 40.64
Malonate ion/NaOH	178.49	49.44 48.73 47.92
Malonate ion/neutral	178.37	48.9
[Co en ₂ mal] ⁺	179.5	~ 42
[Co en mal ₂] ⁻	180.22, 179.93	-
[Co mal ₃] ³⁻	182.81	46.21
uns[CoTMDDAmal] ⁻	178.66, 179.31	43.52 ⁷

acid and +6.65 ppm for benzylmalonic acid. For ethylmalonic acid there is a down field shift for both methylene and methyl carbons in basic media.

The results in Table 8.1 show that the addition of a proton to the anion of benzylmalonic acid produces an upfield shift in the carboxyl and α -carbon resonances both of 6.79 ppm. The CH_2 and C_1 resonances are slightly more shielded, with upfield shifts of 2.07 and 3.09 ppm respectively. The C_2 , C_3 and C_4 resonances show deshielding with small downfield shifts. When the anion is complexed with Al^{3+} , the increased shieldings of the carboxyl and the α -carbons are smaller, 2.62 and 5.8 ppm respectively, and the increased shielding of the CH_2 carbon is smaller, 1.05 ppm. The C_2 and C_3 resonances are resolved in the complex. A similar trend is observed for ethylmalonate and malonate. On acidification, the carboxyl and α -carbon show large increases in shielding of 6.58 and 7.35 ppm, of 6.80 and 6.57 ppm for ethylmalonate and malonate respectively. In ethylmalonate, the ethyl group shows a smaller upfield shift. On coordination to Al^{3+} , there are smaller upfield shifts for the carboxyl and α -carbons, 2.36 and 6.79 ppm, and 2.88 and 6.50 ppm for ethylmalonate and malonate respectively, whereas the methylene carbon of the ethyl group is now deshielded, 2.16 ppm. However, the methyl group carbon is shielded by 0.56 ppm. The results indicate that the resonances for the Al^{3+} complexes fall between those found for the free acids and those for their sodium salts. The ^{13}C n.m.r. spectra of Al (III) complexes show that substitution into the CH_2 group of the malonate chelate by ethyl or benzyl has similar effects on the carboxylate carbon and α -carbon chemical shift values. Thus, the ^{13}C chemical shifts of carboxylate carbon and α -carbon are shifted to lower field ~ 2.0 ppm and 13.0 ppm respectively on going from malonate to ethylmalonate and benzylmalonate

Al (III) complexes.

N.M.R. of Cobalt (III) complexes of Malonic Acid and Ethylmalonic Acid.

The 60 MHz ^1H n.m.r. spectrum of $[\text{Coen}_2\text{mal}]\text{Br}$ has been reported.⁴ The assignments for the signals relative to t-butanol in ppm are as follows: $\text{NH}_2(\text{cis to O})$, 3.13; $\text{NH}_2(\text{trans to O})$, 4.14; $\text{CH}_2(\text{mal})$, 2.11; $\text{CH}_2(\text{en})$, 1.47. The 100 MHz n.m.r. spectrum in the present work shows the CH_2 malonate signal at 2.17 ppm and the methylene groups from the ethylenediamine show the expected splitting; giving signals at 1.57 and 1.47 ppm. In basic media, the $\text{CH}_2(\text{mal})$ signal broadens and then splits into a triplet, showing that deuterium substitution has occurred as in the free malonate anion. The CH_2 signal then disappears with time as in the case of the $[\text{Co en}_2\text{mal}]^+$ ion with D_2SO_4 .⁴

The ^{13}C n.m.r. spectrum of the $[\text{Co en}_2\text{mal}]^+$ ion (ppm vs. TMS) is as follows: carboxyl, 179.5; $\text{CH}_2(\text{en})$, 45.87, 44.25; $\text{CH}_2(\text{mal})$, 42.0. On addition of base to $[\text{Co en}_2\text{mal}]^+$ in D_2O solution the methylene (mal) signals are no longer visible, but changes are noticed in the signals from the ethylenediamine methylenes.

The ^{13}C n.m.r. spectrum of the $[\text{Co mal}_3]^{3-}$ ion shows the carboxyl carbon at 182.81 ppm and the malonato methylene at 46.21 ppm (see Table 8.3).

The ^1H n.m.r. spectrum of $[\text{Co en}_2\text{etmal}]^+$ ion has been reported⁴ and the assignment of the signals relative to t-butanol is as follows: $\text{CH}(\text{mal})$, 1.90 (triplet); CH_2 , 0.72 (quintet); CH_3 , -0.40 (triplet). The ^{13}C n.m.r. spectrum (ppm vs. TMS) shows signals at 183.72 (carboxyl); 56.22 (CH); 47.44, 46.34 (CH_2, en); 26.26 (CH_2); 14.23 (CH_3).

The ^{13}C n.m.r. spectrum of $[\text{Co en}_2\text{mal}]^+$ shows that the malonato group is chelated in neutral solution since there are two signals from the ethylenediamine carbons. A monodentate malonato

group gives rise to more signals.^{9,10} On the addition of base (saturated NaOH in D₂O) to a solution of [Co en₂mal]⁺ the ¹³C n.m.r. spectrum changes as follows: The methylene signals from the two non equivalent methylene groups of ethylenediamine in [Co en₂mal]⁺ are at 45.87 and 44.29 ppm. After the addition of saturated NaOH/D₂O the spectrum shows three signals at 45.60, 45.12 and 44.20 ppm. It has been suggested that in strongly basic solution the [Co en₂mal]⁺ ion exists either as the monodentate malonato species [Co en₂mal OH]⁰ or as the species in which a proton has been removed from the malonato methylene group in the chelate ring.¹³ The three signals observed are consistent with the presence of the monodentate malonato group, three signals from the ethylenediamine methylene groups are expected for a complex of the type [Co en₂XY]. The results are not consistent with the deprotonated species [Co en₂mal(-H)]⁰, since two methylene signals are still expected, nor with a mixture of [Co en₂mal]⁺ and the deprotonated species. After 24 hours three signals appear at 45.13, 44.68 and 44.20 ppm. After 48 hours the mixture was acidified. The malonato carboxyl peak now appears at 172.8 ppm instead of 179.52 in the complex showing the presence of free malonic acid. The three ethylenediamine methylene signals at 46.72, 46.09 and 44.59 ppm result from the equilibrium mixture of cis and trans [Co en₂(OH₂)]³⁺. Thus in neutral solution the coordinated malonate group is stable in [Co en₂mal]⁺. It does not become dechelated, nor do the methylene group protons exchange with deuterium from the solvent. In basic media the malonato group is dechelated and at the same time exchange takes place between the methylene protons and the deuterium of the solvent. The ¹³C n.m.r. results show that the carboxyl carbons are deshielded on coordination with respect to the free acid, but are more shielded than the free anion. In addition the methylene carbon in [Co mal₃]³⁻

is deshielded with respect to the other species (see Table 8.3). The ^{13}C chemical shift of the carbon signals shows a successive downfield shift in the series ethylmalonic acid < ethylmalonate anion < $[\text{Co en}_2 \text{etmal}]^+$.

The ethylenediamine methylene resonances in neutral solution are 45.87 and 44.78 ppm compared with those in $[\text{Co en}_2 \text{CO}_3]^+$ at 45.82 and 44.78 ppm. Thus there is no evidence of strain in the two bidentate ethylenediamine ligands on changing the ring size of the third chelate. However, the $\text{CH}_2(\text{en})$ resonances in $[\text{Co en}_2 \text{etmal}]^+$ are at 47.44 and 46.36 ppm, slightly deshielded with respect to the simple malonato or the carbonato complexes. The shifts to greater shielding are associated with carbons which are sterically perturbed, the steric compression shift.¹⁴ It appears that the ethylenediamine methylene groups in the simple malonato complex are more sterically strained than in the ethylmalonate compound. The presence of the ethyl substituent gives rise to a flat boat conformation of the malonato ring. Thus the malonato ring and the ethyl substituent would be further away from the ethylenediamine groups than the skew boat conformation.

REFERENCES

1. H. Yoneda and Y. Morimoto, *Inorg. Chim. Acta.*, 1967, 413.
2. M.E. Farago and M.A.R. Smith, *Inorg. Chim. Acta.*, 1975, 14, 21.
3. D.A. Buckingham, *Aust. J. Chem.*, 1967, 20, 257.
4. M.E. Farago and M.A.R. Smith, *J. Chem. Soc.*, 1972, 2120.
5. O.W. Howarth, P. Moor and N. Winterton, (a) *Inorg. Nucl. Chem. Lett.*, 1974, 10, 553; (b) *J. Chem. Soc. Dalton.*, 1974, 2271; (c) *J. Chem. Soc. Dalton.*, 1975, 360.
6. G.L. Blackman and T.M. Vickery, *J. Coord. Chem.*, 1974, 3, 225.
7. K.D. Garley, K. Igi and B.E. Douglas, *J. Inorg. Chem.*, 1975, 14, 2956.
8. T.Y. Yasui, *Bull. Chem. Soc. Jap.*, 1975, 41, 454.
9. M. Kojima and K. Yamasaki, *Bull. Chem. Soc. Japan.*, 1975, 48, 1093.
10. D.A. House and J.W. Blunt, *Inorg. Nucl. Chem. Lett.*, 1975, 11, 219.
11. E. Lippmaa and P. Pehk, *Kem. Teollisuus.*, 1967, 24, 1001, reported in "Carbon-13 n.m.r. spectroscopy", by J.B. Storthers, Academic Press (1972), New York and London, p. 295.
12. R. Hagen and J.D. Roberts, *J. Amer. Chem. Soc.*, 1969, 91, 4504.
13. M.E. Farago and J.M. Keefe, *Inorg. Chim. Acta.*, 1975, 15, 5.

CHAPTER IX GENERAL CONCLUSIONS

The compound which has been prepared and studied fall into the following categories.

- (1) Malonato metal complexes
- (2) Ethylmalonato metal complexes
- (3) Benzylmalonato metal complexes

The diffuse reflectance studies have demonstrated the most probable stereochemical shapes of the metal ion. The visible electronic spectra of transition metal ions with the anions of malonic and C-substituted malonic acid have been studied in the solid state. Here, we noticed the similarity of the transition bands in the spectra of malonato, ethyl and benzyl malonato metal compounds. The wavelength of the absorption band recorded of each metal ion in the visible region of the spectrum remains almost constant throughout the series (Chapter III) thus, the substitution on the malonate chelate has no effect on the position of the bands in the visible region in these compounds.

The solid state spectra of bivalent cobalt, nickel and of trivalent cobalt, iron, manganese and chromium possess expected bands in the visible region characteristic of a regular octahedral environment around the metal ions. The diffuse reflectance spectra of copper(II) malonate and C-substituted malonate compounds exhibited a typical broad absorption band representing a single electronic transition as is required theoretically for the tetragonally coordinated Cu^{2+} ion with the usual Jahn-Teller distortion. Recent X-ray analysis of Cu(II) malonate confirmed that the coordination is indeed a distorted octahedron (Chapter I). All the recorded spectra of manganese(III) complexes are similar with two absorptions around 21,000-22,000 and 11,000-15,000 cm^{-1} .

High-spin d^4 complexes are susceptible to Jahn-Teller distortion. The bands were taken to indicate a highly tetragonally distorted structure. Similar results have been reported for the solid state spectra of Mn(III) malonate complexes whose structures have been shown crystallographically to have tetragonal distortion (p. 24).

Infrared spectral studies confirmed that all complexes involve bonding through the carboxyl oxygens. Infrared analysis of these complexes confirmed the presence of two bands between $1600-1550\text{ cm}^{-1}$ and between $1400-1350\text{ cm}^{-1}$. This differs greatly from the position of such bands in the free acids, and this may be rationalised in terms of the nature of the ligand and of the metal, which upon coordination causes these bands to be shifted to lower or higher frequencies. This kind of shifting is a function of the type of bonding between metal and ligand. A previous discussion (Chapt. IV) shows that the assignment of bands in the $1600-1500\text{ cm}^{-1}$ region appears to be full of controversy, as a large number of bands which are important to the complexes in this research, appear in this region. This band may be regarded as a combination of ring and carboxylate absorption, so that only approximate values can be given for these frequencies. There also appears to be slight controversy over the definite assignment of bands in the $1400-1350\text{ cm}^{-1}$ region. In the infrared spectra of metal complexes the OCO anti-symmetric stretching is higher and the symmetric OCO frequency is lower than those of the simple malonate compounds, in good agreement with the recent X-ray analysis results (see Table 1.1). The formation of these complexes through carboxylate oxygen atoms has been confirmed.

The assignment of metal-oxygen frequency bands is difficult, since these are often combination bands and some are very weak in intensity. However, since the results of X-ray analyses

of malonato complexes are available, accordingly the existence of M-O bonding does not require further confirmation.

The magnetic moments of copper(II), nickel(II), cobalt(II), iron(III), manganese(III) and chromium(III) complexes of malonate, ethyl and benzylmalonate were measured between 112-323 K (Chapter V).

The magnetic properties of all the compounds studied were found to be normal, i.e., the susceptibility showed a linear plot and very low values of Curie-Weiss constant were observed over the temperature range studied. Hence the Curie-Weiss law was obeyed. The magnetic data (Tables 5.5 - 5.19) showed that all the compounds studied are of high-spin type and the ligands are distributed octahedrally about the metal ions. The high magnetic moment observed in some cases was thought to be due to the presence of impurity.

The δ , isomer shift values from the Mössbauer spectra suggest a high-spin octahedral environment of iron(III) when in malonate, ethyl and benzylmalonate complexes (Fig. 7.1).

The Mössbauer spectra of iron(III) malonate, ethylmalonate and benzylmalonate complexes have similar patterns and all are within the characteristic region associated with high-spin Fe(III). The values of the isomer shift found for these complexes show the largest s-electron density at the iron nucleus observed with substituted malonate iron(III) complexes, indicating their greater covalency.

Magnetic resonance studies on malonic, ethyl and benzylmalonic acids showed that the α -protons exchange with deuterium from solvent in both acidic and basic D_2O solution. In D_2O solutions the complexes $[Al(mal)_3]^{3-}$, $[Al(etmal)_3]^{3-}$ and $[Al(benzylmal)_3]^{3-}$

are stable to hydrolysis and do not exchange protons with the solvent.

In basic solution the $[\text{Co en}_2(\text{mal})]^+$ ion undergoes a fast ring opening with hydroxide, at the same time the α -protons exchange with deuterium from the solvent.

^{13}C n.m.r. studies showed that the methylene carbon in $[\text{Co}(\text{mal})_3]^{3-}$ is deshielded with respect to those in $[\text{Co en}_2\text{mal}]^+$, free malonic acid or the free anion. The ^{13}C n.m.r. deshielding effect of the carbon signals is more in $[\text{Co en}_2\text{etmal}]^+$ than those in ethylmalonate anion and ethylmalonic acid.

X-ray powder photographs of zinc(II), cadmium(II), calcium(II), barium(II), cobalt(III) and aluminium(III) malonate complexes and zinc(II) ethylmalonate complexes were examined (Chapter VI).

X-ray powder photographs of zinc(II) malonate confirmed it to be isomorphous with cobalt(II) and nickel(II) malonate, all of which crystallise with the formula unit $\text{MC}_3\text{H}_2\text{O}_4 \cdot 2\text{H}_2\text{O}$. According to our electronic spectra results, the cobalt and nickel(II) malonate compounds are octahedral, therefore suggesting similar binding of malonate to Zn(II) ion.

Manganese(II) and magnesium(II) malonates are known to be isomorphous and isostructural from a crystal structure investigation. The Mn^{2+} ion is coordinated by carboxylate oxygens octahedrally hence a similar structure could be proposed for the isomorphous Mg^{2+} malonate compound.

Although barium malonate and strontium malonate show close resemblance in the values of their cell parameters, they are not isomorphous (p.182). The barium compound could only be isolated as microcrystalline powders (see Slides) so that X-ray crystal studies could not be done.

The results of powder photographs of cadmium(II) malonate did not confirm the reported data (see Chapter VI). The reason is not clearly known. We may conclude with respect to this compound that its identity is firmly established but that some doubts remain concerning its structure. However, a detailed structural investigation of this compound by the single-crystal method will lead to more definite results.

The geometry around the cobalt(III) and chromium(III) centres in malonate complexes is octahedral. The malonate ligands are bidentate, each coordinating the metal ions through two carboxylate oxygen atoms, forming a six-membered chelate ring.

The crystal structures of aluminium(III) malonate complexes were studied by powder and single-crystal methods and the cell parameters were obtained (Table 6.3). While we have no further structural data available on this compound, the fact that the tris-malonate complexes of aluminium(III), chromium(III) and iron(III) are known to be isomorphous strongly supports the suggestion of a similar octahedral structure for these complexes. From consideration of our infrared investigation, the strength of coordination increases in benzylmalonate and decreases in ethylmalonate substituents with respect to the malonate itself. It has been pointed out that benzylmalonic acid has greater strength of bonding to the metal ion than malonic acid. However, there are some uncertainties of the assignment of the symmetric and asymmetric stretching frequencies of the carboxyl groups in the infrared spectra of both ethyl and benzylmalonate complexes, since these are often combination bands and the appearance of many bands in this region makes any assignment ambiguous. Thus, prediction of the relative magnitude of metal-ligand bond order for these complexes

from this consideration would be speculative. Considering the results of Mössbauer spectra for Fe(III) malonate and C-substituted malonate complexes, the isomer shift values indicated an increase in covalency in the order malonate, benzylmalonate, ethylmalonate. This is not corroborated by increase in the stability in the order named.

The benzylmalonate complexes have stability constants lower than the malonate complexes and if one accepts this criterion, it implies less covalent bonding. The isomer shift, however, implies that it is somewhat more covalent and that the phenyl group is donating electrons towards the iron. These discrepancies may arise in part from the use of thermodynamic data as a criterion of covalency. Since Mössbauer measurements measure the quality of a bond the results are more reliable. Again, comparing Fe(III) ethylmalonate with the malonate, the stability constant of the ethylmalonate is slightly lower than for the malonate itself; its isomer shift is significantly less, indicating that it is the most covalent of the series. Such a conclusion is supported by the results obtained in the comparative study of the ^{13}C n.m.r. spectra. Because of electron withdrawal by the carboxylate group, the phenyl group appears to have the same electron releasing effects as does the methyl group. Benzylmalonic and ethylmalonic acid have similar pK values and the ^{13}C shieldings of the α -carbon atom are almost the same. Both these acids are weaker than malonic acid itself because both methyl and benzyl groups are overall electron releasing. It is interesting to note that the ^{13}C chemical shift of α -carbon in malonate is $\sim +12.0$ ppm from malonate to ethyl and benzylmalonate anions. This arises from the inductive effect of the ethyl and benzyl groups which remove electron density from the 2p orbital of the α -C atom compared with the malonate. This is associated with an increase in the $\langle r^{-3} \rangle_{2p}$

factor. It is apparent that the electronic effect contributes more to the total than does the steric effect with respect to these complexes.

PUBLICATIONS

^{13}C Magnetic resonance of benzylmalonic acid and of some malonato complexes of aluminium(III). S. Amirhaeri, M.E. Farago and J.N. Wingfield, *Inorganica Chimica Acta*, 31 (1978), L385-L386.

^1H and ^{13}C n.m.r. studies on malonic and ethylmalonic acids and their cobalt(III) complexes. S. Amirhaeri, M.E. Farago, J.A.P. Gluck and M.A.R. Smith, *Inorganica Chimica Acta*, 33 (1979) 57-61.

¹³C Magnetic Resonance of Benzylmalonic Acid and of Some Malonato Complexes of Aluminium(III)

S. AMIRHAERI, M. E. FARAGO

Chemistry Department, Bedford College, Regents Park, London NW1 4NS, U.K.

J. N. WINGFIELD

Molecular Structures Department, Rothamsted Experimental Station, Harpenden, Herts. AL5 2JQ, U.K.

Received July 24, 1978

There has been recent interest in the acidity of the α -protons in the malonate group, both in the esters [1] and in malonate coordinated to cobalt [2].

We report in this paper preliminary results of the ¹H and ¹³C n.m.r. studies of benzylmalonic acid and the aluminium(III) complexes of malonic, ethyl- and benzylmalonic acids. The results show that benzylmalonic acid undergoes exchange with deuterium from solvent D₂O in acid and in basic solution. In neutral solution, no exchange takes place in CDCl₃, but slow exchange occurs in D₂O. The similar observations for malonic and ethylmalonic acids will be reported later [3].

In D₂O solution, the complexes [Al(mal)₃]³⁻, [Al(etmal)₃]³⁻ and [Al(bzylmal)₃]³⁻ are stable to hydrolysis, and do not exchange protons with the solvent.

Experimental

The aluminium malonato complexes were prepared by a modification of the method of Bailar and Jones [4] for the tris(oxalato) complex. Thus,

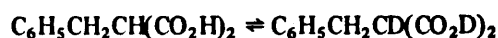
TABLE I. ¹H N.m.r. Signals of Benzylmalonic Acid in CDCl₃ (δ in ppm vs. TMS).

CH ₂	doublet	3.25	(J = 7.63 Hz)
CH	triplet	3.75	
C ₆ H ₅	singlet	7.25	
CO ₂ H	broad	9.36	

potassium tris(malonato)aluminate(III) hexahydrate, potassium tris(ethylmalonato)aluminate(III) trihydrate and potassium tris(benzylmalonato)aluminate(III) trihydrate were prepared by the addition of the appropriate potassium hydrogen malonate to the required amount of freshly prepared aluminium hydroxide. The filtered mixtures were concentrated on a rotary evaporator, and set aside to crystallise. Analyses were satisfactory. The measurement of n.m.r. spectra will be described elsewhere [3].

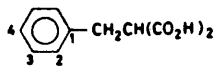
Results and Discussion

The ¹H n.m.r. spectral data of benzylmalonic acid in CDCl₃ are reported in Table I. In this solvent there is no change in the spectrum for 24 hours. In D₂O solution the spectrum is more complicated as a consequence of the slow exchange reaction:



After 30 minutes, the singlet of the high field (CH₂) pattern has increased at the expense of the low field (CH) triplet. After 24 hours the low field triplet has disappeared and the high field pattern has become a singlet, showing the presence of C₆H₅CH₂-CD(CO₂D)₂.

TABLE II. ¹³C N.m.r. Signals of Benzylmalonic Acid and Derivatives (δ in ppm vs. TMS).

				Al(bzylmal) ₃ ³⁻
	D ₂ O soln.	D ₂ O/NaOD	Na ₂ CO ₃ /D ₂ O ^b	
CO ₂ H	173.21	179.86	180.00	177.38
C ₁	138.63	141.66	141.72	140.50
C ₂ , C ₃	129.53	129.38	129.46	129.62, 129.38
C ₄	127.71	126.95	127.04	127.25
CH	54.42 ^c	61.7 ^a	61.21	55.41
CH ₂	35.17	37.11	37.24	36.19

^aSplit signal showing presence of CH and CD. ^bAcid neutralised with Na₂CO₃, salt dried and dissolved in D₂O. ^cSinglet of fresh solution rapidly collapses to split signal of CH and CD.

TABLE III. ^{13}C N.m.r. Signals of Ethylmalonic Acid and Derivatives (δ in ppm vs. TMS).

	D_2O soln. ^a	$\text{D}_2\text{O}/\text{NaOD}^a$	$\text{Na}_2\text{CO}_3/\text{D}_2\text{O}^{a,b}$	$\text{Al}(\text{etmal})_3^{3-}$
CO_2H	174.28	180.88	180.86	178.50
CH	54.05	—	61.64	54.85
CH_2	22.80	22.40	22.38	24.54
CH_3	11.73	13.00	13.04	12.48

^aFrom ref. 3. ^bAs Table II.TABLE IV. ^{13}C N.m.r. Signals of Malonic Acid and Derivatives (δ in ppm vs. TMS).

	D_2O^a	$\text{D}_2\text{O}/\text{NaOD}^a$	$\text{Na}_2\text{CO}_3/\text{D}_2\text{O}^{a,b}$	$\text{Al}(\text{mal})_3^{3-}$
CO_2H	171.57	178.49	178.37	175.49
CH_2	42.33	49.44	48.90	42.40
	41.43	48.73		
	40.64	47.92		

^aFrom ref. 3. ^bAs Table II.

The ^{13}C n.m.r. spectral data of benzylmalonic, ethylmalonic and malonic acids are shown in Tables II–IV.

The addition of a proton to the anion of benzylmalonic acid produces an upfield shift in the carboxyl and α -carbon resonances both of 6.79 ppm. The CH_2 and C_1 resonances are slightly more shielded, with upfield shifts of 2.07 and 3.09 ppm respectively. The C_2 , C_3 and C_4 resonances show deshielding with small downfield shifts. When the anion is complexed with Al^{3+} , the increased shieldings of the carboxyl and the α -carbons are smaller (2.62 and 5.8 ppm, respectively), and the increased shielding of the CH_2 carbon is smaller (1.05 ppm). The C_2 and C_3 resonances are resolved in the complex.

A similar trend is observed for ethylmalonate. On acidification, the carboxyl and α -carbons show large increases in shielding of 6.58 and 7.35 ppm, respectively. The ethyl group shows a smaller upfield shift. On coordination to Al^{3+} , there are smaller upfield shifts for the carboxyl and α -carbons (2.36 and 6.79 ppm), whereas the methylene carbon of the ethyl

group is now deshielded (2.16 ppm). However, the methyl group carbon is shielded by 0.56 ppm.

In general the resonances for the Al^{3+} complexes fall between those found for the free acids and those for their sodium salts, with the exception of the CH_2 resonance in the ethyl group of $[\text{Al}(\text{etmal})_3]^{3-}$. Thus coordination of the anion by Al^{3+} in general produces shielding.

There exists the possibility of geometrical isomers in the tris complexes of C-substituted malonate. This point, and the reactions of such complexes are under investigation.

References

- 1 A. J. Kirby and G. J. Lloyd, *J. Chem. Soc. Perkin II*, 1762 (1975).
- 2 M. E. Farago and M. A. R. Smith, *J. Chem. Soc. Dalton*, 2120 (1972).
- 3 S. Amirhaeri, M. E. Farago, J. A. P. Gluck and J. N. Wingfield, *Inorg. Chim. Acta*, submitted for publication.
- 4 J. C. Bailar and E. M. Jones, *Inorg. Synth.*, 1, 36 (1939).

^1H and ^{13}C NMR Studies on Malonic and Ethylmalonic Acids and their Cobalt(III) Complexes

S. AMIRHAERI, M. E. FARAGO*, J. A. P. GLUCK, M. A. R. SMITH†

Chemistry Department, Bedford College, Regent's Park, London NW1 4NS, U.K.

and J. N. WINGFIELD*

Department of Molecular Structures, Rothamsted Experimental Station, Harpenden, Herts. AL5 2JQ, U.K.

Received July 6, 1978

Magnetic resonance studies on malonic and ethyl malonic acids show that the α -protons exchange with deuterium from solvent in both acid and basic D_2O solution. In basic solution the $[\text{Coen}_2\text{mal}]^+$ ion undergoes a fast ring opening with hydroxide. At the same time the α -protons exchange with deuterium from the solvent. ^{13}C n.m.r. studies show that the methylene carbon in $[\text{Comal}_3]^{3-}$ is deshielded with respect to those in $[\text{Coen}_2\text{mal}]^+$, free malonic acid or the free anion. The ^{13}C n.m.r. shieldings for ethylmalonic acid and $[\text{Coen}_2\text{Etmal}]^+$ are reported.

Introduction

There has been recent interest in the malonate group: crystallographic work has shown that the conformation of the six membered malonato-chelate ring is greatly dependent on its environment in the solid state *e.g.* [1-5]; malonate has been shown to be an important C_2 biosynthetic unit [6] and the acidity of the α -protons in the malonate ligand has been demonstrated [7-10].

In this and subsequent papers we describe further investigations of the malonato group coordinated to metal ions, and present a study of malonic and of C-substituted ethylmalonic acids and their derived complexes in solution by both ^1H and ^{13}C n.m.r. spectroscopy. There have been several investigations of malonato complexes using ^1H n.m.r. particularly those of cobalt(III) [7, 10], and some reports of the application of ^{13}C n.m.r. spectroscopy to the study of cobalt(III) complexes, including those of aminopolycarboxylates [11-13], and of amino acids [14], and of diamines [15].

The aim of this research is three-fold: firstly, the assignment of chemical shifts to malonic acids and their complexes of cobalt and of other metals; secondly, the investigation of the stereochemistry of complexes containing more than one malonate ring each of which carry a C-substituent [10] and thirdly, the elucidation of the first step in the reaction of the metal-malonato ring with hydroxide ions. The kinetic results of this last reaction, in the case of $[\text{Coen}_2\text{mal}]^+$ are explicable either in terms of a ring opening reaction or of a proton extraction from the malonato methylene group [16].

Experimental

^1H n.m.r. spectra were measured with a Perkin Elmer 60 MHz continuous wave spectrometer at 35 °C, or with a Jeol Inc., JNM PS 100 Fourier transform 100 MHz spectrometer in the ^1H mode. Chemical shifts were relative to tertiary butanol as internal standard, or to external TMS. ^{13}C n.m.r. spectra were measured using the Jeol Fourier transform instrument in the ^{13}C mode. Most spectra were obtained using D_2O lock, 8000 data points, repetition times between 3 and 10 seconds, and up to 6000 scans depending on the concentration of the sample. Concentrations were normally about 0.2 g cm^{-3} . Either tertiary butanol or *p*-dioxane were used as internal standards. Most ^{13}C spectra were carried out at Rothamsted (some were measured by P.C.M.U., Harwell, where T.S.P. was used as internal standard, and some by U.L.I.R.S., King's College, London). ^1H n.m.r. spectra were measured at Bedford College.

Preparation of Cobalt Complexes

$[\text{Coen}_2\text{mal}]\text{Br}$ and $\text{K}[\text{Coenmal}_2]\text{H}_2\text{O}$ were prepared as before [10, 16]. $\text{K}_3[\text{Comal}_3]3\text{H}_2\text{O}$ was prepared by both the methods of Lohmiller and Wendlandt, and Al-Obodie and Sharpe [17], and gave satisfactory elemental analyses. $[\text{Coen}_2\text{Etmal}]\text{Br}$

*To whom correspondence should be addressed.

†Present address: BRUKER Spectrospin (Canada) Ltd., 5200 Dixie Road, Suite 116, Mississauga, Ontario, Canada, 14W 1E4.

H₂O was prepared as follows: 10 g of [Coen₂CO₃]Cl prepared by Dwyer's method [18], was treated with the Ag₂O freshly precipitated from 11 g silver nitrate. The silver chloride and the excess of silver oxide was filtered off and ethylmalonic acid (5 g) was added. The mixture was shaken until the evolution of CO₂ had ceased. The volume of the solution was reduced to 40 cm³ on a rotary evaporator and KBr (8 g) was added to the hot solution. The carmine-red leaf crystals were filtered off from the ice-cold solution, washed with ice-cold methanol, cold ether and dried *in vac.* The crude product was recrystallised from warm water and dried as before.

Anal. Calc. for C₉H₂₄N₄CoBrO₅: C, 26.6; H, 5.9; N, 13.8; Co, 14.4. Found: C, 26.6; H, 5.7; N, 14.0; Co, 14.4%.

Results

Uncomplexed Acids

Malonic acid

The ¹H n.m.r. spectrum of malonic acid in D₂SO₄ solution shows the methylene group signal split into a triplet (2.1 ppm vs. *t*-butanol J ~ 7.3 Hz) indicating the presence of the CHD group, where its signal is superimposed on the singlet from the CH₂ group. The intensities of these signals decrease with time as CD₂ is produced.

In NaOD/D₂O solutions a similar trend is noticed: *viz.* the appearance of the triplet, the intensity of which decreases with time. In solution in D₂O and neutralised with Na₂CO₃, malonic acid shows only a singlet from the CH₂ group (1.91 ppm vs. *t*-butanol) which remained unchanged for several hours. A singlet for the methylene signal is also reported for a malonic acid solution in polysol-d [19a].

The ¹³C n.m.r. spectrum of malonic acid in D₂O shows a signal of 171.57 ppm for the carbonyl shielding and a split signal at 42.4 ppm for the CH₂ resonance confirming the presence of CH₂, CHD and CD₂. The carbonyl resonance compares with a value of 170.4 ppm for a saturated solution in methanol [20]. In NaOH solution the carbonyl peak shifts to 178.37 ppm, and the methylene signal is split (Table III). When malonic acid is neutralised in H₂O with Na₂CO₃, then evaporated to dryness and redissolved in D₂O, the proton decoupled spectrum shows a singlet for the CH₂ resonance which persists for several hours. If neutralisation is carried out in D₂O, some exchange occurs during neutralisation, but the spectrum is then 'frozen' for several hours and shows the peaks required for CH₂, CHD and CD₂ species.

Ethylmalonic acid

In D₂O solution ethylmalonic acid gives signals in the ¹H n.m.r. spectrum from the CH₃ group, -0.28 ppm (triplet J ~ 7.5 Hz); CH₂ group, 0.65 ppm

(quintet, J ~ 7.6 Hz); CH, 2.19 ppm (triplet J ~ 7.24 Hz). The spectrum is similar to that reported in trifluoroacetic acid solution [19b]. On standing the CH signal decreases and the CH₂ quintet broadens. Finally the CH triplet disappears and the CH₂ signal sharpens to a quartet. Similar effects are noticed when the acid is neutralised with Na₂CO₃ (Table I). With an excess of NaOD the CH signal has almost disappeared and the CH₂ signal is a quartet when the first measurement is taken in the fresh solution.

TABLE I. Splitting of CH₂ Signal in Ethylmalonic Acid in D₂O/Na₂CO₃ Solution as α-H Exchanges with D from Solvent.

Intensity	Splitting of CH ₂ Signals	Time
CH:CH ₂ :CH ₃		
1:2:3	quintet	fresh solution
0.75:2:2	broad quintet	after two days
0.45:2:3	7 or 8 bands	after seven days
0:2:3	quartet	in excess of NaOD (fresh solution)

The ¹³C n.m.r. spectrum of ethylmalonic acid in fresh D₂O solution exhibits a singlet for the CH resonance; this rapidly collapses to a complex triplet. When ethyl malonic acid is neutralised in H₂O, evaporated to dryness and dissolved in D₂O a singlet results for the CH resonance (doublet in ORD spectrum), which persists for several hours. No resonance is observed for the CH carbon in NaOH solution, indicating fast exchange. The ¹³C n.m.r. spectrum of ethyl malonic acid is given in Table II.

TABLE II. ¹³C N.m.r. Spectrum (ppm vs. TMS) of CH₃CH₂-CH(CO₂H)₂.

	CO ₂ H	CH	CH ₂	CH ₃
D ₂ O solution	174.28	54.05	22.80	11.73
D ₂ O/NaOD	180.88	—	24.40	13.00
D ₂ O/Na ₂ CO ₃	180.86	61.4	24.38	13.04

Cobalt(III) Complexes of Malonic Acid

The 60 MHz ¹H n.m.r. spectrum of [Coen₂mal] Br has been reported [9]. Relative to *t*-butanol the spectrum (in ppm) was reported as follows: NH₂ (*cis* to O), 3.13; NH₂ (*trans* to O), 4.14; CH₂(mal), 2.11; CH₂(en), 1.47. The present work using 100 MHz shows the CH₂(mal) signal at 2.17 ppm and the methylene groups from the ethylenediamine show the expected splitting: giving signals at 1.57 and 1.47 ppm. On the addition of base the CH₂(mal) signal broadens and then splits into a triplet, showing that

TABLE III. ^{13}C N.m.r. Signals from Malonate Group (ppm vs. TMS).

	Carboxyl	Methylene		
Malonic acid/D ₂ O	171.57	42.23	41.43	40.64
Malonate ion/NaOH	178.49	49.44	48.73	47.92
Malonate ion/neutral	178.37	48.9		
[Coen ₂ mal] ⁺	179.5	~42		
[Coenmal ₂] ⁻	180.22, 179.93	-		
[Comal ₃] ³⁻	182.81	46.21		
uns[CoTMDDAmal] ^{-a}	178.66, 179.31	43.52		

^aFrom ref. 13.

deuterium substitution has occurred as in the free malonate anion. The CH₂ signal then disappears with time as in the case of the [Coen₂mal]⁺ ion with D₂SO₄ [9].

The ^{13}C n.m.r. spectrum (ppm vs. TMS) of the [Coen₂mal]⁺ ion is as follows: carboxyl, 179.5; CH₂(en), 45.87, 44.25; CH₂(mal), ~42. On addition of base to [Coen₂mal]⁺ in D₂O solution the methylene(mal) signals are no longer visible, but changes are noticed in the signals from the ethylenediamine methylenes.

The ^{13}C n.m.r. spectrum of the [Comal]³⁻ ion shows the carboxyl carbon at 182.81 and the malonato methylene at 46.21 ppm (see Table III).

Cobalt(III) Complex of Ethylmalonic Acid

[Coen₂Etmal]⁺

The ^1H n.m.r. spectrum (ppm vs. t-butanol) of the [Coen₂Etmal]⁺ ion has been reported [9]. C-H(mal), 1.90 (triplet); CH₂, 0.72 (quintuplet), CH₃, -0.40 (triplet). The ^{13}C n.m.r. spectrum (ppm vs. TMS) shows signals at 183.72 (carboxyl); 56.22 (CH); 47.44, 46.34 (CH₂, en); 26.26 (CH₂); 14.23 (CH₃).

Discussion

Free Acids and Anions

The ^1H n.m.r. spectra show that the >CH₂ protons of malonic acid exchange with deuterium from the solvent in both acidic and basic solution. In neutral solution, however, this exchange is very slow (confirmed by ^{13}C spectrum).

With ethylmalonic acid a similar trend is observed, the reactions are, however, faster than for the unsubstituted compound, in basic solution. Table I shows that initially the CH₂ signal is a quintet, with splitting from neighbouring CH and CH₃ groups. When the exchange of D for H in the CH group is complete, with excess NaOH for example, the coupling of the >CH₂ groups is now only with the methyl group giving a quartet. As the exchange takes place the >CH₂ signal becomes complicated as it arises from the quintet of the >CHCH₂CH₃ group superimposed

on the quartet of the >CDCH₂CH₃ group. When half exchange has taken place this gives rise to seven or eight bands.

The ^{13}C n.m.r. spectra give expected values for the shieldings in both acids. The results in Tables II and III show that on formation of the anion [21] the carboxylate carbon signal shifts to a lower field with a shift of +6.60 ppm for ethylmalonic acid and a similar shift of +6.92 ppm for malonic acid.

For ethylmalonic acid there is a downfield shift for both methylene and methyl carbons in basic media.

Complexes of Malonic Acid and Ethylmalonic Acid

The ^{13}C n.m.r. spectrum of [Coen₂mal]⁺ shows that the malonato group is chelated in neutral solution since there are two signals from the ethylene diamine carbons. A monodentate malonato group should give rise to more signals [15].

On the addition of base (saturated NaOH in D₂O) to a solution of [Coen₂mal]⁺ the changes in ^{13}C n.m.r. spectrum shown in the Figure arise.

Figure 1(a) shows the methylene signals from the two non equivalent methylene groups of ethylenediamine in [Coen₂mal]⁺. These are at 45.87 and 44.29 ppm. The first measurement after the addition of saturated NaOH/D₂O Figure 1(b) shows three signals at 45.60, 45.12 and 44.20 ppm. At this stage in the reaction it has been suggested that in strongly basic solution the [Coen₂mal]⁺ ion exists either as the monodentate malonato species [Coen₂malOH]⁰ or as the species in which a proton has been removed from the malonato methylene group in the chelate ring [16]. The three signals observed are consistent with the presence of the monodentate malonato group, three signals from the ethylenediamine methylene groups are expected for a complex of the type [Coen₂XY]. The results are not consistent with the deprotonated species [Coen₂mal(-H)]⁰, since two methylene signals are still expected, nor with a mixture of [Coen₂mal]⁺ and the deprotonated species. After 24 hours three signals appear at 45.13, 44.68 and 44.20 ppm. After 48 hours the mixture was acidified. The malonato carboxyl peak now

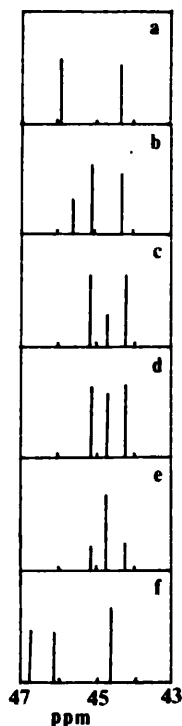


Figure. Changes in the ethylenediamine CH₂ signals when [Coen₂mal]⁺ is treated with NaOH solution. (a) [Coen₂mal]⁺ in D₂O. (b) Scans begun immediately after addition of NaOH solution. (c) Scans begun 1 hour after addition of NaOH. (d) After 24 hours. (e) After 48 hours. (f) Final solution acidified with conc. HCl.

appears at 172.8 ppm instead of 179.52 in the complex showing the presence of free malonic acid. The three ethylenediamine methylene signals at 46.72, 46.09 and 44.59 result from the equilibrium mixture of *cis* and *trans*[Coen₂(OH₂)₂]³⁺.

Thus in neutral solution the coordinated malonate group is stable in [Coen₂mal]⁺. It does not become dechelated, nor do the methylene group protons exchange with deuterium from the solvent. In basic media the malonate group is dechelated and at the same time exchange takes place between the methylene protons and the deuterium of the solvent.

The results in Table III show that the carboxyl carbons are deshielded on coordination with respect to the free acid, but are more shielded than the free anion. In addition the methylene carbon in [Comal₃]³⁻ is deshielded with respect to the other species in Table III.

Complexes of Ethylmalonic Acid

The ¹³C n.m.r. shieldings of ethylmalonic acid species are shown in Table IV.

The carbon signals show a successive downfield shift in the series ethylmalonic acid < ethylmalonate anion < [Coen₂Etmal]⁺.

TABLE IV. ¹³C N.m.r. Signals (ppm vs. TMS) of Ethylmalonic Acid Species.

	Carboxyl	CH	CH ₂	CH ₃
Acid/D ₂ O solution	174.28	54.05	22.80	11.73
NaOD/D ₂ O	180.88	—	24.4	13.00
[Coen ₂ Etmal] ⁺	183.72	56.22	26.26	14.23

The ethylenediamine methylene resonances in neutral solution are 45.87 and 44.78 ppm compared with those in [Coen₂CO₃]⁺ at 45.82 and 44.78 ppm. Thus there is no evidence of strain in the two bidentate ethylenediamine ligands on changing the ring size of the third chelate in contrast to the results of Douglas and co-workers for the quadridentate ligand TMDDA [13]. However the CH₂(en) resonances in [Coen₂(Etmal)]⁺ are at 47.44 and 46.34 ppm slightly deshielded with respect to the simple malonato or the carbonato complex.

¹³C studies on organic compounds show that shifts to greater shielding are associated with carbons which are sterically perturbed — the steric compression shift [20 (b)].

It appears that the ethylenediamine methylene groups in the simple malonato complex are more sterically strained than in the ethyl malonato compound. A possible explanation is that the presence of the ethyl substituent gives rise to a flat boat conformation of the malonato ring. Thus the malonato ring and the ethyl substituent would be further away from the ethylenediamine groups than the skew boat conformations.

Acknowledgements

M.A.R.S. and S.A. acknowledge the award of Studentships from the SRC and the Iranian Government respectively.

MEF thanks the Director of Rothamsted Experimental Station, and Dr. M. R. Truter, Head of the Molecular Structures Department, Rothamsted Experimental Station, Harpenden, Hertfordshire, for hospitality.

References

- 1 K. R. Butler and M. R. Snow, *J. Chem. Soc. Dalton*, 251 (1976).
- 2 K. Toriumi, S. Sato and Y. Saito, *Acta Cryst.*, B33, 1378 (1977).
- 3 E. Hansson, *Acta Chem. Scand.*, 27, 2813 (1973).
- 4 M. L. Post and J. Trotter, *J. Chem. Soc. Dalton*, 1922 (1974).
- 5 B. Briggman and A. Oskarsson, *Acta Cryst.*, B33, 1900 (1977).

- 6 W. B. Turner, "Fungal Metabolites", Academic Press, London (1975); J. A. Elvidge, D. K. Jais Wal, J. R. Jones and R. Thomas, *J. Chem. Soc. Perkin II*, 353 (1976).
- 7 H. Yoneda and Y. Morimoto, *Inorg. Chim. Acta*, **1**, 413 (1967).
- 8 D. A. Buckingham, L. Durham and A. M. Sargeson, *Austral. J. Chem.*, **20**, 257 (1967).
- 9 M. E. Farago and M. A. R. Smith, *J. Chem. Soc. Dalton*, 2120 (1972).
- 10 M. E. Farago and M. A. R. Smith, *Inorg. Chim. Acta*, **14**, 21 (1975).
- 11 O. W. Howarth, P. Moor and N. Winterton: (a) *Inorg. Nucl. Chem. Lett.*, **10**, 553 (1974); (b) *J. Chem. Soc. Dalton*, 2271 (1974); (c) *J. Chem. Soc. Dalton*, 360 (1975).
- 12 G. L. Blackman and T. M. Vickery, *J. Coord. Chem.*, **3**, 225 (1974).
- 13 K. D. Garley, K. Igi and B. E. Douglas, *Inorg. Chem.*, **14**, 2956 (1975).
- 14 T. Y. Yasui, *Bull. Chem. Soc. Jap.*, **41**, 454 (1975).
- 15 M. Kojima and K. Yamasaki, *Bull. Chem. Soc. Jap.*, **48**, 1093 (1975); D. A. House and J. W. Blunt, *Inorg. Nucl. Chem. Letters*, **11**, 219 (1975).
- 16 M. E. Farago and I. M. Keefe, *Inorg. Chim. Acta*, **15**, 5 (1975).
- 17 G. Lohmiller and W. W. Wendlandt, *J. Inorg. Nucl. Chem.*, **31**, 3187 (1969); M. S. Al-Obodie and A. G. Sharpe, *J. Inorg. Nucl. Chem.*, **31**, 2963 (1969).
- 18 F. P. Dwyer, A. M. Sargeson and I. K. Reid, *J. Am. Chem. Soc.*, **85**, 1215 (1963).
- 19 Sadtler n.m.r. (a) Spectrum No. 16010 M, (b) Spectrum No. 891 M.
- 20 (a) E. Lippmaa and P. Pehk, *Kem. Teollisuus*, **24**, 1001 (1967), reported in (b) "Carbon-13 N.m.r. Spectroscopy", by J. B. Storchers, Academic Press (1972) New York and London, p. 295.
- 21 R. Hagen and J. D. Roberts, *J. Am. Chem. Soc.*, **91**, 4504 (1969).